Journal Pre-proof

Molecular markers of response to anti-PD1 therapy in advanced hepatocellular carcinoma

Philipp K. Haber, Florian Castet, Miguel Torres-Martin, Carmen Andreu-Oller, Marc Puigvehí, Miho Maeda, Pompilia Radu, Jean-Francois Dufour, Chris Verslype, Carolin Czauderna, Jens U. Marquardt, Peter R. Galle, Arndt Vogel, Melanie Bathon, Tim Meyer, Ismail Labgaa, Antonia Digklia, Lewis R. Roberts, Mohamed A. Mohamed Ali, Beatriz Mínguez, Davide Citterio, Vincenzo Mazzaferro, Fabian Finkelmeier, Jörg Trojan, Burcin Özdirik, Tobias Müller, Moritz Schmelzle, Anthony Bejjani, Max W. Sung, Myron E. Schwartz, Richard S. Finn, Swan Thung, Augusto Villanueva, Daniela Sia, Josep M. Llovet

PII: S0016-5085(22)01039-3
DOI: https://doi.org/10.1053/j.gastro.2022.09.005
Reference: YGAST 65322

To appear in: *Gastroenterology*
Accepted Date: 2 September 2022

Please cite this article as: Haber PK, Castet F, Torres-Martin M, Andreu-Oller C, Puigvehí M, Maeda M, Radu P, Dufour J-F, Verslype C, Czauderna C, Marquardt JU, Galle PR, Vogel A, Bathon M, Meyer T, Labgaa I, Digklia A, Roberts LR, Mohamed Ali MA, Mínguez B, Citterio D, Mazzaferro V, Finkelmeier F, Trojan J, Özdirik B, Müller T, Schmelzle M, Bejjani A, Sung MW, Schwartz ME, Finn RS, Thung S, Villanueva A, Sia D, Llovet JM, Molecular markers of response to anti-PD1 therapy in advanced hepatocellular carcinoma, *Gastroenterology* (2022), doi: https://doi.org/10.1053/j.gastro.2022.09.005.

Title: Molecular markers of response to anti-PD1 therapy in advanced hepatocellular carcinoma

Authors: Philipp K. Haber[1,2], Florian Castet[3], Miguel Torres-Martin[3], Carmen Andreu-Oller[1], Marc Puigvehí[1,4], Miho Maeda[1], Pompilia Radu[5], Jean-Francois Dufour[5,6], Chris Verslype[7], Carolin Czauderna[8,9], Jens U. Marquardt[8,9], Peter R. Galle[8], Arndt Vogel[10], Melanie Bathon[10], Tim Meyer[11], Ismail Labgaa[12], Antonia Digklia[13], Lewis R. Roberts[14], Mohamed A. Mohamed Ali[14], Beatriz Mínguez[15], Davide Citterio[16], Vincenzo Mazzaferro[16], Fabian Finkelmeier[17], Jörg Trojan[17], Burcin Özdirik[18], Tobias Müller[18], Moritz Schmelzle[2,19], Anthony Bejjani[20], Max W. Sung[1], Myron E. Schwartz[1], Richard S. Finn[20], Swan Thung[1], Augusto Villanueva[1] , Daniela Sia[1], Josep M. Llovet[1,2,21]

Affiliations:

[1]Mount Sinai Liver Cancer Program, Division of Liver Diseases -Department of Medicine, Division of Hematology and Medical Oncology- Tisch Cancer Institute. Recanati/Miller Transplantation Institute, Department of Pathology, Molecular and Cell-Based Medicine, Icahn School of Medicine at Mount Sinai, New York, NY.

[2]Department of Surgery, Campus Charité Mitte and Campus Virchow Klinikum, Charité-Universitätsmedizin Berlin, corporate member of Freie Universität Berlin, Humboldt-Universität zu Berlin, and Berlin Institute of Health, Germany.

[3]Translational Research in Hepatic Oncology, Liver Unit, IDIBAPS, Hospital Clinic, University of Barcelona, Catalonia, Spain

[4]Hepatology Section, Gastroenterology Department, Parc de Salut Mar, IMIM (Hospital del Mar Medical Research Institute), Universitat Autònoma de Barcelona, Barcelona, Spain

[5]University Clinic for Visceral Surgery and Medicine, University of Bern, Inselspital, Bern, Switzerland.

[6]Hepatology, Department of Clinical Research, University of Bern, Bern, Switzerland.

[7]Department of Gastroenterology and Hepatology, KU Leuven, Leuven, Belgium.

[8]Department of Medicine I, University Medical Center of the Johannes-Gutenberg University Mainz, Germany.

[9]Department of Medicine I, University of Lübeck, UKSH – Campus Lübeck, Lübeck, Germany

[10]Department of Gastroenterology, Hepatology and Endocrinology, Hannover Medical School, Hannover, Germany

[11]Department Oncology, University College London Cancer Institute, London, UK.

[12]Department of Visceral Surgery, Lausanne University Hospital and University of Lausanne, Lausanne, Switzerland.

[13]Department of Oncology, Lausanne University Hospital and University of Lausanne, Lausanne, Switzerland.

[14]Division of Gastroenterology and Hepatology, Mayo Clinic College of Medicine and Science, Rochester, MN.

[15]Liver Unit, Hospital Universitari Vall d'Hebron, Liver Diseases Research Group, Vall d'Hebron Institute of Research (VHIR), Vall d'Hebron Barcelona Hospital Campus. CIBERehd, Universitat Autònoma de Barcelona, Barcelona, Spain.

[16]Gastrointestinal Surgery and Liver Transplantation Unit, National Cancer Institute, Milan, Italy.

[17]Department of Gastroenterology, University Liver and Cancer Centre, Frankfurt, Germany.

[18]Department of Hepatology & Gastroenterology, Campus Virchow Klinikum and Campus Charité Mitte, Charité University Medicine Berlin, Germany.

[19] Department of General, Visceral and Transplant Surgery, Hannover Medical School, Hannover, Germany.

[20]Division of Hematology/Oncology, Geffen School of Medicine at UCLA, Los Angeles, CA, USA.

[21]Institució Catalana de Recerca i Estudis Avançats, Barcelona, Catalonia, Spain.

***Corresponding author:**

Josep M. Llovet, M.D., Ph.D.,
Mount Sinai Liver Cancer Program,
Division of Liver Diseases, Tisch Cancer Institute,
Icahn School of Medicine at Mount Sinai, New York, NY, USA .
E-mail: josep.llovet@mssm.edu

Financial disclosures: This study was supported by a research grant from Bayer Pharmaceuticals to JM Llovet, MD.

PKH is supported by the fellowship grant of the German Research Foundation (DFG, HA 8754/1-1). FC is supported by a AECC Clínico Junior grant, ID code (CLJUN20007CAST). CAO is supported by a Fulbright fellowship. MP received a "Juan Rodés" scholarship grant from Asociación Española para el Estudio del Hígado (AEEH). J.U.M. is supported by grants from the German Research Foundation (MA 4443/2-2; SFB1292), the Volkswagen Foundation (Lichtenberg program). AV is funded by the DFG, (SFB/TRR 209 - 314905040, and Vo959/9-1). TM is funded by the NIHR UCH Biomedical Research Centre and Accelerator Award (HUNTER, Ref. C9380/A26813, partnership between the CRUK, AECC and AIRC). LRR and MAMA are supported by the Mayo Clinic Hepatobiliary SPORE (P50 CA210964). MS acknowledges a research grant from the DFG (SCHM2661/3-2). The work of DS is supported by the Tisch Cancer Institute and the PhD Scientist Innovative Research Award. J.M.L. is supported by National Cancer Institute (P30-CA196521), NIDDK (R01 DK128289), US. Department of Defense (CA150272P3), European Commission/Horizon 2020 Program (HEPCAR, Ref. 667273-2), Accelerator Award (CRUK, AECC, AIRC) (HUNTER, Ref. C9380/A26813), Samuel Waxman Cancer Research Foundation, Centro de Investigación Biomédica en Red (CIBER) – ISCIII, Spanish National Health Institute (SAF2016-76390), Generalitat de

Catalunya/AGAUR (SGR-1358) and the Acadèmia de Ciències Mèdiques i de la Salut de Catalunya i de Balears.

Conflicts of interest relevant to this work:

JFD has received consulting fees from Abbvie, Bayer Healthcare, Bristol-Myers Squibb, Falk, Genfit, Genkyotex, Gilead Sciences, HepaRegenix, Intercept, Eli Lilly, Merck, Novartis, Roche. JUM. received honoraria from Roche, Bayer, Ipsen, Merz, AstraZeneca, MSD and Leap-Tx, Eisai. PRG is receiving honoraria from Adaptimmune, Bayer, BMS, AstraZeneca, Sirtex, MSD, Eisai, Ipsen, Roche, Lilly, Guerbet. AV has received consulting fees and honoraria from AstraZeneca, Bayer, BMS, Eisai, Incyte, Ipsen, Janssen, Lilly, Merck, MSD, Novartis, Pierre Fabre, Roche, and Sanofi. TM reports consulting fees from IPSEN, AstraZeneca, Roche, Bayer Healthcare, Adaptimmune, Boston Scientific and Eisai. LRR has received grant funding from Bayer, BTG International, Exact Sciences, Gilead Sciences, GlycoTest, Redhill, TARGET PharmaSolutions and FUJIFILM Medical Systems, and has consulted for AstraZeneca, Bayer, Exact Sciences, Gilead Sciences, GRAIL, QED Therapeutics, and TAVEC. B.M. received consultancy fees from Bayer-Shering Pharma, and speaker fees from Eisai and MSD. MS is receiving honoraria from ERBE, Amgen, Merck and Bayer Healthcare. MWS is receiving consulting fees from Bayer, EISAI and Exelixis. RSF has received consulting fees from AstraZeneca, Bayer Healthcare, Eisai, CStone, Bristol-Myers Sqibb,Eli Lilly, Pfizer, Merck, Roche/ Genenetech, Exelixis. AV has received consulting fees from Guidepoint, Fujifilm, Boehringer Ingelheim, FirstWord, and MHLife. JML is receiving research support from Bayer HealthCare Pharmaceuticals, Eisai Inc, Bristol-Myers Squibb, Boehringer-Ingelheim and Ipsen, and consulting fees from Eli Lilly, Bayer HealthCare Pharmaceuticals, Bristol-Myers Squibb, Eisai Inc, Celsion Corporation, Exelixis, Merck, Ipsen, Genentech, Roche, Glycotest, Nucleix, Sirtex, Mina Alpha Ltd and AstraZeneca. The remaining co-authors have nothing to disclose related to this manuscript.

Author contributions: Study design: PKH, MP, DS, JML. Patient enrolment/sample and data collection: PKH, FC, MP, PR, JFD, CV, CC, JM, PG, AV, MB, TM, IL, AD, LRR, MAM, BM, DC, VM, FF, JT, BÖ, TM, MS, AB, MWS, MES, RSF. Experiments: PKH, MTM, MP, CAO, MM. Analysis: PKH, MTM, CAO, FC, ST, AV, DS, JML. Drafting of manuscript: PKH, DS, JML. All authors gave intellectual input to the manuscript and have approved its final version.

Abbreviations: AFP: α-fetoprotein, aHCC: Advanced hepatocellular carcinoma, AP: Antigen presentation, AUC: Area under the curve, BCLC: Barcelona Clinic Liver Cancer, CR: Complete response, DCR: Disease control rate, ECOG: Eastern Cooperative Oncology Group, FDR: False discovery rate, FOXP3: Forkhead-Box-Protein P3, HNSCC: Head and neck squamous cell carcinoma, ICI: Immune checkpoint inhibitors, IFNγ: Interferon gamma, IRB: Institutional review board, mAB: Monoclonal antibody, MHC: Major histocompatibility complex, mOS: median overall survival, NASH: Non-alcoholic steatohepatitis, NSCLC: Non-small cell lung cancer, OR: Objective response, ORR: objective response rates, OS: Overall survival, PD: Progressive disease, PFS: Progression free survival, PR: Partial response, RECIST: Response evaluation criteria in solid tumors, ROC: Receiver operating characteristic, SD: Stable disease, TKI: tyrosine-kinase inhibitors, VEGF: Vascular endothelial growth factor

Word count: 6960

Abstract word count: 260

Number of figures: 6

Number of tables: 1

ABSTRACT

Background and Aims

Single agent anti-PD1 checkpoint inhibitors convey outstanding clinical benefits in a small fraction (~20%) of patients with advanced hepatocellular carcinoma (aHCC) but the molecular mechanisms determining response are unknown. To fill this gap, we herein analyze the molecular and immune traits of aHCC in patients treated with anti-PD1.

Methods: Overall, 111 tumor samples from patients with aHCC were obtained from 13 centers prior to systemic therapies. We performed molecular analysis and immune deconvolution using whole genome expression data (n=83), mutational analysis (n=72) and histological evaluation with an endpoint of objective response.

Results: Among 83 patients with transcriptomic data, 28 were treated in frontline whereas 55 patients were treated after tyrosine-kinase inhibitors (TKI) either in 2nd or 3rd line. Responders treated in frontline showed upregulated Interferon-γ-signaling and MHCII-related antigen presentation. We generated an 11-gene signature *(IFNAP*), capturing these molecular features, which predicts response and survival in patients treated with anti-PD1 in frontline. The signature was validated in a separate cohort of aHCC and >240 patients with other solid cancer types where it also predicted response and survival. Of note, the same signature was unable to predict response in archival tissue of patients treated with frontline TKIs, highlighting the need for fresh biopsies prior to immunotherapy.

Conclusion: IFN-signaling and MHCII-related genes are key molecular features of HCCs responding to anti-PD1. A novel 11-gene signature predicts response in frontline aHCC - but not in patients pre-treated with TKIs. These results have to be confirmed in prospective studies and highlight the need for biopsies prior immunotherapy to identify biomarkers of response.

Keywords: Hepatocellular carcinoma, biomarkers, predictors of response, Immunotherapy

INTRODUCTION

Hepatocellular carcinoma (HCC) is a leading cause of cancer related mortality globally and incidence rates are on the rise[1]. At advanced stages, where only systemic therapies are effective, outcomes remain dismal. Until recently, the treatment landscape of HCC was dominated by tyrosine-kinase inhibitors (TKIs), such as sorafenib[2] and lenvatinib[3] that have been able to convey a marginal improvement in survival for the majority of the population.

The use of immune checkpoint inhibitors (ICI) has revolutionized clinical care across cancer types. In HCC, the combination of the anti-PD-L1 agent atezolizumab and the monoclonal antibody (mAB) bevacizumab (anti-VEGF) has elicited an outstanding median overall survival (mOS) of 19.2[4] months in patients with advanced HCC (IMbrave150 trial) and is now considered standard of care in frontline[1, 5]. Furthermore, new ICI-based combinations are expected to reshape the treatment scenario such as the combination of durvalumab-tremelimumab[6], which increases overall survival (OS) relative to sorafenib and cabozantinib-atezolizumab, which increases progression-free survival (PFS)[7]. These and other combinations currently under investigation are aimed at enhancing the size of the patient subset that derives a benefit from ICI treatment. In this setting, ICIs are commonly regarded as the driving force in improving outcomes whereas drugs like bevacizumab are thought to expand the immune-sensitive population[8]. Indeed, immunotherapy as standalone treatment is able to convey meaningful benefits in patients with advanced HCC: early efficacy results from anti-PD1 inhibitors nivolumab[9] and pembrolizumab[10] demonstrated objective response rates (ORR) between 15-20%. These responses lasted beyond 16 months[9] and are expected to elicit a mOS >26 months, thereby outperforming the new standard of care. However, the comparatively small size of this subset failed to drive a significant advantage for the entire population leading to the failure of phase III trials both in frontline[11] (vs sorafenib) and 2nd line[12] setting (vs. placebo), hence the utilization of combination treatments. The molecular mechanisms that determine response to anti-PD1 in HCC remain elusive. Thus, the development of predictive biomarkers of response to ICI has the potential to address several unmet clinical needs: (I) to enhance survival in patients likely to respond to therapy, (II) to reduce

the risk of treatment-related adverse effects conveyed through combination drugs like bevacizumab and (III) maximize efficacious application and thereby cost-effectiveness of different treatments.

To address these needs, we established an international consortium of referral centers to identify biomarkers of response in patients treated with anti-PD1. We analysed tissue samples from patients subsequently undergoing anti-PD1 treatment for advanced HCC at the histological, mutational and gene expression levels. Patients responding to anti-PD1 in frontline showed higher baseline levels of intratumoral inflammatory signalling. We generated a gene-expression signature capable of capturing responders and validated it in an independent cohort of aHCC patients and four publicly available datasets of solid cancer types comprising >240 patients. Interestingly, the same signature failed to predict response in patients that were pre-treated with TKIs, suggesting that archival tissue may not be appropriate to predict response to immunotherapy in patients previously treated with TKIs as these drugs may modulate response patterns to 2nd line anti-PD1 therapy. Overall, these findings provide a comprehensive picture of the molecular landscape of patients with advanced HCC responding to anti-PD1 and define a novel tool for patient selection in future clinical trials.

MATERIALS AND METHODS

Study population and endpoints

Under the umbrella of an international consortium comprising thirteen centers in the United States and Europe (**Table S1**), we retrospectively collected samples from 111 patients for this study. Eligible patients were ≥18 years with pathologically confirmed HCC at advanced stage (BCLC stage C) or intermediate stage (stage B) after confirmed progression to locoregional therapies and not amenable to a curative treatment approach. Response assessment was performed at least two months after the initiation of anti-PD1 treatment via modified RECIST (mRECIST[13]) and at least one untreated lesion was required for inclusion. Patients had compensated liver function and Eastern Cooperative Oncology Group (ECOG) performance score 0-2 as well as otherwise adequate organ and bone marrow function (white blood cell counts ≥2000/µL, platelets ≥50×10^3/µL). All patients had archived tissue available obtained from the resection specimen or at the time

of biopsy prior to systemic therapies and underwent anti-PD1 monotherapy. Patients who had been previously treated with an agent targeting T-cell costimulation or checkpoint pathways (including PD-1/PD-L1) were excluded, as were those receiving anti-PD1 or any other treatment neoadjuvantly prior to resection or in combination with other systemic or percutaneous treatments. Further exclusion criteria were: history of other malignancies, other diseases expected to severely limit life expectancy, brain metastases, history of hepatic encephalopathy or clinically significant ascites that required paracentesis. Patients with fibrolamellar HCC, sarcomatoid HCC, or mixed cholangiocarcinoma-HCC were excluded. The present study was conducted in accordance with the Helsinki Declaration and local laws. The institutional review board (IRB) at each contributing center approved the study protocol. All patients alive at the time of study initiation provided written informed consent enabling to use their archived tissues. Consent for already deceased patients was waived by the local IRBs.

Given that different systemic treatments may alter the tumoral microenvironment to the point that it may impact the efficacy of subsequent therapies[14], we stratified patients according to the treatment line in which they received anti-PD1 (**Table S2**).

The primary endpoint applied for the analysis was best objective response (OR), which was assessed in individual centers using mRECIST criteria defining complete response (CR), partial response (PR), stable disease (SD) and progressive disease (PD)[13]. Response was generally assessed 2-3 months after therapy start and every three months thereafter via either computed tomography (CT-scan) or magnetic resonance imaging (MRI). The secondary endpoints were overall- (OS) and progression-free survival (PFS).

Immunohistochemistry, transcriptome analysis, CTNNB1 analysis and molecular data availability

See online supplementary materials and methods.

Statistical analysis

Analyses were performed using the R statistical package and SPSS 24.0 (SPPS Inc., Chicago, USA). Correlations between clinicopathological data and molecular features were performed in case of categorical data with Chi^2 test, whereas continuous data with

non-parametric distribution was assessed by Wilcoxon-rank-sum test. Continuous variables with Gaussian distribution were compared with ANOVA. Survival analysis was performed with Kaplan-Meier estimates and log-rank test with respect to both OS and PFS as well as a Cox logistic regression model. Biomarkers were considered predictive of response or primary resistance to anti-PD1 therapy when two sided $p<0.05$.

RESULTS

Baseline characteristics and clinical courses

Among the 111 HCC samples collected for the study, 83 cases had enough tissue available for molecular analysis, met all inclusion criteria and were thus included in the transcriptomic analysis (**Figure 1A**). The time difference between acquisition of the biological sample and initiation of systemic therapies is depicted in **Figure S1**. Recruited patients were treated with nivolumab (n=67; 80.7%), pembrolizumab (n=14; 16.9%) or tislelizumab (n=2; 2.4%) in either frontline (n=28), 2nd (n=41) or 3rd line (n=14) (**Figure 1B**). All patient demographics and disease characteristics were well balanced between response types (**Table 1**). Among the 83 patients, 25 exhibited OR (ORR:30.1%, 3 CR, 22 PR), whereas 21 cases (25.3%) had SD and 37 cases (44.6%) PD as best response. Median time to response was 3.0 months (range 1.7-12.8 months) and responses were very durable with 67% lasting 18 months or longer. Median duration of treatment was 4.9 months, and patients displaying OR had a significantly longer time on therapy than non-responders (18.2 vs. 3.3 months, $p<0.001$). In terms of outcome, median follow-up was 12.5 months. Responders did not reach mOS during follow up, whereas mOS was 19.5 months and 12.5 months for patients achieving SD and PD, respectively ($p<0.001$, **Figure 1C**). Likewise, responders had significantly longer PFS compared to patients with either SD or PD (median PFS [mPFS]: 28.8 vs. 6.2 vs. 2.5 months, $p<0.0001$) (**Figure 1D**).

Of the 28 patients in the frontline cohort, 12 exhibited OR (ORR:42.9%). These patients had, expectedly, a significantly better outcome than non-responders both in terms of OS and PFS ($p<0.005$ and $p<0.001$, respectively, **Figure 2A,B**). A detailed description of patients treated with anti-PD1 in 1st line is provided in **Table S3**.

Molecular features of HCC patients responding to anti-PD1 in front line

Overall, differential expression analysis identified 427 genes significantly upregulated in responders (p<0.01, **Table S4**), with 140 exhibiting a Fold Change >1.5. Among these, several genes involved in Interferon-γ (IFNγ)-signalling (*STAT1, STAT2, IRF1*, p <0.0005, p<0.05, p<0.05, respectively, **Figure 2C**) and antigen-presentation were significantly upregulated in responding patients. This was particularly evident for MHC class II peptides (*HLA-DRA, HLA-DQA1, HLA-DMA*, p<0.01, p<0.005, p<0.05, **Figure 2C,D**). Metagenes capturing activation of IFN- and T-cell receptor signalling as well as antigen processing and presentation were, likewise, enriched among responders (FDR<0.001). The same patients showed a significant upregulation in the expression of key cytokines involved in chemotaxis (*CXCL9*, *IL18*, p<0.005 and p<0.001, respectively). Gene Ontology (GO) Enrichment Analysis of the top 140 differentially expressed genes confirmed IFNγ signalling, MHC-II assembly and MHC-II dependent antigen presentation as the most overexpressed pathways among responders (**Figure 2E, S2A**). Gene set enrichment analysis using the Hallmark gene sets confirmed enhanced IFN-signalling in responders (FDR<0.001, **Table S5**, **Figure S2B**). Comparison between patients exhibiting disease-control (DCR=OR+SD) and those with PD revealed a significant enrichment in *CD274* (PD-L1) expression in DCR patients, although no difference was observed in PD-L1 staining by immunohistochemistry, a discrepancy previously characterized[15]. Likewise, gene expression of *PDCD1LG2* (PD-L2), the alternative ligand to PD-1, was significantly higher in responders (p<0.01), whereas expression of its common receptor *PDCD1* (PD1) was markedly increased among patients with PD (p<0.05) (**Figure 2C**).

We next sought to correlate clinical response to anti-PD1 therapy with previously established molecular classes of HCC (**Figure 3A**) including the recently characterized HCC *Inflamed class*[16], which further refines our previously published *Immune class* of HCC[17]. The inflamed class entails three subtypes, named *Active, Exhausted, Immune-like* that all share a microenvironment with increased interferon-signalling. Interestingly, patients belonging to the HCC *Inflamed class* showed a higher rate of OR compared to the other classes *Intermediate* and *Excluded* (7/9, vs 5/19, p=0.01), whereas differences

in PFS showed a non-significant trend (p=0.068, **Figure S2C**). Patients with an aggressive and proliferative HCC phenotype (classes *S1* and *S2)* had markedly longer PFS when treated with anti-PD1 compared to the rest (p=0.017, **Figure S2D**). Next, we evaluated previously reported signatures and biomarkers of response to anti-PD1 therapy in our dataset (**Table S6**). Interestingly, we observed that several signatures such as the *IFN signature*[18], *POPLAR*[19] and the *Inflammatory signature*[20] were significantly enriched in HCC responding patients (p<0.01, p<0.01, p<0.05, respectively, **Figure 3B).** In terms of outcome, both *IFN-* and the *Inflammatory signature* were associated with longer PFS (p=0.023 for both, **Figure 3C,D**) whereas no differences were observed for *POPLAR* or the *cytolytic activity* signature (**Figure 3E,F**). However, none of the signatures was able to predict significantly longer OS (**Figure 3G-J**). A summary of the performance of these signatures is provided in **Table S7**. When considering histological markers such as the richness of the immune infiltrate, Tertiary lymphoid structures signature[21] and PD-L1 expression as well as tumor mutational burden inferred through a gene signature[22] no positive correlation with response to ICIs was observed (**Figure S3A,C).**

A novel 11-genes signature accurately predicts response to anti-PD1

Given the paucity of studies identifying candidate biomarkers for anti-PD1 in HCC and that none of the previously reported signatures was able to predict both PFS and OS, we then developed a gene expression signature capable of discriminating responding from non-responding patients (see supplementary methods). The resulting 11-gene set, hereafter named *IFNAP-signature* (Interferon and antigen-presentation, **Table S8**), comprises genes involved in IFN-γ signalling (*STAT1, GBP1*), antigen presentation (*B2M, HLA-DRB5, HLA-DRA*) and chemotaxis (*CXCL9*, **Figure 4A**). Most of these genes were not shared with other published immune response signatures (**Figure S4B)** underscoring the unique composition of IFNAP. The IFN signature and IFNAP shared three individual genes, all of which were predictive of OR and PFS. Likewise, the non-overlapping genes in IFNAP were linked with OR and PFS, whereas the remaining genes in the IFN signature where not (**Figure S5A-C**). Patients with high expression of IFNAP (n=9, defined as those within the upper tertile, see supplementary methods) had superior outcomes both with

regards to PFS (p=0.035) and OS (p=0.039, **Figure 4B,C**). ROC analysis indeed revealed IFNAP as the most efficient geneset at discriminating responding from non-responding patients with an AUC of 0.87 (**Figure 4D**).

We next sought to investigate the robustness of the IFNAP signature by testing its stability across different regions within a given tumor to investigate whether intratumoral heterogeneity, which may cause differences in regional adaptive immune responses, may compromise the reproducibility of signature expression. For this purpose we re-analyzed a cohort published by our group including 30 HCC samples from 15 patients with tumors >4cm[23], we found expression between two distinct regions of the same tumor to be very stable and 90% of cases had the same expression category (low/high) in both samples. Indeed, correlation of IFNAP between two regions of a given tumor was significant (R=0.77, p<0.001, **Figure S4C**).

We tested IFNAP in four independent datasets (see supplementary methods) comprising 240 patients with either NSCLC[24, 25], HNSCC[24] or melanoma[24, 26, 27] treated with anti-PD1/anti-PD-L1. In the first dataset[24], patients with OR had significantly more often high IFNAP expression, which was, moreover, associated with longer mPFS (55% vs. 24.4%, p=0.017 and 6.9 vs. 2.8 months, p=0.039, respectively, **Figure 4E-H**). Likewise, in the second dataset[25] high IFNAP expression was associated with response and longer mPFS (75% vs. 15.8%, p=0.006 and 8.6 vs. 1.2 months, p=0.006, respectively, **Figure 4G-H**). In the third dataset[27], OR was again associated with high IFNAP expression, (42.5% vs. 27.4%, p=0.043, **Figure S6A**), which in turn predicted longer mPFS and mOS (13.3 vs. 3.2 months, p=0.011 and NR vs. 19.7 months, p=0.033, respectively, **Figure S6B,C**). Finally, IFNAP also predicted higher response (46.7% vs. 15.6%, p=0.039, **Figure S6M**) in the fourth dataset [26]. Of note, none of the previously published signatures consistently predicted response or PFS in any of the datasets (**Figure S6D-L,N-P** and **Figure S7A-F, I-L**) with the exception of the *IFN signature* in the Jung et al dataset (**Figure S7G-H**). In summary, the IFNAP signature was able to capture responders to anti-PD1 pre-treatment across cancer types and was associated with longer PFS and OS whereas none of the previously published signatures was capable of consistently eliciting the same significant differences. This is of note as several of these signatures were designed in tumors that

are investigated in the validation datasets[18, 19]. In these, patients were treated with anti-PD1 both in frontline as well as in second line. However, unlike in our cohort, none of the patients underwent TKI treatment prior to immunotherapy and most tissue samples were obtained directly prior to the initiation of anti-PD1 therapy.

Finally, we tested the ability of IFNAP to predict response and longer survival in a dataset of patients treated with either single-agent ICI (n=13, nivolumab) or combination treatment (nivolumab/ipilimumab or spartalizumab/sabatolimab, n=11)[28]. High expression of IFNAP assessed by nanostring was associated with significantly longer OS and a trend towards higher OR (**Figure S8A-B**) to nivolumab but not to combination treatment (**Figure S8C-D)** suggesting molecularly distinct mechanisms of response for the combination.

The IFNAP gene signature captures a unique immune microenvironment

Since the increased expression of IFN- and AP-related genes is not unequivocally associated with a specific cell type but can be conferred through both tumoral and immune cells, we next characterized the immune infiltration in patients with high IFNAP expression. Strikingly, patients with high and low IFNAP expression were not different in terms of actual immune cell infiltration quantified on H&E stained slides (see methods) both in the intratumoral area and at the invasive margin (**Figure 5A**). We next hypothesized that the microenvironmental composition rather than overall infiltration may drive response to anti-PD1 in HCC. Thus, we performed virtual microdissection using CIBERSORTx[29] and found a significant upregulation of plasma cells, CD4-memory activated Tcells and M1 macrophages in patients with high expression of IFNAP (**Figures 5B, S9**). Conversely, patients with low IFNAP showed a significant increase in the infiltration of immunosuppressive regulatory Tcells (Tregs, p=0.001). Indeed, expression of IFNAP showed a negative correlation with expression of Tregs and of Forkhead-Box-Protein P3 (*FOXP3*, **Figure 5C**), a transcription factor active in Tregs which has been previously implicated in driving immunosuppression across cancer types and is linked with hyperprogression after anti-PD1[30]. In our dataset, low expression of Tregs or IFNAP, defined by the 1st tertile, was associated with markedly lower PFS (4.9 vs. NR and 3.6 vs. 28.8 months, p=0.012 and p<0.001, respectively, data not shown). We also considered

other features associated with primary resistance to anti-PD1 and found significant negative correlations between IFNAP and *PDCD1* expression (**Figure 5C**). Interestingly, all these markers of immunosuppression were highly correlated with each other and were negatively correlated to all genes of the IFNAP signature (Pearson correlation, **Figure 5D**). Overall, these data indicate that immunosuppressive expression programs predict poor outcome after anti-PD1 therapy. The presence of Tregs in the microenvironment may be one of the key factors eventually driving resistance while the other factors could represent downstream effects of this microenvironmental composition.

CTNNB1 mutational status is not a dominant feature to predict resistance to anti-PD1 therapy

Mutations in the WNT-CTNNB1 pathway have been implicated in driving resistance in a murine model of HCC[31]. We then investigated whether the presence of *CTNNB1* mutations was able to predict primary resistance to anti-PD1. To this end, we correlated treatment response with tumoral mutational status in 23 cases of frontline-treated patients. We found 4 of 11 responders (36%) and 6 out of 12 non-responders (50%) to have mutations in exon 3 of *CTNNB1*, the dominant hotspot, thereby showing no significant differences in response rates (**Figure 5E**). We considered that patients with *CTNNB1* exhibited less durable responses than non-mutated patients but no differences were observed in PFS and OS. Likewise, no difference in PFS and OS was seen among non-responding patients based on mutational status (**Figure S10**). Next, we compared the gene expression profile of *CTNNB1* mutated patients that exhibited response (n=4) to those patients with mutations that did not (n=6). We observed a trend towards increased inflammatory signalling as captured by the cytolytic activity gene signature[32] in those patients with mutations that responded. Moreover, the same patient subset demonstrated an upregulation in genes associated with an active immune response (*GZMA, CXCL9*; one-sided $p<0.05$).

In summary, *CTNNB1* mutational status did not predict resistance to therapy. A trend towards more inflammatory signalling in responders despite the presence of mutations hints at a more intricate role of *CTNNB1* in this scenario. While previous studies have

shown discrepancies in terms of the role of *CTNNB1* as a driver of immune exclusion[31, 33, 34], our findings provide an explanation to reconcile these inconsistencies. Indeed, our data suggest that patients with *CTNNB1*-driven immune exclusion may be prone to resistance. However, in tumors where this profile is overcome by unknown mechanisms to establish an inflamed microenvironment, the conducive effects of IFN-signaling and the intact antigen-presenting machinery may outweigh the impact of *CTNNB1* mutations.

Prior treatment with TKIs may influence response to subsequent anti-PD1 in 2nd line

Overall, 55 patients underwent anti-PD1 treatment as 2nd (41 cases) or 3rd line (14 cases) therapy after previous exposure to TKIs (54 sorafenib, 1 lenvatinib, **Table S9**). In all but two of these cases, though, histology was obtained prior to first line therapy. Overall, the ORR was 23.6%, and as in frontline treated patients, responders had both markedly longer OS and PFS (p=0.047 and p<0.0001, respectively, **Figure 6A-B**). In this setting, neither IFNAP (n=18 patients in 2nd/3rd line) nor other previously reported signatures were significantly enriched among patients with OR (**Figure 6C, S11A,D,G,J**). This translated to clinical outcome, where no differences were observed between patients with high and low expression of these signatures (**Figure S11B,C,E,F,H,I,K,L**). Likewise, histological severity of the immune infiltrate and inferred presence of Tertiary lymphoid structures signature[21] and high tumor mutational burden (TMB) were not linked to response in patients treated with anti-PD1 in 2nd line either (**Figure S3B,C**).

We thus considered that TKIs may impact the success of subsequent anti-PD1 therapy in a way that renders some tumors that would be expected to respond to anti-PD1 in frontline no longer responsive after prior TKI therapy. Conversely, a subset of tumors that would be expected to exhibit resistance to anti-PD1 when treated in frontline did respond when pretreated with TKIs. In an exploratory analysis, we investigated factors that may guide whether or not TKI therapy is conducive for subsequent anti-PD1 treatment. Patients with low inflammatory signaling and resistance to therapy (IFNAP low NR) showed an upregulation in metabolic signaling pathways compared with patients with low inflammatory signaling that did respond (IFNAP low OR, **Figure S12B**) and retained the

significant enrichment in Tregs infiltration by CIBERSORTx (**Figure S12C**). Conversely, patients with low IFNAP expression and response showed a marked increase in CD4 naïve T cell infiltration. Overall, this data suggested that severe infiltration of regulatory T cells may impede anti-PD1-mediated anti-tumoral immunity even after TKI therapy, as this feature was maintained both in frontline and 2nd/3rd line treated patients. Indeed, markedly worse PFS was observed in the top 20% of patients that harboured the highest infiltration in Tregs in both frontline and 2nd/3rd line (**Figure 6C, D-E**). This same subset of patients presented a significant enrichment in the expression of *SOCS1* and *SOCS3*, key antagonists of JAK/STAT signaling and thus inhibitors of the intracellular IFN-response pathway (**Figure 6C**). In keeping with this, the same subset featured significant downregulation in key genes involved in IFN-signaling and an active antigen presenting machinery.

In the absence of human datasets featuring serial biopsies to investigate the distinct effect of TKIs on the tumoral microenviroment, we explored a recently published murine model in which HCC-bearing mice were treated with either lenvatinib or placebo (**Figure S12D**, see supplementary methods). Comparative gene expression analysis of mice treated with Lenvatinib for two weeks revealed a significant enrichment in inflammatory signaling by TKIs as captured by higher expression of IFNAP and the IFN signatures (**Figure S12E**). Cellular subsets, such as CD4 effector memory cells, that we linked to response to anti-PD1, were, likewise, upregulated after Lenvatinib treatment. Overall this data suggests that TKIs may modulate response to anti-PD1 by altering microenvironmental signalling.

Overall, our findings suggest that fresh tissue should be obtained directly prior to the initiation of a given treatment to enable precision oncology as prior lines of systemic therapy compromise the readout quality of biomarkers. Our data indicates a patient subset, characterized through severe Treg infiltration and overexpression of immune-evasion related genes that is linked to poor outcomes when treated with anti-PD1 both in frontline as well as in 2nd/3rd line.

DISCUSSION

The present study represents a comprehensive characterization of the molecular patterns associated with response and resistance in patients with advanced HCC treated with anti-PD1. Herein, we identified IFN-signalling and AP-related genes to be associated with OR whereas presence of Tregs and pathways associated with immunosuppression are linked to resistance. We developed an 11-gene expression signature capable of predicting response to anti-PD1 in HCC and other solid cancer types when treated with anti-PD1 in the frontline setting. When testing the signature in samples from patients pre-treated with TKIs, we found that neither our signature nor previously reported inflammatory markers predict outcomes to 2nd or 3rd line anti-PD1 therapy suggesting that prior lines of therapy may impact the efficacy of subsequent anti-PD1.

In recent years, several predictive biomarkers of response and resistance to systemic therapies have entered the clinical space. Regarding anti-PD1 therapy, the only FDA-approved biomarkers are high TMB and microsatellite-instability across cancer types. The benefit conveyed by these biomarkers is limited in magnitude (<3% of HCCs) underscoring the need for more refined testing. Earlier studies in melanoma and lung cancer have observed an increase in T-cell infiltration in the tumor microenvironment and enrichment of IFNγ-signalling in patients responding to anti-PD1 therapy[18, 19]. While this observation has been consistently confirmed in early on-treatment samples collected 2-4 weeks after therapy start[35], results in samples collected before the initiation of therapy are conflicting[26].

Among the most relevant findings of our study, we identified a gene expression signature – IFNAP – that predicts response and survival to frontline anti-PD1 in aHCC. Notably, it outperformed previously published signatures of response and was the only one to predict significant increases in ORR, OS and PFS in our dataset as well as in an aHCC validation cohort and four expression datasets from other solid cancer types across different platforms (Nanostring, microarray, RNA-seq). IFNAP identified responders independent of the etiology of the underlying liver disease, where 4/5 responders without viral hepatitis had high expression of the signature. This is particularly relevant in light of a recently published report that draws the efficacy of anti-PD1 therapy in patients with NASH into question[36]. The composition of IFNAP reflects key biological pathways involved in T-cell

directed therapies: (i) Interferon-signalling and (ii) antigen-presentation, which are readouts of nascent cancer cell immunogenicity, that can be leveraged through immunotherapy[18]. IFNAP includes genes such as *B2M*, whose loss of heterozygosity has been implicated as a mechanism of resistance to anti-PD1[37], and *CXCL9* as well *HLA-DRA* that have been linked to response in melanoma[18]. In our dataset, analysis of the immune infiltrate suggested that the composition rather than overall infiltrate might drive response to immunotherapy. Specifically, CD4+ naïve Tcells were consistently upregulated in patients with high IFNAP expression, whereas Treg infiltration was negatively correlated with IFNAP. The presence of immunosuppressive Tregs and their active transcription factor *FOXP3* may in this regard be an impediment towards initiating antitumoral immunity. A recent biomarker analysis of HCC patients treated with atezolizumab and bevacizumab in clinical trials identified that increased IFNy-signalling, active antigen-presentation and low Treg/Effector-T-cell ratio were linked to response. In addition, patients with high Treg infiltration experienced a significantly stronger benefit from combination compared to atezolizumab monotherapy, suggesting synchronous application of ICI with anti-angiogenics may help in overcoming severe Treg infiltration as a driver of resistance to ICI monotherapy[38].

Several investigations in melanoma have shown genetic alterations in the WNT-CTNNB1 pathway to be a tumor-intrinsic driver of immune exclusion and resistance to anti-PD1[39]. In HCC, a preclinical study suggested that *CTNNB1* mutations conveyed defective recruitment of dendritic cells and subsequently impaired cytotoxic T-cell function[31]. These effects were reverted upon overexpression of *CCL5*. One cohort study supported this correlation in patients that underwent biopsy prior to treatment[33], whereas another did not identify *CTNNB1* mutations in liquid biopsy impacting PFS[34]. Our results point towards the fact that *CTNNB1* mutations alone are not associated with resistance, although the underlying biological mechanisms remain elusive. Those patients with inflammatory signalling counterbalancing *CTNNB1*–related immunosuppression showed a trend to better OR, as opposed to those where *CTNNB1* mutations was the dominant molecular feature determining lack of response to anti-PD1. In the former cases, other signalling pathways such as IFN-signalling and an active antigen-presenting machinery may overcome *CTNNB1*-mediated immune exclusion and thus facilitate response.

Finally, the aforementioned differences in expression profiles between responding and non-responding patients were no longer evident in those patients receiving TKIs between sample acquisition and immunotherapy start. This finding could be due to the longer time elapsed between tissue acquisition and anti-PD1 treatment in the 2nd/3rd line when compared to the frontline which may increase the odds of molecular events contributing to immunosuppression, although this is unlikely given the relative stability of driver events during cancer evolution[40]. An alternative hypothesis would be that treatment with TKIs may influence how a patient responds to anti-PD1 therapy in subsequent treatment lines. In the absence of serial biopsies, the molecular mechanisms that guide the impact of TKIs on other treatments remain unknown and it is unclear as to whether an inflamed microenvironment pre-sorafenib remains inflamed thereafter or if the effect of the TKI may ameliorate inflammatory signalling in these tumors.

Data from murine model suggests[41, 42] that TKIs may overall increase inflammatory signalling within the tumor and induce a shift in the composition of the microenvironment. However, it needs to be acknowledged that these models are not fully reflective of human disease course since the molecular analyses were performed on animals during TKI treatment while humans are generally not exposed to anti-PD1 before resistance to TKIs. As previous studies have shown that while sorafenib sensitive tumors display an increase in inflammatory signaling and an enhanced antigen-presentation apparatus, resistance in turn is associated with a less rich T cell infiltration and less overall inflammatory signaling within the tumor[42]. Likewise, a recent biomarker companion study for a phase I clinical trial aiming at converting locally advanced disease to resectable HCC through neoadjuvant cabozantinib and nivolumab confirmed heterogeneous expression of TKI targets and inflammatory markers based on response status[43].

Our data implies that responders in different treatment lines are different populations with some overlap. Conversely, we have identified a subset of patients that exhibit resistance to anti-PD1 regardless of whether treatment is administered in frontline or after exposure to TKIs. This subset was characterized through an increase in Treg infiltration and expression of genes that are direct inhibitors of active JAK/STAT signalling. Overall, our data opens up the enticing perspective that more HCC patients could respond to anti-

PD1 therapy through selective pre-treatment/or combination with TKIs, although some patients may not be suitable for anti-PD1 in any case. Our data ultimately calls for the need of biopsies prior to anti-PD1 treatment start to enable biomarker-based precision oncology regardless of treatment line.

Several limitations of this study need to be addressed: first, the distinction between therapy lines diminishes the sample size considerably and limits the power of the study despite recruitment from 13 international referral centers. The observed response rate of 43% in the first-line cohort is certainly above the expected 15-20% response rate and is a reflection of the inclusion criteria of a minimal duration of 2 months of treatment to evaluate response. While this naturally increases the proportion of responders, it also increases the power of our biomarker analysis. In addition, the use of mRECIST response criteria likely contributes a small further increase in the ORR. Second, the lack of serial biopsies between systemic treatments precludes a refined analysis on how precisely TKI therapy alters the microenvironment and impacts efficacy of subsequent immunotherapy. Finally, validation of IFNAP could only be performed in a comparatively small HCC dataset as well as cohorts with other cancer types. Therefore, validation of IFNAP in future larger HCC cohorts remains a critical unmet need particularly in light of the limited number of cases that were used for the construction of the signature.

In summary, our study defines the key molecular drivers of response to anti-PD1 in HCC. We generated and validated a signature recapitulating these pathways that predict response and longer survival in HCC and other cancer types and therefore has potential to maximize the efficiency of anti-PD1 application. The final value of this signature needs to be explored within phase III investigations. In patients treated with 2nd and 3rd line anti-PD1, prior TKI therapy likely impairs the predictive potential of the IFNAP signature, although further studies will be required to clarify the reasons for this observation.

REFERENCES

1. Llovet JM, Kelley RK, Villanueva A, et al. Hepatocellular carcinoma. Nat Rev Dis Primers 2021;7:6.

2. Llovet JM, Ricci S, Mazzaferro V, et al. Sorafenib in advanced hepatocellular carcinoma. N Engl J Med 2008;359:378-90.
3. Kudo M, Finn RS, Qin S, et al. Lenvatinib versus sorafenib in first-line treatment of patients with unresectable hepatocellular carcinoma: a randomised phase 3 non-inferiority trial. The Lancet 2018;391:1163-1173.
4. Finn RS, Qin S, Ikeda M, et al. IMbrave150: Updated overall survival (OS) data from a global, randomized, open-label phase III study of atezolizumab (atezo) + bevacizumab (bev) versus sorafenib (sor) in patients (pts) with unresectable hepatocellular carcinoma (HCC). Journal of Clinical Oncology 2021;39:267-267.
5. Finn RS, Qin S, Ikeda M, et al. Atezolizumab plus Bevacizumab in Unresectable Hepatocellular Carcinoma. N Engl J Med 2020;382:1894-1905.
6. Abou-Alfa Ghassan K, Lau G, Kudo M, et al. Tremelimumab plus Durvalumab in Unresectable Hepatocellular Carcinoma. NEJM Evidence;0:EVIDoa2100070.
7. **Kelley RK, Rimassa L**, Cheng A-L, et al. Cabozantinib plus atezolizumab versus sorafenib for advanced hepatocellular carcinoma (COSMIC-312): a multicentre, open-label, randomised, phase 3 trial. The Lancet Oncology.
8. Greten TF, Lai CW, Li G, et al. Targeted and Immune-Based Therapies for Hepatocellular Carcinoma. Gastroenterology 2019;156:510-524.
9. El-Khoueiry AB, Sangro B, Yau T, et al. Nivolumab in patients with advanced hepatocellular carcinoma (CheckMate 040): an open-label, non-comparative, phase 1/2 dose escalation and expansion trial. Lancet 2017;389:2492-2502.
10. Zhu AX, Finn RS, Edeline J, et al. Pembrolizumab in patients with advanced hepatocellular carcinoma previously treated with sorafenib (KEYNOTE-224): a non-randomised, open-label phase 2 trial. The Lancet Oncology 2018;19:940-952.
11. Yau T, Park JW, Finn RS, et al. CheckMate 459: A randomized, multi-center phase III study of nivolumab (NIVO) vs sorafenib (SOR) as first-line (1L) treatment in patients (pts) with advanced hepatocellular carcinoma (aHCC). Ann Oncol 2019;30 (suppl_5):v851-v934.
12. Finn RS, Ryoo BY, Merle P, et al. Pembrolizumab As Second-Line Therapy in Patients With Advanced Hepatocellular Carcinoma in KEYNOTE-240: A Randomized, Double-Blind, Phase III Trial. J Clin Oncol 2020;38:193-202.
13. Llovet JM, Lencioni R. mRECIST for HCC: Performance and novel refinements. J Hepatol 2020;72:288-306.
14. **Isomoto K, Haratani K**, Hayashi H, et al. Impact of EGFR-TKI Treatment on the Tumor Immune Microenvironment in EGFR Mutation-Positive Non-Small Cell Lung Cancer. Clin Cancer Res 2020;26:2037-2046.
15. Lee H-H, Wang Y-N, Xia W, et al. Removal of N-Linked Glycosylation Enhances PD-L1 Detection and Predicts Anti-PD-1/PD-L1 Therapeutic Efficacy. Cancer Cell 2019;36:168-178.e4.
16. **Montironi C, Castet F, Haber PK**, et al. Inflamed and non-inflamed classes of HCC: a revised immunogenomic classification. Gut 2022.
17. Sia D, Jiao Y, Martinez-Quetglas I, et al. Identification of an Immune-specific Class of Hepatocellular Carcinoma, Based on Molecular Features. Gastroenterology 2017;153:812-826.
18. Ayers M, Lunceford J, Nebozhyn M, et al. IFN-γ-related mRNA profile predicts clinical response to PD-1 blockade. J Clin Invest 2017;127:2930-2940.
19. Fehrenbacher L, Spira A, Ballinger M, et al. Atezolizumab versus docetaxel for patients with previously treated non-small-cell lung cancer (POPLAR): a multicentre, open-label, phase 2 randomised controlled trial. The Lancet 2016;387:1837-1846.

20. **Sangro B, Melero I,** Wadhawan S, et al. Association of inflammatory biomarkers with clinical outcomes in nivolumab-treated patients with advanced hepatocellular carcinoma. J Hepatol 2020;73:1460-1469.
21. Finkin S, Yuan D, Stein I, et al. Ectopic lymphoid structures function as microniches for tumor progenitor cells in hepatocellular carcinoma. Nat Immunol 2015;16:1235-44.
22. Tian S, Roepman P, Popovici V, et al. A robust genomic signature for the detection of colorectal cancer patients with microsatellite instability phenotype and high mutation frequency. J Pathol 2012;228:586-95.
23. **Torrecilla S, Sia D, Harrington AN**, et al. Trunk mutational events present minimal intra- and inter-tumoral heterogeneity in hepatocellular carcinoma. J Hepatol 2017;67:1222-1231.
24. Prat A, Navarro A, Paré L, et al. Immune-Related Gene Expression Profiling After PD-1 Blockade in Non–Small Cell Lung Carcinoma, Head and Neck Squamous Cell Carcinoma, and Melanoma. Cancer Research 2017;77:3540-3550.
25. **Jung H, Kim HS**, Kim JY, et al. DNA methylation loss promotes immune evasion of tumours with high mutation and copy number load. Nature Communications 2019;10:4278.
26. **Hugo W, Zaretsky JM**, Sun L, et al. Genomic and Transcriptomic Features of Response to Anti-PD-1 Therapy in Metastatic Melanoma. Cell 2016;165:35-44.
27. **Liu D, Schilling B**, Liu D, et al. Integrative molecular and clinical modeling of clinical outcomes to PD1 blockade in patients with metastatic melanoma. Nature Medicine 2019;25:1916-1927.
28. Hsu CL, Ou DL, Bai LY, et al. Exploring Markers of Exhausted CD8 T Cells to Predict Response to Immune Checkpoint Inhibitor Therapy for Hepatocellular Carcinoma. Liver Cancer 2021;10:346-359.
29. Newman AM, Steen CB, Liu CL, et al. Determining cell type abundance and expression from bulk tissues with digital cytometry. Nature Biotechnology 2019;37:773-782.
30. Kamada T, Togashi Y, Tay C, et al. PD-1⁺ regulatory T cells amplified by PD-1 blockade promote hyperprogression of cancer. Proceedings of the National Academy of Sciences 2019;116:9999.
31. Ruiz de Galarreta M, Bresnahan E, Molina-Sánchez P, et al. β-Catenin Activation Promotes Immune Escape and Resistance to Anti-PD-1 Therapy in Hepatocellular Carcinoma. Cancer Discov 2019;9:1124-1141.
32. Rooney MS, Shukla SA, Wu CJ, et al. Molecular and genetic properties of tumors associated with local immune cytolytic activity. Cell 2015;160:48-61.
33. Harding JJ, Nandakumar S, Armenia J, et al. Prospective Genotyping of Hepatocellular Carcinoma: Clinical Implications of Next-Generation Sequencing for Matching Patients to Targeted and Immune Therapies. Clin Cancer Res 2019;25:2116-2126.
34. von Felden J, Craig AJ, Garcia-Lezana T, et al. Mutations in circulating tumor DNA predict primary resistance to systemic therapies in advanced hepatocellular carcinoma. Oncogene 2021;40:140-151.
35. **Chen P-L, Roh W**, Reuben A, et al. Analysis of Immune Signatures in Longitudinal Tumor Samples Yields Insight into Biomarkers of Response and Mechanisms of Resistance to Immune Checkpoint Blockade. Cancer Discovery 2016;6:827-837.
36. Pfister D, Núñez NG, Pinyol R, et al. NASH limits anti-tumour surveillance in immunotherapy-treated HCC. Nature 2021.
37. **Sade-Feldman M, Jiao YJ**, Chen JH, et al. Resistance to checkpoint blockade therapy through inactivation of antigen presentation. Nature Communications 2017;8:1136.
38. Zhu AX, Abbas AR, de Galarreta MR, et al. Molecular correlates of clinical response and resistance to atezolizumab in combination with bevacizumab in advanced hepatocellular carcinoma. Nature Medicine 2022;28:1599-1611.

39. Spranger S, Bao R, Gajewski TF. Melanoma-intrinsic β-catenin signalling prevents anti-tumour immunity. Nature 2015;523:231-235.
40. van de Haar J, Hoes LR, Roepman P, et al. Limited evolution of the actionable metastatic cancer genome under therapeutic pressure. Nature Medicine 2021;27:1553-1563.
41. Torrens L, Montironi C, Puigvehí M, et al. Immunomodulatory Effects of Lenvatinib Plus Anti-Programmed Cell Death Protein 1 in Mice and Rationale for Patient Enrichment in Hepatocellular Carcinoma. Hepatology 2021.
42. Tovar V, Cornella H, Moeini A, et al. Tumour initiating cells and IGF/FGF signalling contribute to sorafenib resistance in hepatocellular carcinoma. Gut 2017;66:530-540.
43. **Ho WJ, Zhu Q**, Durham J, et al. Neoadjuvant Cabozantinib and Nivolumab Converts Locally Advanced HCC into Resectable Disease with Enhanced Antitumor Immunity. Nat Cancer 2021;2:891-903.

Table 1

	All (n = 83)	Objective response (n = 25)	Stable disease (n = 21)	Progressive disease (n = 37)	p
Median age (range)	66 (22-86)	65 (29-86)	63 (22-79)	66 (28-83)	0.79
Gender, male (%)	65 (77.1)	21 (84.0)	17 (81.0)	26 (70.3)	0.4
Etiology (%)					
HBV	16 (19.3)	8 (32.0)	3 (14.3)	5 (13.5)	0.16
HCV	24 (28.9)	6 (24.0)	7 (33.3)	11 (29.7)	0.78
NASH	13 (15.7)	5 (20.0)	4 (19.0)	4 (10.8)	0.79
Other Uninfected	31 (37.3)	7 (28.0)	7 (33.3)	17 (45.9)	0.323
Child Pugh Score (%)*					0.45
A	72 (88.9)	20 (83.3)	20 (95.2)	32 (88.9)	
B	9 (11.1)	4 (16.7)	1 (4.8)	4 (11.1)	
Fibrosis F3/F4	25 (48.1)	10 (55.6)	7 (50.0)	8 (40.0)	0.62
Platelets <100,000 / mm3 (%)* **	17 (21.3)	4 (16.7)	6 (28.6)	7 (20.0)	0.61
BCLC stage (%)					0.35
Intermediate (B)	17 (20.5)	3 (12.0)	4 (19.0)	10 (27.0)	
Advanced (C)	66 (79.5)	22 (88.0)	17 (81.0)	28 (73.0)	
Macrovascular invasion (%)#	23 (28.0)	10 (40.0)	6 (28.6)	7 (19.4)	0.21
Extrahepatic disease (%)	53 (63.9)	17 (68.0)	14 (66.7)	22 (59.5)	0.75
Sample origin (%)					0.12
Primary tumor	73 (88.0)	22 (88.0)	16 (76.2)	35 (94.6)	
Metastasis	10 (12.0)	3 (12.0)	5 (23.8)	2 (5.4)	
Specimen type (%)					0.61
Resection	49 (59.0)	14 (56.0)	11 (52.4)	24 (64.9)	
Biopsy	34 (41.0)	11 (44.0)	10 (47.6)	13 (35.1)	
AFP (ng/ml) > 200 (%)#	30 (36.6)	7 (28.0)	10 (47.6)	13 (36.1)	0.39
Anti-PD1 drug (%)					0.67
Nivolumab	67 (80.7)	19 (76.0)	16 (76.2)	32 (86.5)	
Pembrolizumab	14 (16.9)	5 (20.0)	4 (19.0)	5 (13.5)	
Tislelizumab	2 (2.4)	1 (4.0)	1 (4.8)	0 (0)	
Median time on therapy in month (range)	4.9 (0.47-45.4)	18.2 (3.1-45.4)	4.9 (0.5-25.7)	2.3 (0.47-33.6)	<0.001
Events					
Deceased	32 (38.6)	3 (12.0)	10 (47.6)	19 (51.4)	<0.01
Progression	58 (69.9)	8 (32.0)	14 (66.7)	37 (100)	<0.001
Median time to response in months (range) ##		3 (1.7-12.8)			

*BCLC – Barcelona clinic liver cancer; AFP – Alpha fetoprotein; *Data missing from 2 cases; **Data missing from 31 cases;***Data missing from 3 cases; #Data missing from one case; ##Data missing from 7 cases*

FIGURE LEGENDS

Figure 1. Cohort overview and outcomes. (A) Study flowchart: Of the 111 samples collected for this study, 83 cases, treated with anti-PD1 in either frontline or after exposure to TKIs were eventually included in the transcriptomic analysis. (B) Alluvial plot showing response patterns based on treatment line. The numbers in the boxes represent the number of patients with that specific response (C,D) Kaplan-Meier (KM) estimates of all patients included in the transcriptomic analysis are shown for OS (C) and PFS (D) based on whether patients exhibited objective response (OR), stable disease (SD) or progressive disease (PD). P values in KM curves represent log-rank tests.

Figure 2. Upregulation of inflammation and antigen-presentation associated genes in responders. (A,B) KM estimates for OS (A) and (PFS) for all 28 patients treated with anti-PD1 in frontline based on whether patients exhibited OR or non-response (NR). (C) Heatmap of gene expression analysis based on observed response types. Each signature or individual gene is significantly upregulated in one response subgroup relative to the others, whereas no differences were observed regarding PD-L1 by IHC. (D) Volcano plot showing differentially expressed genes in responders compared to non-responders. Genes differentially expressed at $p<0.05$ are depicted in red, all others in orange. (E) GeneOntology gene set enrichment analysis of differentially expressed genes using the *biological processes* classification. P values in KM curves represent log-rank tests.

Figure 3. Association of previously reported gene signatures and HCC molecular classes with response and resistance to anti-PD1. (A) Circular classification plot integrating response types with molecular classes of HCC. Each sector represents one patient. Significant enrichment of the *S1/2* classes and the *Inflamed HCC* subgroup is observed in responders. (B) Boxplot comparison for the expression of previously reported gene signatures based on observed response. (C-J) KM estimates for PFS (C-F) and OS (G-J) based on expression of previously reported signatures. P values in boxplot comparison represents Mann-Whitney test, while those in the KM curves represent log-rank tests.

Figure 4. Generation and validation of expression signature associated with response. (a) Heatmap of genes incorporated in the IFNAP signature. (B,C) KM

estimates for PFS (B) and OS (C) are shown based on expression of IFNAP. (D) Receiver operating characteristic (ROC) curve is shown for IFNAP and previously characterized signatures of response. (E-F) Validation of IFNAP in two independent datasets of anti-PD1/anti-PDL1 treated patients with melanoma, non-small cell lung cancer (NSCLC) and head and neck squamous cell cancer (E,G) and NSCLC (F,H), respectively. Patients with response showed marked enrichment in IFNAP (E,F) which was associated with longer PFS (G,H). P values for KM analysis derive from log-rank test whereas those in the barplots represent 2-sided Chi^2 test.

Figure 5. Characterization of IFNAP and correlates of resistance to anti-PD1. (A) Histological assessment of the immune infiltrate, applying a previously characterized semi-quantitative score[17], in the intratumoral compartment and at the invasive margin. (B) Boxplot representation of virtual-microdissection with CIBERSORTx based on IFNAP expression. (C) Correlation of IFNAP expression with previously characterized resistance markers. (D) Correlation heatmap with unsupervised clustering of factors associated with response and resistance to anti-PD1 therapy. (E) Heatmap of patients treated in frontline with anti-PD1 ordered by response and CTNNB1 mutational status. No differences in response rates were observed, while a trend towards increased inflammatory signaling in responders with CTNNB1 mutations compared to non-responders with mutations was noted. P values in boxplot comparison represents Mann-Whitney test, while those in the correlation plots represent Pearson tests.

Figure 6. TKI therapy compromises predictive potential of response-signatures. (A-B) Kaplan-Meier estimates for PFS and OS in patients treated with anti-PD1 in 2^{nd}/3^{rd} line. (C) Heatmap of patients treated with anti-PD1 in 2^{nd} and 3^{rd} line highlights inability of previously characterized markers to capture responders to anti-PD1 after TKI therapy. (D-E) Forest plots showing log Hazard ratios from a Cox regression model for PFS defines high infiltration of Tregs (Top 20%) as a poor prognostic marker in patients treated with anti-PD1 both in frontline (D) and after exposure to TKIs (E). P values in KM curves represent a log-rank test.

Figure 1

A

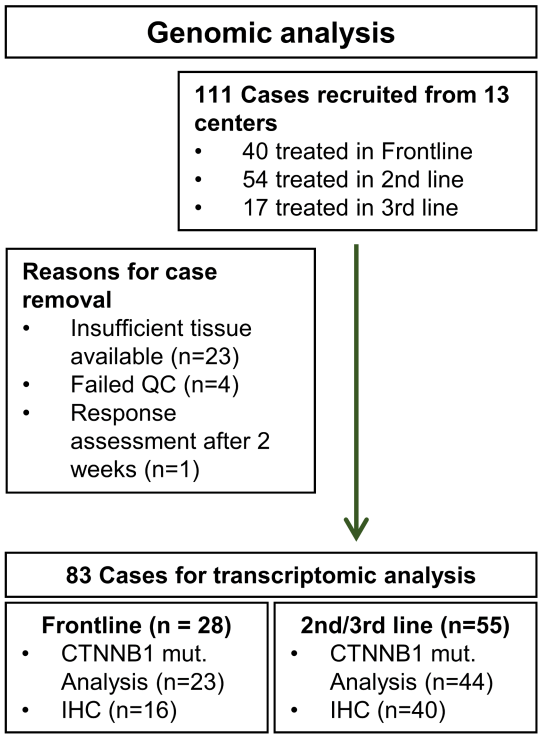

B

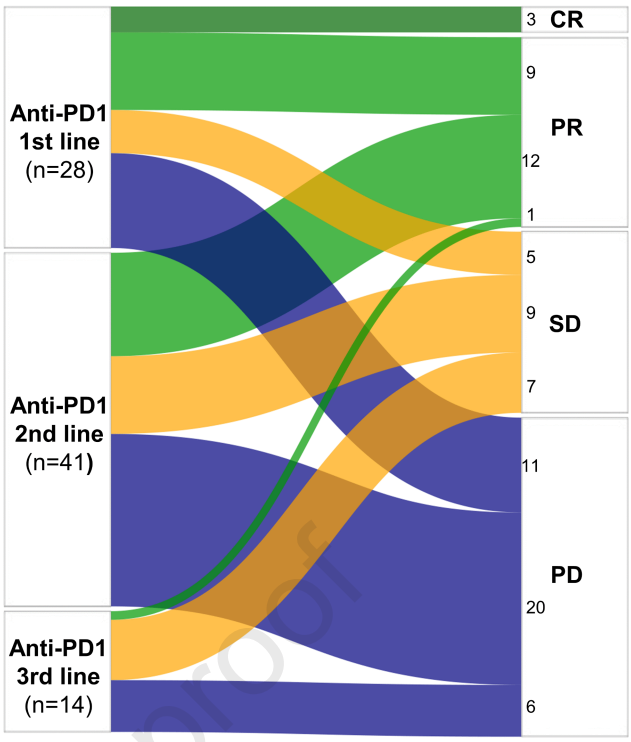

C

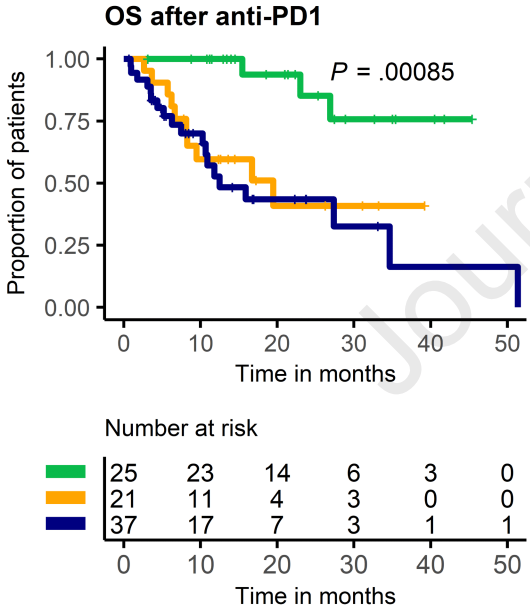

D

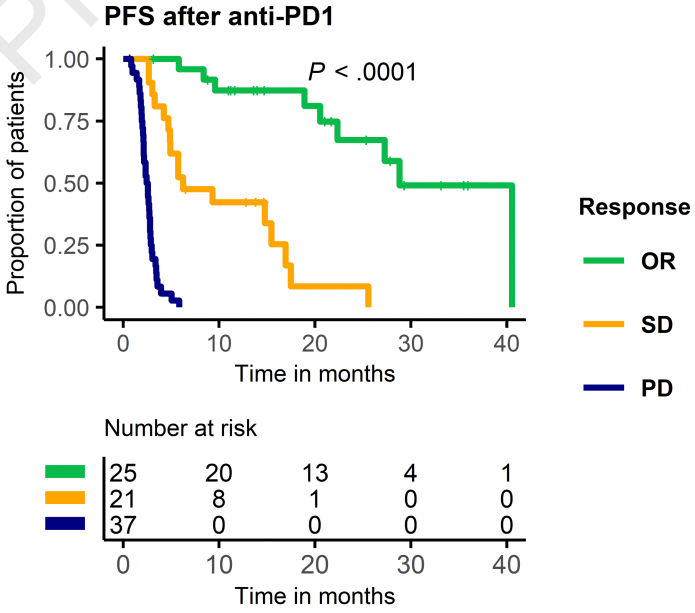

Figure 2

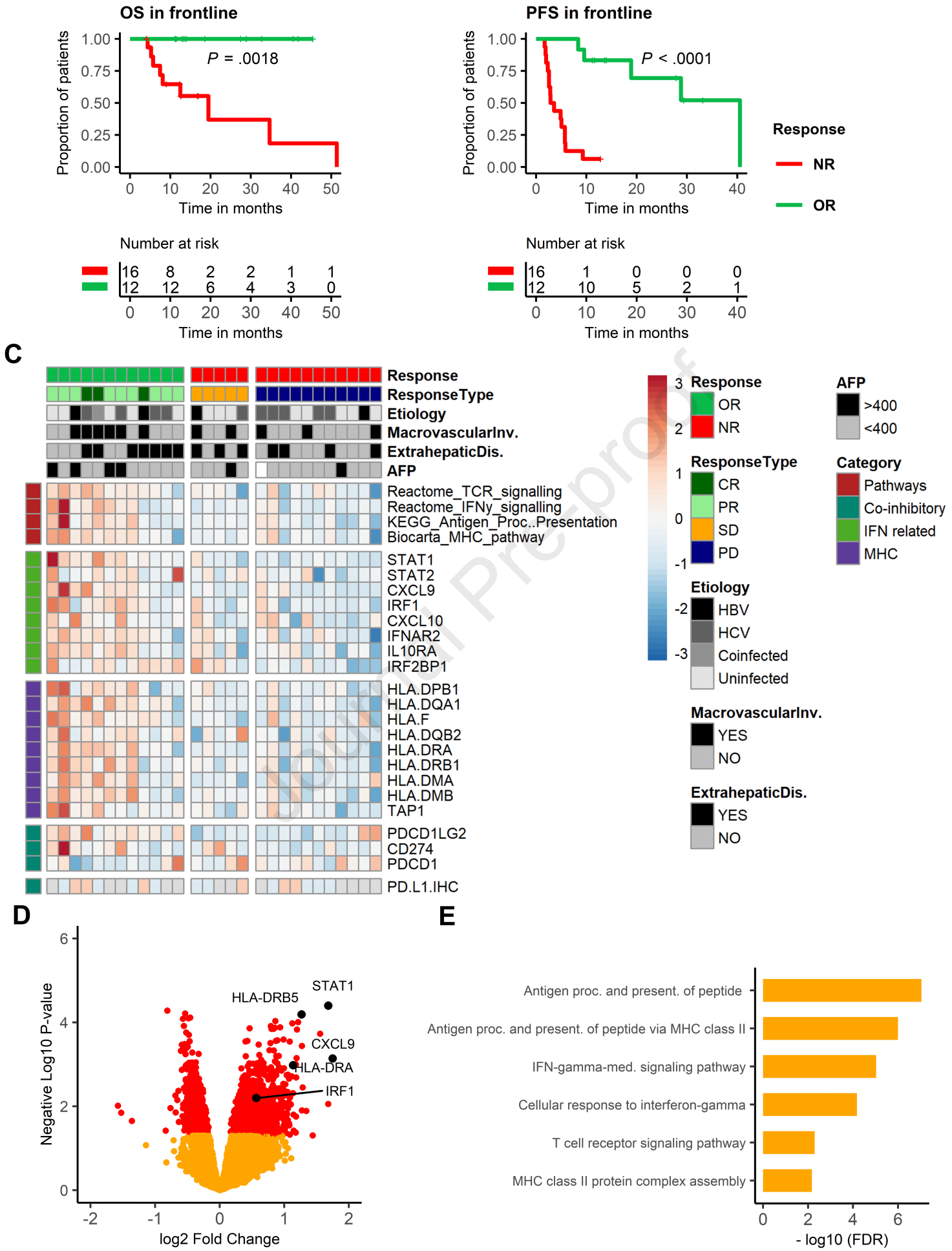

Figure 3

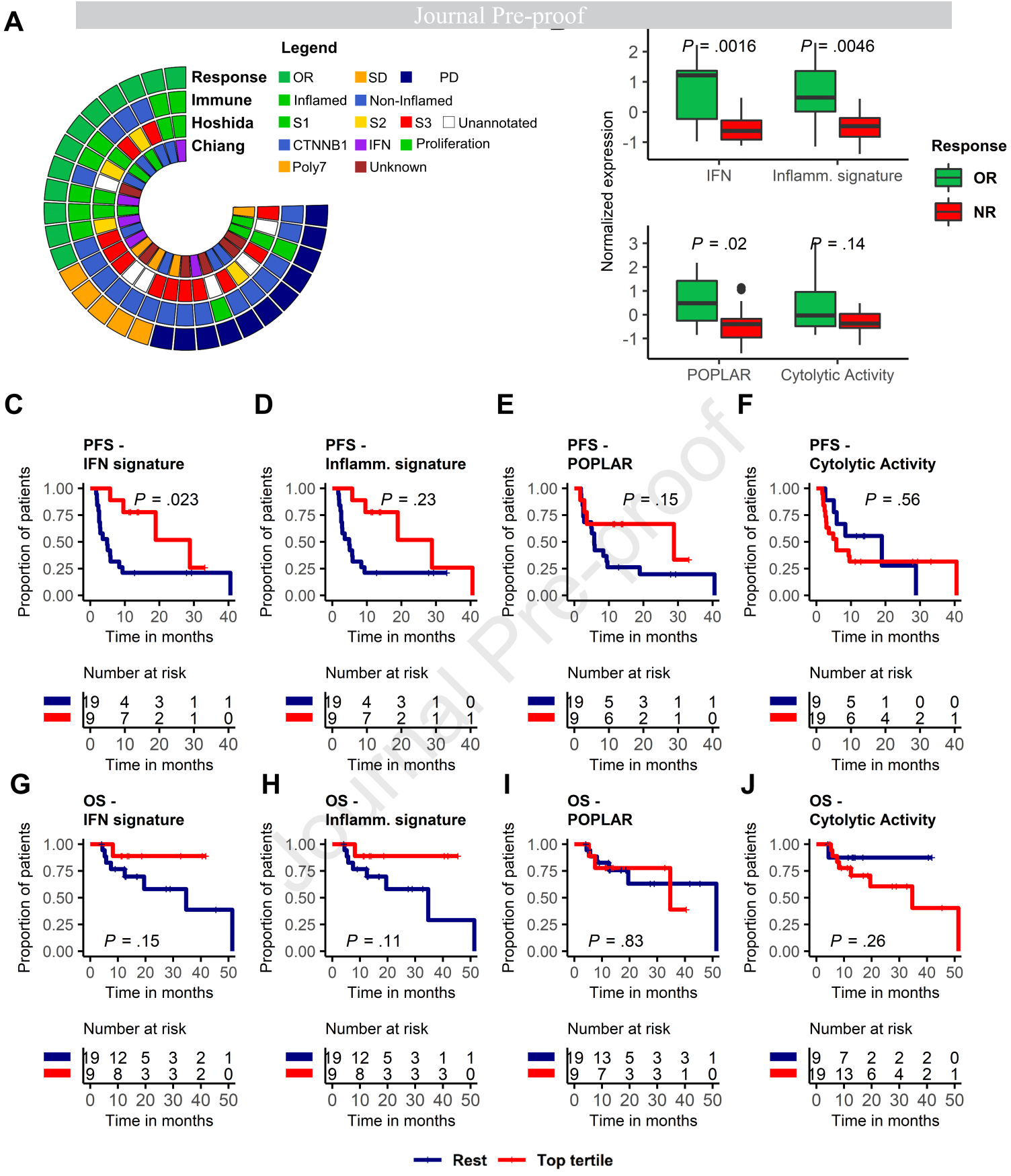

Figure 4

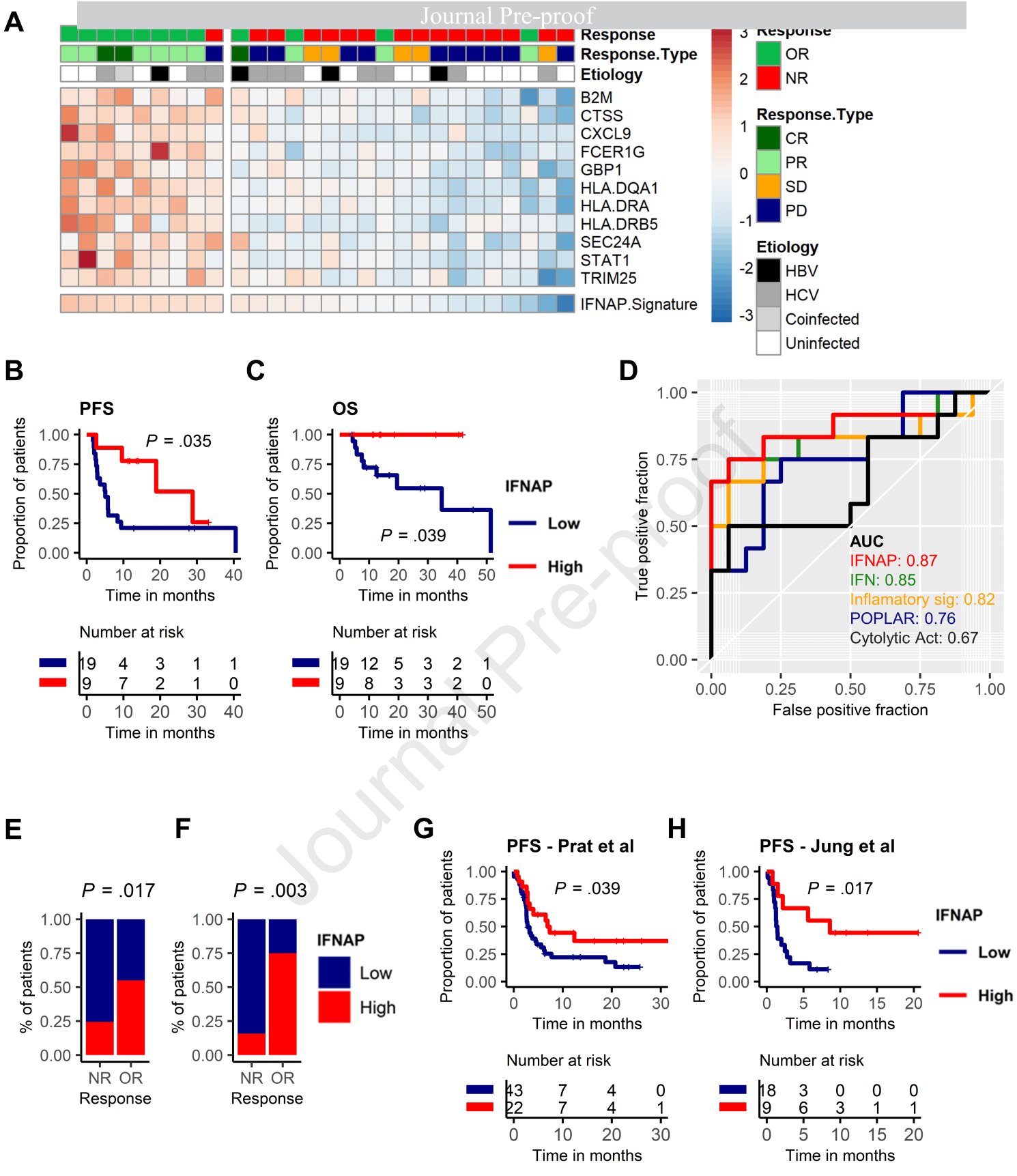

Figure 5

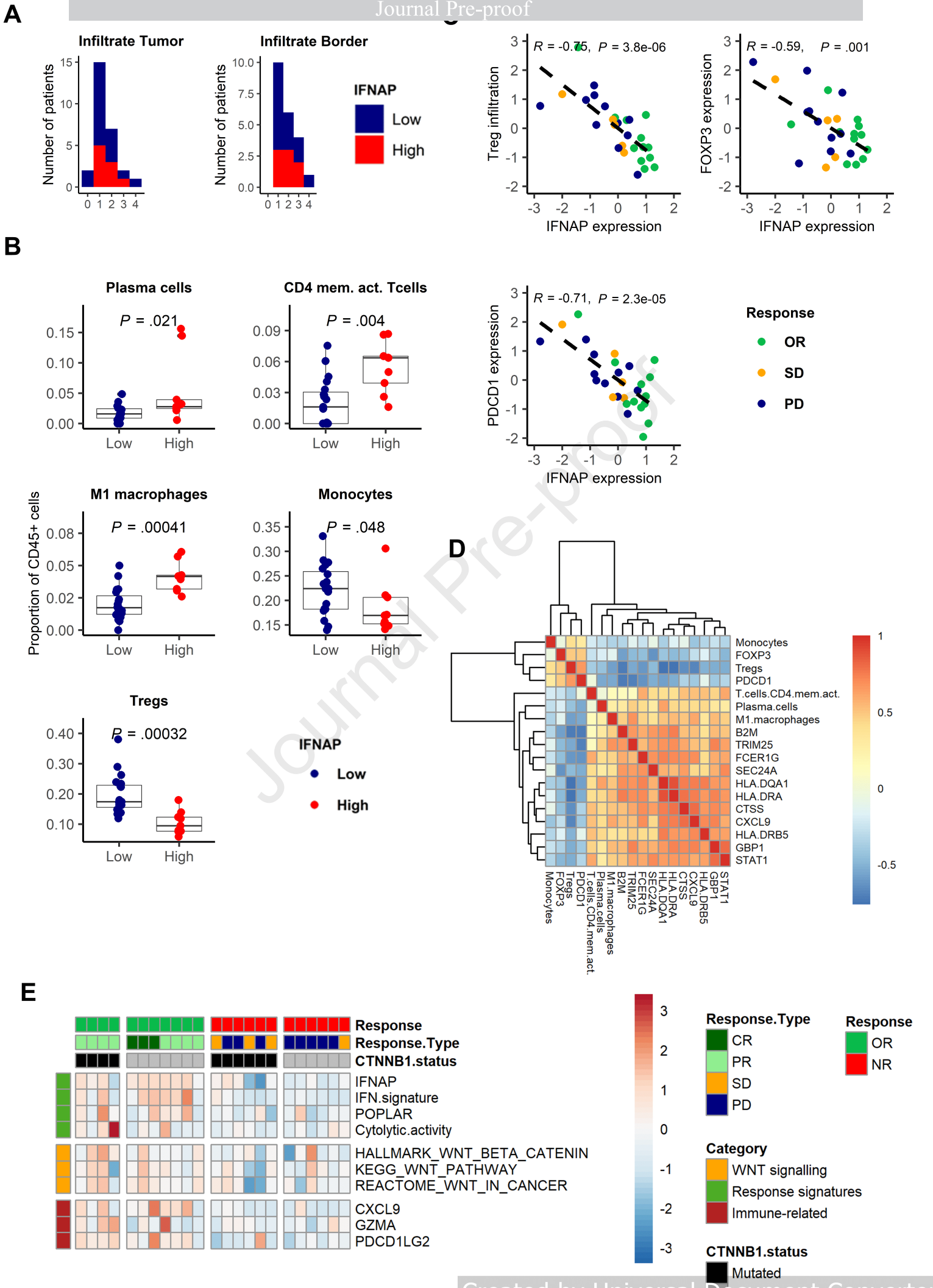

Figure 6

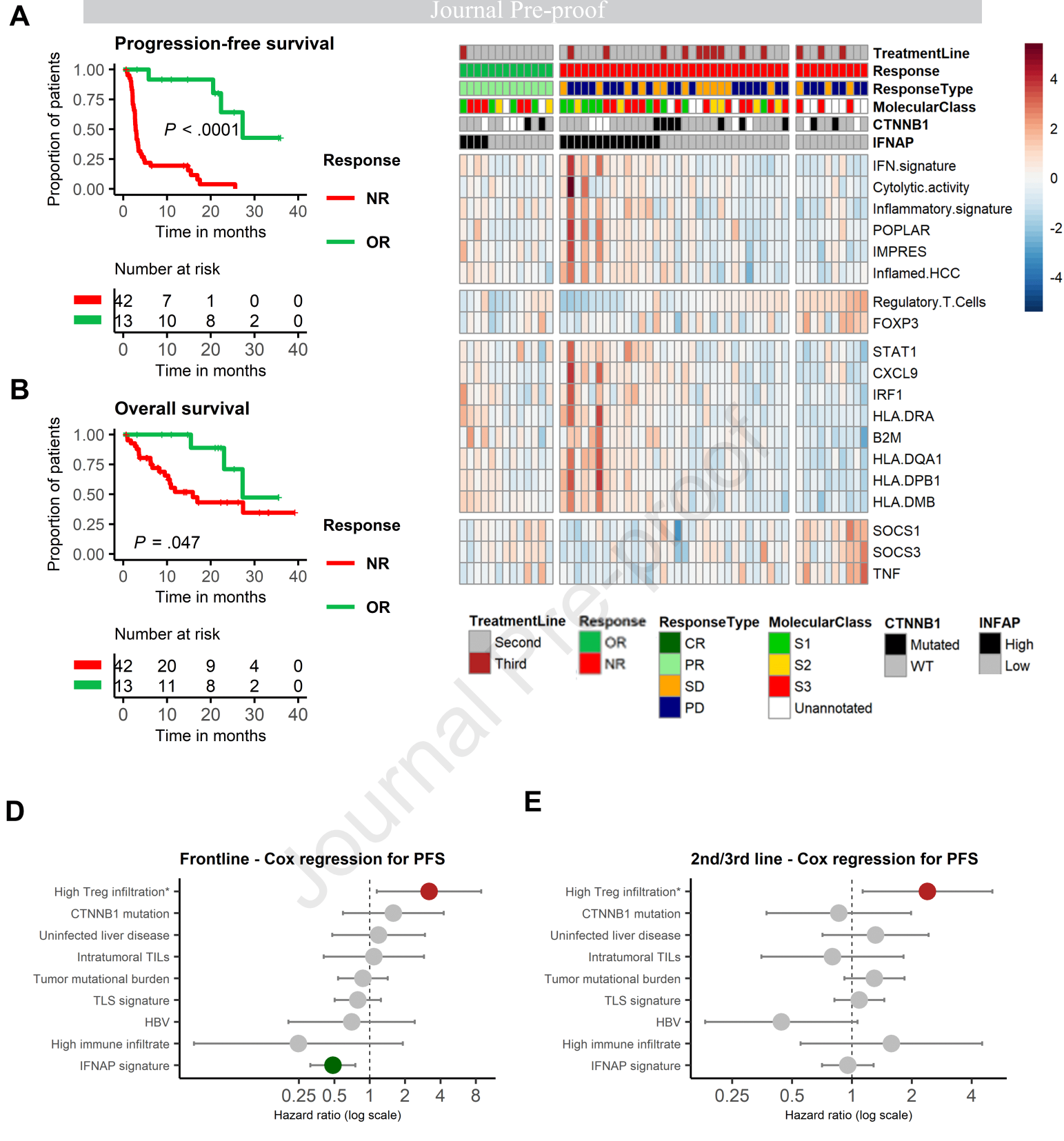

Lay summary

Here, we define the molecular factors associated with response to frontline anti-PD1 in advanced HCC and develop a predictive signature, IFNAP, that can maximize the effectiveness of anti-PD1 in HCC.

What you need to know

BACKGROUND AND CONTEXT:

Only 15-20% of patients with advanced HCC patients treated with anti-PD1 exhibit a strong benefit but an understanding of the molecular underpinnings that would enable precision oncology is still amiss.

NEW FINDINGS

We develop a tissue-based genomic tool to predict response in patients treated with anti-PD1 in frontline. Treatment with tyrosine-kinase-inhibitors between tissue acquisition and anti-PD1 compromises the predictive ability of this marker.

LIMITATIONS

Due to the absence of serial biopsies, an understanding of how TKIs reshape the tumoral microenvironment to mitigate applicability of biomarkers in patients receiving anti-PD1 in 2^{nd}/3^{rd} line remains unclear.

IMPACT

We provide a comprehensive molecular characterization of responders to anti-PD1. Discrepancies between patients treated in frontline and in 2^{nd}/3^{rd} line highlight the need for fresh biopsies directly prior to anti-PD1.

Table S1: Participating centers

Center	Recruited cases
Mount Sinai	21
University of Bern	12
University of Leuven	11
University of Mainz	9
University of Hannover	9
Royal Free Hospital	8
University of Lausanne	7
Mayo Clinic	3
Hosp. Vall d'Hebron	4
Istituto Nazionale dei Tumori	1
University of Frankfurt	10
UCLA	8
Charité	8

Table S2: Cohort characteristics based on treatment line

	Frontline (n=28)	2nd/3rd line (n=55)	p
Median age (range)	66.5 (22-85)	63.0 (28-86)	0.55
Gender, male (%)	22 (78.6)	42 (76.4)	1
Etiology (%)			0.31
HBV	5 (17.9)	11 (20.0)	
HCV	11 (39.3)	13 (23.6)	
Uninfected	13 (46.4)	31 (56.4)	
Child Pugh Score (%)*			0.71
A	24 (92.3)	48 (87.3)	
B	2 (7.7)	7 (12.7)	
Advanced Fibrosis F3/4(%)**	10 (55.6)	15 (44.1)	0.56
Platelets <100,000 / mm3 (%)***	3 (12)	14 (25.5)	0.24
BCLC stage (%)			0.78
Intermediate (B)	5 (17.9)	12 (21.8)	
Advanced (C)	23 (82.1)	43 (78.2)	
Macrovascular invasion (%)#	11 (39.3)	12 (22.2)	0.12
Extrahepatic disease (%)	14 (50.0)	39 (70.9)	0.09
Sample origin (%)			0.73
Primary tumor	24 (85.7)	49 (89.1)	
Metastasis	4 (14.3)	6 (10.9)	
Specimen type (%)			0.248
Resection	14 (50.0)	35 (63.6)	
Biopsy	14 (50.0)	20 (36.4)	
AFP (ng/ml) > 200 (%)#	7 (25.9)	23 (41.8)	0.22
Anti-PD1 drug (%)			0.22
Nivolumab	25 (89.3)	42 (76.4)	
Pembrolizumab	2 (7.1)	12 (21.8)	
Tislelizumab	1 (3.6)	1 (1.8)	
Objective response (%)##	12 (42.9)	13 (23.6%)	0.08
Disease control (%)##	17 (60.7)	29 (52.7)	0.64
Median time on therapy in month	6.25	3.9	0.36
Events			
Deceased	9 (32.1)	23 (41.8)	0.48
Progression	19 (67.9)	40 (72.7)	0.80

* data missing from 2 cases
** data missing from 31 cases
*** data missing from 3 cases
# data missing from one case
Assessment in 2 centers (11 patients) via RECIST 1.1

Table S3: Clinicopathological characteristics of patients treated with anti-PD1 in frontline

	All (n = 28)	Objective response (n=12)	No response (n=16)	p
Age (years), median (range)	66.5 (22-85)	66.5 (29-85)	66.5 (22-79)	0.91
>65 years, n(%)	19 (67.9)	7 (58.3)	12 (75.0)	0.43
Sex, n (%)				0.80
Male	22 (78.6)	9 (75)	13 (81.2)	
Female	6 (21.4)	3 (25)	3 (18.8)	
Region, n (%)				0.05
US	17 (60.7)	10 (83.3)	7 (43.8)	
Europe	11 (39.3)	2 (16.7)	9 (56.2)	
Aetiology, n (%)				
HBV	5 (17.9)	3 (25.0)	2 (12.5)	0.63
HCV	11 (39.3)	5 (41.7)	6 (37.5)	1.0
Uninfected	13 (46.4)	5 (41.7)	8 (50.0)	0.71
BCLC stage, n (%)				0.48
Intermediate (B)	5 (17.9)	1 (8.3)	4 (25.0)	
Advanced (C)	23 (82.1)	11 (91.7)	12 (75.0)	
Sample origin, n (%)				0.66
Primary tumor	24 (85.7)	11 (91.7)	13 (81.2)	
Metastasis	4 (14.3)	1 (8.3)	3 (18.8)	
Specimen type, n (%)				0.54
Resection	14 (50.0)	5 (41.7)	9 (56.3)	
Biopsy	14 (50.0)	7 (58.3)	7 (43.7)	
Child Pugh Score, n (%)*				1.0
A	24 (92.3)	10 (90.9)	14 (93.3)	
B	2 (7.7)	1 (9.1)	1 (6.7)	
Advanced Fibrosis F3-4, n (%)**	10 (55.6)	6 (66.7)	4 (44.4)	0.71
Platelets >100,000 / mm3, n (%)***	22 (88)	10 (90.9)	12 (85.7)	1.0
AFP (ng/mL), median (range)*	15 (2-78981)	20 (2-78981)	15 (2-1780)	0.91
AFP (ng/ml) > 200, n (%)*	7 (25.9)	4 (33.3)	3 (20.0)	0.66
Macrovascular invasion, n (%)	11 (39.3)	6 (50.0)	5 (31.3)	0.44
Extrahepatic disease, n (%)	14 (50.0)	7 (58.3)	7 (43.8)	0.70
Anti-PD1 drug, n (%)				0.63
Nivolumab	25 (89.3)	10 (83.3)	15 (93.8)	
Pembrolizumab	2 (7.1)	1 (8.3)	1 (6.3)	
Tislelizumab	1 (3.6)	1 (8.3)	0 (0.0)	
Median time on therapy (months), median (range)	6.25	13.8	3.8	<0.001

* data missing from 2 cases
** data missing from 10 cases
*** data missing from 3 cases

Table S4: Differentially expressed genes between responders and non-responders in frontline treated patients

Gene	logFC	FC	Wilcoxon p upregulated in OR
LIN9	0.045117382	1.031767124	0.026344429
BACE1	0.055614396	1.039301613	0.045311299
RAP2A	0.055883361	1.039495391	0.023457892
OTUD4	0.065624121	1.046537582	0.036746083
EID3	0.067156124	1.047649495	0.020832926
SLC38A2	0.068823633	1.048861099	0.032970758
TSPAN31	0.085555799	1.06109645	0.011041353
ARHGAP8	0.085834713	1.061301611	0.029509206
MIPOL1	0.085852306	1.061314553	0.020832926
GCG	0.090346649	1.064625958	0.040853946
RXYLT1	0.090977593	1.065091661	0.029509206
GALNT2	0.092254855	1.066035037	0.009640554
RHEB	0.093882142	1.067238149	0.040853946
ZSWIM8	0.0970303	1.069569551	0.032970758
CSNK1E	0.102473039	1.07361225	0.045311299
ARL4A	0.102940823	1.073960418	0.040853946
FGFR1OP2	0.104827961	1.075366147	0.040853946
USP37	0.104896163	1.075416985	0.032970758
SGCE	0.109035283	1.078506808	0.032970758
TRMT10A	0.110509033	1.079609093	0.045311299
FAM20C	0.111481887	1.080337352	0.032970758
IMMP2L	0.112367225	1.081000526	0.040853946
AKNAD1	0.112462324	1.081071785	0.014355333
SOCS5	0.11296337	1.081447305	0.029509206
BBS10	0.113345959	1.081734132	0.029509206
ADIRF	0.116383117	1.084013796	0.045311299
AGAP11	0.116383117	1.084013796	0.045311299
FCHO2	0.117376551	1.0847605	0.045311299
JHY	0.118206331	1.08538459	0.045311299
NPHP3	0.118766342	1.085805985	0.026344429
SHQ1	0.119699336	1.086508406	0.040853946
RNF212B	0.120907979	1.087419029	0.029509206
UFSP1	0.120920373	1.087428371	0.029509206
GTF2H3	0.121050927	1.08752678	0.003995217
MRPL37	0.121338752	1.087743769	0.040853946
CHPT1	0.121563362	1.08791313	0.045311299
MICU3	0.124473146	1.090109566	0.029509206
GLA	0.125357524	1.090778012	0.023457892
TIPRL	0.125580614	1.090946697	0.009640554
CCDC66	0.126567595	1.091693294	0.023457892
TRMT10C	0.126949985	1.091982688	0.036746083
DEFB114	0.127014161	1.092031265	0.026344429
KDM4C	0.12778562	1.092615368	0.026344429

MTERF2	0.128655766	1.093274566	0.036746083
PREB	0.128867812	1.093435266	0.045311299
PTPDC1	0.129952769	1.094257877	0.032970758
MARK4	0.130567708	1.094724397	0.032970758
FUCA2	0.132300215	1.096039821	0.040853946
GSTCD	0.132392077	1.096109612	0.026344429
ANKRD26	0.132591936	1.096261469	0.032970758
PRSS48	0.133448204	1.096912315	0.040853946
HIST1H2AC	0.133916092	1.097268118	0.026344429
RFTN2	0.135166828	1.098219801	0.029509206
UCHL3	0.137050827	1.09965489	0.036746083
ELOVL2	0.13832529	1.100626744	0.040853946
IQCD	0.138404	1.100686793	0.029509206
OMG	0.138881561	1.101051203	0.018451648
CCDC65	0.139021683	1.101158148	0.014355333
MIR6890	0.141343166	1.10293148	0.036746083
QARS	0.141343166	1.10293148	0.036746083
WRNIP1	0.142083453	1.10349757	0.029509206
SGF29	0.142214972	1.103598172	0.020832926
LOC100133315	0.142490156	1.103808696	0.00466565
PIGK	0.142772282	1.104024572	0.023457892
ZC3H7B	0.142865787	1.104096129	0.045311299
RAP1GDS1	0.143393422	1.104500002	0.023457892
LOC653513	0.143434409	1.104531382	0.026344429
PDE4DIP	0.143434409	1.104531382	0.026344429
CDC7	0.144861823	1.105624755	0.026344429
RRAGA	0.146428054	1.106825705	0.045311299
KAAG1	0.147930202	1.107978742	0.040853946
NFYB	0.149123617	1.108895655	0.023457892
AGBL3	0.151405805	1.110651197	0.012608351
CLTA	0.151407061	1.110652163	0.040853946
FAR2	0.152441647	1.11144892	0.029509206
CPPED1	0.152449965	1.111455328	0.045311299
SCFD1	0.152623315	1.111588886	0.020832926
OPA1	0.152671749	1.111626204	0.032970758
CARD6	0.153253171	1.112074293	0.016298131
TUBB1	0.153756984	1.112462715	0.040853946
OSBPL1A	0.154881395	1.113330087	0.032970758
ARIH1	0.15635548	1.114468222	0.018451648
MIR630	0.15635548	1.114468222	0.018451648
LRRTM2	0.157835308	1.115611962	0.029509206
TSC22D2	0.158322536	1.11598879	0.023457892
VPS26B	0.159119646	1.116605561	0.003995217
HSPA4	0.159388116	1.116813369	0.029509206
RPRD1B	0.160511105	1.117683031	0.026344429
ENPP2	0.161054213	1.118103866	0.040853946
PPP1R3C	0.163076408	1.119672187	0.026344429

RBM4	0.163157603	1.119735204	0.002454436
WDR27	0.163239374	1.119798672	0.014355333
AIFM1	0.16401848	1.120403566	0.040853946
PLPP1	0.164993279	1.121160855	0.026344429
RNF138P1	0.164993279	1.121160855	0.026344429
MIR7855	0.165042408	1.121199035	0.032970758
SPTB	0.165042408	1.121199035	0.032970758
DCAF17	0.165684854	1.121698427	0.032970758
ATPAF1	0.166243008	1.122132477	0.036746083
EPHX4	0.167132891	1.122824844	0.020832926
ZNF174	0.167435996	1.12306077	0.011041353
CEP295	0.167586471	1.123177913	0.026344429
HADHB	0.167713162	1.12327655	0.023457892
CCDC73	0.168109743	1.123585369	0.023457892
C1orf53	0.168500108	1.12388943	0.016298131
GTF2B	0.168653921	1.12400926	0.036746083
SEC61B	0.168881522	1.124186599	0.040853946
MID1	0.169361187	1.124560428	0.045311299
MYPN	0.169967496	1.125033137	0.001456447
C6orf106	0.170710234	1.125612483	0.036746083
DLGAP1	0.171108843	1.125923527	0.016298131
PLD3	0.171319022	1.126087569	0.045311299
C5orf15	0.171336329	1.126101078	0.029509206
CDCA2	0.171764944	1.126435685	0.045311299
LRP5	0.172810869	1.127252625	0.012608351
FIGNL1	0.173376852	1.127694944	0.040853946
TUBG1	0.173822997	1.12804373	0.040853946
CAAP1	0.173883967	1.128091404	0.040853946
SEC22A	0.173907314	1.12810966	0.020832926
VAMP2	0.173917573	1.128117681	0.016298131
ZNF623	0.174732834	1.128755356	0.045311299
KIAA1107	0.175253279	1.129162623	0.001456447
SLC25A16	0.175605069	1.129437994	0.036746083
LACTB	0.17629913	1.129981482	0.040853946
ASAH2	0.177154002	1.130651253	0.036746083
PPARG	0.17722447	1.130706481	0.045311299
TMEM147	0.177291457	1.130758983	0.001740183
PPFIBP1	0.177555669	1.130966087	0.011041353
HABP4	0.178933002	1.132046329	0.032970758
ERI2	0.179229018	1.132278629	0.036746083
METAP1D	0.179600626	1.132570318	0.002898085
UBA5	0.179923254	1.132823622	0.036746083
SPATC1L	0.179968787	1.132859375	0.032970758
GALNT1	0.180059189	1.132930364	0.045311299
ST3GAL6	0.182612339	1.134937097	0.045311299
CFAP69	0.18266831	1.134981128	0.026344429
SCRN3	0.182714448	1.135017426	0.011041353

FAM81A	0.18277948	1.135068591	0.014355333
PPP6R3	0.1838499	1.135911077	0.032970758
SDAD1	0.184019276	1.136044444	0.032970758
RARB	0.184230427	1.136210725	0.00466565
TRIP13	0.184294482	1.136261174	0.032970758
HIST1H3G	0.185591883	1.137283462	0.045311299
SMU1	0.1861536	1.137726352	0.023457892
TTC23	0.186193933	1.13775816	0.036746083
CAMK1D	0.186431539	1.137945559	0.045311299
SENP1	0.18685455	1.138279264	0.026344429
ANKEF1	0.187117881	1.13848705	0.036746083
GSPT1	0.187628822	1.138890325	0.020832926
KANSL1	0.187755528	1.138990353	0.029509206
KIF16B	0.188789777	1.139807173	0.023457892
SH3GL1	0.189298106	1.140208851	0.023457892
ZBP1	0.189589828	1.140439432	0.032970758
KRT18	0.189963346	1.140734733	0.045311299
POP5	0.190325803	1.141021363	0.040853946
TMEM9	0.190328597	1.141023573	0.032970758
HTR2B	0.190855657	1.141440499	0.032970758
ZNF398	0.191525855	1.141970874	0.036746083
MTREX	0.192642006	1.142854709	0.007281815
IL1R1	0.192761566	1.142949425	0.016298131
CXCL10	0.193020544	1.143154614	0.040853946
LSM3	0.193052392	1.14317985	0.018451648
PNPT1	0.193337754	1.14340599	0.045311299
PIGF	0.193893369	1.143846427	0.029509206
NR1D2	0.194035035	1.143958753	0.020832926
ZAR1L	0.194222796	1.144107645	0.018451648
IFT74	0.195260688	1.144931026	0.014355333
C20orf194	0.195480229	1.145105268	0.036746083
AZI2	0.195533244	1.145147347	0.023457892
CREG1	0.195865765	1.145411319	0.032970758
CBL	0.196046423	1.145554759	0.036746083
SCAF11	0.19628652	1.145745421	0.045311299
WFDC10A	0.196322665	1.145774127	0.007281815
GORAB	0.196608102	1.146000841	0.012608351
RSPH9	0.196756842	1.146118998	0.020832926
ATG4A	0.197256659	1.146516136	0.003408791
ARHGAP1	0.197596995	1.146786634	0.007281815
PARP4	0.197731983	1.14689394	0.016298131
ETFDH	0.198189098	1.147257389	0.040853946
P4HA2	0.19859402	1.147579435	0.023457892
KIF9	0.198655039	1.147627973	0.023457892
LACTB2	0.19931052	1.14814951	0.018451648
ERGIC2	0.200840513	1.149367781	0.014355333
TESK2	0.201094581	1.14957021	0.011041353

IKZF5	0.201683675	1.150039708	0.023457892
NAPA	0.201958445	1.150258761	0.011041353
TADA2A	0.202498355	1.150689311	0.040853946
MLH3	0.202892901	1.151004043	0.016298131
WNT5B	0.203012601	1.151099545	0.045311299
NDUFB11	0.204439638	1.152238715	0.029509206
MGMT	0.204777709	1.152508754	0.023457892
ACAD10	0.20531724	1.152939843	0.040853946
MFAP3	0.205554766	1.153129679	0.029509206
RALGAPA2	0.205794149	1.153321032	0.040853946
DLX6	0.2068949	1.154201331	0.045311299
CDKL5	0.206984243	1.154272811	0.006298355
ZNF518A	0.207361526	1.154574707	0.026344429
FAM83H	0.207507273	1.154691353	0.003408791
HIBCH	0.207657326	1.154811457	0.029509206
ARL15	0.208043814	1.155120864	0.023457892
SIAH1	0.21005977	1.156736106	0.040853946
DNAJB5	0.210160065	1.156816524	0.023457892
TMF1	0.210579305	1.157152738	0.036746083
MMAB	0.210825645	1.157350339	0.014355333
FLJ30679	0.211176283	1.157631659	0.016298131
MYH9	0.211457745	1.157857529	0.018451648
SASH1	0.211534156	1.157918855	0.036746083
CCT8	0.212147809	1.158411483	0.016298131
BCL6	0.212668641	1.158829761	0.029509206
EIF4G3	0.212733936	1.158882209	0.036746083
INSIG2	0.212752747	1.15889732	0.032970758
LIMS1	0.213517653	1.159511921	0.011041353
FBXO22	0.213820242	1.159755141	0.029509206
SPATA6	0.213929229	1.159842757	0.023457892
ARMC10	0.21468895	1.16045369	0.014355333
STAT2	0.214791179	1.160535922	0.032970758
UPRT	0.214937013	1.16065324	0.026344429
SSRP1	0.215055534	1.160748594	0.040853946
ING2	0.215369747	1.161001429	0.011041353
KIAA2026	0.216805671	1.162157556	0.001213644
KAT2A	0.217828694	1.162981941	0.045311299
FYTTD1	0.218295927	1.163358647	0.011041353
BAZ1B	0.218884027	1.163832975	0.040853946
SCYL2	0.219288635	1.16415942	0.020832926
CEP112	0.219386155	1.164238116	0.003408791
MAPK9	0.219463306	1.164300377	0.026344429
XPA	0.219759787	1.164539671	0.018451648
FAM86C1	0.22021449	1.164906764	0.011041353
ARPP19	0.220796098	1.165376479	0.012608351
FASTKD1	0.220995817	1.165537818	0.045311299
PRKD3	0.221016625	1.165554629	0.029509206

PPP2CB	0.221040428	1.16557386	0.029509206
POP4	0.221168407	1.16567726	0.00466565
CCDC146	0.221283311	1.165770105	0.018451648
GTF2F1	0.221954651	1.166312708	0.018451648
IRF2BP1	0.222015626	1.166362003	0.006298355
ABI2	0.223544021	1.167598304	0.029509206
RAP2B	0.224314913	1.168222368	0.045311299
CEP41	0.224530127	1.16839665	0.020832926
RIC1	0.225102353	1.168860171	0.011041353
PCYT2	0.225163534	1.168909741	0.016298131
TRIM5	0.225285887	1.169008878	0.018451648
MMS19	0.22603473	1.16961582	0.020832926
MMP15	0.226386927	1.169901386	0.018451648
SHLD1	0.22654551	1.170029991	0.016298131
ACP2	0.227046002	1.170435961	0.009640554
NPAT	0.227413457	1.17073411	0.040853946
TMEM144	0.227790354	1.171039999	0.009640554
MED29	0.227941476	1.171162672	0.016298131
ZNF267	0.228487685	1.171606161	0.040853946
SMARCD1	0.229790165	1.172664376	0.023457892
LOC388436	0.22980634	1.172677525	0.029509206
LOC79999	0.22980634	1.172677525	0.029509206
HCFC1	0.229883475	1.172740224	0.045311299
PRKCA	0.230087492	1.172906078	0.014355333
BRK1	0.230639613	1.173355036	0.012608351
DLST	0.231319783	1.173908354	0.036746083
AIDA	0.231520385	1.174071593	0.032970758
UBTF	0.232759247	1.175080218	0.036746083
SOX13	0.233815477	1.175940836	0.016298131
SLC25A4	0.23410661	1.176178163	0.023457892
ATR	0.234175215	1.176234095	0.029509206
DNTTIP1	0.234421261	1.176434714	0.002898085
TLR3	0.234578145	1.176562651	0.045311299
DNAJC3	0.234619146	1.176596089	0.020832926
PRDX2	0.235414475	1.177244902	0.016298131
PTPN12	0.23597366	1.177701287	0.040853946
PPID	0.236299062	1.177966949	0.005430149
PARL	0.236563556	1.17818293	0.014355333
SERPINB6	0.236587325	1.178202342	0.012608351
LINC01549	0.236753734	1.17833825	0.032970758
HECW2	0.237379418	1.178849396	0.018451648
ZACN	0.237532805	1.178974738	0.002898085
SHARPIN	0.237954632	1.179319506	0.032970758
RHOBTB1	0.238219477	1.179536021	0.011041353
PATZ1	0.238362594	1.179653039	0.040853946
BTF3L4	0.23954678	1.180621713	0.018451648
TBCD	0.24051331	1.181412933	0.045311299

TTLL1	0.240538961	1.181433938	0.014355333
AK4	0.241412763	1.182149718	0.040853946
CD40	0.242644589	1.183159512	0.029509206
FBXL5	0.242684037	1.183191864	0.026344429
MAPRE2	0.242737445	1.183235666	0.003408791
SLC25A44	0.243105757	1.183537778	0.029509206
ZFYVE9	0.243186299	1.183603854	0.018451648
SF3B5	0.243242447	1.183649919	0.008391519
XPC	0.243668768	1.183999743	0.007281815
ERGIC1	0.243905261	1.184193846	0.045311299
RGPD1	0.244468372	1.184656149	0.032970758
RGPD2	0.244468372	1.184656149	0.032970758
ZFYVE16	0.244533713	1.184709804	0.045311299
PTGFR	0.245384917	1.185409001	0.026344429
ATAD1	0.24541217	1.185431393	0.036746083
MFSD8	0.24615081	1.186038474	0.011041353
RAB3GAP1	0.247410583	1.187074585	0.000296775
KNTC1	0.24811661	1.187655658	0.012608351
ASNA1	0.248516609	1.187984991	0.023457892
UBXN8	0.24854609	1.188009267	0.036746083
OTUD1	0.248557254	1.18801846	0.014355333
HS6ST1	0.24860955	1.188061525	0.018451648
BCHE	0.248670856	1.188112012	0.014355333
ZYG11B	0.249592015	1.188870862	0.036746083
SLC35F5	0.249657461	1.188924795	0.009640554
SIRT2	0.249807293	1.189048278	0.003995217
HACL1	0.249869395	1.189099463	0.040853946
DNAJC25-GNG10	0.249956646	1.189171379	0.020832926
RABEP1	0.25039915	1.189536178	0.023457892
PSMG3-AS1	0.252321704	1.191122426	0.007281815
METAP2	0.252347504	1.191143727	0.036746083
HAO1	0.252402213	1.191188898	0.018451648
NAPB	0.252502662	1.191271838	0.006298355
PLEKHA3	0.253040636	1.191716141	0.036746083
SOCS4	0.253074198	1.191743864	0.040853946
MIR4742	0.253104165	1.191768619	0.045311299
WDR26	0.253104165	1.191768619	0.045311299
AKR1B1	0.253773187	1.192321407	0.026344429
ETFA	0.253952085	1.192469267	0.009640554
WRN	0.25414591	1.192629486	0.012608351
EIF2A	0.254274504	1.192735795	0.005430149
SETX	0.254360401	1.192806812	0.020832926
DYNC2LI1	0.254593812	1.192999809	0.023457892
LGALSL	0.255289507	1.193575235	0.020832926
CXorf56	0.255565394	1.193803504	0.009640554
UMAD1	0.25575555	1.193960865	0.023457892
RHBDL3	0.255951208	1.194122801	0.045311299

TSPAN15	0.255996837	1.194160569	0.020832926
NDUFA2	0.256017924	1.194178023	0.016298131
SLC28A3	0.256150865	1.194288069	0.029509206
SETD5	0.256174291	1.194307462	0.029509206
APOBEC3G	0.256217214	1.194342995	0.036746083
HNRNPA2B1	0.257847263	1.195693203	0.040853946
THAP5	0.258290605	1.196060697	0.036746083
COA4	0.258724693	1.19642063	0.029509206
C1orf174	0.258957389	1.19661362	0.020832926
SNRPD3	0.258980874	1.1966331	0.020832926
MBNL3	0.259042368	1.196684106	0.020832926
DCAF10	0.259263569	1.196867601	0.007281815
CLIC6	0.259509631	1.197071753	0.032970758
LGMN	0.259536836	1.197094327	0.026344429
BUB3	0.259730692	1.197255192	0.014355333
GPRC5D	0.259806536	1.197318134	0.029509206
MAF	0.259856067	1.197359242	0.045311299
EPG5	0.260017924	1.197493582	0.006298355
BCL2L13	0.261182977	1.198461013	0.018451648
CDK12	0.261225315	1.198496183	0.00466565
PIGS	0.261688472	1.198881006	0.045311299
KIAA1958	0.261995038	1.199135789	0.045311299
PCNX4	0.262094693	1.199218623	0.008391519
NAIP	0.2624319	1.199498955	0.008391519
RPL29	0.263311726	1.200230691	0.011041353
VASH1	0.26336726	1.200276892	0.005430149
NEK6	0.264327775	1.201076276	0.020832926
STARD3NL	0.264850685	1.20151169	0.007281815
FEN1	0.265074077	1.20169775	0.020832926
RGMB	0.265214219	1.201814488	0.029509206
GLCE	0.265310274	1.201894507	0.045311299
NR2F1	0.265346774	1.201924916	0.023457892
PDE5A	0.265472224	1.202029434	0.005430149
TRAF6	0.265587979	1.202125883	0.016298131
GLB1	0.265606297	1.202141147	0.045311299
TMPPE	0.265606297	1.202141147	0.045311299
CPSF3	0.265614641	1.2021481	0.018451648
DIRC2	0.266158851	1.202601656	0.032970758
CDKL1	0.266828872	1.203160302	0.029509206
WHAMM	0.267473934	1.203698383	0.040853946
EIF3A	0.26785422	1.204015713	0.023457892
DYM	0.268878638	1.204870955	0.040853946
ZNF614	0.269161767	1.205107434	0.029509206
LTV1	0.269267169	1.205195481	0.023457892
HDHD3	0.269329074	1.205247197	0.009640554
BTG3	0.269471831	1.205366464	0.006298355
KIDINS220	0.269728966	1.205581318	0.016298131

RNF31	0.270898422	1.206558965	0.032970758
LRCH1	0.271006289	1.20664918	0.002070906
TSPYL4	0.271171169	1.206787091	0.014355333
SREBF2	0.271650155	1.20718782	0.040853946
TNPO3	0.271810049	1.20732162	0.016298131
RGSL1	0.272554044	1.207944394	0.045311299
ROCK1	0.27257393	1.207961044	0.018451648
MPHOSPH9	0.273379872	1.208636044	0.040853946
PHB	0.273402666	1.20865514	0.023457892
MFN2	0.273682674	1.208889747	0.040853946
PPM1G	0.274474973	1.209553827	0.023457892
ARHGAP11B	0.275037518	1.210025556	0.036746083
ST3GAL5	0.275298099	1.210244132	0.026344429
PIK3C2A	0.275519577	1.210429939	0.029509206
GDE1	0.275959086	1.210798746	0.020832926
AP1B1	0.27647353	1.211230576	0.045311299
RHOT1	0.276808487	1.211511825	0.001740183
MT4	0.277450536	1.21205111	0.009640554
MED4	0.278228607	1.212704967	0.026344429
CINP	0.27857889	1.212999444	0.00466565
HSBP1L1	0.278755551	1.213147988	0.020832926
GRB14	0.27888064	1.213253178	0.045311299
NFIA	0.27898584	1.213341652	0.012608351
PSMA1	0.279386503	1.213678666	0.023457892
MAP7D2	0.279465252	1.213744915	0.007281815
IBTK	0.279629323	1.213882957	0.018451648
ACTL6A	0.279820129	1.214043512	0.023457892
ATP5MC3	0.279883604	1.214096927	0.036746083
CD180	0.280205982	1.214368254	0.029509206
MIR6132	0.280532254	1.21464292	0.032970758
ST7	0.280532254	1.21464292	0.032970758
ST7-OT3	0.280532254	1.21464292	0.032970758
ST7-OT4	0.280532254	1.21464292	0.032970758
TMCC1	0.28093971	1.214986016	0.003995217
APOA2	0.281158443	1.21517024	0.029509206
SRRT	0.281199692	1.215204984	0.016298131
SAP30L	0.281560086	1.215508587	0.009640554
FAM76B	0.2822877	1.216121776	0.045311299
ARID1B	0.282333749	1.216160594	0.002454436
DNM2	0.282566246	1.216356599	0.045311299
DNAJC13	0.283738139	1.21734504	0.008391519
EP300	0.284045812	1.217604682	0.00466565
MIR1281	0.284045812	1.217604682	0.00466565
TMX2-CTNND1	0.284964553	1.218380327	0.036746083
RER1	0.285130233	1.218520255	0.023457892
INTS6	0.285380628	1.218731761	0.014355333
COPZ1	0.285386962	1.218737112	0.029509206

EPM2A	0.285678841	1.218983706	0.026344429
SLC30A1	0.285768424	1.2190594	0.023457892
MAIP1	0.285829971	1.219111407	0.040853946
UHRF2	0.285985565	1.219242895	0.045311299
ANKRD36	0.286121312	1.219357622	0.032970758
COMMD4	0.286686347	1.21983528	0.036746083
DHX15	0.287358203	1.220403483	0.023457892
APOBEC3F	0.287422007	1.220457458	0.040853946
SETD1B	0.287807953	1.220783995	0.045311299
RARS2	0.288045076	1.220984661	0.007281815
ZNF282	0.288060098	1.220997375	0.026344429
FMN1	0.288400897	1.221285837	0.012608351
PAK4	0.288496023	1.221366367	0.036746083
AKAP1	0.288944959	1.221746489	0.014355333
LAMTOR3	0.289321621	1.222065507	0.020832926
SOS1	0.28933078	1.222073266	0.023457892
KALRN	0.289737078	1.22241748	0.023457892
DTYMK	0.289944435	1.222593189	0.018451648
SEC22B	0.290037487	1.222672047	0.023457892
COG2	0.290367691	1.222951925	0.032970758
RCAN2	0.291286245	1.223730817	0.023457892
ATXN2	0.291304097	1.22374596	0.002070906
AGFG2	0.291751876	1.224125841	0.026344429
NEK1	0.291994794	1.224331975	0.014355333
SLC22A12	0.292127186	1.224444333	0.020832926
SPCS1	0.292158692	1.224471073	0.026344429
ZNF567	0.293072105	1.225246567	0.029509206
PMPCB	0.293105508	1.225274936	0.029509206
CPNE3	0.293316385	1.225454046	0.040853946
GOLGB1	0.293836949	1.225896303	0.020832926
TOGARAM1	0.293852033	1.225909121	0.005430149
OXSR1	0.293892924	1.225943868	0.040853946
POM121	0.294165463	1.226175482	0.007281815
PEA15	0.29422898	1.226229468	0.045311299
TEX10	0.294637074	1.226576379	0.023457892
ADIPOR2	0.294986827	1.226873775	0.001456447
SCFD2	0.294996982	1.226882411	0.036746083
MRRF	0.295174125	1.227033064	0.011041353
DNAJC22	0.296209868	1.227914295	0.036746083
GTF2H5	0.296234926	1.227935622	0.026344429
PRLR	0.296512648	1.228172026	0.023457892
FBXO5	0.296706494	1.228337058	0.002070906
PRKAA2	0.297235001	1.228787122	0.008391519
CENPU	0.298336103	1.229725322	0.001740183
RNF13	0.298357514	1.229743572	0.016298131
DHX29	0.298436754	1.229811117	0.045311299
PREP	0.298918476	1.230221826	0.011041353

PLSCR1	0.299079562	1.230359195	0.040853946
MRPL40	0.299306302	1.230552579	0.009640554
IFT81	0.300074879	1.231208314	0.036746083
CTSD	0.300340736	1.231435219	0.026344429
TENT2	0.300455138	1.231532873	0.040853946
NDRG3	0.30088551	1.231900308	0.045311299
FAM149B1	0.301320056	1.232271417	0.023457892
PLAUR	0.301340652	1.23228901	0.006298355
KIAA0754	0.302185993	1.233011276	0.005430149
MACF1	0.302185993	1.233011276	0.005430149
MTIF2	0.302278281	1.233090153	0.006298355
NTAN1	0.303227224	1.233901494	0.018451648
PKIB	0.303421436	1.23406761	0.040853946
LATS1	0.303449848	1.234091913	0.032970758
ILVBL	0.303550032	1.234177615	0.00466565
LYNX1	0.303720575	1.234323517	0.045311299
COX7A2L	0.303819276	1.234407965	0.029509206
SYNJ2	0.304154173	1.234694545	0.036746083
ZNF639	0.304646826	1.235116242	0.036746083
CREBRF	0.305090153	1.23549584	0.005430149
PATJ	0.305213014	1.23560106	0.045311299
SNX4	0.305492942	1.235840828	0.029509206
FKBP1A	0.305784079	1.236090248	0.026344429
MIR6869	0.305784079	1.236090248	0.026344429
ABCB7	0.305816947	1.236118409	0.032970758
THUMPD1	0.306200734	1.236447286	0.011041353
MTFR1L	0.306283502	1.236518223	0.045311299
DMD	0.306741417	1.23691076	0.032970758
COX8A	0.307001927	1.237134131	0.005430149
MTAP	0.3071817	1.237288299	0.045311299
C6orf48	0.307221054	1.237322051	0.036746083
SNORD48	0.307221054	1.237322051	0.036746083
SNORD52	0.307221054	1.237322051	0.036746083
SPATA5	0.307390899	1.237467726	0.014355333
POLR2L	0.307419347	1.237492127	0.026344429
CACHD1	0.307555952	1.237609307	0.001740183
DENND6A	0.307738181	1.237765642	0.003408791
ADRA1A	0.30785336	1.237864464	0.029509206
DCDC2	0.30789966	1.237904191	0.00466565
RBBP6	0.307932164	1.237932081	0.036746083
GLTP	0.309124073	1.238955245	0.006298355
IREB2	0.309439365	1.23922604	0.045311299
PTPRO	0.309674859	1.239428338	0.040853946
LSM8	0.310435019	1.240081568	0.009640554
ABHD17B	0.31106564	1.240623742	0.040853946
TANK	0.31116196	1.240706575	0.003408791
UBE3D	0.311199879	1.240739184	0.018451648

NEK7	0.312022664	1.241446994	0.023457892
SPICE1	0.312094609	1.241508905	0.006298355
ZNF512	0.312199856	1.241599478	0.026344429
C1QB	0.312304815	1.24168981	0.040853946
02. Sep	0.313160584	1.242426566	0.029509206
ELOVL6	0.314139825	1.24327016	0.006298355
BBOF1	0.314274247	1.243386006	0.016298131
HNRNPL	0.314620861	1.243684771	0.036746083
TMEM183B	0.314639545	1.243700877	0.045311299
FBXO25	0.314719348	1.243769675	0.036746083
NDUFB9	0.314913111	1.243936733	0.036746083
SHPRH	0.315353562	1.244316561	0.040853946
CSNK1D	0.315556201	1.244491348	0.045311299
CRLF3	0.315672006	1.244591248	0.032970758
SNX24	0.31610208	1.244962321	0.032970758
TRIM4	0.316124927	1.244982037	0.009640554
KIFAP3	0.31618358	1.245032653	0.007281815
EIF4ENIF1	0.317245792	1.24594967	0.000559323
GPBP1L1	0.317305804	1.246001499	0.002454436
FNDC3A	0.317481483	1.246153236	0.018451648
TATDN3	0.317918689	1.246530938	0.023457892
MIR4741	0.318119009	1.246704031	0.000455291
RBBP8	0.318119009	1.246704031	0.000455291
PERP	0.318229024	1.246799105	0.026344429
KLC4	0.318436043	1.246978027	0.036746083
EIF4H	0.318478905	1.247015074	0.020832926
OSBPL2	0.3198159	1.248171261	0.020832926
GCNT1	0.320111975	1.248427442	0.029509206
HLTF	0.320549071	1.248805737	0.016298131
RBBP5	0.320935369	1.249140164	0.007281815
PRIMPOL	0.321056395	1.249244957	0.029509206
GFM2	0.322080583	1.250132128	0.018451648
PSMD10	0.322561007	1.250548496	0.032970758
KLF3	0.322935831	1.250873442	0.036746083
HIVEP2	0.323065937	1.250986254	0.006298355
CDC73	0.324336758	1.252088691	0.026344429
HPF1	0.324671378	1.252379135	0.014355333
KIAA0825	0.325104297	1.252755001	0.032970758
MINPP1	0.325405553	1.253016622	0.029509206
TBC1D14	0.325552403	1.253144171	0.029509206
ANXA5	0.325601397	1.253186729	0.036746083
ADAT2	0.327863787	1.25515348	0.020832926
MITD1	0.328170958	1.255420749	0.005430149
MIR937	0.328180508	1.255429059	0.002070906
SCRIB	0.328180508	1.255429059	0.002070906
LNPEP	0.328241718	1.255482324	0.020832926
ATP5MGL	0.328433904	1.255649583	0.040853946

THUMPD3-AS1	0.329174365	1.256294208	0.026344429
SNX3	0.329435498	1.256521623	0.007281815
KLHDC3	0.329658645	1.256715989	0.018451648
MAP2K4	0.329902803	1.25692869	0.029509206
MIR744	0.329902803	1.25692869	0.029509206
TMEM60	0.33020176	1.257189179	0.023457892
NPRL2	0.330299334	1.25727421	0.018451648
CCNY	0.330329295	1.257300321	0.020832926
COX20	0.330396112	1.257358553	0.029509206
SWAP70	0.330956529	1.25784707	0.008391519
FOXJ2	0.331468879	1.258293854	0.012608351
FAM208A	0.331545247	1.258360462	0.020832926
SF3A1	0.332133167	1.258873368	0.005430149
PTEN	0.33217315	1.258908257	0.006298355
SDHC	0.332895212	1.259538492	0.040853946
TYSND1	0.332988989	1.259620367	0.002070906
DDX6	0.333145137	1.259756707	0.016298131
ENPEP	0.333166722	1.259775554	0.003408791
RMDN1	0.33319016	1.259796021	0.018451648
CALML4	0.333841375	1.260364806	0.023457892
LACC1	0.334775859	1.261181453	0.0000233
MBTPS1	0.33489986	1.261289857	0.032970758
MTMR10	0.33508532	1.261452008	0.026344429
COIL	0.335429198	1.261752721	0.006298355
NDUFA10	0.335893366	1.262158739	0.020832926
KIAA0232	0.336015347	1.26226546	0.016298131
ATG12	0.336437748	1.262635087	0.018451648
AGO1	0.336516643	1.262704137	0.018451648
TTK	0.337155296	1.263263236	0.045311299
PTPRG	0.337491503	1.263557662	0.012608351
MRPL30	0.338380827	1.2643368	0.016298131
ZNF713	0.338598914	1.26452794	0.029509206
ATE1	0.338916513	1.264806348	0.018451648
ZNF638	0.339649937	1.265449501	0.045311299
PRDX5	0.340072103	1.265819855	0.026344429
ETF1	0.340207077	1.265938287	0.014355333
ARHGAP29	0.341132273	1.26675039	0.018451648
CHST9	0.341827033	1.267360567	0.040853946
INVS	0.342250307	1.267732454	0.018451648
COP1	0.342466444	1.267922393	0.016298131
SREK1	0.342739827	1.26816268	0.018451648
G3BP2	0.34282727	1.268239547	0.040853946
SERINC2	0.343319957	1.268672731	0.029509206
ARHGAP5	0.343561796	1.268885416	0.045311299
CSRP2	0.343853226	1.269141762	0.026344429
FAM214A	0.344073066	1.269335171	0.003408791
IPO7	0.344836279	1.27000685	0.000455291

SNORA23	0.344836279	1.27000685	0.000455291
NCOA4	0.345250888	1.270371884	0.040853946
CCDC125	0.345359215	1.270467275	0.001456447
HDHD2	0.345703015	1.270770069	0.003408791
DEFB1	0.345940049	1.270978873	0.036746083
MRPS18C	0.346149218	1.271163159	0.045311299
PPP4R3B	0.346536578	1.271504509	0.040853946
UGGT1	0.346622628	1.27158035	0.032970758
HSF1	0.346624162	1.271581702	0.023457892
PLXND1	0.346958603	1.27187651	0.011041353
UBA3	0.34731657	1.272192133	0.008391519
ANO6	0.347568029	1.272413892	0.008391519
TSPAN3	0.347650635	1.27248675	0.012608351
SQSTM1	0.34843759	1.27318105	0.016298131
KRTAP21-3	0.348804334	1.273504744	0.020832926
CEPT1	0.349105827	1.273770907	0.00100707
NISCH	0.349238747	1.273888269	0.008391519
SLFN5	0.349308225	1.27394962	0.012608351
CEP192	0.349600994	1.274208171	0.005430149
TTC32	0.349619649	1.274224647	0.026344429
MOB1A	0.349961515	1.274526628	0.005430149
FH	0.349984037	1.274546525	0.026344429
NUP35	0.350175144	1.274715369	0.036746083
VPS13A	0.350468571	1.274974658	0.040853946
RNF169	0.350582234	1.27507511	0.005430149
TSPYL1	0.350603471	1.27509388	0.032970758
CDC14B	0.350851086	1.275312748	0.040853946
RTRAF	0.350966931	1.275415157	0.009640554
FAM49A	0.35133327	1.27573906	0.002454436
CSDE1	0.352135571	1.276448712	0.045311299
H1F0	0.352366833	1.276653341	0.023457892
GOPC	0.352523968	1.276792399	0.018451648
PHF6	0.35307037	1.277276059	0.018451648
CSNK2A2	0.353129918	1.277328781	0.032970758
ATF4	0.353500382	1.277656822	0.020832926
PAICS	0.353709353	1.277841902	0.014355333
ALKBH5	0.353897232	1.278008323	0.007281815
GNG10	0.353932319	1.278039405	0.009640554
NUPL2	0.354691079	1.278711744	0.005430149
GALNT10	0.355621003	1.279536234	0.002454436
EIF5B	0.355717246	1.279621596	0.011041353
BCAS2	0.355948942	1.279827119	0.020832926
NAT8	0.355962166	1.27983885	0.014355333
ZNF24	0.356430984	1.280254814	0.036746083
YWHAEP7	0.356707988	1.280500652	0.014355333
ZNF780B	0.356848258	1.280625159	0.032970758
PBX3	0.357209569	1.280945921	0.020832926

DNAJC21	0.357340741	1.281062392	0.014355333
SMIM14	0.357682262	1.281365686	0.011041353
ANKRD40	0.359314462	1.282816186	0.012608351
TRIM21	0.359657543	1.283121283	0.006298355
NCOA6	0.360510629	1.283880235	0.045311299
REEP3	0.360622059	1.283979403	0.026344429
GNPAT	0.360914571	1.284239761	0.012608351
MAP3K8	0.361376582	1.284651094	0.016298131
PAM	0.361487016	1.284749433	0.014355333
LXN	0.362012551	1.285217518	0.002898085
ARFGAP3	0.362094594	1.285290609	0.023457892
RBAK	0.36321628	1.286290302	0.007281815
RBAK-RBAKDN	0.36321628	1.286290302	0.007281815
RBAKDN	0.36321628	1.286290302	0.007281815
RBMS2	0.363291564	1.286357426	0.018451648
TMEM59	0.363320425	1.28638316	0.002898085
09. Sep	0.363543054	1.286581683	0.012608351
METTL14	0.363553821	1.286591285	0.001740183
RPARP-AS1	0.36355877	1.286595698	0.016298131
KCNJ2	0.363931421	1.286928071	0.029509206
FGD6	0.364100742	1.28707912	0.008391519
WASHC2C	0.364131332	1.28710641	0.040853946
RAVER2	0.364259414	1.287220684	0.00466565
FAM86B1	0.364318541	1.287273441	0.026344429
TMEM184B	0.364825192	1.287725589	0.029509206
ZNF480	0.36522962	1.288086626	0.040853946
IQCJ	0.36526662	1.288119661	0.014355333
IQCJ-SCHIP1	0.36526662	1.288119661	0.014355333
SCHIP1	0.36526662	1.288119661	0.014355333
PI4KB	0.366140227	1.288899903	0.009640554
TRMT1L	0.366888527	1.289568605	0.002070906
COL6A3	0.366909299	1.289587173	0.014355333
MIR6839	0.367086788	1.289745835	0.036746083
ZNF107	0.367086788	1.289745835	0.036746083
C3orf67	0.367549338	1.290159414	0.014355333
BRAF	0.368645682	1.291140214	0.032970758
HARS2	0.368666226	1.2911586	0.045311299
JOSD1	0.369060735	1.291511719	0.029509206
PTCH1	0.36932637	1.29174954	0.003408791
TBCEL	0.369440698	1.29185191	0.018451648
BRD7	0.369647233	1.292036864	0.012608351
IFI44L	0.369826569	1.292197482	0.005430149
DPF2	0.370093454	1.292436549	0.014355333
GHR	0.370260849	1.292586518	0.018451648
OSBP	0.370675608	1.292958176	0.008391519
LYRM2	0.370975381	1.293226863	0.026344429
ZBTB44	0.371696965	1.29387385	0.026344429

RBM18	0.371943924	1.294095353	0.003995217
CHAMP1	0.372019578	1.294163217	0.020832926
LARP4	0.372901653	1.29495472	0.036746083
DCTN4	0.372947142	1.294995551	0.045311299
VAPB	0.373093614	1.295127035	0.045311299
TSG101	0.373698912	1.295670533	0.026344429
EIF3G	0.373880645	1.295833756	0.009640554
PLEC	0.37404637	1.295982619	0.040853946
CTNNBL1	0.374347833	1.296253454	0.045311299
GTPBP4	0.374977154	1.296819019	0.045311299
PTPN4	0.375368152	1.297170529	0.007281815
WDR45B	0.37564265	1.297417362	0.023457892
MIR3615	0.376299245	1.298007973	0.045311299
SLC9A3R1	0.376299245	1.298007973	0.045311299
HSPD1	0.377096501	1.298725471	0.026344429
VKORC1L1	0.377293381	1.298902716	0.003408791
KIAA0556	0.37801985	1.299556942	0.036746083
MIR8072	0.378294823	1.299804658	0.020832926
SBNO1	0.378294823	1.299804658	0.020832926
AP3B1	0.378331026	1.299837275	0.032970758
PIK3C2B	0.378711854	1.300180439	0.023457892
KCTD3	0.379052029	1.300487046	0.002898085
HNRNPF	0.379085477	1.300517197	0.029509206
POLR2A	0.379239608	1.300656146	0.026344429
APH1B	0.379330714	1.300738285	0.020832926
PWARSN	0.379504224	1.300894731	0.020832926
SNORD107	0.379504224	1.300894731	0.020832926
SNRPN	0.379504224	1.300894731	0.020832926
SNURF	0.379504224	1.300894731	0.020832926
THYN1	0.379624657	1.301003332	0.032970758
PRKAR1A	0.380178079	1.301502496	0.040853946
TMEM165	0.380860411	1.302118196	0.012608351
NHLRC2	0.381092706	1.302327873	0.020832926
RTF1	0.381424269	1.302627211	0.045311299
ARFGAP2	0.381551134	1.302741764	0.036746083
GTDC1	0.381721978	1.302896044	0.007281815
CCDC7	0.381862038	1.303022538	0.007281815
SPATS2	0.382404725	1.303512778	0.029509206
USF3	0.382427532	1.303533384	0.009640554
KITLG	0.382522495	1.303619191	0.023457892
ZRANB2	0.382532665	1.30362838	0.007281815
PRPF4B	0.382702595	1.303781938	0.029509206
BLMH	0.382856318	1.303920868	0.011041353
APIP	0.383128486	1.304166878	0.040853946
RAB6A	0.383248854	1.304275693	0.020832926
EMP3	0.384094874	1.305040767	0.032970758
TBC1D13	0.384255402	1.305185986	0.023457892

ICK	0.384744941	1.30562894	0.032970758
AMBRA1	0.385294044	1.306125969	0.014355333
SUCO	0.385384242	1.306207631	0.023457892
CBX1	0.385425422	1.306244916	0.008391519
DDRGK1	0.385835944	1.306616664	0.006298355
PUM1	0.385941745	1.306712489	0.016298131
FAM120A	0.386425654	1.30715086	0.007281815
MIR611	0.387214144	1.307865465	0.032970758
TMEM258	0.387214144	1.307865465	0.032970758
TMEM41B	0.387222788	1.307873301	0.009640554
ZMYND11	0.38723423	1.307883674	0.018451648
TARBP1	0.387621644	1.308234934	0.026344429
HNRNPC	0.387946327	1.308529389	0.020832926
LYPLAL1	0.38831862	1.308867104	0.040853946
ADSS	0.388332775	1.308879946	0.007281815
SLC25A20	0.388462757	1.308997876	0.003408791
07. Sep	0.388514079	1.309044444	0.045311299
GNG11	0.389035432	1.309517584	0.007281815
SLC30A10	0.389248703	1.309711182	0.036746083
UBE4A	0.389500565	1.309939848	0.005430149
RB1CC1	0.389591017	1.31002198	0.012608351
AGXT2	0.389752858	1.310168945	0.029509206
RPL15	0.389860366	1.310266581	0.012608351
WDR44	0.389937737	1.310336852	0.026344429
GATAD1	0.390082603	1.310468434	0.006298355
RNASEH2B	0.390108087	1.310491583	0.009640554
ILK	0.390124242	1.310506257	0.040853946
NDUFB3	0.391133722	1.311423564	0.026344429
ARSB	0.391407837	1.31167276	0.007281815
LINC00174	0.391569645	1.311819881	0.000831696
SFT2D2	0.391712285	1.311949588	0.040853946
MALSU1	0.391912139	1.312131342	0.011041353
ZNF652	0.392081353	1.312285252	0.020832926
OSTC	0.392108941	1.312310346	0.023457892
POLK	0.392476842	1.312645041	0.029509206
TBC1D1	0.392638031	1.312791708	0.018451648
TNKS2	0.393140985	1.313249455	0.018451648
SRP9	0.393542017	1.313614555	0.002070906
RPL22L1	0.393981257	1.314014556	0.000455291
TP53INP1	0.394197454	1.314211484	0.029509206
PACRGL	0.394366559	1.314365538	0.023457892
PRKCQ	0.394787603	1.314749186	0.045311299
ZNF12	0.394877276	1.314830908	0.008391519
CISD2	0.39606761	1.315916192	0.007281815
POLDIP2	0.396525819	1.316334202	0.012608351
SNAPC3	0.39708059	1.31684048	0.020832926
LYRM1	0.397089633	1.316848734	0.014355333

CNNM2	0.39713334	1.316888629	0.00466565
LCMT1	0.397523071	1.317244423	0.026344429
LDB2	0.397953361	1.317637355	0.003408791
SMAP1	0.398210794	1.317872494	0.026344429
RUFY3	0.398607053	1.318234518	0.0000414
CCDC198	0.398654502	1.318277874	0.014355333
CTNNB1	0.399501626	1.31905217	0.045311299
IPO11	0.399569022	1.319113791	0.002070906
IPO11-LRRC70	0.399569022	1.319113791	0.002070906
LRRC70	0.399569022	1.319113791	0.002070906
H2AFY	0.399605601	1.319147238	0.045311299
SNX9	0.399879641	1.319397833	0.014355333
CCDC144B	0.400297348	1.319779897	0.029509206
FAM106A	0.400297348	1.319779897	0.029509206
USP32P2	0.400297348	1.319779897	0.029509206
ME1	0.401614397	1.320985286	0.009640554
MSRB2	0.401710129	1.321072945	0.002070906
PSMF1	0.402042193	1.32137705	0.018451648
DLEU2	0.402084499	1.321415799	0.029509206
MIR15A	0.402084499	1.321415799	0.029509206
MIR16-1	0.402084499	1.321415799	0.029509206
MIR3613	0.402084499	1.321415799	0.029509206
CROT	0.402116849	1.32144543	0.012608351
MAN1A1	0.402384858	1.321690937	0.029509206
GNAI3	0.402426738	1.321729306	0.00100707
YAE1	0.402499769	1.321796214	0.040853946
WDR76	0.403216368	1.322452925	0.020832926
CTHRC1	0.404106118	1.32326877	0.014355333
TARDBP	0.404308285	1.323454214	0.016298131
TMEM126A	0.404712156	1.323824757	0.045311299
PCNA	0.405265989	1.324333055	0.036746083
RPL24	0.405652644	1.324688035	0.036746083
ESF1	0.405660044	1.32469483	0.020832926
SEC24C	0.405711833	1.324742384	0.012608351
ANKIB1	0.405749008	1.32477652	0.026344429
PTPA	0.405873421	1.324890769	0.009640554
CAMLG	0.406650555	1.325604638	0.018451648
NCL	0.407071693	1.325991652	0.032970758
SLC2A13	0.40709279	1.326011043	0.009640554
NRIP1	0.407515821	1.326399917	0.006298355
TNPO2	0.408004653	1.32684942	0.009640554
TBC1D7	0.408006226	1.326850867	0.018451648
UGP2	0.408535681	1.327337897	0.006298355
ARL3	0.408850304	1.327627395	0.003408791
MAP4	0.409169077	1.327920775	0.014355333
GFM1	0.409181127	1.327931866	0.026344429
HNF4G	0.409253097	1.327998113	0.026344429

SMARCE1	0.409329014	1.328067996	0.020832926
RAB5A	0.409469294	1.328197137	0.045311299
UHRF1BP1	0.410007163	1.328692411	0.001740183
ARHGEF12	0.410170448	1.328842802	0.032970758
ZBTB2	0.410432729	1.329084406	0.026344429
MIR1287	0.410671586	1.329304472	0.032970758
PYROXD2	0.410671586	1.329304472	0.032970758
RPS5	0.410789183	1.32941283	0.040853946
APOO	0.410933774	1.329546075	0.029509206
COX6B1	0.41121262	1.329803076	0.036746083
PTBP2	0.411879944	1.330418324	0.020832926
MIR99AHG	0.412957964	1.331412819	0.009640554
NDUFV2	0.4133265	1.331752972	0.032970758
ENOPH1	0.413897006	1.33227971	0.040853946
MRPL52	0.414065318	1.33243515	0.003408791
TMEM209	0.414436685	1.332778178	0.011041353
KMT2A	0.414455831	1.332795866	0.023457892
FAM122A	0.414809339	1.333122485	0.003995217
CAPZA1	0.415062777	1.333356695	0.032970758
ADAR	0.415826777	1.33406298	0.002898085
MAP2K6	0.416644746	1.334819572	0.023457892
ATP6V1B2	0.417122528	1.335261702	0.016298131
HAUS6	0.417450069	1.335564887	0.012608351
SDC3	0.417518742	1.335628462	0.032970758
ASH2L	0.417623888	1.335725808	0.029509206
ZNF33A	0.41769656	1.335793093	0.023457892
KIF21A	0.417776345	1.335866969	0.011041353
CHD1	0.418315548	1.336366338	0.045311299
CALM3	0.418503668	1.336540604	0.012608351
PIK3C3	0.418633695	1.33666107	0.020832926
HEATR5B	0.418912758	1.336919648	0.007281815
GATAD2B	0.419042215	1.337039618	0.026344429
SNRPD2	0.419167264	1.337155514	0.032970758
SUSD1	0.419272751	1.337253289	0.009640554
NMI	0.419519227	1.337481769	0.040853946
DAP3	0.420309758	1.338214849	0.032970758
ANXA13	0.420790221	1.338660592	0.029509206
ATG5	0.421264505	1.339100747	0.032970758
ACACB	0.421376915	1.339205088	0.032970758
ILF2	0.422547435	1.340292084	0.012608351
RAB5C	0.424179798	1.34180944	0.036746083
FLRT3	0.424659819	1.342255968	0.026344429
LINC00266-1	0.424690594	1.3422846	0.018451648
MIR6844	0.424759358	1.34234858	0.016298131
TATDN1	0.424759358	1.34234858	0.016298131
NDUFA12	0.425131935	1.342695287	0.029509206
GUF1	0.425460642	1.343001245	0.026344429

VPS33A	0.425802055	1.343319103	0.020832926
KIF2A	0.426806246	1.344254449	0.032970758
MLX	0.427783273	1.345165118	0.0000014
ARFIP1	0.428051824	1.345415537	0.001456447
C6orf62	0.428432553	1.34577064	0.040853946
THOC5	0.428860317	1.346169726	0.009640554
ZNF44	0.428891225	1.346198566	0.012608351
BPHL	0.429019136	1.346317927	0.040853946
CAPZB	0.429674201	1.34692937	0.011041353
SH3GLB1	0.430627103	1.347819312	0.008391519
TRIM37	0.430739952	1.347924744	0.026344429
STK39	0.43101808	1.348184627	0.023457892
TMEM38B	0.431617244	1.348744657	0.005430149
FAM133B	0.431874907	1.348985562	0.029509206
SMIM11A	0.432464856	1.349537304	0.007281815
DHFR	0.432542575	1.349610006	0.036746083
RPL17-C18orf32	0.432646837	1.349707545	0.045311299
RPF2	0.432804612	1.349855159	0.012608351
SPG21	0.432805481	1.349855971	0.026344429
FUBP3	0.433080293	1.350113123	0.040853946
DNAJC1	0.433427753	1.350438325	0.000296775
HERC4	0.434061789	1.351031946	0.011041353
MAPK1	0.43429972	1.351254778	0.000831696
VRK1	0.434893337	1.351810886	0.014355333
CSNK1G3	0.434920413	1.351836256	0.023457892
MPRIP	0.435016009	1.351925835	0.029509206
SLC7A8	0.435148245	1.352049757	0.032970758
DDX59	0.435500007	1.352379457	0.012608351
NFE2L2	0.436337729	1.353164965	0.012608351
DCP2	0.436454069	1.353274089	0.026344429
MELK	0.437041551	1.35382527	0.026344429
CISD1	0.438001687	1.354726561	0.040853946
GRB10	0.438770628	1.355448809	0.00466565
PARD3	0.438961503	1.355628153	0.003995217
MAN2A1	0.439585257	1.35621439	0.029509206
SETD2	0.439598367	1.356226714	0.020832926
ANK3	0.439748865	1.356368199	0.000296775
FBXO8	0.440276078	1.356863956	0.020832926
VPS45	0.440426057	1.35700502	0.036746083
FAM104B	0.441293105	1.357820813	0.018451648
RNF20	0.441621593	1.358130011	0.001213644
NDUFB2	0.44201725	1.358502528	0.023457892
NFX1	0.442048946	1.358532374	0.023457892
ZBED6	0.442787454	1.359227978	0.036746083
ZC3H11A	0.442787454	1.359227978	0.036746083
FNIP1	0.44305608	1.359481087	0.002454436
VPS41	0.443371779	1.359778608	0.014355333

SMARCB1	0.444240491	1.360597639	0.020832926
KLHL5	0.44450672	1.360848742	0.029509206
TMEM131	0.445962388	1.36222252	0.026344429
MTCH2	0.446604325	1.362828785	0.014355333
ZNF17	0.448429907	1.364554396	0.016298131
RPS11	0.448786183	1.364891417	0.007281815
SNORD35B	0.448786183	1.364891417	0.007281815
SLAIN2	0.448812381	1.364916202	0.012608351
PTPRA	0.44899701	1.365090889	0.023457892
RASSF5	0.449797192	1.365848238	0.032970758
RAB11FIP2	0.450114116	1.366148314	0.029509206
TMEM64	0.450283704	1.366308913	0.009640554
BET1	0.450755271	1.366755585	0.005430149
RALGPS2	0.451036452	1.367021991	0.009640554
N4BP1	0.451207362	1.367183947	0.011041353
ELF2	0.451369161	1.367337285	0.001740183
AFDN	0.451377433	1.367345126	0.006298355
TFB2M	0.451408715	1.367374774	0.008391519
ITCH	0.451538582	1.367497867	0.036746083
RPS4X	0.451578019	1.367535248	0.040853946
ZNF791	0.452364042	1.368280525	0.029509206
EIF3L	0.452366781	1.368283122	0.018451648
XRN2	0.454522241	1.370328936	0.009640554
ATP5MG	0.455629935	1.371381471	0.018451648
RWDD4	0.455776272	1.371520581	0.026344429
PLRG1	0.457572024	1.373228804	0.032970758
RSU1	0.457669712	1.373321792	0.036746083
RPL36A	0.457811362	1.373456637	0.045311299
QRICH1	0.458049395	1.373683265	0.003995217
IL18	0.458601685	1.374209236	0.000237495
NECTIN3	0.458635556	1.3742415	0.002454436
TPK1	0.459270568	1.374846515	0.018451648
PHLDB2	0.459656495	1.375214341	0.023457892
PLCXD2	0.459656495	1.375214341	0.023457892
HDGF	0.460384011	1.375908003	0.018451648
NPAS2	0.460788673	1.376293986	0.036746083
RNF217	0.46101371	1.376508682	0.032970758
GBP3	0.461231207	1.376716218	0.029509206
FAM129A	0.461338561	1.376818666	0.009640554
RAD23B	0.461576514	1.377045771	0.023457892
RNF115	0.461954921	1.377407007	0.008391519
CAPNS1	0.462071934	1.377518729	0.045311299
SHTN1	0.462477699	1.377906217	0.014355333
HSD17B12	0.462525791	1.37795215	0.032970758
SUPT4H1	0.462756066	1.378172109	0.032970758
SPPL3	0.463048589	1.378451578	0.026344429
ZBTB24	0.463274376	1.378667327	0.001456447

STYX	0.463280839	1.378673503	0.029509206
ERMAP	0.463811578	1.379180784	0.026344429
COA5	0.464048979	1.379407751	0.023457892
PON2	0.46443674	1.379778552	0.011041353
PSMB9	0.465428764	1.38072764	0.040853946
XPO7	0.465585141	1.380877308	0.012608351
ELMOD2	0.465815417	1.381097735	0.036746083
HNRNPD	0.465857522	1.381138043	0.009640554
PHF21A	0.465914817	1.381192894	0.045311299
EMC2	0.465992368	1.381267141	0.016298131
DPY19L1	0.466121576	1.381390853	0.036746083
NHSL1	0.467019568	1.382250955	0.001456447
RAD18	0.468502039	1.383672045	0.040853946
TBC1D8B	0.468625721	1.383790672	0.002070906
ZNF780A	0.46977868	1.384896998	0.032970758
ZDHHC20	0.470926122	1.38599891	0.045311299
SCAPER	0.472163629	1.387188294	0.005430149
MSC	0.472515556	1.387526721	0.045311299
PTGFRN	0.47322445	1.388208676	0.014355333
MFSD14B	0.473583319	1.388554034	0.00466565
SLC30A6	0.473687798	1.388654595	0.012608351
ITSN2	0.474282241	1.38922689	0.029509206
LPCAT3	0.474457774	1.389395928	0.045311299
ANKRD17	0.476435257	1.39130166	0.029509206
ASPN	0.477416169	1.39224795	0.014355333
MIR6805	0.47751723	1.392345482	0.018451648
RPL28	0.47751723	1.392345482	0.018451648
PHF20	0.47764069	1.392464638	0.00100707
ABCA5	0.477736234	1.392556859	0.001213644
UBR3	0.478810888	1.393594551	0.026344429
NEK4	0.479850618	1.394599257	0.020832926
WBP11	0.480347368	1.39507953	0.036746083
UBTD2	0.480390546	1.395121283	0.012608351
EPC1	0.480641361	1.395363848	0.002454436
TMA16	0.48078846	1.395506128	0.036746083
URI1	0.480794562	1.39551203	0.005430149
SEC61A2	0.480848932	1.395564624	0.026344429
MARCHF2	0.48087866	1.395593381	0.020832926
FN1	0.480930069	1.395643113	0.011041353
KIAA1586	0.480980865	1.395692253	0.036746083
C2CD2	0.481152598	1.395858401	0.007281815
ACP1	0.481434734	1.396131404	0.032970758
CERK	0.482091479	1.396767096	0.016298131
YPEL2	0.482463319	1.397127145	0.018451648
CARD16	0.482512854	1.397175116	0.012608351
CKAP2	0.482631294	1.397289824	0.012608351
EFCAB14	0.482701598	1.397357917	0.040853946

RPS14	0.483576241	1.398205331	0.026344429
CUL3	0.484188612	1.398798944	0.032970758
STK3	0.484370908	1.398975704	0.045311299
BUD31	0.484713644	1.399308093	0.029509206
SNX6	0.485112789	1.399695288	0.005430149
SLC35F6	0.485185469	1.399765804	0.003995217
CHP1	0.485338562	1.399914349	0.011041353
WTAP	0.485651208	1.400217758	0.007281815
CNOT4	0.48575577	1.400319244	0.012608351
S100A10	0.486644472	1.401182109	0.014355333
MGST2	0.486752899	1.40128742	0.029509206
ATP5PD	0.487031164	1.401557724	0.040853946
CALD1	0.487858881	1.40236207	0.003408791
TBC1D15	0.488321012	1.402811353	0.016298131
COBLL1	0.489763884	1.404215039	0.045311299
LYRM7	0.49010838	1.404550386	0.003995217
RTN4	0.491002085	1.405420732	0.045311299
RAD17	0.491061526	1.405478638	0.000831696
CPQ	0.491304657	1.405715517	0.029509206
KIF5B	0.491314387	1.405724997	0.001213644
HSPA4L	0.491432626	1.405840211	0.029509206
PNPLA3	0.492008985	1.406401959	0.045311299
ORMDL1	0.493316513	1.407677171	0.016298131
SLBP	0.494099194	1.408441062	0.036746083
AMD1	0.49414459	1.408485381	0.020832926
SRP19	0.494636874	1.408966074	0.011041353
SIL1	0.494829525	1.409154233	0.029509206
ANKHD1	0.49600347	1.410301352	0.009640554
ANKHD1-EIF4EBP3	0.49600347	1.410301352	0.009640554
EIF4EBP3	0.49600347	1.410301352	0.009640554
PPP6C	0.496411836	1.410700606	0.001213644
PIBF1	0.496448829	1.410736779	0.00466565
CARNMT1	0.49711065	1.411384088	0.005430149
ATP13A3	0.497979825	1.412234655	0.020832926
PDP1	0.498421342	1.412666916	0.014355333
CTDSPL2	0.498872	1.413108263	0.032970758
MXI1	0.498905406	1.413140984	0.040853946
RIN2	0.499024181	1.413257332	0.002070906
FRS2	0.499046568	1.413279262	0.003995217
YBX1	0.499117917	1.413349158	0.045311299
ADPRM	0.499328981	1.413555943	0.002070906
BCAP29	0.499565396	1.413787602	0.008391519
OXR1	0.499838231	1.414054996	0.000455291
ATG3	0.499998913	1.414212497	0.032970758
ZHX1	0.500911002	1.415106862	0.016298131
ATP5MPL	0.501359257	1.415546613	0.020832926
CEP170	0.501506264	1.415690861	0.020832926

FAM111A	0.501542037	1.415725965	0.005430149
LSMEM1	0.501792921	1.41597218	0.029509206
LYPLA1	0.501793779	1.415973023	0.016298131
NUP88	0.501846439	1.416024708	0.000237495
STT3B	0.502168677	1.416341024	0.045311299
ARL17A	0.502618058	1.416782265	0.014355333
ARL17B	0.502618058	1.416782265	0.014355333
PLAA	0.503015511	1.417172633	0.009640554
TNFAIP1	0.503317139	1.417468956	0.00466565
NIPAL2	0.503516047	1.4176644	0.045311299
DOCK7	0.504162327	1.418299609	0.005430149
NECTIN1	0.504467359	1.418599514	0.023457892
RAB11A	0.504742756	1.418870338	0.032970758
CHURC1-FNTB	0.505105608	1.419227242	0.045311299
UBB	0.505183745	1.41930411	0.032970758
RNF220	0.505382398	1.419499556	0.007281815
PSMG2	0.505734286	1.419845829	0.029509206
SERINC3	0.505933597	1.420041997	0.005430149
CCDC90B	0.505943591	1.420051834	0.045311299
CUL1	0.50637317	1.420474733	0.009640554
MS4A7	0.506888714	1.420982427	0.018451648
WEE1	0.507119415	1.421209675	0.020832926
AGFG1	0.507163553	1.421253156	0.040853946
MIR5703	0.507163553	1.421253156	0.040853946
RNF149	0.507264582	1.421352687	0.011041353
ATP5PO	0.508325273	1.422398071	0.045311299
KLF10	0.508332079	1.422404782	0.026344429
DUSP3	0.509764431	1.42381769	0.009640554
NRP2	0.511794266	1.425822375	0.011041353
THRA	0.511839946	1.425867522	0.026344429
PDCD1LG2	0.512662423	1.426680637	0.003995217
SYNRG	0.51315591	1.42716873	0.023457892
TAB3	0.513502468	1.427511599	0.006298355
C5orf24	0.513751516	1.427758048	0.00466565
GNG5	0.513838544	1.427844177	0.045311299
ZDHHC4	0.514627564	1.428625288	0.016298131
TNS3	0.515085735	1.429079063	0.026344429
ARPC1A	0.515230406	1.429222376	0.008391519
RFX3	0.515311186	1.429302404	0.032970758
SLC11A2	0.515647365	1.429635501	0.002070906
CDK4	0.516134567	1.430118374	0.018451648
ORC3	0.516244789	1.430227639	0.018451648
PPIP5K2	0.516583406	1.43056337	0.012608351
RNF11	0.516798747	1.430776915	0.000237495
PRKAG1	0.517063006	1.431039016	0.007281815
TMED2	0.517277023	1.43125132	0.040853946
EIF3F	0.517835734	1.431805705	0.029509206

USP33	0.517976335	1.431945252	0.002898085
PIAS1	0.51940015	1.433359156	0.018451648
RPS16	0.519499092	1.433457461	0.032970758
GPBP1	0.519513338	1.433471616	0.012608351
NOA1	0.520300961	1.434254417	0.023457892
FBXO7	0.521065494	1.435014679	0.016298131
TIA1	0.521596285	1.435542741	0.006298355
GLUD1	0.521714503	1.435660378	0.032970758
TNRC6B	0.521767569	1.435713186	0.002070906
NDUFA4	0.522140018	1.43608388	0.023457892
GOLIM4	0.522524952	1.436467101	0.009640554
CCDC14	0.522758778	1.436699937	0.045311299
RGPD5	0.523100604	1.437040383	0.036746083
RGPD8	0.523100604	1.437040383	0.036746083
NT5C3B	0.523307567	1.437246549	0.036746083
CHCHD3	0.523551879	1.437489959	0.023457892
CCDC58	0.52443545	1.438370612	0.018451648
TRIM24	0.524837571	1.438771584	0.029509206
INO80	0.525710791	1.439642693	0.023457892
LRRC37A3	0.526430925	1.440361482	0.018451648
UBE2L3	0.527109076	1.441038695	0.026344429
EBLN2	0.527290753	1.441220176	0.00466565
AP2B1	0.527307842	1.441237247	0.036746083
ARRDC3	0.52760645	1.441535584	0.045311299
AGAP4	0.527674615	1.441603696	0.045311299
RGL1	0.528382639	1.442311357	0.020832926
HSD17B4	0.529222586	1.443151326	0.032970758
MAP3K7	0.52984813	1.443777204	0.014355333
SCARB1	0.53057313	1.44450293	0.020832926
TMEM50A	0.531232261	1.445163038	0.016298131
MYL6	0.531269991	1.445200833	0.032970758
PLXDC2	0.531377243	1.445308275	0.012608351
TIMM23	0.531573847	1.445505248	0.005430149
TRIM2	0.532904469	1.446839078	0.012608351
PSAP	0.53315329	1.447088634	0.014355333
ZDHHC3	0.533177532	1.447112951	0.012608351
GMFG	0.533793329	1.447730765	0.032970758
HSPB11	0.534072166	1.448010602	0.011041353
TGOLN2	0.535262469	1.449205784	0.011041353
GRHPR	0.537415799	1.451370447	0.005430149
RPA3	0.537458421	1.451413326	0.032970758
TXNRD2	0.537568156	1.451523728	0.023457892
EDNRA	0.538852332	1.452816338	0.029509206
RBM5	0.538943497	1.452908146	0.029509206
TSSK3	0.539493029	1.453461673	0.009640554
GSR	0.539678129	1.453648166	0.029509206
ADAM1A	0.540485535	1.45446193	0.020832926

MAPKAPK5	0.540485535	1.45446193	0.020832926
NR1H4	0.54089211	1.454871879	0.000368536
RNF213	0.541179454	1.455161677	0.020832926
RAP1A	0.541493764	1.455478737	0.045311299
STX8	0.543087185	1.457087166	0.003995217
RASAL2	0.543147403	1.457147986	0.002454436
RUFY2	0.543481395	1.457485363	0.040853946
DKK3	0.544220067	1.458231799	0.011041353
SHOC2	0.544225573	1.458237364	0.016298131
YBEY	0.544515563	1.458530507	0.023457892
TGIF1	0.544525521	1.458540575	0.009640554
PABPN1	0.544877633	1.458896598	0.045311299
LSM12	0.544901117	1.458920346	0.020832926
WDR33	0.545088107	1.459109451	0.011041353
PCM1	0.54514597	1.459167974	0.011041353
CDC42SE2	0.54551459	1.45954085	0.016298131
RPL3	0.545809068	1.459838797	0.012608351
SNORD139	0.545809068	1.459838797	0.012608351
SNORD43	0.545809068	1.459838797	0.012608351
SNORD83B	0.545809068	1.459838797	0.012608351
FMO3	0.546409088	1.460446074	0.029509206
KIAA1551	0.546440019	1.460477386	0.023457892
RPS7	0.547121418	1.461167346	0.016298131
PPP1CC	0.547218431	1.461265605	0.040853946
OSGIN2	0.547805468	1.461860319	0.014355333
LINC01578	0.548046756	1.462104833	0.045311299
RBM27	0.549175698	1.463249411	0.026344429
CD58	0.549893702	1.463977825	0.008391519
APOL2	0.550370552	1.46446179	0.009640554
SYMPK	0.550779371	1.464876836	0.014355333
GSK3B	0.551772905	1.465885993	0.040853946
DNAJB9	0.551851811	1.46596617	0.026344429
ZNF302	0.552333809	1.466456025	0.045311299
CFL1	0.552588624	1.46671506	0.040853946
SBDS	0.552635608	1.466762826	0.020832926
C7orf31	0.553921657	1.468070913	0.011041353
GPAM	0.554608403	1.468769905	0.029509206
SYNPO	0.554851425	1.46901734	0.016298131
MIR3658	0.555043633	1.469213067	0.040853946
UCK2	0.555043633	1.469213067	0.040853946
APOBEC3D	0.555251928	1.469425206	0.012608351
SCAF8	0.55532362	1.469498228	0.026344429
RPL22	0.55600458	1.470192004	0.032970758
IMPACT	0.556203919	1.470395156	0.006298355
SDCBP	0.557250696	1.471462419	0.014355333
JCAD	0.558234015	1.472465687	0.005430149
DHX36	0.558987964	1.473235395	0.014355333

BNIP3L	0.559274148	1.473527666	0.029509206
PRPF38A	0.559341566	1.473596526	0.026344429
IDI1	0.559946531	1.474214579	0.020832926
DENND1B	0.560468858	1.474748415	0.040853946
SP1	0.561409282	1.475710046	0.009640554
CALR	0.561630283	1.475936122	0.032970758
VEZF1	0.561985677	1.476299749	0.006298355
RPL37A	0.561991224	1.476305425	0.040853946
CALU	0.562172991	1.476491439	0.020832926
SAMD9L	0.562327473	1.476649547	0.006298355
NUP153	0.562371907	1.476695028	0.020832926
TAGLN2	0.56396294	1.478324455	0.029509206
SMYD2	0.5643415	1.478712415	0.012608351
PSME1	0.564872845	1.479257126	0.029509206
LMAN1	0.564950347	1.479336594	0.023457892
ORC4	0.565397474	1.479795148	0.045311299
CDV3	0.56550808	1.479908603	0.029509206
ARF3	0.565797004	1.480205009	0.040853946
FKBP11	0.565797004	1.480205009	0.040853946
ARHGAP12	0.566121461	1.480537939	0.000455291
IRF1	0.5667741	1.48120785	0.029509206
SGCB	0.567172489	1.48161693	0.009640554
DYRK1A	0.56868398	1.483170012	0.011041353
CYTH1	0.569296877	1.483800238	0.018451648
ADD1	0.56955679	1.484067581	0.009640554
CDC27	0.569647026	1.484160407	0.026344429
UBE2B	0.571624112	1.486195712	0.008391519
TDRD3	0.571779384	1.486355675	0.005430149
PDZK1	0.572017965	1.486601496	0.023457892
CD36	0.572045109	1.486629467	0.002454436
WIPI2	0.572083128	1.486668644	0.002898085
ARV1	0.573794689	1.48843342	0.008391519
DALRD3	0.573795485	1.488434241	0.020832926
CHKB	0.573801143	1.488440078	0.005430149
SKIL	0.573997775	1.488642959	0.006298355
RPL11	0.575055063	1.48973432	0.045311299
PALMD	0.57541589	1.490106959	0.032970758
ARHGAP35	0.575573982	1.490270255	0.006298355
FAM107B	0.575629975	1.490328096	0.00100707
MYO9A	0.575797701	1.49050137	0.0000414
CPLANE1	0.576177121	1.490893413	0.002070906
QSER1	0.576701656	1.491435572	0.045311299
ZSWIM6	0.57772944	1.492498457	0.003408791
SNX25	0.578398385	1.493190656	0.018451648
SLC39A8	0.57867846	1.493480561	0.002070906
EVI2A	0.578792421	1.493598538	0.023457892
EVI2B	0.578792421	1.493598538	0.023457892

LPGAT1	0.579496091	1.494327214	0.026344429
LEPR	0.580478791	1.49534543	0.040853946
LEPROT	0.580478791	1.49534543	0.040853946
MRPS15	0.581066637	1.495954853	0.032970758
RGPD6	0.582629114	1.49757589	0.029509206
EEF1A1	0.582677064	1.497625665	0.012608351
RPL32	0.58314727	1.498113853	0.012608351
SNORA7A	0.58314727	1.498113853	0.012608351
FGD4	0.583421724	1.498398877	0.014355333
UBE2D1	0.583892049	1.498887442	0.018451648
ACOT13	0.584989799	1.500028383	0.045311299
NGDN	0.585371711	1.500425525	0.029509206
DGAT1	0.585372828	1.500426687	0.023457892
MIR6848	0.585372828	1.500426687	0.023457892
ATP5F1B	0.585771077	1.500840929	0.045311299
TAPBPL	0.585945683	1.501022583	0.040853946
SAMM50	0.587302927	1.502435365	0.036746083
USP16	0.587862561	1.503018286	0.040853946
TRMO	0.589834375	1.505073951	0.023457892
UQCR10	0.589881369	1.505122978	0.029509206
CASK	0.590965847	1.506254809	0.029509206
ANAPC15	0.591226158	1.506526612	0.012608351
ZNF268	0.59172313	1.507045662	0.016298131
FAM117B	0.591900953	1.507231428	0.007281815
ZCCHC10	0.592841575	1.508214448	0.00466565
PPAT	0.593815689	1.509233145	0.045311299
BANF1	0.595160806	1.510640956	0.036746083
KAT2B	0.595796453	1.511306686	0.00466565
SETBP1	0.59595844	1.511476386	0.009640554
PRC1-AS1	0.596453431	1.511995065	0.036746083
CDK9	0.596543081	1.512089024	0.008391519
GAPDH	0.597422501	1.513011026	0.036746083
TMA7	0.597709942	1.513312506	0.040853946
FARP1	0.598351478	1.513985594	0.002070906
MIR3170	0.598351478	1.513985594	0.002070906
UBN2	0.599381149	1.515066532	0.029509206
CS	0.599602984	1.515299513	0.012608351
EPRS	0.600092907	1.515814179	0.032970758
ENPP1	0.602498192	1.518343478	0.032970758
SMG1	0.602808376	1.518669961	0.003995217
HSPA8	0.605070123	1.521052683	0.029509206
SNORD14C	0.605070123	1.521052683	0.029509206
SNORD14D	0.605070123	1.521052683	0.029509206
A1CF	0.605994531	1.522027611	0.016298131
CACUL1	0.606034516	1.522069796	0.029509206
MRAP2	0.606581708	1.522647203	0.029509206
PIK3AP1	0.607373826	1.523483448	0.001456447

EIF2AK2	0.60742331	1.523535704	0.029509206
SEC62	0.60851031	1.524684046	0.014355333
TFG	0.608580645	1.52475838	0.023457892
RPS20	0.608800695	1.524990965	0.023457892
SNORD54	0.608800695	1.524990965	0.023457892
SEC24A	0.608987359	1.525188289	0.00100707
MRPS7	0.609580528	1.525815505	0.032970758
INHBA	0.609780398	1.526026905	0.011041353
PPIL4	0.609828063	1.526077324	0.014355333
USP14	0.61092679	1.527239995	0.026344429
NGLY1	0.611380868	1.527720759	0.016298131
BCLAF1	0.611471991	1.527817256	0.026344429
COQ5	0.612065273	1.528445672	0.000683798
EFEMP1	0.612323581	1.528719358	0.003995217
CHRNA10	0.61269078	1.529108502	0.045311299
NUP98	0.61269078	1.529108502	0.045311299
HNRNPK	0.61284847	1.529275646	0.011041353
MIR7-1	0.61284847	1.529275646	0.011041353
RNF128	0.613010447	1.529447353	0.003408791
CLINT1	0.613129168	1.529573219	0.018451648
NEK9	0.615225016	1.531796892	0.014355333
PSME4	0.615382087	1.531963673	0.018451648
ALG2	0.615403379	1.531986282	0.045311299
NUP214	0.615605671	1.532201109	0.007281815
VPS26A	0.616831472	1.533503513	0.040853946
FTH1	0.617483104	1.534196318	0.026344429
PPIA	0.617967124	1.534711123	0.018451648
CTR9	0.618084521	1.534836012	0.006298355
SRRM1	0.618385822	1.53515659	0.032970758
POLR3C	0.619033332	1.535845753	0.032970758
AASDHPPT	0.619453838	1.536293475	0.023457892
EPS15	0.619659941	1.536512966	0.012608351
NCOR1	0.62010418	1.536986166	0.016298131
MAP3K4	0.621939143	1.538942302	0.003995217
RPL31	0.622142173	1.539158891	0.023457892
TXNDC11	0.623393385	1.540494343	0.029509206
FAM114A2	0.624669868	1.541857961	0.029509206
CYP3A7	0.62645502	1.543766996	0.045311299
CYP3A7-CYP3A51P	0.62645502	1.543766996	0.045311299
RPS6	0.62703289	1.544385474	0.014355333
ACAP2	0.627255844	1.544624161	0.003995217
EZH1	0.627625008	1.545019459	0.020832926
GPR65	0.627858463	1.545269492	0.007281815
NR2C1	0.628212555	1.545648806	0.002898085
UQCRH	0.628899512	1.54638496	0.045311299
VDAC2	0.632110468	1.549830529	0.016298131
SEPSECS	0.632728357	1.550494444	0.007281815

RDX	0.633479267	1.551301673	0.023457892
PAG1	0.633544494	1.551371812	0.036746083
FCGR3B	0.633587854	1.551418439	0.014355333
LARS	0.634209135	1.552086684	0.018451648
HSP90AA1	0.635470153	1.553443912	0.040853946
HMGN3	0.635883663	1.553889229	0.016298131
UBE2E1	0.636566111	1.55462445	0.023457892
GTF3C6	0.637220931	1.555330233	0.006298355
RBPJ	0.638206731	1.556393361	0.040853946
HECTD2	0.638432655	1.556637108	0.006298355
MOSPD2	0.638714657	1.556941413	0.000149389
UBE2D3	0.640287689	1.558639938	0.036746083
AGAP5	0.640331833	1.558687631	0.026344429
FAF1	0.640885859	1.559286316	0.036746083
RFX5	0.641023426	1.559435006	0.036746083
SYNCRIP	0.641136913	1.559557682	0.026344429
RAB2A	0.641608315	1.560067352	0.045311299
RNF43	0.641657039	1.56012004	0.011041353
DROSHA	0.642135174	1.560637178	0.005430149
WASL	0.643207079	1.561797144	0.018451648
DOCK11	0.64333379	1.561934321	0.007281815
SRI	0.644274709	1.562953339	0.011041353
EIF2AK1	0.64440996	1.563099872	0.023457892
CFAP97	0.644954054	1.563689486	0.007281815
NR5A2	0.645575957	1.564363691	0.001740183
PSMA2	0.646120295	1.564954047	0.016298131
RPS3A	0.64694181	1.565845434	0.002070906
SNORD73A	0.64694181	1.565845434	0.002070906
SNORA31	0.646955023	1.565859775	0.040853946
TPT1	0.646955023	1.565859775	0.040853946
TICAM2	0.647506592	1.566458547	0.040853946
TMED7	0.647506592	1.566458547	0.040853946
TMED7-TICAM2	0.647506592	1.566458547	0.040853946
LANCL2	0.648884483	1.567955356	0.000368536
RFC1	0.649083057	1.568171186	0.014355333
ARL8A	0.64971064	1.568853501	0.001740183
MIR4523	0.650086761	1.569262566	0.011041353
TAOK1	0.650086761	1.569262566	0.011041353
FAM20A	0.650708962	1.569939499	0.018451648
PICALM	0.651707024	1.571025964	0.020832926
TRAPPC11	0.652052698	1.571402432	0.003408791
MRPL51	0.653359437	1.572826394	0.014355333
ARFGEF1	0.65450014	1.57407048	0.029509206
DHCR24	0.655831767	1.575524039	0.006298355
LAPTM4A	0.656200121	1.575926359	0.036746083
MIR6850	0.657196268	1.577014875	0.008391519
RPL8	0.657196268	1.577014875	0.008391519

SYVN1	0.659436222	1.579465278	0.045311299
SMLR1	0.659909078	1.579983047	0.005430149
DUSP6	0.660572614	1.580709893	0.014355333
FGL2	0.66166451	1.581906696	0.045311299
EIF5	0.663274076	1.583672562	0.012608351
LOC100506548	0.663712321	1.584153704	0.036746083
RPL37	0.663712321	1.584153704	0.036746083
AGAP9	0.664180646	1.584668032	0.032970758
BMS1P2	0.664180646	1.584668032	0.032970758
PPT1	0.664355278	1.584859861	0.032970758
MLEC	0.664680772	1.585217471	0.032970758
CCNI	0.665384568	1.585990982	0.020832926
RPS12	0.665787934	1.586434474	0.036746083
CSTA	0.667375392	1.588181056	0.014355333
PCTP	0.667464166	1.588278785	0.023457892
STAM	0.667918054	1.588778554	0.012608351
GPR34	0.66813293	1.589015205	0.023457892
PNISR	0.668899488	1.589859733	0.040853946
PGM1	0.669832315	1.590888047	0.005430149
UBE2J1	0.671458287	1.592682049	0.020832926
EEF1G	0.671913184	1.593184318	0.026344429
MIR3654	0.671913184	1.593184318	0.026344429
AMZ2	0.672807746	1.594172498	0.032970758
MED24	0.674326387	1.595851475	0.011041353
MIR6884	0.674326387	1.595851475	0.011041353
MIR4534	0.675724403	1.597398654	0.026344429
MIR6820	0.675724403	1.597398654	0.026344429
POLR2F	0.675724403	1.597398654	0.026344429
TLK2	0.677121304	1.598946097	0.012608351
TBCA	0.67758886	1.599464375	0.040853946
TTLL5	0.677902853	1.599812526	0.00100707
CYP4V2	0.67807753	1.600006238	0.014355333
MIR423	0.678703699	1.600700835	0.020832926
NSRP1	0.678703699	1.600700835	0.020832926
LPAR6	0.67950041	1.601585047	0.003995217
CCNK	0.680995161	1.603245281	0.012608351
CUL2	0.681112044	1.603375177	0.023457892
TCTEX1D2	0.683335851	1.605848567	0.020832926
SNAP29	0.68368625	1.606238639	0.011041353
RPL12	0.686735613	1.609637267	0.018451648
CD63	0.688184029	1.6112541	0.012608351
OLA1	0.691679453	1.615162649	0.045311299
MATR3	0.692667206	1.616268862	0.029509206
SNHG4	0.692667206	1.616268862	0.029509206
SNORA74A	0.692667206	1.616268862	0.029509206
GABARAP	0.695160892	1.619064984	0.018451648
RRAGD	0.695232055	1.619144849	0.029509206

UBE2K	0.696620559	1.620703924	0.026344429
UQCRC2	0.698146844	1.62241944	0.009640554
EIF4B	0.698350052	1.622647979	0.045311299
CLDN2	0.700821421	1.625429993	0.012608351
PIP5K1A	0.701293465	1.625961914	0.007281815
NUP50	0.702582784	1.627415667	0.005430149
C8orf44-SGK3	0.703243931	1.628161637	0.029509206
BIRC2	0.703529057	1.628483448	0.032970758
RNF38	0.704124304	1.62915549	0.026344429
RNF130	0.706499609	1.631839999	0.016298131
HEBP2	0.707560267	1.633040157	0.020832926
ENY2	0.709293451	1.63500319	0.029509206
ZFR	0.709701884	1.635466132	0.012608351
PKN2	0.709986678	1.635789012	0.008391519
TCERG1	0.711735315	1.637772893	0.002070906
DYNC1LI2	0.712073905	1.638157312	0.026344429
THOC7	0.712767429	1.638944987	0.011041353
EVI5	0.714907804	1.641378321	0.020832926
TSC22D1	0.716075531	1.642707402	0.014355333
CD47	0.717404781	1.644221634	0.009640554
COX6C	0.717534206	1.644369144	0.045311299
CD164	0.719718291	1.646860428	0.040853946
CEP70	0.720021729	1.647206844	0.029509206
DEPDC5	0.721366535	1.648743001	0.036746083
PLCB1	0.722481871	1.650018124	0.045311299
CSNK1A1	0.722769692	1.650347339	0.032970758
HSDL2	0.722797263	1.650378879	0.003408791
CDC26	0.725171161	1.653096748	0.006298355
ARNT	0.72729007	1.655526461	0.018451648
RPS27L	0.730109198	1.65876464	0.032970758
CD302	0.73030519	1.65899	0.005430149
LY75	0.73030519	1.65899	0.005430149
LY75-CD302	0.73030519	1.65899	0.005430149
LRRC37A4P	0.731791377	1.660699883	0.008391519
ETV1	0.735184689	1.664610554	0.040853946
CCNT2	0.736608054	1.666253671	0.009640554
MEIS2	0.737599131	1.667398718	0.018451648
MS4A6A	0.738968101	1.668981659	0.023457892
NDUFA6	0.73928302	1.669346014	0.014355333
GLUL	0.739538166	1.669641269	0.040853946
DENND4A	0.740731672	1.671023093	0.016298131
NSA2	0.743605222	1.674354743	0.040853946
ZC3H7A	0.743977329	1.674786656	0.040853946
UBE2V2	0.744907326	1.675866614	0.001456447
WASHC3	0.746075856	1.677224554	0.007281815
ME2	0.747784806	1.679212494	0.014355333
ODF2L	0.749121665	1.680769241	0.040853946

AIF1	0.749809949	1.681571297	0.029509206
TAX1BP1	0.750887899	1.6828282	0.001456447
PCNX1	0.752202512	1.684362325	0.032970758
ANTXR1	0.753056095	1.685359188	0.005430149
OGFRL1	0.755490851	1.688205876	0.040853946
DBI	0.757589004	1.690662869	0.003995217
VAPA	0.759094606	1.692428172	0.016298131
PDS5A	0.760232218	1.693763233	0.014355333
CNOT9	0.762029171	1.695874219	0.045311299
NADK2	0.763435268	1.697527878	0.020832926
EWSR1	0.763969938	1.698157108	0.006298355
NNT	0.764427749	1.698696069	0.026344429
TAF2	0.764900359	1.699252634	0.016298131
SRP72	0.765072958	1.699455938	0.016298131
RNPS1	0.769661163	1.704869324	0.001213644
B2M	0.769901778	1.705153689	0.011041353
TPM3	0.770960016	1.706404902	0.009640554
THADA	0.771454477	1.706989847	0.036746083
TRAM1	0.771507964	1.707053133	0.032970758
DYNLT1	0.772705889	1.708471154	0.020832926
PLPPR1	0.774094742	1.710116655	0.029509206
PLEK	0.774822918	1.710980026	0.036746083
FAM200B	0.775252903	1.711490047	0.029509206
SGK3	0.780075993	1.717221324	0.008391519
MAX	0.780124397	1.717278939	0.020832926
SELENOW	0.781635384	1.71907845	0.026344429
BST2	0.782625447	1.720258589	0.020832926
RPL14	0.782630541	1.720264663	0.020832926
DOK2	0.783100106	1.720824662	0.029509206
PARP9	0.783129798	1.720860079	0.032970758
TMEM14C	0.785113971	1.723228446	0.029509206
ACACA	0.785724	1.72395725	0.000559323
GOLGA7	0.787792424	1.726430699	0.029509206
VSTM4	0.789494684	1.728468946	0.011041353
PSMB4	0.789625934	1.728626201	0.008391519
RGS10	0.791553367	1.730937181	0.026344429
ZHX2	0.79194372	1.731405588	0.001213644
RAB1A	0.792779199	1.732408551	0.001740183
DYNLL2	0.794475831	1.73444709	0.0000708
MIR4709	0.795089685	1.735185239	0.045311299
NPC2	0.795089685	1.735185239	0.045311299
PARK7	0.795644398	1.735852542	0.032970758
ATF7IP	0.796636868	1.737047093	0.005430149
CBX3	0.796982003	1.737462696	0.026344429
GAB1	0.799051466	1.739956775	0.032970758
UBC	0.801985134	1.743498514	0.005430149
TP53BP1	0.802156921	1.74370613	0.002070906

YWHAZ	0.802445727	1.74405523	0.009640554
BHLHE41	0.802778021	1.744456981	0.016298131
SLC22A3	0.803505648	1.745337024	0.040853946
SLAMF7	0.805922847	1.748263744	0.026344429
UBE2D2	0.807103854	1.749695478	0.023457892
HLA-F	0.807503441	1.750180163	0.023457892
INTS8	0.807693501	1.750410746	0.023457892
PALLD	0.808425636	1.751299266	0.018451648
JMJD1C	0.81070496	1.754068343	0.018451648
GTF2I	0.817200011	1.761983008	0.009640554
IFNAR2	0.818259662	1.763277649	0.032970758
MKLN1	0.818746604	1.763872896	0.018451648
ATRAID	0.820217342	1.765671972	0.023457892
GNB1	0.820232173	1.765690123	0.020832926
HLA-DMB	0.822159909	1.768051023	0.036746083
PAPOLA	0.822230619	1.768137682	0.036746083
MIR7703	0.822406287	1.76835299	0.026344429
PSME2	0.822406287	1.76835299	0.026344429
SECISBP2	0.822494516	1.768461138	0.007281815
RRM2B	0.823320192	1.769473545	0.009640554
HLA-DMA	0.824138077	1.77047697	0.014355333
HADH	0.824292395	1.770666358	0.020832926
METTL23	0.828055227	1.775290632	0.036746083
UBE2H	0.829579122	1.777166833	0.003995217
NUS1	0.83052717	1.778335058	0.029509206
CCDC91	0.831386774	1.779394963	0.045311299
CUX1	0.831660656	1.779732796	0.000683798
MTO1	0.833451359	1.78194321	0.002898085
RPS8	0.834097542	1.78274152	0.045311299
SNORD38A	0.834097542	1.78274152	0.045311299
SNORD38B	0.834097542	1.78274152	0.045311299
SNORD46	0.834097542	1.78274152	0.045311299
SNORD55	0.834097542	1.78274152	0.045311299
ZNF706	0.834635279	1.783406128	0.001456447
RELN	0.836609806	1.785848635	0.012608351
ZNF143	0.83738378	1.786806961	0.026344429
ARL8B	0.837479688	1.786925749	0.002070906
SELENOT	0.840712982	1.790935006	0.016298131
GNAI1	0.843335137	1.794193061	0.032970758
R3HDM1	0.845101689	1.796391361	0.003995217
POM121C	0.846923317	1.798661018	0.006298355
CSTB	0.847096863	1.798877397	0.020832926
IQGAP1	0.847941526	1.799930905	0.029509206
UBXN4	0.848575997	1.800722656	0.036746083
KDELR2	0.848755986	1.800947326	0.036746083
SLC2A14	0.848836057	1.801047283	0.026344429
PGRMC2	0.849363721	1.801706134	0.009640554

SELENOF	0.849493448	1.801868151	0.040853946
LMBRD1	0.851481621	1.804353011	0.011041353
CRYZ	0.851590986	1.804489797	0.00466565
PTP4A2	0.851866796	1.804834807	0.029509206
SAT1	0.854038496	1.807553685	0.045311299
TSPAN5	0.854766175	1.808465624	0.040853946
BMP2K	0.854926732	1.808666898	0.001740183
DDAH1	0.85561437	1.809529176	0.001456447
DDX17	0.85888426	1.813635153	0.023457892
LIMA1	0.860236396	1.815335743	0.0000414
TMEM123	0.861213706	1.816565902	0.005430149
DR1	0.86373573	1.81974428	0.002454436
ITGB1	0.864373702	1.820549165	0.032970758
TMSB10	0.866787826	1.823598119	0.045311299
IK	0.868098644	1.825255774	0.032970758
MIR3655	0.868098644	1.825255774	0.032970758
BLOC1S1	0.869150518	1.826587059	0.003995217
ASAH1	0.870729438	1.828587215	0.002070906
TOM1	0.872183536	1.830431185	0.00100707
AFTPH	0.873014181	1.831485375	0.001740183
CEMIP2	0.874855969	1.833824998	0.011041353
NCF1	0.87563558	1.834816237	0.006298355
RPL23A	0.878418415	1.838358857	0.026344429
SNORD42A	0.878418415	1.838358857	0.026344429
SNORD42B	0.878418415	1.838358857	0.026344429
SNORD4B	0.878418415	1.838358857	0.026344429
LRRC37A	0.880344703	1.840815075	0.016298131
NPIPA2	0.882868654	1.844038343	0.023457892
NPIPA3	0.882868654	1.844038343	0.023457892
LAP3	0.88290986	1.844091013	0.023457892
DHX8	0.88402001	1.845510582	0.005430149
CD3D	0.88552108	1.847431766	0.023457892
WAC	0.888714699	1.85152586	0.040853946
UBE2D4	0.890219093	1.853457576	0.012608351
CPVL	0.891639213	1.855282929	0.001456447
HLA-DQA1	0.892372045	1.856225578	0.001456447
ARPC2	0.894045976	1.858380571	0.026344429
BPTF	0.895903552	1.860774913	0.007281815
PREX1	0.897207899	1.86245801	0.016298131
ATF2	0.901382403	1.867854921	0.012608351
DRG1	0.901439566	1.867928931	0.029509206
ACSM3	0.907008823	1.875153661	0.018451648
RIOK3	0.907461377	1.875741964	0.032970758
AOX1	0.909414031	1.878282455	0.029509206
RCN1	0.912592769	1.8824255	0.005430149
EFR3A	0.913336358	1.883395984	0.003995217
PPWD1	0.914642002	1.885101235	0.002070906

PHACTR2	0.918354462	1.889958376	0.000831696
ITM2C	0.92099716	1.893423535	0.029509206
NOP10	0.921497736	1.894080616	0.020832926
SOD2	0.922738621	1.895710446	0.006298355
SOD2-OT1	0.922738621	1.895710446	0.006298355
S100A11	0.926187859	1.900248188	0.026344429
ATXN10	0.932741691	1.908900216	0.005430149
MEF2A	0.934640374	1.91141411	0.020832926
TFEC	0.936105257	1.913355907	0.002454436
SPTBN1	0.939837089	1.918311608	0.011041353
UTP6	0.943124648	1.922687969	0.014355333
ETV5	0.948343836	1.929656208	0.026344429
PARP14	0.954813011	1.93832839	0.026344429
PRDM1	0.955665271	1.939473779	0.012608351
CUL5	0.959860874	1.945122309	0.011041353
GOSR1	0.961425097	1.947232425	0.014355333
LENG8	0.963383047	1.9498769	0.032970758
SCD	0.963505252	1.950042075	0.002070906
MAL2	0.965381755	1.95258013	0.032970758
QKI	0.967998235	1.956124554	0.003995217
ATP5MF	0.977324515	1.968810852	0.018451648
UTRN	0.977646429	1.96925021	0.014355333
HLA-DRB1	0.983673848	1.977494728	0.032970758
WARS	0.985900212	1.980548749	0.036746083
HBS1L	0.988555129	1.984196806	0.007281815
GBP5	0.988821302	1.984562918	0.00466565
CASD1	0.989236574	1.985134246	0.00466565
TMEM230	0.989877813	1.98601678	0.012608351
LIPA	0.991476868	1.988219263	0.011041353
FAM91A1	0.991646779	1.988453436	0.029509206
SEC63	0.993728455	1.991324663	0.005430149
CD74	0.99430097	1.99211505	0.020832926
GLT8D1	0.999336606	1.999080552	0.018451648
RPL30	1.006824467	2.009483132	0.026344429
AHR	1.012046373	2.016769735	0.036746083
EIF4A2	1.014271665	2.019882911	0.014355333
MIR1248	1.014271665	2.019882911	0.014355333
SNORA4	1.014271665	2.019882911	0.014355333
SNORA63	1.014271665	2.019882911	0.014355333
SNORA81	1.014271665	2.019882911	0.014355333
SNORD2	1.014271665	2.019882911	0.014355333
EPB41	1.016726595	2.023322926	0.007281815
UBE2Q1	1.018068806	2.0252062	0.023457892
ELOC	1.027248833	2.038133896	0.036746083
ECPAS	1.037983321	2.053355352	0.002898085
ATM	1.039205566	2.055095683	0.023457892
SDHAF2	1.039690014	2.055785887	0.005430149

FABP5	1.049845517	2.070308148	0.020832926
SUB1	1.055290644	2.078136824	0.020832926
COPS3	1.055499441	2.078437609	0.003995217
MIR3614	1.057322983	2.081066379	0.002454436
TRIM25	1.057322983	2.081066379	0.002454436
HEXB	1.068572685	2.097357342	0.00466565
ASAP1	1.07237142	2.102887135	0.007281815
ASAP1-IT2	1.07237142	2.102887135	0.007281815
FNDC3B	1.074594425	2.106129907	0.023457892
NT5E	1.076822872	2.109385637	0.005430149
TAB2	1.083171409	2.118688379	0.000296775
ATG7	1.086149586	2.123066537	0.016298131
PGM3	1.087162353	2.124557446	0.009640554
TXNL4A	1.101141861	2.145244166	0.008391519
STK10	1.116453618	2.168133539	0.011041353
CTSS	1.124857292	2.180799736	0.002454436
KRIT1	1.135147204	2.196409725	0.011041353
HLA-DRA	1.137393158	2.199831707	0.008391519
CASP4	1.143170907	2.208659324	0.006298355
HSPE1	1.177562022	2.261942134	0.032970758
KCNRG	1.17926042	2.264606551	0.001740183
TRIM13	1.17926042	2.264606551	0.001740183
MBD2	1.182357756	2.269473679	0.036746083
FCER1G	1.182741253	2.27007703	0.008391519
SAMHD1	1.189232692	2.280314307	0.002454436
ANKRD12	1.195699642	2.29055887	0.001456447
EPSTI1	1.213880104	2.319606529	0.000559323
HLA-DRB5	1.268893187	2.409766212	0.00100707
ATP5PF	1.271918934	2.414825489	0.007281815
GBP1	1.2719597	2.414893725	0.003408791
ROBO1	1.284714757	2.436338778	0.002454436
DAD1	1.340464468	2.532328325	0.005430149
EPB41L2	1.554489572	2.937297862	0.002898085
TNFAIP3	1.679064586	3.202202595	0.045311299
STAT1	1.681927515	3.208563455	0.000189018
CXCL9	1.74870221	3.360561276	0.009640554

Table S5: GSEA between responding and non-responding patients treated in frontline

NAME	SIZE	ES	NES	NOM p-val	FDR q-val	FWER p-val	RANK AT MAX	LEADING EDGE
HALLMARK_ADIPOGENESIS	198	-0.40265	-1.7275	0	0.002	0.029	4121	tags=34%, list=20%, signal=43%
HALLMARK_ALLOGRAFT_REJECTION	196	-0.49353	-2.1355	0	0.000	0	4701	tags=39%, list=23%, signal=51%
HALLMARK_ANDROGEN_RESPONSE	99	-0.53868	-2.1358	0	0.000	0	3816	tags=41%, list=19%, signal=51%
HALLMARK_ANGIOGENESIS	36	-0.18875	-0.6225	0.94876	0.991	1	6857	tags=50%, list=34%, signal=75%
HALLMARK_APICAL_JUNCTION	200	-0.27231	-1.1787	0.14158	0.207	1	4694	tags=29%, list=23%, signal=37%
HALLMARK_APICAL_SURFACE	44	-0.22084	-0.7671	0.8319	0.963	1	5852	tags=32%, list=29%, signal=45%
HALLMARK_APOPTOSIS	160	-0.44949	-1.9037	0	0.000	0.003	4284	tags=35%, list=21%, signal=44%
HALLMARK_BILE_ACID_METABOLISM	112	-0.24113	-0.9805	0.51449	0.587	1	4104	tags=24%, list=20%, signal=30%
HALLMARK_CHOLESTEROL_HOMEOSTASIS	73	-0.47837	-1.8141	0	0.000	0.006	3215	tags=36%, list=16%, signal=42%
HALLMARK_COAGULATION	138	-0.29409	-1.2213	0.13876	0.165	0.998	4491	tags=28%, list=22%, signal=36%
HALLMARK_COMPLEMENT	200	-0.45723	-1.9821	0	0.000	0	4524	tags=39%, list=22%, signal=50%
HALLMARK_DNA_REPAIR	150	-0.48858	-2.0518	0	0.000	0	4850	tags=43%, list=24%, signal=56%
HALLMARK_E2F_TARGETS	198	-0.35215	-1.51	0	0.013	0.263	5121	tags=38%, list=25%, signal=50%
HALLMARK_EPITHELIAL_MESENCHYMAL_TRANSITION	198	-0.30748	-1.3262	0.03737	0.079	0.891	2472	tags=16%, list=12%, signal=18%
HALLMARK_ESTROGEN_RESPONSE_EARLY	198	-0.16878	-0.7314	0.96334	0.959	1	4472	tags=20%, list=22%, signal=25%
HALLMARK_ESTROGEN_RESPONSE_LATE	198	-0.28077	-1.2098	0.12358	0.176	0.998	3884	tags=24%, list=19%, signal=30%
HALLMARK_FATTY_ACID_METABOLISM	156	-0.42036	-1.7512	0	0.001	0.021	4068	tags=35%, list=20%, signal=44%
HALLMARK_G2M_CHECKPOINT	195	-0.46318	-1.991	0	0.000	0	5101	tags=46%, list=25%, signal=61%
HALLMARK_GLYCOLYSIS	199	-0.2836	-1.2243	0.10274	0.165	0.998	4876	tags=30%, list=24%, signal=39%
HALLMARK_HEDGEHOG_SIGNALING	36	-0.37613	-1.2497	0.14977	0.144	0.99	4989	tags=39%, list=25%, signal=51%
HALLMARK_HEME_METABOLISM	194	-0.43083	-1.8578	0	0.000	0.003	3098	tags=30%, list=15%, signal=35%
HALLMARK_HYPOXIA	197	-0.30602	-1.3149	0.03819	0.085	0.916	3891	tags=25%, list=19%, signal=31%
HALLMARK_IL2_STAT5_SIGNALING	199	-0.36663	-1.5834	0.00111	0.007	0.129	5580	tags=39%, list=28%, signal=54%
HALLMARK_IL6_JAK_STAT3_SIGNALING	87	-0.40655	-1.5744	0.00379	0.007	0.14	2960	tags=23%, list=15%, signal=27%
HALLMARK_INFLAMMATORY_RESPONSE	200	-0.34134	-1.4793	0	0.018	0.368	4504	tags=29%, list=22%, signal=37%
HALLMARK_INTERFERON_ALPHA_RESPONSE	96	-0.63697	-2.5177	0	0.000	0	3700	tags=50%, list=18%, signal=61%
HALLMARK_INTERFERON_GAMMA_RESPONSE	199	-0.58403	-2.4995	0	0.000	0	3750	tags=43%, list=19%, signal=52%
HALLMARK_KRAS_SIGNALING_UP	199	-0.36915	-1.5912	0.00113	0.006	0.119	4895	tags=34%, list=24%, signal=45%
HALLMARK_MITOTIC_SPINDLE	198	-0.49911	-2.1748	0	0.000	0	4087	tags=39%, list=20%, signal=48%
HALLMARK_MTORC1_SIGNALING	197	-0.51467	-2.2067	0	0.000	0	4547	tags=47%, list=22%, signal=60%
HALLMARK_MYC_TARGETS_V1	196	-0.55225	-2.3766	0	0.000	0	4743	tags=51%, list=23%, signal=65%

HALLMARK_MYC_TARGETS_V2	58	-0.25618	-0.9186	0.61872	0.714	1	4327	tags=28%, list=21%, signal=35%
HALLMARK_NOTCH_SIGNALING	32	-0.22266	-0.735	0.86217	0.978	1	4543	tags=28%, list=22%, signal=36%
HALLMARK_OXIDATIVE_PHOSPHORYLATION	200	-0.51833	-2.2424	0	0.000	0	4454	tags=46%, list=22%, signal=58%
HALLMARK_P53_PATHWAY	195	-0.20345	-0.8742	0.73513	0.793	1	4694	tags=25%, list=23%, signal=32%
HALLMARK_PEROXISOME	104	-0.36857	-1.47	0.00899	0.020	0.409	4085	tags=31%, list=20%, signal=38%
HALLMARK_PI3K_AKT_MTOR_SIGNALING	104	-0.50055	-2.0053	0	0.000	0	4890	tags=48%, list=24%, signal=63%
HALLMARK_PROTEIN_SECRETION	96	-0.59667	-2.3656	0	0.000	0	4392	tags=57%, list=22%, signal=73%
HALLMARK_REACTIVE_OXYGEN_SPECIES_PATHWAY	49	-0.42209	-1.5	0.02532	0.015	0.291	4876	tags=47%, list=24%, signal=62%
HALLMARK_TGF_BETA_SIGNALING	54	-0.4792	-1.7509	0.00137	0.001	0.021	4916	tags=44%, list=24%, signal=59%
HALLMARK_TNFA_SIGNALING_VIA_NFKB	199	-0.27737	-1.2044	0.12306	0.178	0.999	4992	tags=30%, list=25%, signal=40%
HALLMARK_UNFOLDED_PROTEIN_RESPONSE	110	-0.52227	-2.0883	0	0.000	0	4429	tags=46%, list=22%, signal=59%
HALLMARK_UV_RESPONSE_DN	143	-0.43616	-1.824	0	0.000	0.006	5020	tags=43%, list=25%, signal=56%
HALLMARK_UV_RESPONSE_UP	156	-0.37222	-1.5766	0.00115	0.007	0.135	4525	tags=33%, list=22%, signal=42%
HALLMARK_WNT_BETA_CATENIN_SIGNALING	42	-0.41789	-1.4334	0.0493	0.029	0.544	1323	tags=19%, list=7%, signal=20%
HALLMARK_XENOBIOTIC_METABOLISM	198	-0.28525	-1.2283	0.10421	0.165	0.998	4876	tags=32%, list=24%, signal=41%
KEGG_ABC_TRANSPORTERS	44	-0.2888	-0.9978	0.4625	0.564	1	4107	tags=27%, list=20%, signal=34%
KEGG_ACUTE_MYELOID_LEUKEMIA	57	-0.31179	-1.1361	0.26694	0.362	1	5294	tags=33%, list=26%, signal=45%
KEGG_ADHERENS_JUNCTION	73	-0.51783	-1.9541	0	0.001	0.01	3713	tags=40%, list=18%, signal=48%
KEGG_ADIPOCYTOKINE_SIGNALING_PATHWAY	67	-0.2599	-0.9748	0.49204	0.605	1	4752	tags=31%, list=23%, signal=41%
KEGG_ALANINE_ASPARTATE_AND_GLUTAMATE_METABOLISM	30	-0.37348	-1.1961	0.21045	0.299	1	2163	tags=23%, list=11%, signal=26%
KEGG_ALLOGRAFT_REJECTION	35	-0.60716	-2.0141	0	0.000	0.002	4800	tags=51%, list=24%, signal=67%
KEGG_ALZHEIMERS_DISEASE	157	-0.46504	-1.9668	0	0.001	0.007	4421	tags=39%, list=22%, signal=49%
KEGG_AMINO_SUGAR_AND_NUCLEOTIDE_SUGAR_METABOLISM	43	-0.41438	-1.4476	0.04661	0.091	0.992	3980	tags=28%, list=20%, signal=35%
KEGG_AMINOACYL_TRNA_BIOSYNTHESIS	22	-0.25833	-0.7678	0.76508	0.900	1	3922	tags=27%, list=19%, signal=34%
KEGG_AMYOTROPHIC_LATERAL_SCLEROSIS_ALS	53	-0.33241	-1.1853	0.21526	0.311	1	4111	tags=28%, list=20%, signal=35%
KEGG_ANTIGEN_PROCESSING_AND_PRESENTATION	85	-0.52481	-2.046	0	0.000	0.001	4370	tags=40%, list=22%, signal=51%
KEGG_APOPTOSIS	87	-0.33635	-1.3202	0.07398	0.175	1	4626	tags=34%, list=23%, signal=44%
KEGG_ARGININE_AND_PROLINE_METABOLISM	54	-0.28387	-1.0304	0.4148	0.518	1	3591	tags=22%, list=18%, signal=27%
KEGG_ASCORBATE_AND_ALDARATE_METABOLISM	25	-0.62613	-1.9209	0.00146	0.002	0.026	6308	tags=84%, list=31%, signal=122%
KEGG_ASTHMA	28	-0.67627	-2.1111	0	0.000	0.001	476	tags=29%, list=2%, signal=29%
KEGG_AUTOIMMUNE_THYROID_DISEASE	50	-0.51988	-1.8223	0	0.005	0.104	4492	tags=42%, list=22%, signal=54%
KEGG_AXON_GUIDANCE	129	-0.24852	-1.0201	0.42822	0.533	1	4420	tags=28%, list=22%, signal=35%

KEGG_B_CELL_RECEPTOR_SIGNALING_PATHWAY	75	-0.35906	-1.3636	0.05828	0.138	1	5925	tags=41%, list=29%, signal=58%
KEGG_BASAL_TRANSCRIPTION_FACTORS	35	-0.49651	-1.6233	0.01114	0.029	0.67	5640	tags=51%, list=28%, signal=71%
KEGG_BASE_EXCISION_REPAIR	33	-0.36148	-1.1913	0.22831	0.304	1	4558	tags=30%, list=22%, signal=39%
KEGG_BETA_ALANINE_METABOLISM	22	-0.41158	-1.2355	0.19545	0.254	1	5536	tags=45%, list=27%, signal=62%
KEGG_BIOSYNTHESIS_OF_UNSATURATED_FATTY_ACIDS	22	-0.4136	-1.2457	0.18731	0.242	1	2644	tags=23%, list=13%, signal=26%
KEGG_BUTANOATE_METABOLISM	34	-0.38807	-1.2712	0.15892	0.218	1	5453	tags=41%, list=27%, signal=56%
KEGG_CARDIAC_MUSCLE_CONTRACTION	73	-0.31954	-1.2019	0.15817	0.299	1	3361	tags=27%, list=17%, signal=33%
KEGG_CELL_ADHESION_MOLECULES_CAMS	131	-0.37158	-1.5316	0.00735	0.056	0.916	1586	tags=16%, list=8%, signal=17%
KEGG_CELL_CYCLE	124	-0.45566	-1.8544	0	0.003	0.063	5354	tags=48%, list=26%, signal=65%
KEGG_CHEMOKINE_SIGNALING_PATHWAY	188	-0.34355	-1.4592	0.00794	0.086	0.991	4796	tags=31%, list=24%, signal=40%
KEGG_CHRONIC_MYELOID_LEUKEMIA	73	-0.41478	-1.5699	0.00661	0.042	0.842	5199	tags=44%, list=26%, signal=59%
KEGG_CITRATE_CYCLE_TCA_CYCLE	30	-0.41891	-1.3309	0.11259	0.165	1	3614	tags=33%, list=18%, signal=41%
KEGG_COLORECTAL_CANCER	62	-0.4778	-1.7453	0.00136	0.011	0.251	4752	tags=45%, list=23%, signal=59%
KEGG_COMPLEMENT_AND_COAGULATION_CASCADES	69	-0.39101	-1.4595	0.02696	0.087	0.991	4705	tags=39%, list=23%, signal=51%
KEGG_CYSTEINE_AND_METHIONINE_METABOLISM	34	-0.32083	-1.0743	0.37113	0.453	1	3718	tags=32%, list=18%, signal=40%
KEGG_CYTOKINE_CYTOKINE_RECEPTOR_INTERACTION	264	-0.18624	-0.8313	0.84358	0.816	1	4707	tags=21%, list=23%, signal=27%
KEGG_CYTOSOLIC_DNA_SENSING_PATHWAY	54	-0.26764	-0.9713	0.51499	0.597	1	4818	tags=30%, list=24%, signal=39%
KEGG_DNA_REPLICATION	36	-0.37951	-1.2726	0.13083	0.218	1	3276	tags=25%, list=16%, signal=30%
KEGG_DRUG_METABOLISM_CYTOCHROME_P450	71	-0.29985	-1.146	0.25752	0.352	1	2231	tags=21%, list=11%, signal=24%
KEGG_DRUG_METABOLISM_OTHER_ENZYMES	51	-0.33428	-1.1846	0.22253	0.309	1	1954	tags=25%, list=10%, signal=28%
KEGG_ENDOCYTOSIS	181	-0.39809	-1.6948	0	0.018	0.402	3550	tags=29%, list=18%, signal=35%
KEGG_ENDOMETRIAL_CANCER	52	-0.393	-1.3964	0.064	0.117	1	4626	tags=37%, list=23%, signal=47%
KEGG_EPITHELIAL_CELL_SIGNALING_IN_HELICOBACTER_PYLORI_INFECTION	68	-0.38734	-1.4503	0.03846	0.091	0.991	3549	tags=31%, list=18%, signal=37%
KEGG_ERBB_SIGNALING_PATHWAY	87	-0.34168	-1.3318	0.08601	0.166	1	4796	tags=36%, list=24%, signal=46%
KEGG_ETHER_LIPID_METABOLISM	33	-0.24544	-0.8022	0.76358	0.859	1	4924	tags=30%, list=24%, signal=40%
KEGG_FC_EPSILON_RI_SIGNALING_PATHWAY	79	-0.28861	-1.1171	0.26512	0.389	1	6019	tags=41%, list=30%, signal=57%
KEGG_FC_GAMMA_R_MEDIATED_PHAGOCYTOSIS	95	-0.44252	-1.7649	0	0.009	0.207	4756	tags=41%, list=23%, signal=53%
KEGG_FOCAL_ADHESION	199	-0.27473	-1.1843	0.1352	0.306	1	6145	tags=41%, list=30%, signal=58%
KEGG_FRUCTOSE_AND_MANNOSE_METABOLISM	33	-0.21857	-0.7104	0.88174	0.945	1	4050	tags=24%, list=20%, signal=30%
KEGG_GALACTOSE_METABOLISM	26	-0.36385	-1.1167	0.31921	0.386	1	5515	tags=38%, list=27%, signal=53%
KEGG_GAP_JUNCTION	89	-0.20365	-0.7944	0.8075	0.866	1	5132	tags=28%, list=25%, signal=37%
KEGG_GLIOMA	65	-0.26061	-0.973	0.50524	0.599	1	5088	tags=32%, list=25%, signal=43%

KEGG_GLUTATHIONE_METABOLISM	49	-0.26696	-0.9375	0.56125	0.649	1	4915	tags=29%, list=24%, signal=38%
KEGG_GLYCEROPHOSPHOLIPID_METABOLISM	77	-0.25662	-0.9689	0.51337	0.597	1	2564	tags=14%, list=13%, signal=16%
KEGG_GLYCOLYSIS_GLUCONEOGENESIS	62	-0.19657	-0.7239	0.9028	0.937	1	5574	tags=29%, list=28%, signal=40%
KEGG_GLYCOSAMINOGLYCAN_DEGRADATION	21	-0.28259	-0.8412	0.67236	0.805	1	1810	tags=14%, list=9%, signal=16%
KEGG_GLYCOSPHINGOLIPID_BIOSYNTHESIS_GANGLIO_SERIES	15	-0.23119	-0.6282	0.91009	0.976	1	5254	tags=33%, list=26%, signal=45%
KEGG_GLYOXYLATE_AND_DICARBOXYLATE_METABOLISM	16	-0.55335	-1.5207	0.04252	0.061	0.933	3687	tags=44%, list=18%, signal=53%
KEGG_GNRH_SIGNALING_PATHWAY	101	-0.17633	-0.6995	0.95107	0.942	1	2653	tags=13%, list=13%, signal=15%
KEGG_GRAFT_VERSUS_HOST_DISEASE	38	-0.60566	-2.0494	0	0.000	0.001	3269	tags=34%, list=16%, signal=41%
KEGG_HEMATOPOIETIC_CELL_LINEAGE	85	-0.38728	-1.5028	0.01675	0.065	0.959	960	tags=13%, list=5%, signal=14%
KEGG_HOMOLOGOUS_RECOMBINATION	28	-0.219	-0.7008	0.88355	0.947	1	4871	tags=29%, list=24%, signal=38%
KEGG_HUNTINGTONS_DISEASE	172	-0.51741	-2.1923	0	0.000	0	4421	tags=44%, list=22%, signal=56%
KEGG_HYPERTROPHIC_CARDIOMYOPATHY_HCM	83	-0.2259	-0.8796	0.67588	0.751	1	3521	tags=22%, list=17%, signal=26%
KEGG_INOSITOL_PHOSPHATE_METABOLISM	54	-0.38163	-1.3842	0.06098	0.123	1	4298	tags=31%, list=21%, signal=40%
KEGG_INSULIN_SIGNALING_PATHWAY	137	-0.27593	-1.1498	0.20813	0.349	1	5925	tags=42%, list=29%, signal=59%
KEGG_INTESTINAL_IMMUNE_NETWORK_FOR_IGA_PRODUCTION	46	-0.50919	-1.8065	0.00281	0.006	0.126	1163	tags=20%, list=6%, signal=21%
KEGG_JAK_STAT_SIGNALING_PATHWAY	155	-0.30065	-1.2503	0.10409	0.244	1	4965	tags=32%, list=24%, signal=42%
KEGG_LEISHMANIA_INFECTION	70	-0.56675	-2.1204	0	0.000	0.001	3038	tags=33%, list=15%, signal=39%
KEGG_LEUKOCYTE_TRANSENDOTHELIAL_MIGRATION	116	-0.3475	-1.4062	0.03776	0.115	1	4535	tags=34%, list=22%, signal=43%
KEGG_LINOLEIC_ACID_METABOLISM	29	-0.24138	-0.7666	0.8218	0.896	1	4345	tags=24%, list=21%, signal=31%
KEGG_LONG_TERM_DEPRESSION	70	-0.29581	-1.1302	0.26418	0.369	1	5132	tags=31%, list=25%, signal=42%
KEGG_LONG_TERM_POTENTIATION	70	-0.30576	-1.1679	0.21974	0.330	1	4310	tags=29%, list=21%, signal=36%
KEGG_LYSINE_DEGRADATION	44	-0.40199	-1.3744	0.06999	0.130	1	5448	tags=45%, list=27%, signal=62%
KEGG_LYSOSOME	121	-0.47686	-1.9464	0	0.001	0.014	3593	tags=35%, list=18%, signal=42%
KEGG_MAPK_SIGNALING_PATHWAY	267	-0.24816	-1.094	0.26172	0.420	1	4777	tags=26%, list=24%, signal=34%
KEGG_MELANOMA	71	-0.17303	-0.6472	0.968	0.973	1	5112	tags=25%, list=25%, signal=34%
KEGG_METABOLISM_OF_XENOBIOTICS_BY_CYTOCHROME_P450	69	-0.33414	-1.246	0.14726	0.244	1	2231	tags=20%, list=11%, signal=23%
KEGG_MISMATCH_REPAIR	23	-0.49518	-1.5117	0.04893	0.063	0.942	4584	tags=52%, list=23%, signal=67%
KEGG_MTOR_SIGNALING_PATHWAY	52	-0.40693	-1.4431	0.04485	0.091	0.993	5834	tags=48%, list=29%, signal=67%
KEGG_N_GLYCAN_BIOSYNTHESIS	46	-0.46034	-1.6329	0.0123	0.028	0.639	4180	tags=37%, list=21%, signal=46%
KEGG_NATURAL_KILLER_CELL_MEDIATED_CYTOTOXICITY	136	-0.28485	-1.1963	0.1649	0.302	1	4535	tags=27%, list=22%, signal=35%

KEGG_NEUROTROPHIN_SIGNALING_PATHWAY	126	-0.28238	-1.1566	0.21403	0.340	1	4752	tags=31%, list=23%, signal=40%
KEGG_NICOTINATE_AND_NICOTINAMIDE_METABOLISM	24	-0.5495	-1.6715	0.01791	0.021	0.49	3738	tags=42%, list=18%, signal=51%
KEGG_NOD_LIKE_RECEPTOR_SIGNALING_PATHWAY	62	-0.43503	-1.6065	0.01173	0.033	0.736	3275	tags=29%, list=16%, signal=35%
KEGG_NON_SMALL_CELL_LUNG_CANCER	54	-0.36355	-1.3047	0.09485	0.190	1	5088	tags=37%, list=25%, signal=49%
KEGG_NOTCH_SIGNALING_PATHWAY	47	-0.34695	-1.2018	0.21795	0.296	1	5299	tags=28%, list=26%, signal=37%
KEGG_NUCLEOTIDE_EXCISION_REPAIR	44	-0.52517	-1.8039	0.00138	0.006	0.13	4960	tags=52%, list=24%, signal=69%
KEGG_ONE_CARBON_POOL_BY_FOLATE	17	-0.31188	-0.8749	0.64465	0.754	1	4002	tags=29%, list=20%, signal=37%
KEGG_OOCYTE_MEIOSIS	112	-0.3492	-1.4061	0.03431	0.113	1	4636	tags=36%, list=23%, signal=46%
KEGG_OTHER_GLYCAN_DEGRADATION	16	-0.46769	-1.2785	0.1633	0.213	1	3778	tags=38%, list=19%, signal=46%
KEGG_OXIDATIVE_PHOSPHORYLATION	116	-0.5411	-2.1906	0	0.000	0	4421	tags=50%, list=22%, signal=64%
KEGG_P53_SIGNALING_PATHWAY	68	-0.35092	-1.2853	0.10861	0.209	1	4264	tags=29%, list=21%, signal=37%
KEGG_PANCREATIC_CANCER	70	-0.41945	-1.5923	0.00652	0.034	0.782	4890	tags=41%, list=24%, signal=54%
KEGG_PANTOTHENATE_AND_COA_BIOSYNTHESIS	16	-0.5986	-1.6729	0.02299	0.021	0.483	4868	tags=63%, list=24%, signal=82%
KEGG_PARKINSONS_DISEASE	112	-0.56379	-2.2737	0	0.000	0	4421	tags=52%, list=22%, signal=66%
KEGG_PATHOGENIC_ESCHERICHIA_COLI_INFECTION	54	-0.53056	-1.9199	0	0.001	0.026	4495	tags=52%, list=22%, signal=66%
KEGG_PATHWAYS_IN_CANCER	325	-0.33836	-1.5062	0	0.064	0.953	4918	tags=34%, list=24%, signal=44%
KEGG_PENTOSE_AND_GLUCURONATE_INTERCONVERSIONS	28	-0.62163	-1.9391	0	0.001	0.015	4611	tags=57%, list=23%, signal=74%
KEGG_PENTOSE_PHOSPHATE_PATHWAY	27	-0.20109	-0.6208	0.94682	0.973	1	5248	tags=30%, list=26%, signal=40%
KEGG_PEROXISOME	78	-0.27906	-1.0623	0.36582	0.468	1	4104	tags=27%, list=20%, signal=34%
KEGG_PHOSPHATIDYLINOSITOL_SIGNALING_SYSTEM	76	-0.26842	-1.0198	0.44162	0.529	1	4535	tags=26%, list=22%, signal=34%
KEGG_PORPHYRIN_AND_CHLOROPHYLL_METABOLISM	40	-0.48657	-1.6537	0.00853	0.024	0.548	1217	tags=25%, list=6%, signal=27%
KEGG_PPAR_SIGNALING_PATHWAY	69	-0.33144	-1.2466	0.14304	0.246	1	4068	tags=29%, list=20%, signal=36%
KEGG_PRIMARY_BILE_ACID_BIOSYNTHESIS	16	-0.51167	-1.4283	0.07753	0.099	0.997	2520	tags=38%, list=12%, signal=43%
KEGG_PRIMARY_IMMUNODEFICIENCY	35	-0.43679	-1.4431	0.04499	0.093	0.993	2486	tags=20%, list=12%, signal=23%
KEGG_PRION_DISEASES	35	-0.38802	-1.2831	0.14204	0.209	1	4396	tags=31%, list=22%, signal=40%
KEGG_PROGESTERONE_MEDIATED_OOCYTE_MATURATION	85	-0.27738	-1.0712	0.35104	0.455	1	5120	tags=34%, list=25%, signal=45%
KEGG_PROPANOATE_METABOLISM	31	-0.4546	-1.472	0.04271	0.080	0.988	5250	tags=48%, list=26%, signal=65%
KEGG_PROSTATE_CANCER	89	-0.25819	-1.0087	0.44183	0.547	1	4626	tags=27%, list=23%, signal=35%
KEGG_PROTEASOME	44	-0.52745	-1.8144	0.00138	0.006	0.119	3554	tags=36%, list=18%, signal=44%
KEGG_PROTEIN_EXPORT	23	-0.6857	-2.053	0	0.000	0.001	4410	tags=65%, list=22%, signal=83%
KEGG_PROXIMAL_TUBULE_BICARBONATE_RECLAMATION	23	-0.28275	-0.874	0.62388	0.750	1	2919	tags=26%, list=14%, signal=30%
KEGG_PURINE_METABOLISM	157	-0.33786	-1.3953	0.02712	0.116	1	3867	tags=27%, list=19%, signal=34%
KEGG_PYRIMIDINE_METABOLISM	98	-0.42608	-1.6856	0	0.019	0.433	3867	tags=36%, list=19%, signal=44%

KEGG_PYRUVATE_METABOLISM	40	-0.3634	-1.2333	0.16034	0.255	1	3693	tags=30%, list=18%, signal=37%
KEGG_REGULATION_OF_ACTIN_CYTOSKELETON	211	-0.32121	-1.4001	0.01359	0.115	1	4721	tags=33%, list=23%, signal=43%
KEGG_REGULATION_OF_AUTOPHAGY	35	-0.45759	-1.5166	0.03506	0.062	0.938	4179	tags=40%, list=21%, signal=50%
KEGG_RENAL_CELL_CARCINOMA	70	-0.52037	-1.9767	0	0.000	0.005	4722	tags=49%, list=23%, signal=63%
KEGG_RENIN_ANGIOTENSIN_SYSTEM	17	-0.35272	-0.9734	0.49534	0.603	1	3547	tags=29%, list=17%, signal=36%
KEGG_RETINOL_METABOLISM	64	-0.29857	-1.1079	0.30476	0.398	1	1331	tags=17%, list=7%, signal=18%
KEGG_RIBOFLAVIN_METABOLISM	15	-0.35652	-0.9676	0.514	0.595	1	3861	tags=40%, list=19%, signal=49%
KEGG_RIBOSOME	87	-0.66426	-2.57	0	0.000	0	4780	tags=74%, list=24%, signal=96%
KEGG_RIG_I_LIKE_RECEPTOR_SIGNALING_PATHWAY	70	-0.29954	-1.139	0.24482	0.361	1	4278	tags=31%, list=21%, signal=40%
KEGG_RNA_DEGRADATION	57	-0.50897	-1.8539	0.00137	0.003	0.063	4699	tags=46%, list=23%, signal=59%
KEGG_RNA_POLYMERASE	29	-0.50017	-1.5962	0.01413	0.035	0.765	3867	tags=41%, list=19%, signal=51%
KEGG_SELENOAMINO_ACID_METABOLISM	25	-0.23752	-0.7288	0.83094	0.938	1	2436	tags=16%, list=12%, signal=18%
KEGG_SMALL_CELL_LUNG_CANCER	84	-0.40195	-1.5469	0.00624	0.051	0.896	4918	tags=42%, list=24%, signal=55%
KEGG_SNARE_INTERACTIONS_IN_VESICULAR_TRANSPORT	38	-0.48152	-1.6424	0.01034	0.026	0.602	5811	tags=53%, list=29%, signal=74%
KEGG_SPHINGOLIPID_METABOLISM	39	-0.31061	-1.0586	0.36963	0.472	1	5094	tags=36%, list=25%, signal=48%
KEGG_SPLICEOSOME	126	-0.53365	-2.197	0	0.000	0	5945	tags=57%, list=29%, signal=80%
KEGG_STARCH_AND_SUCROSE_METABOLISM	52	-0.40963	-1.438	0.03787	0.094	0.996	3025	tags=37%, list=15%, signal=43%
KEGG_STEROID_BIOSYNTHESIS	17	-0.56953	-1.594	0.024	0.035	0.774	3883	tags=41%, list=19%, signal=51%
KEGG_STEROID_HORMONE_BIOSYNTHESIS	55	-0.43817	-1.5965	0.00652	0.035	0.765	6181	tags=53%, list=30%, signal=76%
KEGG_SYSTEMIC_LUPUS_ERYTHEMATOSUS	55	-0.61312	-2.2088	0	0.000	0	3990	tags=45%, list=20%, signal=56%
KEGG_T_CELL_RECEPTOR_SIGNALING_PATHWAY	108	-0.40486	-1.6193	0.00124	0.030	0.69	4800	tags=34%, list=24%, signal=45%
KEGG_TERPENOID_BACKBONE_BIOSYNTHESIS	15	-0.60446	-1.6555	0.01958	0.024	0.545	3546	tags=53%, list=17%, signal=65%
KEGG_TGF_BETA_SIGNALING_PATHWAY	85	-0.29985	-1.1657	0.1972	0.328	1	3625	tags=26%, list=18%, signal=31%
KEGG_THYROID_CANCER	29	-0.40751	-1.3004	0.15015	0.192	1	2992	tags=31%, list=15%, signal=36%
KEGG_TIGHT_JUNCTION	132	-0.33781	-1.3862	0.02722	0.122	1	4021	tags=33%, list=20%, signal=40%
KEGG_TOLL_LIKE_RECEPTOR_SIGNALING_PATHWAY	102	-0.41003	-1.638	0.00127	0.027	0.622	4752	tags=38%, list=23%, signal=50%
KEGG_TRYPTOPHAN_METABOLISM	39	-0.34653	-1.1664	0.23521	0.330	1	5980	tags=49%, list=30%, signal=69%
KEGG_TYPE_I_DIABETES_MELLITUS	41	-0.52989	-1.8283	0	0.005	0.096	3269	tags=34%, list=16%, signal=41%
KEGG_UBIQUITIN_MEDIATED_PROTEOLYSIS	134	-0.54703	-2.2679	0	0.000	0	3356	tags=39%, list=17%, signal=46%
KEGG_VALINE_LEUCINE_AND_ISOLEUCINE_DEGRADATION	43	-0.40803	-1.4018	0.07876	0.115	1	5763	tags=49%, list=28%, signal=68%
KEGG_VASCULAR_SMOOTH_MUSCLE_CONTRACTION	114	-0.23104	-0.9297	0.60025	0.659	1	4420	tags=24%, list=22%, signal=30%
KEGG_VASOPRESSIN_REGULATED_WATER_REABSORPTION	44	-0.42694	-1.4902	0.03017	0.071	0.975	3913	tags=39%, list=19%, signal=48%

KEGG_VEGF_SIGNALING_PATHWAY	76	-0.27439	-1.0543	0.36435	0.476	1	4626	tags=30%, list=23%, signal=39%
KEGG_VIBRIO_CHOLERAE_INFECTION	54	-0.46293	-1.6779	0.00268	0.020	0.46	4107	tags=44%, list=20%, signal=56%
KEGG_VIRAL_MYOCARDITIS	68	-0.45514	-1.7101	0.00387	0.016	0.352	4545	tags=44%, list=22%, signal=57%
KEGG_WNT_SIGNALING_PATHWAY	150	-0.32398	-1.3596	0.03529	0.140	1	4420	tags=31%, list=22%, signal=40%
REACTOME_A_TETRASACCHARIDE_LINKER_SEQUENCE_IS_REQUIRED_FOR_GAG_SYNTHESIS	26	-0.22272	-0.685	0.89808	0.945	1	1922	tags=15%, list=9%, signal=17%
REACTOME_ABC_FAMILY_PROTEINS_MEDIATED_TRANSPORT	103	-0.48203	-1.9039	0.00122	0.002	0.25	4255	tags=39%, list=21%, signal=49%
REACTOME_ABC_TRANSPORTER_DISORDERS	77	-0.54918	-2.0725	0	0.000	0.021	4255	tags=45%, list=21%, signal=57%
REACTOME_ABERRANT_REGULATION_OF_MITOTIC_EXIT_IN_CANCER_DUE_TO_RB1_DEFECTS	20	-0.67775	-1.9422	0	0.001	0.15	1991	tags=35%, list=10%, signal=39%
REACTOME_ABERRANT_REGULATION_OF_MITOTIC_G1_S_TRANSITION_IN_CANCER_DUE_TO_RB1_DEFECTS	17	-0.49708	-1.3604	0.09934	0.117	1	6786	tags=65%, list=33%, signal=97%
REACTOME_ABORTIVE_ELONGATION_OF_HIV_1_TRANSCRIPT_IN_THE_ABSENCE_OF_TAT	23	-0.63922	-1.9197	0.00157	0.001	0.202	4452	tags=57%, list=22%, signal=72%
REACTOME_ACTIVATED_NOTCH1_TRANSMITS_SIGNAL_TO_THE_NUCLEUS	31	-0.39334	-1.2618	0.16788	0.194	1	3760	tags=29%, list=19%, signal=36%
REACTOME_ACTIVATED_TAK1_MEDIATES_P38_MAPK_ACTIVATION	23	-0.61188	-1.8538	0.00309	0.003	0.423	3356	tags=52%, list=17%, signal=62%
REACTOME_ACTIVATION_OF_AMPK_DOWNSTREAM_OF_NMDARS	28	-0.29693	-0.9357	0.54985	0.637	1	2359	tags=21%, list=12%, signal=24%
REACTOME_ACTIVATION_OF_ANTERIOR_HOX_GENES_IN_HINDBRAIN_DEVELOPMENT_DURING_EARLY_EMBRYOGENESIS	62	-0.47134	-1.7264	0.00271	0.009	0.918	3029	tags=35%, list=15%, signal=42%
REACTOME_ACTIVATION_OF_ATR_IN_RESPONSE_TO_REPLICATION_STRESS	37	-0.42519	-1.4189	0.07255	0.085	1	4525	tags=43%, list=22%, signal=56%
REACTOME_ACTIVATION_OF_BAD_AND_TRANSLOCATION_TO_MITOCHONDRIA_	15	-0.51138	-1.3857	0.09641	0.101	1	4626	tags=53%, list=23%, signal=69%
REACTOME_ACTIVATION_OF_BH3_ONLY_PROTEINS	30	-0.47382	-1.5322	0.03683	0.042	1	4890	tags=47%, list=24%, signal=61%
REACTOME_ACTIVATION_OF_GENE_EXPRESSION_BY_SREBF_SREBP_	42	-0.62011	-2.111	0	0.000	0.008	3883	tags=48%, list=19%, signal=59%
REACTOME_ACTIVATION_OF_IRF3_IRF7_MEDIATED_BY_TBK1_IKK_EPSILON	17	-0.52601	-1.4818	0.04603	0.058	1	3558	tags=47%, list=18%, signal=57%
REACTOME_ACTIVATION_OF_KAINATE_RECEPTORS_UPON_GLUTAMATE_BINDING	30	-0.39815	-1.2775	0.14353	0.181	1	2772	tags=27%, list=14%, signal=31%
REACTOME_ACTIVATION_OF_SMO	18	-0.26025	-0.7466	0.81064	0.893	1	768	tags=11%, list=4%, signal=12%

REACTOME_ACTIVATION_OF_THE_MRNA_UPON_BINDING_OF_THE_CAP_BINDING_COMPLEX_AND_EIFS_AND_SUBSEQUENT_BINDING_TO_43S	60	-0.63269	-2.3078	0	0.000	0.001	5503	tags=77%, list=27%, signal=105%
REACTOME_ACTIVATION_OF_THE_PRE_REPLICATIVE_COMPLEX	33	-0.36519	-1.1949	0.21875	0.264	1	5538	tags=45%, list=27%, signal=62%
REACTOME_ACYL_CHAIN_REMODELLING_OF_PC	26	-0.20493	-0.634	0.94351	0.972	1	828	tags=8%, list=4%, signal=8%
REACTOME_ACYL_CHAIN_REMODELLING_OF_PE	24	-0.18854	-0.5687	0.96626	0.987	1	5637	tags=29%, list=28%, signal=40%
REACTOME_ACYL_CHAIN_REMODELLING_OF_PS	21	-0.30841	-0.9046	0.58859	0.686	1	2416	tags=19%, list=12%, signal=22%
REACTOME_ADHERENS_JUNCTIONS_INTERACTIONS	33	-0.31701	-1.0391	0.39972	0.476	1	1238	tags=15%, list=6%, signal=16%
REACTOME_ADP_SIGNALLING_THROUGH_P2Y_PURINOCEPTOR_1	25	-0.37888	-1.1731	0.26617	0.288	1	3496	tags=32%, list=17%, signal=39%
REACTOME_ADP_SIGNALLING_THROUGH_P2Y_PURINOCEPTOR_12	22	-0.52921	-1.6001	0.03053	0.026	1	2462	tags=36%, list=12%, signal=41%
REACTOME_ADRENALINE_NORADRENALINE_INHIBITS_INSULIN_SECRETION	28	-0.37528	-1.1777	0.2381	0.283	1	2462	tags=25%, list=12%, signal=28%
REACTOME_AGGREPHAGY	43	-0.4992	-1.7386	0.00668	0.008	0.888	4217	tags=47%, list=21%, signal=59%
REACTOME_AMINO_ACIDS_REGULATE_MTORC1	55	-0.46114	-1.6699	0.00282	0.015	0.988	3218	tags=35%, list=16%, signal=41%
REACTOME_AMYLOID_FIBER_FORMATION	51	-0.47845	-1.6806	0.00274	0.013	0.982	3760	tags=39%, list=19%, signal=48%
REACTOME_ANCHORING_OF_THE_BASAL_BODY_TO_THE_PLASMA_MEMBRANE	95	-0.4695	-1.8524	0	0.003	0.429	4582	tags=37%, list=23%, signal=47%
REACTOME_ANTIGEN_ACTIVATES_B_CELL_RECEPTOR_BCR_LEADING_TO_GENERATION_OF_SECOND_MESSENGERS	30	-0.36351	-1.1711	0.22907	0.290	1	2483	tags=23%, list=12%, signal=27%
REACTOME_ANTIGEN_PRESENTATION_FOLDING_ASSEMBLY_AND_PEPTIDE_LOADING_OF_CLASS_I_MHC	25	-0.68731	-2.1028	0	0.000	0.009	4370	tags=68%, list=22%, signal=87%
REACTOME_ANTIGEN_PROCESSING_CROSS_PRESENTATION	99	-0.53807	-2.1284	0	0.000	0.005	3269	tags=35%, list=16%, signal=42%
REACTOME_ANTIGEN_PROCESSING_UBIQUITINATION_PROTEASOME_DEGRADATION	308	-0.42772	-1.9097	0	0.002	0.23	3356	tags=31%, list=17%, signal=36%
REACTOME_ANTIVIRAL_MECHANISM_BY_IFN_STIMULATED_GENES	80	-0.62805	-2.4149	0	0.000	0	4388	tags=54%, list=22%, signal=68%
REACTOME_APC_C_CDC20_MEDIATED_DEGRADATION_OF_CYCLIN_B	24	-0.68752	-2.1045	0	0.000	0.009	3235	tags=46%, list=16%, signal=54%
REACTOME_APC_C_CDH1_MEDIATED_DEGRADATION_OF_CDC20_AND_OTHER_APC_C_CDH1_TARGETED_PROTEINS_IN_LATE_MITOSIS_EARLY_G1	74	-0.5702	-2.1748	0	0.000	0.002	3235	tags=38%, list=16%, signal=45%
REACTOME_APC_C_MEDIATED_DEGRADATION_OF_CELL_CYCLE_PROTEINS	88	-0.54853	-2.1502	0	0.000	0.004	3264	tags=36%, list=16%, signal=43%

REACTOME_APC_CDC20_MEDIATED_DEGRADATION_OF_NEK2A	26	-0.69584	-2.1911	0	0.000	0.002	3264	tags=50%, list=16%, signal=60%
REACTOME_APOPTOTIC_CLEAVAGE_OF_CELLULAR_PROTEINS	38	-0.41698	-1.4019	0.06745	0.094	1	3972	tags=37%, list=20%, signal=46%
REACTOME_APOPTOTIC_EXECUTION_PHASE	46	-0.39835	-1.3932	0.05172	0.097	1	3972	tags=35%, list=20%, signal=43%
REACTOME_APOPTOTIC_FACTOR_MEDIATED_RESPONSE	17	-0.5432	-1.515	0.05651	0.047	1	4241	tags=47%, list=21%, signal=59%
REACTOME_AQUAPORIN_MEDIATED_TRANSPORT	52	-0.29464	-1.054	0.37052	0.455	1	2496	tags=21%, list=12%, signal=24%
REACTOME_ASPARAGINE_N_LINKED_GLYCOSYLATION	302	-0.45972	-2.0503	0	0.000	0.035	4255	tags=37%, list=21%, signal=46%
REACTOME_ASSEMBLY_OF_ACTIVE_LPL_AND_LIPC_LIPASE_COMPLEXES	19	-0.27129	-0.7692	0.77977	0.870	1	3724	tags=32%, list=18%, signal=39%
REACTOME_ASSEMBLY_OF_COLLAGEN_FIBRILS_AND_OTHER_MULTIMERIC_STRUCTURES	61	-0.24679	-0.9196	0.59615	0.665	1	1752	tags=11%, list=9%, signal=13%
REACTOME_ASSEMBLY_OF_THE_HIV_VIRION	16	-0.62906	-1.7368	0.00985	0.008	0.891	3113	tags=44%, list=15%, signal=52%
REACTOME_ASSEMBLY_OF_THE_PRE_REPLICATIVE_COMPLEX	68	-0.49089	-1.816	0.00133	0.004	0.575	5555	tags=53%, list=27%, signal=73%
REACTOME_ASSOCIATION_OF_TRIC_CCT_WITH_TARGET_PROTEINS_DURING_BIOSYNTHESIS	39	-0.43957	-1.4797	0.03953	0.059	1	4977	tags=46%, list=25%, signal=61%
REACTOME_ASYMMETRIC_LOCALIZATION_OF_PCP_PROTEINS	64	-0.49832	-1.8499	0	0.003	0.442	3178	tags=33%, list=16%, signal=39%
REACTOME_ATF4_ACTIVATES_GENES_IN_RESPONSE_TO_ENDOPLASMIC_RETICULUM_STRESS	27	-0.4834	-1.5184	0.04056	0.046	1	4699	tags=52%, list=23%, signal=67%
REACTOME_ATTENUATION_PHASE	28	-0.50192	-1.5922	0.01368	0.028	1	5241	tags=46%, list=26%, signal=63%
REACTOME_AUF1_HNRNP_D0_BINDS_AND_DESTABILIZES_MRNA	55	-0.53415	-1.9358	0	0.001	0.158	3178	tags=38%, list=16%, signal=45%
REACTOME_AURKA_ACTIVATION_BY_TPX2	71	-0.51491	-1.9437	0	0.001	0.147	4264	tags=41%, list=21%, signal=52%
REACTOME_AUTOPHAGY	150	-0.50549	-2.1061	0	0.000	0.009	3942	tags=43%, list=19%, signal=53%
REACTOME_B_WICH_COMPLEX_POSITIVELY_REGULATES_RRNA_EXPRESSION	31	-0.48344	-1.561	0.01493	0.035	1	4580	tags=52%, list=23%, signal=67%
REACTOME_BASE_EXCISION_REPAIR	44	-0.41343	-1.4379	0.04871	0.076	1	4558	tags=32%, list=22%, signal=41%
REACTOME_BASE_EXCISION_REPAIR_AP_SITE_FORMATION	17	-0.19949	-0.5618	0.96849	0.988	1	16230	tags=100%, list=80%, signal=501%
REACTOME_BASIGIN_INTERACTIONS	25	-0.46794	-1.4388	0.06366	0.075	1	4630	tags=48%, list=23%, signal=62%
REACTOME_BBSOME_MEDIATED_CARGO_TARGETING_TO_CILIUM	23	-0.42784	-1.2824	0.14619	0.176	1	3253	tags=30%, list=16%, signal=36%
REACTOME_BETA_CATENIN_INDEPENDENT_WNT_SIGNALING	146	-0.43542	-1.8174	0	0.004	0.57	4124	tags=35%, list=20%, signal=44%

REACTOME_BETA_CATENIN_PHOSPHORYLATION_CASCADE	17	-0.62156	-1.7247	0.00483	0.009	0.919	4021	tags=59%, list=20%, signal=73%
REACTOME_BILE_ACID_AND_BILE_SALT_METABOLISM	43	-0.3307	-1.1454	0.28135	0.325	1	4294	tags=35%, list=21%, signal=44%
REACTOME_BINDING_AND_UPTAKE_OF_LIGANDS_BY_SCAVENGER_RECEPTORS	42	-0.48918	-1.6917	0.00283	0.012	0.971	5215	tags=40%, list=26%, signal=54%
REACTOME_BIOLOGICAL_OXIDATIONS	216	-0.22132	-0.9567	0.58929	0.606	1	5076	tags=27%, list=25%, signal=36%
REACTOME_BIOSYNTHESIS_OF_SPECIALIZED_PRORESOLVING_MEDIATORS_SPMS_	19	-0.30284	-0.8724	0.6458	0.733	1	4274	tags=32%, list=21%, signal=40%
REACTOME_BIOSYNTHESIS_OF_THE_N_GLYCAN_PRECURSOR_DOLICHOL_LIPID_LINKED_OLIGOSACCHARIDE_LLO_AND_TRANSFER_TO_A_NASCENT_PROTEIN	77	-0.30964	-1.1758	0.19433	0.284	1	3815	tags=22%, list=19%, signal=27%
REACTOME_BMAL1_CLOCK_NPAS2_ACTIVATES_CIRCADIAN_GENE_EXPRESSION	27	-0.3573	-1.1203	0.29762	0.358	1	2013	tags=19%, list=10%, signal=21%
REACTOME_BRANCHED_CHAIN_AMINO_ACID_CATABOLISM	21	-0.17582	-0.5181	0.98033	0.994	1	5335	tags=33%, list=26%, signal=45%
REACTOME_BUDDING_AND_MATURATION_OF_HIV_VIRION	28	-0.49905	-1.5615	0.02481	0.035	1	3550	tags=43%, list=18%, signal=52%
REACTOME_BUTYRATE_RESPONSE_FACTOR_1_BRF1_BINDS_AND_DESTABILIZES_MRNA	17	-0.54446	-1.524	0.03616	0.044	1	4699	tags=59%, list=23%, signal=77%
REACTOME_C_TYPE_LECTIN_RECEPTORS_CLRS_	140	-0.46198	-1.9103	0	0.002	0.228	3356	tags=30%, list=17%, signal=36%
REACTOME_CA2_PATHWAY	62	-0.40132	-1.4878	0.02513	0.056	1	4038	tags=34%, list=20%, signal=42%
REACTOME_CALNEXIN_CALRETICULIN_CYCLE	25	-0.66285	-2.0191	0	0.000	0.05	5873	tags=72%, list=29%, signal=101%
REACTOME_CARGO_CONCENTRATION_IN_THE_ER	33	-0.49389	-1.6155	0.00846	0.024	1	5783	tags=58%, list=29%, signal=80%
REACTOME_CARGO_RECOGNITION_FOR_CLATHRIN_MEDIATED_ENDOCYTOSIS	105	-0.45054	-1.7985	0	0.005	0.658	4483	tags=38%, list=22%, signal=49%
REACTOME_CARGO_TRAFFICKING_TO_THE_PERICILIARY_MEMBRANE	51	-0.37614	-1.3431	0.09877	0.128	1	3285	tags=25%, list=16%, signal=30%
REACTOME_CASPASE_ACTIVATION_VIA_DEATH_RECEPTORS_IN_THE_PRESENCE_OF_LIGAND	16	-0.46203	-1.2752	0.1504	0.182	1	4188	tags=44%, list=21%, signal=55%
REACTOME_CASPASE_ACTIVATION_VIA_EXTRINSIC_APOPTOTIC_SIGNALLING_PATHWAY	26	-0.32434	-1.0041	0.45399	0.533	1	4188	tags=31%, list=21%, signal=39%
REACTOME_CD209_DC_SIGN_SIGNALING	21	-0.4176	-1.2325	0.20313	0.221	1	6940	tags=62%, list=34%, signal=94%
REACTOME_CD28_CO_STIMULATION	33	-0.31031	-1.0119	0.4344	0.521	1	4626	tags=39%, list=23%, signal=51%
REACTOME_CD28_DEPENDENT_PI3K_AKT_SIGNALING	22	-0.27711	-0.8198	0.7394	0.810	1	4626	tags=36%, list=23%, signal=47%
REACTOME_CELL_CELL_COMMUNICATION	130	-0.31038	-1.2866	0.07942	0.173	1	3064	tags=23%, list=15%, signal=27%
REACTOME_CELL_CELL_JUNCTION_ORGANIZATION	65	-0.26982	-1.0075	0.45103	0.528	1	1586	tags=15%, list=8%, signal=17%
REACTOME_CELL_CYCLE_CHECKPOINTS	258	-0.49176	-2.1813	0	0.000	0.002	4729	tags=43%, list=23%, signal=55%

REACTOME_CELL_CYCLE_MITOTIC	497	-0.46799	-2.1365	0	0.000	0.005	5041	tags=43%, list=25%, signal=56%
REACTOME_CELL_DEATH_SIGNALLING_VIA_NRAGE_NRIF_AND_NADE	76	-0.33239	-1.2754	0.12278	0.182	1	3760	tags=29%, list=19%, signal=35%
REACTOME_CELL_EXTRACELLULAR_MATRIX_INTERACTIONS	18	-0.43658	-1.2318	0.20099	0.222	1	3713	tags=33%, list=18%, signal=41%
REACTOME_CELL_JUNCTION_ORGANIZATION	92	-0.28159	-1.1011	0.29498	0.385	1	2005	tags=17%, list=10%, signal=19%
REACTOME_CELL_SURFACE_INTERACTIONS_AT_THE_VASCULAR_WALL	137	-0.32622	-1.3483	0.04028	0.125	1	4765	tags=32%, list=24%, signal=42%
REACTOME_CELLULAR_RESPONSE_TO_HEAT_STRESS	100	-0.5653	-2.2585	0	0.000	0.002	5086	tags=54%, list=25%, signal=72%
REACTOME_CELLULAR_RESPONSE_TO_HYPOXIA	75	-0.58676	-2.2235	0	0.000	0.002	3625	tags=43%, list=18%, signal=52%
REACTOME_CELLULAR_SENESCENCE	130	-0.37869	-1.5649	0.00573	0.034	1	4957	tags=36%, list=24%, signal=48%
REACTOME_CHAPERONE_MEDIATED_AUTOPHAGY	22	-0.59627	-1.7871	0.00466	0.005	0.701	4217	tags=59%, list=21%, signal=75%
REACTOME_CHEMOKINE_RECEPTORS_BIND_CHEMOKINES	58	-0.23782	-0.8749	0.68895	0.730	1	2940	tags=14%, list=15%, signal=16%
REACTOME_CHOLESTEROL_BIOSYNTHESIS	25	-0.57052	-1.7386	0.00613	0.008	0.888	3883	tags=44%, list=19%, signal=54%
REACTOME_CHONDROITIN_SULFATE_DERMATAN_SULFATE_METABOLISM	50	-0.24821	-0.8729	0.66529	0.733	1	1922	tags=16%, list=9%, signal=18%
REACTOME_CHROMATIN_MODIFYING_ENZYMES	207	-0.44551	-1.927	0	0.001	0.179	5041	tags=43%, list=25%, signal=57%
REACTOME_CHROMOSOME_MAINTENANCE	92	-0.39111	-1.5338	0.01161	0.042	1	5171	tags=39%, list=26%, signal=52%
REACTOME_CILIUM_ASSEMBLY	199	-0.39805	-1.722	0	0.009	0.923	4283	tags=32%, list=21%, signal=40%
REACTOME_CIRCADIAN_CLOCK	70	-0.40663	-1.5264	0.01289	0.044	1	5443	tags=46%, list=27%, signal=62%
REACTOME_CITRIC_ACID_CYCLE_TCA_CYCLE_	22	-0.52701	-1.5786	0.03135	0.031	1	3614	tags=36%, list=18%, signal=44%
REACTOME_CLASS_I_MHC_MEDIATED_ANTIGEN_PROCESSING_PRESENTATION	370	-0.44897	-2.0305	0	0.000	0.045	3356	tags=32%, list=17%, signal=38%
REACTOME_CLATHRIN_MEDIATED_ENDOCYTOSIS	144	-0.47236	-1.9597	0	0.001	0.111	4483	tags=42%, list=22%, signal=53%
REACTOME_CLEC7A_DECTIN_1_SIGNALING	100	-0.5433	-2.1651	0	0.000	0.002	3554	tags=38%, list=18%, signal=46%
REACTOME_COBALAMIN_CBL_VITAMIN_B12_TRANSPORT_AND_METABOLISM	19	-0.35457	-1.0184	0.44704	0.511	1	4233	tags=37%, list=21%, signal=47%
REACTOME_COLLAGEN_FORMATION	90	-0.22954	-0.9025	0.65461	0.689	1	1752	tags=10%, list=9%, signal=11%
REACTOME_COMMON_PATHWAY_OF_FIBRIN_CLOT_FORMATION	22	-0.20805	-0.6251	0.93274	0.975	1	4279	tags=23%, list=21%, signal=29%
REACTOME_COMPLEMENT_CASCADE	58	-0.38053	-1.4028	0.05665	0.094	1	6161	tags=50%, list=30%, signal=72%
REACTOME_COMPLEX_I_BIOGENESIS	49	-0.53503	-1.8748	0	0.002	0.335	4646	tags=51%, list=23%, signal=66%
REACTOME_CONSTITUTIVE_SIGNALING_BY_EGFRVIII	15	-0.67677	-1.8283	0.00479	0.004	0.538	4222	tags=60%, list=21%, signal=76%

REACTOME_CONSTITUTIVE_SIGNALING_BY_LIGAND_RESPONSIVE_EGFR_CANCER_VARIANTS	19	-0.70973	-2.0575	0	0.000	0.03	4222	tags=68%, list=21%, signal=86%
REACTOME_CONVERSION_FROM_APC_C_CDC20_TO_APC_C_CDH1_IN_LATE_ANAPHASE	20	-0.66094	-1.9149	0.00156	0.001	0.216	1394	tags=30%, list=7%, signal=32%
REACTOME_COOPERATION_OF_PDCL_PHLP1_AND_TRIC_CCT_IN_G_PROTEIN_BETA_FOLDING	42	-0.51639	-1.7863	0.00142	0.005	0.703	3496	tags=40%, list=17%, signal=49%
REACTOME_COOPERATION_OF_PREFOLDIN_AND_TRIC_CCT_IN_ACTIN_AND_TUBULIN_FOLDING	33	-0.33724	-1.0804	0.35451	0.412	1	4380	tags=36%, list=22%, signal=46%
REACTOME_COPI_DEPENDENT_GOLGI_TO_ER_RETROGRADE_TRAFFIC	99	-0.38607	-1.534	0.00862	0.042	1	4169	tags=35%, list=21%, signal=44%
REACTOME_COPI_INDEPENDENT_GOLGI_TO_ER_RETROGRADE_TRAFFIC	52	-0.45857	-1.635	0.00541	0.020	0.999	4053	tags=38%, list=20%, signal=48%
REACTOME_COPI_MEDIATED_ANTEROGRADE_TRANSPORT	101	-0.52325	-2.0783	0	0.000	0.019	3185	tags=40%, list=16%, signal=47%
REACTOME_COPII_MEDIATED_VESICLE_TRANSPORT	68	-0.52062	-1.9414	0	0.001	0.15	3413	tags=37%, list=17%, signal=44%
REACTOME_COSTIMULATION_BY_THE_CD28_FAMILY	67	-0.53716	-2.0143	0	0.000	0.052	4722	tags=49%, list=23%, signal=64%
REACTOME_CRISTAE_FORMATION	27	-0.66434	-2.0953	0	0.000	0.013	3868	tags=56%, list=19%, signal=69%
REACTOME_CROSS_PRESENTATION_OF_SOLUBLE_EXOGENOUS_ANTIGENS_ENDOSOMES_	50	-0.46638	-1.6498	0.00277	0.018	0.994	3554	tags=32%, list=18%, signal=39%
REACTOME_CROSSLINKING_OF_COLLAGEN_FIBRILS	18	-0.25567	-0.7294	0.83333	0.907	1	1752	tags=11%, list=9%, signal=12%
REACTOME_CTLA4_INHIBITORY_SIGNALING	21	-0.56516	-1.6906	0.0126	0.012	0.973	4722	tags=62%, list=23%, signal=81%
REACTOME_CYCLIN_A_B1_B2_ASSOCIATED_EVENTS_DURING_G2_M_TRANSITION	25	-0.52666	-1.6015	0.01385	0.026	1	5101	tags=48%, list=25%, signal=64%
REACTOME_CYCLIN_A_CDK2_ASSOCIATED_EVENTS_AT_S_PHASE_ENTRY	85	-0.5132	-2.0173	0	0.000	0.05	5555	tags=53%, list=27%, signal=73%
REACTOME_CYCLIN_D_ASSOCIATED_EVENTS_IN_G1	47	-0.5349	-1.8676	0.00134	0.002	0.367	4062	tags=49%, list=20%, signal=61%
REACTOME_CYTOCHROME_P450_ARRANGED_BY_SUBSTRATE_TYPE	64	-0.23612	-0.8754	0.69419	0.731	1	1184	tags=11%, list=6%, signal=12%
REACTOME_CYTOSOLIC_SENSORS_OF_PATHOGEN_ASSOCIATED_DNA_	62	-0.4141	-1.5271	0.02937	0.044	1	4188	tags=34%, list=21%, signal=43%
REACTOME_DAP12_INTERACTIONS	45	-0.23529	-0.8156	0.74826	0.815	1	5399	tags=36%, list=27%, signal=48%
REACTOME_DAP12_SIGNALING	29	-0.3642	-1.1497	0.28125	0.319	1	5399	tags=48%, list=27%, signal=66%
REACTOME_DARPP_32_EVENTS	24	-0.36433	-1.1275	0.27217	0.349	1	4038	tags=38%, list=20%, signal=47%
REACTOME_DDX58_IFIH1_MEDIATED_INDUCTION_OF_INTERFERON_ALPHA_BETA	78	-0.47488	-1.8249	0.00131	0.004	0.549	4278	tags=42%, list=21%, signal=53%

REACTOME_DEACTIVATION_OF_THE_BETA_CATENIN_TRANSACTIVATING_COMPLEX	42	-0.3765	-1.2983	0.14794	0.163	1	4989	tags=43%, list=25%, signal=57%
REACTOME_DEADENYLATION_DEPENDENT_MRNA_DECAY	56	-0.52328	-1.8952	0	0.002	0.276	4790	tags=46%, list=24%, signal=61%
REACTOME_DEADENYLATION_OF_MRNA	25	-0.50459	-1.5728	0.01502	0.033	1	2576	tags=28%, list=13%, signal=32%
REACTOME_DEATH_RECEPTOR_SIGNALLING	141	-0.36709	-1.5193	0.01061	0.046	1	5299	tags=40%, list=26%, signal=54%
REACTOME_DECTIN_1_MEDIATED_NONCANONICAL_NF_KB_SIGNALING	62	-0.55075	-2.0426	0	0.000	0.037	3178	tags=35%, list=16%, signal=42%
REACTOME_DECTIN_2_FAMILY	26	-0.25649	-0.7827	0.78681	0.855	1	1691	tags=12%, list=8%, signal=13%
REACTOME_DEFECTIVE_B4GALT7_CAUSES_EDS_PROGEROID_TYPE	20	-0.30817	-0.8955	0.60938	0.700	1	1922	tags=20%, list=9%, signal=22%
REACTOME_DEFECTIVE_CFTR_CAUSES_CYSTIC_FIBROSIS	61	-0.60114	-2.2206	0	0.000	0.002	4255	tags=51%, list=21%, signal=64%
REACTOME_DEFECTS_IN_VITAMIN_AND_COFACTOR_METABOLISM	20	-0.40262	-1.1941	0.24057	0.264	1	4233	tags=35%, list=21%, signal=44%
REACTOME_DEGRADATION_OF_AXIN	55	-0.55866	-2.0279	0	0.000	0.046	3178	tags=38%, list=16%, signal=45%
REACTOME_DEGRADATION_OF_BETA_CATENIN_BY_THE_DESTRUCTION_COMPLEX	84	-0.52808	-2.0691	0	0.000	0.021	4124	tags=43%, list=20%, signal=54%
REACTOME_DEGRADATION_OF_DVL	57	-0.55032	-2.0048	0	0.000	0.054	3625	tags=40%, list=18%, signal=49%
REACTOME_DEGRADATION_OF_GLI1_BY_THE_PROTEASOME	60	-0.56071	-2.0559	0	0.000	0.03	3625	tags=42%, list=18%, signal=51%
REACTOME_DEPOLYMERISATION_OF_THE_NUCLEAR_LAMINA	15	-0.27438	-0.738	0.8273	0.901	1	6775	tags=60%, list=33%, signal=90%
REACTOME_DEPOSITION_OF_NEW_CENPA_CONTAINING_NUCLEOSOMES_AT_THE_CENTROMERE	28	-0.43359	-1.3966	0.09385	0.096	1	6150	tags=54%, list=30%, signal=77%
REACTOME_DETOXIFICATION_OF_REACTIVE_OXYGEN_SPECIES	37	-0.58291	-1.9739	0	0.001	0.086	4111	tags=43%, list=20%, signal=54%
REACTOME_DEUBIQUITINATION	263	-0.42375	-1.8675	0	0.002	0.367	4658	tags=40%, list=23%, signal=51%
REACTOME_DISASSEMBLY_OF_THE_DESTRUCTION_COMPLEX_AND_RECRUITMENT_OF_AXIN_TO_THE_MEMBRANE	31	-0.39112	-1.2595	0.17034	0.195	1	4545	tags=42%, list=22%, signal=54%
REACTOME_DISEASES_ASSOCIATED_WITH_GLYCOSAMINOGLYCAN_METABOLISM	41	-0.23387	-0.7956	0.81093	0.840	1	1922	tags=15%, list=9%, signal=16%
REACTOME_DISEASES_ASSOCIATED_WITH_GLYCOSYLATION_PRECURSOR_BIOSYNTHESIS	18	-0.49427	-1.3942	0.08903	0.097	1	6107	tags=56%, list=30%, signal=79%
REACTOME_DISEASES_ASSOCIATED_WITH_N_GLYCOSYLATION_OF_PROTEINS	17	-0.346	-0.9474	0.55869	0.620	1	3815	tags=24%, list=19%, signal=29%
REACTOME_DISEASES_OF_CARBOHYDRATE_METABOLISM	34	-0.30479	-1.0005	0.45545	0.536	1	5071	tags=35%, list=25%, signal=47%
REACTOME_DISEASES_OF_GLYCOSYLATION	142	-0.1868	-0.7815	0.89252	0.855	1	3104	tags=15%, list=15%, signal=18%

REACTOME_DISEASES_OF_IMMUNE_SYSTEM	24	-0.32845	-1.0012	0.4584	0.536	1	3558	tags=25%, list=18%, signal=30%
REACTOME_DISEASES_OF_METABOLISM	243	-0.21166	-0.9252	0.64074	0.656	1	3870	tags=20%, list=19%, signal=24%
REACTOME_DISEASES_OF_MITOTIC_CELL_CYCLE	36	-0.52637	-1.7839	0.00147	0.005	0.713	4895	tags=39%, list=24%, signal=51%
REACTOME_DISEASES_OF_PROGRAMMED_CELL_DEATH	24	-0.41105	-1.2543	0.17451	0.200	1	3644	tags=29%, list=18%, signal=36%
REACTOME_DISEASES_OF_SIGNAL_TRANSDUCTION_BY_GROWTH_FACTOR_RECEPTORS_AND_SECOND_MESSENGERS	385	-0.40538	-1.8404	0	0.003	0.481	4737	tags=37%, list=23%, signal=48%
REACTOME_DISORDERS_OF_TRANSMEMBRANE_TRANSPORTERS	175	-0.46598	-1.9761	0	0.001	0.082	4729	tags=42%, list=23%, signal=54%
REACTOME_DNA_DAMAGE_BYPASS	48	-0.56592	-1.9913	0	0.001	0.066	5120	tags=60%, list=25%, signal=81%
REACTOME_DNA_DAMAGE_RECOGNITION_IN_GG_NER	38	-0.53078	-1.7671	0	0.006	0.789	5097	tags=53%, list=25%, signal=70%
REACTOME_DNA_DAMAGE_TELOMERE_STRESS_INDUCED_SENESCENCE	28	-0.38359	-1.202	0.21557	0.255	1	6786	tags=54%, list=33%, signal=80%
REACTOME_DNA_DOUBLE_STRAND_BREAK_REPAIR	132	-0.43764	-1.8112	0.00118	0.004	0.592	4940	tags=41%, list=24%, signal=54%
REACTOME_DNA_DOUBLE_STRAND_BREAK_RESPONSE	43	-0.5145	-1.7833	0	0.005	0.716	4710	tags=49%, list=23%, signal=63%
REACTOME_DNA_REPAIR	284	-0.45044	-1.9815	0	0.001	0.078	5120	tags=44%, list=25%, signal=58%
REACTOME_DNA_REPLICATION	128	-0.47709	-1.9575	0	0.001	0.121	5555	tags=48%, list=27%, signal=65%
REACTOME_DNA_REPLICATION_PRE_INITIATION	85	-0.47582	-1.8757	0	0.002	0.332	5555	tags=51%, list=27%, signal=69%
REACTOME_DNA_STRAND_ELONGATION	32	-0.3073	-0.9912	0.47669	0.548	1	5538	tags=38%, list=27%, signal=52%
REACTOME_DOWNREGULATION_OF_ERBB2_SIGNALING	29	-0.39079	-1.2371	0.17262	0.218	1	4626	tags=34%, list=23%, signal=45%
REACTOME_DOWNREGULATION_OF_SMAD2_3_SMAD4_TRANSCRIPTIONAL_ACTIVITY	23	-0.65938	-1.9462	0	0.001	0.14	3244	tags=61%, list=16%, signal=72%
REACTOME_DOWNREGULATION_OF_TGF_BETA_RECEPTOR_SIGNALING	26	-0.53296	-1.6356	0.01089	0.020	0.999	3335	tags=42%, list=16%, signal=51%
REACTOME_DOWNSTREAM_SIGNAL_TRANSDUCTION	29	-0.46782	-1.4875	0.04208	0.056	1	5349	tags=55%, list=26%, signal=75%
REACTOME_DOWNSTREAM_SIGNALING_EVENTS_OF_B_CELL_RECEPTOR_BCR_	81	-0.51325	-1.98	0	0.001	0.079	5555	tags=52%, list=27%, signal=71%
REACTOME_DOWNSTREAM_SIGNALING_OF_ACTIVATED_FGFR1	31	-0.33906	-1.1044	0.33191	0.380	1	2525	tags=19%, list=12%, signal=22%
REACTOME_DOWNSTREAM_SIGNALING_OF_ACTIVATED_FGFR2	30	-0.26864	-0.8506	0.68971	0.768	1	2525	tags=17%, list=12%, signal=19%
REACTOME_DOWNSTREAM_SIGNALING_OF_ACTIVATED_FGFR3	25	-0.31497	-0.984	0.48372	0.561	1	5088	tags=36%, list=25%, signal=48%
REACTOME_DOWNSTREAM_SIGNALING_OF_ACTIVATED_FGFR4	27	-0.31873	-0.9972	0.45092	0.540	1	5088	tags=33%, list=25%, signal=44%
REACTOME_DUAL_INCISION_IN_GG_NER	41	-0.56707	-1.9815	0	0.001	0.078	4960	tags=56%, list=24%, signal=74%

REACTOME_DUAL_INCISION_IN_TC_NER	65	-0.55469	-2.0468	0	0.000	0.035	4960	tags=54%, list=24%, signal=71%
REACTOME_E2F_MEDIATED_REGULATION_OF_DNA_REPLICATION	22	-0.53208	-1.5862	0.01917	0.030	1	5170	tags=59%, list=26%, signal=79%
REACTOME_E3_UBIQUITIN_LIGASES_UBIQUITINATE_TARGET_PROTEINS	44	-0.63318	-2.1991	0	0.000	0.002	3951	tags=61%, list=19%, signal=76%
REACTOME_EGFR_DOWNREGULATION	31	-0.46756	-1.5022	0.04296	0.051	1	4698	tags=45%, list=23%, signal=59%
REACTOME_EGR2_AND_SOX10_MEDIATED_INITIATION_OF_SCHWANN_CELL_MYELINATION	29	-0.42068	-1.3235	0.13112	0.142	1	4146	tags=45%, list=20%, signal=56%
REACTOME_ELASTIC_FIBRE_FORMATION	45	-0.27075	-0.9476	0.53324	0.621	1	2171	tags=13%, list=11%, signal=15%
REACTOME_ENDOGENOUS_STEROLS	26	-0.5489	-1.7201	0.00939	0.010	0.926	2185	tags=27%, list=11%, signal=30%
REACTOME_ENDOSOMAL_SORTING_COMPLEX_REQUIRED_FOR_TRANSPORT_ESCRT_	31	-0.56942	-1.8397	0	0.003	0.483	3550	tags=42%, list=18%, signal=51%
REACTOME_ENERGY_DEPENDENT_REGULATION_OF_MTOR_BY_LKB1_AMPK	29	-0.59239	-1.8959	0	0.002	0.276	2613	tags=41%, list=13%, signal=47%
REACTOME_EPH_EPHRIN_MEDIATED_REPULSION_OF_CELLS	51	-0.18899	-0.6762	0.94519	0.949	1	4464	tags=24%, list=22%, signal=30%
REACTOME_EPH_EPHRIN_SIGNALING	91	-0.39948	-1.5709	0.0051	0.033	1	4495	tags=40%, list=22%, signal=51%
REACTOME_EPHB_MEDIATED_FORWARD_SIGNALING	41	-0.56942	-1.9657	0	0.001	0.099	4495	tags=56%, list=22%, signal=72%
REACTOME_EPHRIN_SIGNALING	19	-0.36044	-1.0392	0.42857	0.477	1	6826	tags=68%, list=34%, signal=103%
REACTOME_EPIGENETIC_REGULATION_OF_GENE_EXPRESSION	88	-0.46969	-1.8278	0	0.004	0.539	4580	tags=43%, list=23%, signal=56%
REACTOME_ER_QUALITY_CONTROL_COMPARTMENT_ERQC_	20	-0.66579	-1.9353	0	0.001	0.161	5162	tags=65%, list=25%, signal=87%
REACTOME_ER_TO_GOLGI_ANTEROGRADE_TRANSPORT	154	-0.4974	-2.0842	0	0.000	0.018	3413	tags=37%, list=17%, signal=44%
REACTOME_ERCC6_CSB_AND_EHMT2_G9A_POSITIVELY_REGULATE_RRNA_EXPRESSION	16	-0.42057	-1.1794	0.25402	0.281	1	6646	tags=56%, list=33%, signal=84%
REACTOME_ERK_MAPK_TARGETS	22	-0.58206	-1.7316	0.0077	0.009	0.903	4362	tags=50%, list=22%, signal=64%
REACTOME_ESR_MEDIATED_SIGNALING	161	-0.46945	-1.9772	0	0.001	0.08	5137	tags=48%, list=25%, signal=64%
REACTOME_ESTROGEN_DEPENDENT_GENE_EXPRESSION	90	-0.53851	-2.1174	0	0.000	0.007	3858	tags=43%, list=19%, signal=53%
REACTOME_ESTROGEN_DEPENDENT_NUCLEAR_EVENTS_DOWNSTREAM_OF_ESR_MEMBRANE_SIGNALING	24	-0.20344	-0.6227	0.94108	0.974	1	4643	tags=29%, list=23%, signal=38%
REACTOME_EUKARYOTIC_TRANSLATION_ELONGATION	94	-0.66761	-2.6288	0	0.000	0	4780	tags=73%, list=24%, signal=96%
REACTOME_EUKARYOTIC_TRANSLATION_INITIATION	120	-0.64501	-2.6051	0	0.000	0	4795	tags=72%, list=24%, signal=93%
REACTOME_EXPORT_OF_VIRAL_RIBONUCLEOPROTEINS_FROM_NUCLEUS	32	-0.68298	-2.2246	0	0.000	0.002	4729	tags=66%, list=23%, signal=85%

REACTOME_EXTENSION_OF_TELOMERES	51	-0.34009	-1.2255	0.16938	0.228	1	5171	tags=35%, list=26%, signal=47%
REACTOME_EXTRA_NUCLEAR_ESTROGEN_SIGNALING	75	-0.36328	-1.3827	0.04193	0.103	1	5137	tags=43%, list=25%, signal=57%
REACTOME_EXTRACELLULAR_MATRIX_ORGANIZATION	301	-0.17234	-0.7674	0.95156	0.870	1	2732	tags=12%, list=13%, signal=14%
REACTOME_FACTORS_INVOLVED_IN_MEGAKARYOCYTE_DEVELOPMENT_AND_PLATELET_PRODUCTION	154	-0.30916	-1.2989	0.06139	0.162	1	4026	tags=29%, list=20%, signal=36%
REACTOME_FANCONI_ANEMIA_PATHWAY	39	-0.37534	-1.2651	0.13924	0.191	1	5444	tags=38%, list=27%, signal=52%
REACTOME_FATTY_ACID_METABOLISM	175	-0.3299	-1.3965	0.01732	0.096	1	4294	tags=31%, list=21%, signal=40%
REACTOME_FATTY_ACYL_COA_BIOSYNTHESIS	36	-0.41608	-1.3904	0.07937	0.099	1	4125	tags=39%, list=20%, signal=49%
REACTOME_FC_EPSILON_RECEPTOR_FCERI_SIGNALING	131	-0.49629	-2.047	0	0.000	0.035	4222	tags=40%, list=21%, signal=51%
REACTOME_FCERI_MEDIATED_CA_2_MOBILIZATION	31	-0.43878	-1.4066	0.08423	0.092	1	4764	tags=48%, list=24%, signal=63%
REACTOME_FCERI_MEDIATED_MAPK_ACTIVATION	32	-0.44692	-1.4586	0.04209	0.067	1	5655	tags=53%, list=28%, signal=74%
REACTOME_FCERI_MEDIATED_NF_KB_ACTIVATION	81	-0.58469	-2.2391	0	0.000	0.002	3554	tags=42%, list=18%, signal=51%
REACTOME_FCGAMMA_RECEPTOR_FCGR_DEPENDENT_PHAGOCYTOSIS	85	-0.47964	-1.8787	0	0.002	0.323	4495	tags=45%, list=22%, signal=57%
REACTOME_FCGR3A_MEDIATED_IL10_SYNTHESIS	38	-0.24374	-0.8062	0.75444	0.826	1	3662	tags=21%, list=18%, signal=26%
REACTOME_FGFR1_MUTANT_RECEPTOR_ACTIVATION	30	-0.52238	-1.6553	0.00913	0.017	0.992	3032	tags=33%, list=15%, signal=39%
REACTOME_FGFR2_ALTERNATIVE_SPLICING	27	-0.58768	-1.8684	0	0.002	0.366	5293	tags=63%, list=26%, signal=85%
REACTOME_FGFR2_MUTANT_RECEPTOR_ACTIVATION	33	-0.24147	-0.7857	0.80535	0.852	1	4412	tags=27%, list=22%, signal=35%
REACTOME_FLT3_SIGNALING	292	-0.33132	-1.4731	0.00107	0.062	1	4238	tags=29%, list=21%, signal=36%
REACTOME_FORMATION_OF_ATP_BY_CHEMIOSMOTIC_COUPLING	16	-0.71335	-1.9964	0	0.001	0.061	3476	tags=56%, list=17%, signal=68%
REACTOME_FORMATION_OF_FIBRIN_CLOT_CLOTTING_CASCADE_	39	-0.2092	-0.7136	0.88099	0.924	1	4312	tags=28%, list=21%, signal=36%
REACTOME_FORMATION_OF_INCISION_COMPLEX_IN_GG_NER	43	-0.6594	-2.3036	0	0.000	0.001	3625	tags=60%, list=18%, signal=73%
REACTOME_FORMATION_OF_RNA_POL_II_ELONGATION_COMPLEX_	58	-0.6352	-2.2741	0	0.000	0.002	4571	tags=57%, list=23%, signal=73%
REACTOME_FORMATION_OF_TC_NER_PRE_INCISION_COMPLEX	53	-0.57955	-2.0806	0	0.000	0.018	5296	tags=60%, list=26%, signal=82%
REACTOME_FORMATION_OF_THE_BETA_CATENIN_TCF_TRANSACTIVATING_COMPLEX	31	-0.37312	-1.1834	0.2311	0.276	1	3090	tags=26%, list=15%, signal=30%
REACTOME_FORMATION_OF_THE_EARLY_ELONGATION_COMPLEX	33	-0.62119	-2.0582	0	0.000	0.029	4571	tags=58%, list=23%, signal=74%
REACTOME_FORMATION_OF_TUBULIN_FOLDING_INTERMEDIATES_BY_CCT_TRIC	26	-0.30484	-0.9389	0.56203	0.632	1	4380	tags=35%, list=22%, signal=44%

REACTOME_FOXO_MEDIATED_TRANSCRIPTION	66	-0.3256	-1.2045	0.16422	0.252	1	5199	tags=41%, list=26%, signal=55%
REACTOME_FOXO_MEDIATED_TRANSCRIPTION_OF_CELL_CYCLE_GENES	17	-0.21039	-0.586	0.96135	0.983	1	5199	tags=35%, list=26%, signal=47%
REACTOME_FOXO_MEDIATED_TRANSCRIPTION_OF_CELL_DEATH_GENES	16	-0.44683	-1.2283	0.20712	0.225	1	4121	tags=38%, list=20%, signal=47%
REACTOME_FRS_MEDIATED_FGFR4_SIGNALING	22	-0.15584	-0.4584	1	0.998	1	2020	tags=9%, list=10%, signal=10%
REACTOME_G_ALPHA_12_13_SIGNALLING_EVENTS	80	-0.26503	-1.0021	0.48721	0.535	1	3516	tags=24%, list=17%, signal=29%
REACTOME_G_ALPHA_Z_SIGNALLING_EVENTS	48	-0.34906	-1.2342	0.16735	0.220	1	2728	tags=25%, list=13%, signal=29%
REACTOME_G_BETA_GAMMA_SIGNALLING_THROUGH_CDC42	20	-0.47573	-1.4061	0.07583	0.092	1	2462	tags=35%, list=12%, signal=40%
REACTOME_G_BETA_GAMMA_SIGNALLING_THROUGH_PI3KGAMMA	25	-0.42245	-1.29	0.14832	0.170	1	5834	tags=56%, list=29%, signal=79%
REACTOME_G_PROTEIN_ACTIVATION	28	-0.44602	-1.4281	0.05689	0.081	1	2462	tags=29%, list=12%, signal=32%
REACTOME_G_PROTEIN_BETA_GAMMA_SIGNALLING	32	-0.42563	-1.384	0.06942	0.102	1	4983	tags=44%, list=25%, signal=58%
REACTOME_G_PROTEIN_MEDIATED_EVENTS	54	-0.23006	-0.8262	0.75653	0.803	1	2496	tags=15%, list=12%, signal=17%
REACTOME_G0_AND_EARLY_G1	27	-0.49242	-1.5309	0.03835	0.043	1	4890	tags=44%, list=24%, signal=58%
REACTOME_G1_S_DNA_DAMAGE_CHECKPOINTS	68	-0.53464	-2.0061	0	0.000	0.054	4124	tags=41%, list=20%, signal=52%
REACTOME_G1_S_SPECIFIC_TRANSCRIPTION	29	-0.35919	-1.1179	0.30588	0.360	1	6272	tags=55%, list=31%, signal=80%
REACTOME_G2_M_CHECKPOINTS	134	-0.51576	-2.1254	0	0.000	0.005	4599	tags=45%, list=23%, signal=58%
REACTOME_G2_M_DNA_DAMAGE_CHECKPOINT	61	-0.53212	-1.9602	0	0.001	0.109	4710	tags=48%, list=23%, signal=62%
REACTOME_GAB1_SIGNALOSOME	17	-0.49614	-1.3897	0.10769	0.099	1	4722	tags=47%, list=23%, signal=61%
REACTOME_GABA_B_RECEPTOR_ACTIVATION	43	-0.33603	-1.1793	0.22283	0.281	1	2462	tags=23%, list=12%, signal=26%
REACTOME_GABA_RECEPTOR_ACTIVATION	60	-0.27347	-1.0029	0.44583	0.534	1	2645	tags=20%, list=13%, signal=23%
REACTOME_GABA_SYNTHESIS_RELEASE_REUPTAKE_AND_DEGRADATION	19	-0.24169	-0.6881	0.87616	0.944	1	4788	tags=32%, list=24%, signal=41%
REACTOME_GAP_FILLING_DNA_REPAIR_SYNTHESIS_AND_LIGATION_IN_GG_NER	25	-0.60345	-1.8559	0.00301	0.003	0.416	3276	tags=44%, list=16%, signal=52%
REACTOME_GASTRIN_CREB_SIGNALLING_PATHWAY_VIA_PKC_AND_MAPK	18	-0.36852	-1.0177	0.42857	0.511	1	5088	tags=39%, list=25%, signal=52%
REACTOME_GENE_AND_PROTEIN_EXPRESSION_BY_JAK_STAT_SIGNALING_AFTER_INTERLEUKIN_12_STIMULATION	38	-0.47954	-1.6496	0.01262	0.018	0.994	5655	tags=58%, list=28%, signal=80%
REACTOME_GENE_SILENCING_BY_RNA	77	-0.53677	-2.0831	0	0.000	0.018	4102	tags=43%, list=20%, signal=54%
REACTOME_GENERATION_OF_SECOND_MESSENGER_MOLECULES	32	-0.63967	-2.0821	0	0.000	0.018	4437	tags=50%, list=22%, signal=64%
REACTOME_GLOBAL_GENOME_NUCLEOTIDE_EXCISION_REPAIR_GG_NER_	84	-0.5706	-2.2312	0	0.000	0.002	3625	tags=45%, list=18%, signal=55%

REACTOME_GLUCAGON_LIKE_PEPTIDE_1_GLP1_REGULATES_INSULIN_SECRETION	42	-0.42838	-1.4764	0.04848	0.060	1	2496	tags=29%, list=12%, signal=33%
REACTOME_GLUCAGON_SIGNALING_IN_METABOLIC_REGULATION	33	-0.31596	-1.0222	0.43091	0.505	1	2496	tags=24%, list=12%, signal=28%
REACTOME_GLUCAGON_TYPE_LIGAND_RECEPTORS	33	-0.27629	-0.9057	0.61007	0.685	1	2462	tags=21%, list=12%, signal=24%
REACTOME_GLUCOSE_METABOLISM	91	-0.39437	-1.5463	0.01623	0.039	1	4102	tags=32%, list=20%, signal=40%
REACTOME_GLUCURONIDATION	25	-0.67741	-2.0878	0	0.000	0.016	5076	tags=72%, list=25%, signal=96%
REACTOME_GLYCEROPHOSPHOLIPID_BIOSYNTHESIS	123	-0.30645	-1.2627	0.10291	0.193	1	5637	tags=37%, list=28%, signal=51%
REACTOME_GLYCOGEN_METABOLISM	27	-0.39306	-1.2332	0.18667	0.221	1	3113	tags=33%, list=15%, signal=39%
REACTOME_GLYCOGEN_STORAGE_DISEASES	16	-0.52868	-1.4594	0.0736	0.067	1	3113	tags=38%, list=15%, signal=44%
REACTOME_GLYCOGEN_SYNTHESIS	16	-0.62601	-1.7117	0.0114	0.010	0.945	3113	tags=50%, list=15%, signal=59%
REACTOME_GLYCOLYSIS	71	-0.48385	-1.8138	0	0.004	0.58	4102	tags=39%, list=20%, signal=49%
REACTOME_GLYCOSPHINGOLIPID_METABOLISM	44	-0.44444	-1.5331	0.02361	0.042	1	4479	tags=36%, list=22%, signal=47%
REACTOME_GLYOXYLATE_METABOLISM_AND_GLYCINE_DEGRADATION	31	-0.22551	-0.7359	0.84179	0.901	1	5207	tags=35%, list=26%, signal=48%
REACTOME_GOLGI_ASSOCIATED_VESICLE_BIOGENESIS	56	-0.54197	-1.9475	0	0.001	0.136	3854	tags=54%, list=19%, signal=66%
REACTOME_GOLGI_TO_ER_RETROGRADE_TRANSPORT	133	-0.44666	-1.8327	0	0.003	0.519	4169	tags=39%, list=21%, signal=49%
REACTOME_GPVI_MEDIATED_ACTIVATION_CASCADE	35	-0.41655	-1.3603	0.09207	0.117	1	4722	tags=43%, list=23%, signal=56%
REACTOME_GRB2_SOS_PROVIDES_LINKAGE_TO_MAPK_SIGNALING_FOR_INTEGRINS_	15	-0.58317	-1.5479	0.02908	0.038	1	4185	tags=67%, list=21%, signal=84%
REACTOME_GROWTH_HORMONE_RECEPTOR_SIGNALING	24	-0.52406	-1.6217	0.0162	0.023	1	2483	tags=33%, list=12%, signal=38%
REACTOME_HATS_ACETYLATE_HISTONES	80	-0.52072	-2.0139	0	0.000	0.052	6243	tags=58%, list=31%, signal=83%
REACTOME_HCMV_EARLY_EVENTS	74	-0.52968	-2.013	0	0.000	0.053	4102	tags=43%, list=20%, signal=54%
REACTOME_HCMV_INFECTION	98	-0.4946	-1.9328	0	0.001	0.168	4102	tags=40%, list=20%, signal=50%
REACTOME_HCMV_LATE_EVENTS	53	-0.56424	-2.0425	0	0.000	0.037	4102	tags=45%, list=20%, signal=57%
REACTOME_HDACS_DEACETYLATE_HISTONES	32	-0.43371	-1.412	0.06637	0.089	1	4165	tags=41%, list=21%, signal=51%
REACTOME_HDMS_DEMETHYLATE_HISTONES	23	-0.25573	-0.7577	0.79613	0.881	1	5041	tags=35%, list=25%, signal=46%
REACTOME_HDR_THROUGH_HOMOLOGOUS_RECOMBINATION_HRR_	67	-0.49113	-1.8425	0	0.003	0.471	4525	tags=42%, list=22%, signal=54%
REACTOME_HDR_THROUGH_SINGLE_STRAND_ANNEALING_SSA_	37	-0.47592	-1.5791	0.00971	0.031	1	4525	tags=41%, list=22%, signal=52%
REACTOME_HEDGEHOG_LIGAND_BIOGENESIS	65	-0.54181	-2.0283	0	0.000	0.045	3178	tags=38%, list=16%, signal=45%
REACTOME_HEDGEHOG_OFF_STATE	113	-0.42278	-1.7001	0	0.012	0.958	4217	tags=35%, list=21%, signal=43%
REACTOME_HEDGEHOG_ON_STATE	86	-0.4704	-1.845	0	0.003	0.459	3625	tags=35%, list=18%, signal=42%

REACTOME_HIV_ELONGATION_ARREST_AND_RECOVERY	33	-0.68017	-2.2301	0	0.000	0.002	4452	tags=61%, list=22%, signal=78%
REACTOME_HIV_INFECTION	230	-0.53769	-2.3351	0	0.000	0	4176	tags=42%, list=21%, signal=53%
REACTOME_HIV_LIFE_CYCLE	148	-0.5596	-2.3466	0	0.000	0	4729	tags=49%, list=23%, signal=63%
REACTOME_HIV_TRANSCRIPTION_ELONGATION	43	-0.61874	-2.155	0	0.000	0.003	4571	tags=56%, list=23%, signal=72%
REACTOME_HIV_TRANSCRIPTION_INITIATION	47	-0.55472	-1.9439	0	0.001	0.147	5640	tags=57%, list=28%, signal=79%
REACTOME_HOMOLOGOUS_DNA_PAIRING_AND_STRAND_EXCHANGE	42	-0.42867	-1.4486	0.04762	0.072	1	4871	tags=40%, list=24%, signal=53%
REACTOME_HOMOLOGY_DIRECTED_REPAIR	104	-0.48527	-1.9402	0	0.001	0.152	4525	tags=41%, list=22%, signal=53%
REACTOME_HOST_INTERACTIONS_OF_HIV_FACTORS	130	-0.57664	-2.3655	0	0.000	0	4124	tags=45%, list=20%, signal=56%
REACTOME_HS_GAG_BIOSYNTHESIS	31	-0.32311	-1.0459	0.40262	0.467	1	1922	tags=19%, list=9%, signal=21%
REACTOME_HS_GAG_DEGRADATION	22	-0.27377	-0.8204	0.71293	0.810	1	1922	tags=18%, list=9%, signal=20%
REACTOME_HSF1_ACTIVATION	31	-0.55945	-1.7966	0	0.005	0.672	5241	tags=48%, list=26%, signal=65%
REACTOME_HSF1_DEPENDENT_TRANSACTIVATION	38	-0.39562	-1.3289	0.1092	0.139	1	5241	tags=39%, list=26%, signal=53%
REACTOME_HSP90_CHAPERONE_CYCLE_FOR_STEROID_HORMONE_RECEPTORS_SHR_	56	-0.45532	-1.6423	0.00683	0.019	0.997	3942	tags=36%, list=19%, signal=44%
REACTOME_HYALURONAN_METABOLISM	17	-0.24133	-0.6743	0.8955	0.949	1	137	tags=6%, list=1%, signal=6%
REACTOME_IKK_COMPLEX_RECRUITMENT_MEDIATED_BY_RIP1	23	-0.65744	-1.9736	0	0.001	0.086	3356	tags=61%, list=17%, signal=73%
REACTOME_IMMUNOREGULATORY_INTERACTIONS_BETWEEN_A_LYMPHOID_AND_A_NON_LYMPHOID_CELL	131	-0.26117	-1.0849	0.31535	0.405	1	1205	tags=9%, list=6%, signal=10%
REACTOME_INCRETIN_SYNTHESIS_SECRETION_AND_INACTIVATION	23	-0.27203	-0.8167	0.73016	0.814	1	3353	tags=26%, list=17%, signal=31%
REACTOME_INFECTION_WITH_MYCOBACTERIUM_TUBERCULOSIS	27	-0.64784	-2.0577	0	0.000	0.03	3113	tags=37%, list=15%, signal=44%
REACTOME_INFLAMMASOMES	20	-0.42428	-1.2507	0.15704	0.204	1	5901	tags=50%, list=29%, signal=70%
REACTOME_INFLUENZA_INFECTION	156	-0.65766	-2.7805	0	0.000	0	4780	tags=69%, list=24%, signal=89%
REACTOME_INHIBITION_OF_DNA_RECOMBINATION_AT_TELOMERE	20	-0.55508	-1.6013	0.016	0.026	1	5085	tags=50%, list=25%, signal=67%
REACTOME_INHIBITION_OF_THE_PROTEOLYTIC_ACTIVITY_OF_APC_C_REQUIRED_FOR_THE_ONSET_OF_ANAPHASE_BY_MITOTIC_SPINDLE_CHECKPOINT_COMPONENTS	21	-0.64062	-1.9147	0.0015	0.001	0.218	3264	tags=38%, list=16%, signal=45%
REACTOME_INITIAL_TRIGGERING_OF_COMPLEMENT	23	-0.33453	-1.0118	0.46154	0.521	1	4639	tags=35%, list=23%, signal=45%
REACTOME_INITIATION_OF_NUCLEAR_ENVELOPE_NE_REFORMATION	19	-0.46475	-1.3446	0.12837	0.127	1	4264	tags=42%, list=21%, signal=53%
REACTOME_INLB_MEDIATED_ENTRY_OF_LISTERIA_MONOCYTOGENES_INTO_HOST_CELL	15	-0.64856	-1.7477	0.00503	0.008	0.863	4363	tags=67%, list=22%, signal=85%

REACTOME_INOSITOL_PHOSPHATE_METABOLISM	48	-0.25503	-0.9058	0.62674	0.686	1	2595	tags=15%, list=13%, signal=17%
REACTOME_INSERTION_OF_TAIL_ANCHORED_PROTEINS_INTO_THE_ENDOPLASMIC_RETICULUM_MEMBRANE	20	-0.35358	-1.0363	0.42974	0.481	1	6080	tags=55%, list=30%, signal=78%
REACTOME_INSULIN_PROCESSING	27	-0.40324	-1.267	0.16962	0.189	1	5107	tags=41%, list=25%, signal=54%
REACTOME_INSULIN_RECEPTOR_RECYCLING	26	-0.49845	-1.5324	0.025	0.042	1	3218	tags=42%, list=16%, signal=50%
REACTOME_INTEGRATION_OF_ENERGY_METABOLISM	108	-0.35121	-1.4302	0.03342	0.080	1	3742	tags=29%, list=18%, signal=35%
REACTOME_INTEGRIN_SIGNALING	27	-0.47584	-1.5075	0.04812	0.049	1	4626	tags=48%, list=23%, signal=62%
REACTOME_INTERACTIONS_OF_REV_WITH_HOST_CELLULAR_PROTEINS	36	-0.6608	-2.222	0	0.000	0.002	4729	tags=61%, list=23%, signal=80%
REACTOME_INTERACTIONS_OF_VPR_WITH_HOST_CELLULAR_PROTEINS	36	-0.65491	-2.1963	0	0.000	0.002	4729	tags=58%, list=23%, signal=76%
REACTOME_INTERCONVERSION_OF_NUCLEOTIDE_DI_AND_TRIPHOSPHATES	29	-0.47525	-1.5273	0.03303	0.044	1	4098	tags=41%, list=20%, signal=52%
REACTOME_INTERFERON_ALPHA_BETA_SIGNALING	70	-0.47171	-1.8024	0	0.004	0.64	4370	tags=39%, list=22%, signal=49%
REACTOME_INTERFERON_GAMMA_SIGNALING	90	-0.54077	-2.1611	0	0.000	0.002	3990	tags=43%, list=20%, signal=54%
REACTOME_INTERFERON_SIGNALING	198	-0.54223	-2.3278	0	0.000	0.001	4388	tags=45%, list=22%, signal=57%
REACTOME_INTERLEUKIN_1_FAMILY_SIGNALING	139	-0.4334	-1.7928	0	0.005	0.685	3748	tags=32%, list=18%, signal=39%
REACTOME_INTERLEUKIN_1_SIGNALING	102	-0.46617	-1.8466	0	0.003	0.456	4360	tags=37%, list=22%, signal=47%
REACTOME_INTERLEUKIN_10_SIGNALING	46	-0.3596	-1.267	0.13807	0.190	1	2940	tags=24%, list=15%, signal=28%
REACTOME_INTERLEUKIN_12_FAMILY_SIGNALING	57	-0.47805	-1.7198	0.00136	0.010	0.927	3686	tags=39%, list=18%, signal=47%
REACTOME_INTERLEUKIN_12_SIGNALING	47	-0.42944	-1.5074	0.02408	0.049	1	5655	tags=53%, list=28%, signal=74%
REACTOME_INTERLEUKIN_17_SIGNALING	71	-0.52604	-1.9884	0	0.001	0.07	3356	tags=38%, list=17%, signal=45%
REACTOME_INTERLEUKIN_2_FAMILY_SIGNALING	44	-0.39732	-1.3561	0.0765	0.120	1	4800	tags=41%, list=24%, signal=53%
REACTOME_INTERLEUKIN_3_INTERLEUKIN_5_AND_GM_CSF_SIGNALING	48	-0.4962	-1.7392	0.00139	0.008	0.886	4800	tags=50%, list=24%, signal=65%
REACTOME_INTERLEUKIN_37_SIGNALING	21	-0.47407	-1.426	0.07098	0.081	1	3354	tags=38%, list=17%, signal=46%
REACTOME_INTERLEUKIN_4_AND_INTERLEUKIN_13_SIGNALING	108	-0.3306	-1.3279	0.06197	0.139	1	4773	tags=28%, list=24%, signal=36%
REACTOME_INTERLEUKIN_6_FAMILY_SIGNALING	24	-0.34541	-1.0437	0.41654	0.470	1	2751	tags=21%, list=14%, signal=24%
REACTOME_INTERLEUKIN_7_SIGNALING	23	-0.43102	-1.301	0.12894	0.161	1	4796	tags=43%, list=24%, signal=57%
REACTOME_INTERLEUKIN_RECEPTOR_SHC_SIGNALING	27	-0.42459	-1.3169	0.13077	0.147	1	4800	tags=48%, list=24%, signal=63%
REACTOME_INTRA_GOLGI_AND_RETROGRADE_GOLGI_TO_ER_TRAFFIC	202	-0.45606	-1.9643	0	0.001	0.102	4053	tags=36%, list=20%, signal=45%
REACTOME_INTRA_GOLGI_TRAFFIC	44	-0.58286	-2.0272	0	0.000	0.046	2925	tags=39%, list=14%, signal=45%

REACTOME_INTRACELLULAR_SIGNALING_BY_SECOND_MESSENGERS	304	-0.29955	-1.3451	0.01197	0.127	1	5586	tags=37%, list=28%, signal=50%
REACTOME_INTRAFLAGELLAR_TRANSPORT	54	-0.44542	-1.5855	0.0082	0.030	1	4235	tags=39%, list=21%, signal=49%
REACTOME_INTRINSIC_PATHWAY_FOR_APOPTOSIS	52	-0.50143	-1.7784	0.00131	0.006	0.732	4241	tags=44%, list=21%, signal=56%
REACTOME_INWARDLY_RECTIFYING_K_CHANNELS	35	-0.32642	-1.0851	0.35139	0.405	1	2462	tags=23%, list=12%, signal=26%
REACTOME_ION_CHANNEL_TRANSPORT	184	-0.22147	-0.9434	0.59577	0.625	1	3298	tags=18%, list=16%, signal=22%
REACTOME_ION_HOMEOSTASIS	54	-0.26519	-0.9615	0.53498	0.599	1	2696	tags=20%, list=13%, signal=23%
REACTOME_ION_TRANSPORT_BY_P_TYPE_ATPASES	55	-0.19585	-0.7135	0.91351	0.922	1	4851	tags=27%, list=24%, signal=36%
REACTOME_IRE1ALPHA_ACTIVATES_CHAPERONES	50	-0.46114	-1.6409	0.00567	0.019	0.997	4891	tags=42%, list=24%, signal=55%
REACTOME_IRON_UPTAKE_AND_TRANSPORT	58	-0.59486	-2.1463	0	0.000	0.004	3517	tags=53%, list=17%, signal=64%
REACTOME_JNK_C_JUN_KINASES_PHOSPHORYLATION_AND_ACTIVATION_MEDIATED_BY_ACTIVATED_HUMAN_TAK1	22	-0.64759	-1.9119	0	0.002	0.227	3356	tags=59%, list=17%, signal=71%
REACTOME_KINESINS	60	-0.21389	-0.7797	0.8293	0.857	1	4026	tags=25%, list=20%, signal=31%
REACTOME_KSRP_KHSRP_BINDS_AND_DESTABILIZES_MRNA	17	-0.51722	-1.4702	0.05449	0.063	1	4699	tags=47%, list=23%, signal=61%
REACTOME_L1CAM_INTERACTIONS	120	-0.31285	-1.2769	0.08261	0.181	1	4005	tags=30%, list=20%, signal=37%
REACTOME_LAGGING_STRAND_SYNTHESIS	20	-0.39867	-1.154	0.27129	0.314	1	5170	tags=40%, list=26%, signal=54%
REACTOME_LAMININ_INTERACTIONS	30	-0.19905	-0.638	0.9289	0.971	1	5932	tags=33%, list=29%, signal=47%
REACTOME_LATE_ENDOSOMAL_MICROAUTOPHAGY	34	-0.47018	-1.5366	0.0225	0.042	1	4217	tags=41%, list=21%, signal=52%
REACTOME_LDL_CLEARANCE	19	-0.61684	-1.8152	0.00468	0.004	0.577	2670	tags=42%, list=13%, signal=48%
REACTOME_LEISHMANIA_INFECTION	248	-0.25573	-1.1262	0.21222	0.350	1	4495	tags=25%, list=22%, signal=32%
REACTOME_LISTERIA_MONOCYTOGENES_ENTRY_INTO_HOST_CELLS	20	-0.60291	-1.7881	0.00472	0.005	0.698	4363	tags=65%, list=22%, signal=83%
REACTOME_LYSOSOME_VESICLE_BIOGENESIS	35	-0.34324	-1.1279	0.30949	0.349	1	4771	tags=40%, list=24%, signal=52%
REACTOME_M_PHASE	353	-0.50002	-2.258	0	0.000	0.002	5075	tags=46%, list=25%, signal=60%
REACTOME_MAP2K_AND_MAPK_ACTIVATION	40	-0.48407	-1.6458	0.01156	0.018	0.995	5174	tags=45%, list=26%, signal=60%
REACTOME_MAP3K8_TPL2_DEPENDENT_MAPK1_3_ACTIVATION	16	-0.63736	-1.7342	0.00503	0.008	0.898	3113	tags=44%, list=15%, signal=52%
REACTOME_MAPK_FAMILY_SIGNALING_CASCADES	324	-0.33243	-1.4969	0.00107	0.053	1	4264	tags=29%, list=21%, signal=36%
REACTOME_MAPK_TARGETS_NUCLEAR_EVENTS_MEDIATED_BY_MAP_KINASES	31	-0.59211	-1.9235	0.00148	0.001	0.187	4752	tags=55%, list=23%, signal=72%
REACTOME_MAPK6_MAPK4_SIGNALING	90	-0.46838	-1.8434	0	0.003	0.465	5729	tags=50%, list=28%, signal=69%
REACTOME_MECP2_REGULATES_NEURONAL_RECEPTORS_AND_CHANNELS	18	-0.39865	-1.1248	0.29708	0.352	1	3072	tags=33%, list=15%, signal=39%
REACTOME_MEIOSIS	58	-0.34745	-1.2716	0.1358	0.186	1	5085	tags=34%, list=25%, signal=46%

REACTOME_MEIOTIC_RECOMBINATION	26	-0.4507	-1.4153	0.06785	0.087	1	4871	tags=42%, list=24%, signal=56%
REACTOME_MEIOTIC_SYNAPSIS	33	-0.2587	-0.8463	0.69152	0.774	1	6879	tags=45%, list=34%, signal=69%
REACTOME_MET_ACTIVATES_PTK2_SIGNALING	30	-0.40401	-1.327	0.1021	0.140	1	5019	tags=43%, list=25%, signal=58%
REACTOME_MET_PROMOTES_CELL_MOTILITY	41	-0.49	-1.6634	0.00424	0.016	0.989	5019	tags=49%, list=25%, signal=65%
REACTOME_METABOLIC_DISORDERS_OF_BIOLOGICAL_OXIDATION_ENZYMES	36	-0.2682	-0.894	0.62797	0.701	1	3728	tags=22%, list=18%, signal=27%
REACTOME_METABOLISM_OF_AMINO_ACIDS_AND_DERIVATIVES	365	-0.33989	-1.5447	0	0.039	1	5581	tags=42%, list=28%, signal=58%
REACTOME_METABOLISM_OF_ANGIOTENSINOGEN_TO_ANGIOTENSINS	17	-0.33914	-0.9462	0.55296	0.621	1	6916	tags=59%, list=34%, signal=89%
REACTOME_METABOLISM_OF_CARBOHYDRATES	292	-0.20556	-0.9221	0.66703	0.661	1	4815	tags=25%, list=24%, signal=32%
REACTOME_METABOLISM_OF_COFACTORS	19	-0.45429	-1.315	0.15123	0.149	1	3542	tags=32%, list=17%, signal=38%
REACTOME_METABOLISM_OF_FAT_SOLUBLE_VITAMINS	48	-0.25943	-0.8953	0.64022	0.699	1	4622	tags=31%, list=23%, signal=40%
REACTOME_METABOLISM_OF_NITRIC_OXIDE_NOS3_ACTIVATION_AND_REGULATION	15	-0.62083	-1.6651	0.02284	0.016	0.988	1079	tags=33%, list=5%, signal=35%
REACTOME_METABOLISM_OF_NUCLEOTIDES	97	-0.39343	-1.5582	0.00493	0.035	1	4111	tags=34%, list=20%, signal=42%
REACTOME_METABOLISM_OF_POLYAMINES	59	-0.47017	-1.7233	0.00404	0.009	0.922	3178	tags=31%, list=16%, signal=36%
REACTOME_METABOLISM_OF_PORPHYRINS	26	-0.40644	-1.2604	0.17798	0.195	1	5744	tags=46%, list=28%, signal=64%
REACTOME_METABOLISM_OF_STEROIDS	151	-0.44803	-1.8805	0	0.002	0.314	4373	tags=38%, list=22%, signal=49%
REACTOME_METABOLISM_OF_VITAMINS_AND_COFACTORS	187	-0.33375	-1.4375	0.00575	0.076	1	4626	tags=31%, list=23%, signal=40%
REACTOME_METABOLISM_OF_WATER_SOLUBLE_VITAMINS_AND_COFACTORS	121	-0.35564	-1.4441	0.02068	0.073	1	4233	tags=29%, list=21%, signal=36%
REACTOME_METAL_ION_SLC_TRANSPORTERS	26	-0.56318	-1.7463	0.00897	0.008	0.868	3590	tags=50%, list=18%, signal=61%
REACTOME_METALLOPROTEASE_DUBS	20	-0.71132	-2.0676	0	0.000	0.021	3113	tags=60%, list=15%, signal=71%
REACTOME_MHC_CLASS_II_ANTIGEN_PRESENTATION	123	-0.52773	-2.1694	0	0.000	0.002	4026	tags=45%, list=20%, signal=55%
REACTOME_MICRORNA_MIRNA_BIOGENESIS	25	-0.51989	-1.6014	0.01695	0.026	1	4086	tags=52%, list=20%, signal=65%
REACTOME_MISCELLANEOUS_TRANSPORT_AND_BINDING_EVENTS	25	-0.28579	-0.8821	0.64706	0.720	1	741	tags=8%, list=4%, signal=8%
REACTOME_MISMATCH_REPAIR	15	-0.5156	-1.4071	0.10535	0.091	1	4584	tags=47%, list=23%, signal=60%
REACTOME_MITOCHONDRIAL_BIOGENESIS	90	-0.52501	-2.0711	0	0.000	0.021	4977	tags=46%, list=25%, signal=60%
REACTOME_MITOCHONDRIAL_CALCIUM_ION_TRANSPORT	23	-0.56031	-1.6831	0.00602	0.013	0.982	4578	tags=65%, list=23%, signal=84%
REACTOME_MITOCHONDRIAL_FATTY_ACID_BETA_OXIDATION	36	-0.44808	-1.4758	0.03343	0.061	1	3396	tags=33%, list=17%, signal=40%
REACTOME_MITOCHONDRIAL_PROTEIN_IMPORT	65	-0.42351	-1.5749	0.00788	0.032	1	4266	tags=38%, list=21%, signal=49%

REACTOME_MITOCHONDRIAL_TRANSLATION	94	-0.36649	-1.4438	0.02471	0.073	1	4059	tags=30%, list=20%, signal=37%
REACTOME_MITOPHAGY	29	-0.56602	-1.8006	0.00147	0.005	0.65	3934	tags=55%, list=19%, signal=68%
REACTOME_MITOTIC_G1_PHASE_AND_G1_S_TRANSITION	149	-0.47455	-2.0089	0	0.000	0.054	4124	tags=40%, list=20%, signal=50%
REACTOME_MITOTIC_G2_G2_M_PHASES	198	-0.44266	-1.9138	0	0.002	0.223	4124	tags=34%, list=20%, signal=42%
REACTOME_MITOTIC_METAPHASE_AND_ANAPHASE	235	-0.45902	-2.0072	0	0.000	0.054	4997	tags=43%, list=25%, signal=56%
REACTOME_MITOTIC_PROMETAPHASE	201	-0.43413	-1.8807	0	0.002	0.313	4997	tags=40%, list=25%, signal=52%
REACTOME_MITOTIC_PROPHASE	81	-0.61267	-2.3665	0	0.000	0	5075	tags=60%, list=25%, signal=80%
REACTOME_MITOTIC_SPINDLE_CHECKPOINT	111	-0.4633	-1.8499	0	0.003	0.442	4994	tags=41%, list=25%, signal=55%
REACTOME_MOLECULES_ASSOCIATED_WITH_ELASTIC_FIBRES	38	-0.20614	-0.685	0.91323	0.944	1	2171	tags=11%, list=11%, signal=12%
REACTOME_MRNA_CAPPING	29	-0.59564	-1.8688	0	0.002	0.366	4571	tags=59%, list=23%, signal=76%
REACTOME_MRNA_DECAY_BY_3_TO_5_EXORIBONUCLEASE	16	-0.57227	-1.5502	0.02782	0.038	1	4699	tags=56%, list=23%, signal=73%
REACTOME_MRNA_DECAY_BY_5_TO_3_EXORIBONUCLEASE	15	-0.53943	-1.4596	0.07642	0.067	1	4529	tags=47%, list=22%, signal=60%
REACTOME_MRNA_SPLICING	188	-0.55303	-2.3755	0	0.000	0	5296	tags=55%, list=26%, signal=74%
REACTOME_MRNA_SPLICING_MINOR_PATHWAY	52	-0.57475	-2.0757	0	0.000	0.019	5293	tags=56%, list=26%, signal=75%
REACTOME_MTOR_SIGNALLING	40	-0.52314	-1.784	0.00284	0.005	0.713	2774	tags=38%, list=14%, signal=43%
REACTOME_MTORC1_MEDIATED_SIGNALLING	23	-0.52457	-1.5736	0.02065	0.033	1	5561	tags=61%, list=27%, signal=84%
REACTOME_MYD88_INDEPENDENT_TLR4_CASCADE_	97	-0.5097	-2.0463	0	0.000	0.036	4021	tags=42%, list=20%, signal=52%
REACTOME_MYOGENESIS	29	-0.4756	-1.511	0.02655	0.048	1	6275	tags=59%, list=31%, signal=85%
REACTOME_N_GLYCAN_ANTENNAE_ELONGATION	15	-0.24457	-0.6517	0.91558	0.964	1	6818	tags=47%, list=34%, signal=70%
REACTOME_N_GLYCAN_ANTENNAE_ELONGATION_IN_THE_MEDIAL_TRANS_GOLGI	26	-0.22582	-0.6922	0.87048	0.942	1	1845	tags=12%, list=9%, signal=13%
REACTOME_N_GLYCAN_TRIMMING_IN_THE_ER_AND_CALNEXIN_CALRETICULIN_CYCLE	34	-0.67968	-2.245	0	0.000	0.002	4255	tags=56%, list=21%, signal=71%
REACTOME_NEDDYLATION	234	-0.34389	-1.4947	0.00221	0.054	1	3400	tags=24%, list=17%, signal=29%
REACTOME_NEF_MEDIATES_DOWN_MODULATION_OF_CELL_SURFACE_RECEPTORS_BY_RECRUITING_THEM_TO_CLATHRIN_ADAPTERS	21	-0.46523	-1.3981	0.0858	0.095	1	3565	tags=33%, list=18%, signal=40%
REACTOME_NEGATIVE_EPIGENETIC_REGULATION_OF_RRNA_EXPRESSION	49	-0.49638	-1.7661	0.00275	0.006	0.797	4580	tags=47%, list=23%, signal=60%
REACTOME_NEGATIVE_REGULATION_OF_FGFR1_SIGNALING	33	-0.44602	-1.4577	0.04155	0.068	1	3249	tags=33%, list=16%, signal=40%
REACTOME_NEGATIVE_REGULATION_OF_FGFR2_SIGNALING	34	-0.40795	-1.3466	0.1016	0.126	1	3249	tags=32%, list=16%, signal=38%

REACTOME_NEGATIVE_REGULATION_OF_FGFR3_SIGNALING	29	-0.45598	-1.469	0.04348	0.063	1	3249	tags=38%, list=16%, signal=45%
REACTOME_NEGATIVE_REGULATION_OF_FGFR4_SIGNALING	31	-0.45939	-1.4951	0.04769	0.054	1	3249	tags=35%, list=16%, signal=42%
REACTOME_NEGATIVE_REGULATION_OF_MAPK_PATHWAY	43	-0.45738	-1.5651	0.01269	0.034	1	5174	tags=44%, list=26%, signal=59%
REACTOME_NEGATIVE_REGULATION_OF_MET_ACTIVITY	21	-0.633	-1.8761	0	0.002	0.332	4363	tags=62%, list=22%, signal=79%
REACTOME_NEGATIVE_REGULATION_OF_NOTCH4_SIGNALING	54	-0.56299	-2.0214	0	0.000	0.049	5729	tags=59%, list=28%, signal=82%
REACTOME_NEGATIVE_REGULATION_OF_THE_PI3K_AKT_NETWORK	110	-0.24878	-0.9985	0.47292	0.538	1	4722	tags=30%, list=23%, signal=39%
REACTOME_NEGATIVE_REGULATORS_OF_DDX58_IFIH1_SIGNALING	34	-0.66122	-2.176	0	0.000	0.002	3558	tags=62%, list=18%, signal=75%
REACTOME_NEPHRIN_FAMILY_INTERACTIONS	23	-0.4803	-1.4512	0.05023	0.071	1	4003	tags=48%, list=20%, signal=60%
REACTOME_NETRIN_1_SIGNALING	50	-0.34275	-1.2217	0.19359	0.233	1	4722	tags=34%, list=23%, signal=44%
REACTOME_NEUTROPHIL_DEGRANULATION	475	-0.45552	-2.0888	0	0.000	0.014	4491	tags=39%, list=22%, signal=49%
REACTOME_NICOTINAMIDE_SALVAGING	19	-0.35602	-1.0248	0.44601	0.501	1	4436	tags=32%, list=22%, signal=40%
REACTOME_NICOTINATE_METABOLISM	31	-0.4431	-1.4243	0.06259	0.082	1	1973	tags=19%, list=10%, signal=21%
REACTOME_NOD1_2_SIGNALING_PATHWAY	36	-0.67901	-2.2298	0	0.000	0.002	3356	tags=56%, list=17%, signal=66%
REACTOME_NON_INTEGRIN_MEMBRANE_ECM_INTERACTIONS	59	-0.21472	-0.7884	0.80079	0.849	1	5019	tags=29%, list=25%, signal=38%
REACTOME_NONHOMOLOGOUS_END_JOINING_NHEJ_	35	-0.50377	-1.6613	0.00576	0.016	0.99	4940	tags=43%, list=24%, signal=57%
REACTOME_NONSENSE_MEDIATED_DECAY_NMD_	116	-0.63384	-2.5971	0	0.000	0	5581	tags=74%, list=28%, signal=102%
REACTOME_NOTCH_HLH_TRANSCRIPTION_PATHWAY	28	-0.42036	-1.3417	0.10557	0.129	1	1782	tags=18%, list=9%, signal=20%
REACTOME_NOTCH1_INTRACELLULAR_DOMAIN_REGULATES_TRANSCRIPTION	48	-0.40575	-1.4446	0.04237	0.073	1	5351	tags=44%, list=26%, signal=59%
REACTOME_NOTCH2_ACTIVATION_AND_TRANSMISSION_OF_SIGNAL_TO_THE_NUCLEUS	22	-0.40893	-1.2209	0.20934	0.233	1	3760	tags=32%, list=19%, signal=39%
REACTOME_NOTCH3_ACTIVATION_AND_TRANSMISSION_OF_SIGNAL_TO_THE_NUCLEUS	25	-0.32315	-0.9964	0.47786	0.541	1	3760	tags=28%, list=19%, signal=34%
REACTOME_NOTCH3_INTRACELLULAR_DOMAIN_REGULATES_TRANSCRIPTION	25	-0.45405	-1.3957	0.09119	0.096	1	2465	tags=20%, list=12%, signal=23%
REACTOME_NOTCH4_INTRACELLULAR_DOMAIN_REGULATES_TRANSCRIPTION	20	-0.44962	-1.3171	0.15712	0.147	1	5142	tags=30%, list=25%, signal=40%
REACTOME_NR1H2_AND_NR1H3_MEDIATED_SIGNALING	47	-0.41894	-1.4493	0.02991	0.071	1	3873	tags=36%, list=19%, signal=45%
REACTOME_NR1H3_NR1H2_REGULATE_GENE_EXPRESSION_LINKED_TO_CHOLESTEROL_TRANSPORT_AND_EFFLUX	37	-0.36861	-1.2524	0.14577	0.202	1	6335	tags=49%, list=31%, signal=71%

REACTOME_NRAGE_SIGNALS_DEATH_THROUGH_JNK	59	-0.23394	-0.8451	0.71486	0.774	1	2753	tags=17%, list=14%, signal=20%
REACTOME_NRIF_SIGNALS_CELL_DEATH_FROM_THE_NUCLEUS	16	-0.55185	-1.4885	0.04368	0.056	1	3760	tags=56%, list=19%, signal=69%
REACTOME_NS1_MEDIATED_EFFECTS_ON_HOST_PATHWAYS	40	-0.62846	-2.0978	0	0.000	0.011	4729	tags=58%, list=23%, signal=75%
REACTOME_NUCLEAR_ENVELOPE_BREAKDOWN	52	-0.59973	-2.1399	0	0.000	0.004	4729	tags=58%, list=23%, signal=75%
REACTOME_NUCLEAR_ENVELOPE_NE_REASSEMBLY	75	-0.39912	-1.5344	0.00895	0.042	1	4811	tags=41%, list=24%, signal=54%
REACTOME_NUCLEAR_EVENTS_KINASE_AND_TRANSCRIPTION_FACTOR_ACTIVATION_	61	-0.3634	-1.3272	0.08784	0.140	1	4362	tags=34%, list=22%, signal=44%
REACTOME_NUCLEAR_IMPORT_OF_REV_PROTEIN	33	-0.67409	-2.2147	0	0.000	0.002	4729	tags=64%, list=23%, signal=83%
REACTOME_NUCLEAR_PORE_COMPLEX_NPC_DISASSEMBLY	35	-0.68924	-2.2595	0	0.000	0.002	4729	tags=66%, list=23%, signal=86%
REACTOME_NUCLEAR_RECEPTOR_TRANSCRIPTION_PATHWAY	53	-0.37767	-1.348	0.0762	0.125	1	2992	tags=23%, list=15%, signal=26%
REACTOME_NUCLEAR_SIGNALING_BY_ERBB4	32	-0.34026	-1.106	0.31399	0.378	1	3760	tags=25%, list=19%, signal=31%
REACTOME_NUCLEOBASE_CATABOLISM	36	-0.42459	-1.434	0.05832	0.078	1	2341	tags=28%, list=12%, signal=31%
REACTOME_NUCLEOTIDE_BINDING_DOMAIN_LEUCINE_RICH_REPEAT_CONTAINING_RECEPTOR_NLR_SIGNALING_PATHWAYS	55	-0.58323	-2.142	0	0.000	0.004	3892	tags=45%, list=19%, signal=56%
REACTOME_NUCLEOTIDE_EXCISION_REPAIR	110	-0.55445	-2.2623	0	0.000	0.002	3625	tags=44%, list=18%, signal=53%
REACTOME_NUCLEOTIDE_LIKE_PURINERGIC_RECEPTORS	16	-0.33616	-0.9172	0.59868	0.668	1	100	tags=6%, list=0%, signal=6%
REACTOME_ONCOGENE_INDUCED_SENESCENCE	34	-0.46502	-1.507	0.02774	0.049	1	3113	tags=38%, list=15%, signal=45%
REACTOME_ONCOGENIC_MAPK_SIGNALING	82	-0.4558	-1.7832	0	0.005	0.716	5174	tags=44%, list=26%, signal=59%
REACTOME_OPIOID_SIGNALLING	90	-0.26612	-1.0522	0.39272	0.458	1	4038	tags=26%, list=20%, signal=32%
REACTOME_ORC1_REMOVAL_FROM_CHROMATIN	71	-0.49279	-1.8671	0	0.002	0.368	5555	tags=52%, list=27%, signal=72%
REACTOME_ORGANELLE_BIOGENESIS_AND_MAINTENANCE	289	-0.43927	-1.9336	0	0.001	0.166	4379	tags=35%, list=22%, signal=44%
REACTOME_OTHER_INTERLEUKIN_SIGNALING	24	-0.32877	-0.9988	0.46606	0.539	1	5793	tags=42%, list=29%, signal=58%
REACTOME_OTHER_SEMAPHORIN_INTERACTIONS	19	-0.44229	-1.2844	0.17863	0.175	1	2465	tags=21%, list=12%, signal=24%
REACTOME_OVARIAN_TUMOR_DOMAIN_PROTEASES	38	-0.56226	-1.8736	0	0.002	0.34	4420	tags=53%, list=22%, signal=67%
REACTOME_OXIDATIVE_STRESS_INDUCED_SENESCENCE	65	-0.43472	-1.5875	0.01459	0.029	1	3113	tags=32%, list=15%, signal=38%
REACTOME_P130CAS_LINKAGE_TO_MAPK_SIGNALING_FOR_INTEGRINS	15	-0.53196	-1.4592	0.06209	0.067	1	4090	tags=53%, list=20%, signal=67%
REACTOME_P75_NTR_RECEPTOR_MEDIATED_SIGNALLING	97	-0.30618	-1.2207	0.14568	0.233	1	3760	tags=27%, list=19%, signal=33%
REACTOME_P75NTR_SIGNALS_VIA_NF_KB	16	-0.37944	-1.0471	0.40226	0.466	1	3507	tags=38%, list=17%, signal=45%

REACTOME_PARASITE_INFECTION	58	-0.54263	-1.9967	0	0.001	0.06	4495	tags=52%, list=22%, signal=66%
REACTOME_PCNA_DEPENDENT_LONG_PATCH_BASE_EXCISION_REPAIR	21	-0.554	-1.6656	0.0181	0.016	0.988	4558	tags=52%, list=22%, signal=68%
REACTOME_PCP_CE_PATHWAY	92	-0.45637	-1.7695	0	0.006	0.778	4599	tags=38%, list=23%, signal=49%
REACTOME_PD_1_SIGNALING	21	-0.75807	-2.2035	0	0.000	0.002	1070	tags=43%, list=5%, signal=45%
REACTOME_PEPTIDE_HORMONE_METABOLISM	89	-0.27576	-1.0857	0.31959	0.405	1	3353	tags=21%, list=17%, signal=25%
REACTOME_PERK_REGULATES_GENE_EXPRESSION	32	-0.48593	-1.5778	0.01986	0.032	1	4911	tags=53%, list=24%, signal=70%
REACTOME_PEROXISOMAL_LIPID_METABOLISM	29	-0.34317	-1.0904	0.32799	0.400	1	3866	tags=28%, list=19%, signal=34%
REACTOME_PEROXISOMAL_PROTEIN_IMPORT	63	-0.38774	-1.4253	0.04768	0.082	1	4104	tags=35%, list=20%, signal=44%
REACTOME_PHASE_I_FUNCTIONALIZATION_OF_COMPOUNDS	102	-0.2174	-0.8648	0.74969	0.744	1	2287	tags=13%, list=11%, signal=14%
REACTOME_PHASE_II_CONJUGATION_OF_COMPOUNDS	107	-0.30511	-1.2298	0.14007	0.224	1	5076	tags=36%, list=25%, signal=47%
REACTOME_PHOSPHOLIPID_METABOLISM	206	-0.36678	-1.5886	0	0.029	1	5886	tags=44%, list=29%, signal=61%
REACTOME_PHOSPHORYLATION_OF_THE_APC_C	20	-0.64365	-1.8794	0	0.002	0.318	4264	tags=45%, list=21%, signal=57%
REACTOME_PHOSPHORYLATION_SITE_MUTANTS_OF_CTNNB1_ARE_NOT_TARGETED_TO_THE_PROTEASOME_BY_THE_DESTRUCTION_COMPLEX	15	-0.71326	-1.9271	0	0.001	0.179	4021	tags=67%, list=20%, signal=83%
REACTOME_PI_3K_CASCADE_FGFR1	21	-0.32952	-0.9742	0.48237	0.578	1	2525	tags=19%, list=12%, signal=22%
REACTOME_PI_3K_CASCADE_FGFR2	23	-0.28205	-0.8453	0.67647	0.775	1	2525	tags=17%, list=12%, signal=20%
REACTOME_PI_3K_CASCADE_FGFR3	18	-0.3337	-0.9533	0.5084	0.611	1	2525	tags=22%, list=12%, signal=25%
REACTOME_PI_3K_CASCADE_FGFR4	20	-0.33754	-0.9925	0.45455	0.547	1	2525	tags=20%, list=12%, signal=23%
REACTOME_PI_METABOLISM	84	-0.46696	-1.8142	0	0.004	0.58	4685	tags=43%, list=23%, signal=56%
REACTOME_PI3K_EVENTS_IN_ERBB2_SIGNALING	16	-0.33525	-0.9181	0.59242	0.667	1	2525	tags=19%, list=12%, signal=21%
REACTOME_PINK1_PRKN_MEDIATED_MITOPHAGY	22	-0.55539	-1.6334	0.00987	0.020	0.999	3934	tags=55%, list=19%, signal=68%
REACTOME_PIWI_INTERACTING_RNA_PIRNA_BIOGENESIS	29	-0.41112	-1.3075	0.12329	0.155	1	2692	tags=24%, list=13%, signal=28%
REACTOME_PKMTS_METHYLATE_HISTONE_LYSINES	44	-0.49011	-1.71	0.00297	0.010	0.948	4710	tags=48%, list=23%, signal=62%
REACTOME_PLASMA_LIPOPROTEIN_ASSEMBLY	19	-0.48595	-1.4006	0.08889	0.094	1	2496	tags=32%, list=12%, signal=36%
REACTOME_PLASMA_LIPOPROTEIN_ASSEMBLY_REMODELING_AND_CLEARANCE	71	-0.4226	-1.6048	0.00133	0.026	1	2768	tags=28%, list=14%, signal=33%
REACTOME_PLASMA_LIPOPROTEIN_CLEARANCE	33	-0.48303	-1.5635	0.02458	0.034	1	2768	tags=30%, list=14%, signal=35%
REACTOME_PLASMA_LIPOPROTEIN_REMODELING	32	-0.24087	-0.8035	0.76117	0.830	1	3724	tags=25%, list=18%, signal=31%
REACTOME_PLATELET_ACTIVATION_SIGNALING_AND_AGGREGATION	260	-0.37273	-1.6535	0	0.017	0.993	4722	tags=37%, list=23%, signal=48%

REACTOME_PLATELET_ADHESION_TO_EXPOSED_COLLAGEN	15	-0.43609	-1.2161	0.22692	0.238	1	2440	tags=27%, list=12%, signal=30%
REACTOME_PLATELET_AGGREGATION_PLUG_FORMATION_	39	-0.31993	-1.0913	0.34907	0.399	1	4626	tags=36%, list=23%, signal=46%
REACTOME_PLATELET_HOMEOSTASIS	85	-0.30443	-1.1767	0.19338	0.284	1	4983	tags=35%, list=25%, signal=47%
REACTOME_PLATELET_SENSITIZATION_BY_LDL	17	-0.63337	-1.77	0.00319	0.006	0.776	4722	tags=59%, list=23%, signal=77%
REACTOME_POLO_LIKE_KINASE_MEDIATED_EVENTS	16	-0.3281	-0.9167	0.5616	0.668	1	4087	tags=25%, list=20%, signal=31%
REACTOME_POLYMERASE_SWITCHING_ON_THE_C_STRAND_OF_THE_TELOMERE	26	-0.26159	-0.8068	0.76347	0.826	1	5170	tags=35%, list=26%, signal=46%
REACTOME_POSITIVE_EPIGENETIC_REGULATION_OF_RRNA_EXPRESSION	46	-0.4553	-1.5989	0.00954	0.027	1	4580	tags=46%, list=23%, signal=59%
REACTOME_POSTMITOTIC_NUCLEAR_PORE_COMPLEX_NPC_REFORMATION	27	-0.59216	-1.8314	0.00157	0.003	0.523	6259	tags=70%, list=31%, signal=102%
REACTOME_POTENTIAL_THERAPEUTICS_FOR_SARS	37	-0.54415	-1.877	0	0.002	0.331	4749	tags=51%, list=23%, signal=67%
REACTOME_PRE_NOTCH_EXPRESSION_AND_PROCESSING	49	-0.43284	-1.5213	0.02436	0.045	1	3060	tags=29%, list=15%, signal=34%
REACTOME_PRE_NOTCH_PROCESSING_IN_GOLGI	18	-0.48368	-1.3785	0.09524	0.105	1	3792	tags=39%, list=19%, signal=48%
REACTOME_PRESYNAPTIC_FUNCTION_OF_KAINATE_RECEPTORS	21	-0.47454	-1.4114	0.10079	0.089	1	2462	tags=33%, list=12%, signal=38%
REACTOME_PROCESSING_OF_CAPPED_INTRON_CONTAINING_PRE_MRNA	241	-0.56523	-2.4771	0	0.000	0	5454	tags=57%, list=27%, signal=77%
REACTOME_PROCESSING_OF_CAPPED_INTRONLESS_PRE_MRNA	28	-0.61221	-1.903	0.00292	0.002	0.254	5293	tags=54%, list=26%, signal=72%
REACTOME_PROCESSING_OF_DNA_DOUBLE_STRAND_BREAK_ENDS	64	-0.51262	-1.9257	0	0.001	0.182	4710	tags=47%, list=23%, signal=61%
REACTOME_PROCESSING_OF_INTRONLESS_PRE_MRNAS	19	-0.65637	-1.8779	0	0.002	0.326	5293	tags=58%, list=26%, signal=78%
REACTOME_PROCESSING_OF_SMDT1	16	-0.61223	-1.697	0.00954	0.012	0.96	4467	tags=69%, list=22%, signal=88%
REACTOME_PROCESSIVE_SYNTHESIS_ON_THE_C_STRAND_OF_THE_TELOMERE	19	-0.50796	-1.4526	0.05984	0.070	1	3112	tags=32%, list=15%, signal=37%
REACTOME_PROCESSIVE_SYNTHESIS_ON_THE_LAGGING_STRAND	15	-0.42893	-1.16	0.27869	0.305	1	3112	tags=27%, list=15%, signal=31%
REACTOME_PROGRAMMED_CELL_DEATH	173	-0.43563	-1.8461	0	0.003	0.457	4241	tags=38%, list=21%, signal=47%
REACTOME_PROLACTIN_RECEPTOR_SIGNALING	15	-0.4031	-1.0964	0.34053	0.391	1	5351	tags=47%, list=26%, signal=63%
REACTOME_PROSTACYCLIN_SIGNALLING_THROUGH_PROSTACYCLIN_RECEPTOR	19	-0.48127	-1.3925	0.09682	0.098	1	2462	tags=37%, list=12%, signal=42%
REACTOME_PROTEIN_FOLDING	102	-0.39575	-1.5735	0.00745	0.032	1	4130	tags=34%, list=20%, signal=43%
REACTOME_PROTEIN_LOCALIZATION	162	-0.36476	-1.5337	0.00116	0.042	1	4266	tags=33%, list=21%, signal=42%
REACTOME_PROTEIN_METHYLATION	17	-0.34904	-0.9683	0.50579	0.588	1	4751	tags=41%, list=23%, signal=54%

REACTOME_PROTEIN_UBIQUITINATION	64	-0.56881	-2.103	0	0.000	0.009	3951	tags=50%, list=19%, signal=62%
REACTOME_PTEN_REGULATION	139	-0.49715	-2.0649	0	0.000	0.023	5561	tags=52%, list=27%, signal=71%
REACTOME_PURINE_CATABOLISM	18	-0.52881	-1.4981	0.05354	0.053	1	4462	tags=44%, list=22%, signal=57%
REACTOME_PURINERGIC_SIGNALING_IN_LEISHMANIASIS_INFECTION	24	-0.58393	-1.7666	0.00291	0.006	0.794	4455	tags=50%, list=22%, signal=64%
REACTOME_PYRUVATE_METABOLISM	31	-0.43601	-1.3941	0.07895	0.097	1	3941	tags=32%, list=19%, signal=40%
REACTOME_PYRUVATE_METABOLISM_AND_CITRIC_ACID_TCA_CYCLE	55	-0.4485	-1.6166	0.00962	0.024	1	3941	tags=35%, list=19%, signal=43%
REACTOME_RAB_GEFS_EXCHANGE_GTP_FOR_GDP_ON_RABS	89	-0.46723	-1.8607	0	0.003	0.397	2642	tags=27%, list=13%, signal=31%
REACTOME_RAB_GERANYLGERANYLATION	65	-0.38756	-1.4475	0.02914	0.072	1	3403	tags=23%, list=17%, signal=28%
REACTOME_RAB_REGULATION_OF_TRAFFICKING	121	-0.4832	-1.9782	0	0.001	0.079	2642	tags=29%, list=13%, signal=33%
REACTOME_RAF_ACTIVATION	34	-0.48325	-1.5726	0.02305	0.033	1	5088	tags=50%, list=25%, signal=67%
REACTOME_RAF_INDEPENDENT_MAPK1_3_ACTIVATION	23	-0.31403	-0.9468	0.52221	0.620	1	4722	tags=30%, list=23%, signal=40%
REACTOME_RAP1_SIGNALLING	16	-0.40986	-1.1288	0.30141	0.348	1	2774	tags=25%, list=14%, signal=29%
REACTOME_RAS_PROCESSING	24	-0.49446	-1.4988	0.0471	0.052	1	3113	tags=33%, list=15%, signal=39%
REACTOME_RECOGNITION_OF_DNA_DAMAGE_BY_PCNA_CONTAINING_REPLICATION_COMPLEX	30	-0.58181	-1.8597	0.00144	0.003	0.404	4960	tags=60%, list=24%, signal=79%
REACTOME_RECRUITMENT_OF_MITOTIC_CENTROSOME_PROTEINS_AND_COMPLEXES	80	-0.45139	-1.7601	0	0.007	0.826	4264	tags=34%, list=21%, signal=43%
REACTOME_RECRUITMENT_OF_NUMA_TO_MITOTIC_CENTROSOMES	93	-0.38931	-1.526	0.00627	0.044	1	4264	tags=31%, list=21%, signal=39%
REACTOME_RECYCLING_OF_BILE_ACIDS_AND_SALTS	16	-0.27237	-0.7362	0.80909	0.902	1	3193	tags=25%, list=16%, signal=30%
REACTOME_RECYCLING_PATHWAY_OF_L1	48	-0.42159	-1.5098	0.0195	0.049	1	4342	tags=40%, list=21%, signal=50%
REACTOME_REGULATION_OF_CHOLESTEROL_BIOSYNTHESIS_BY_SREBP_SREBF_	55	-0.62968	-2.2385	0	0.000	0.002	3485	tags=49%, list=17%, signal=59%
REACTOME_REGULATION_OF_EXPRESSION_OF_SLITS_AND_ROBOS	172	-0.58531	-2.5023	0	0.000	0	5581	tags=65%, list=28%, signal=89%
REACTOME_REGULATION_OF_FZD_BY_UBIQUITINATION	21	-0.37035	-1.0876	0.3791	0.402	1	3774	tags=38%, list=19%, signal=47%
REACTOME_REGULATION_OF_GENE_EXPRESSION_IN_LATE_STAGE_BRANCHING_MORPHOGENESIS_PANCREATIC_BUD_PRECURSOR_CELLS	16	-0.56229	-1.5343	0.05065	0.042	1	5142	tags=44%, list=25%, signal=59%
REACTOME_REGULATION_OF_GLUCOKINASE_BY_GLUCOKINASE_REGULATORY_PROTEIN	31	-0.64588	-2.0719	0	0.000	0.021	4729	tags=65%, list=23%, signal=84%
REACTOME_REGULATION_OF_HSF1_MEDIATED_HEAT_SHOCK_RESPONSE	81	-0.58648	-2.2669	0	0.000	0.002	5086	tags=57%, list=25%, signal=76%

REACTOME_REGULATION_OF_IFNA_SIGNALING	26	-0.43784	-1.3346	0.10189	0.134	1	4179	tags=38%, list=21%, signal=48%
REACTOME_REGULATION_OF_INSULIN_LIKE_GROWTH_FACTOR_IGF_TRANSPORT_AND_UPTAKE_BY_INSULIN_LIKE_GROWTH_FACTOR_BINDING_PROTEINS_IGFBPS_	123	-0.29231	-1.1905	0.16141	0.268	1	5895	tags=43%, list=29%, signal=60%
REACTOME_REGULATION_OF_INSULIN_SECRETION	78	-0.34151	-1.3369	0.06971	0.132	1	3742	tags=27%, list=18%, signal=33%
REACTOME_REGULATION_OF_KIT_SIGNALING	16	-0.44702	-1.2421	0.19449	0.213	1	4185	tags=50%, list=21%, signal=63%
REACTOME_REGULATION_OF_LIPID_METABOLISM_BY_PPARALPHA	118	-0.47023	-1.917	0	0.001	0.208	4152	tags=38%, list=20%, signal=48%
REACTOME_REGULATION_OF_MECP2_EXPRESSION_AND_ACTIVITY	31	-0.38295	-1.219	0.21439	0.235	1	5642	tags=45%, list=28%, signal=62%
REACTOME_REGULATION_OF_MRNA_STABILITY_BY_PROTEINS_THAT_BIND_AU_RICH_ELEMENTS	87	-0.52579	-2.0993	0	0.000	0.01	5582	tags=56%, list=28%, signal=77%
REACTOME_REGULATION_OF_PLK1_ACTIVITY_AT_G2_M_TRANSITION	86	-0.53755	-2.086	0	0.000	0.017	4264	tags=41%, list=21%, signal=51%
REACTOME_REGULATION_OF_PTEN_GENE_TRANSCRIPTION	61	-0.41603	-1.5275	0.00904	0.044	1	5561	tags=46%, list=27%, signal=63%
REACTOME_REGULATION_OF_PTEN_STABILITY_AND_ACTIVITY	69	-0.55039	-2.0519	0	0.000	0.034	5555	tags=57%, list=27%, signal=78%
REACTOME_REGULATION_OF_PYRUVATE_DEHYDROGENASE_PDH_COMPLEX	16	-0.5042	-1.3747	0.109	0.107	1	451	tags=13%, list=2%, signal=13%
REACTOME_REGULATION_OF_RAS_BY_GAPS	68	-0.50446	-1.907	0	0.002	0.241	4173	tags=40%, list=21%, signal=50%
REACTOME_REGULATION_OF_RUNX1_EXPRESSION_AND_ACTIVITY	17	-0.51993	-1.4655	0.0656	0.065	1	6101	tags=59%, list=30%, signal=84%
REACTOME_REGULATION_OF_RUNX2_EXPRESSION_AND_ACTIVITY	73	-0.52123	-1.974	0	0.001	0.086	3625	tags=37%, list=18%, signal=45%
REACTOME_REGULATION_OF_RUNX3_EXPRESSION_AND_ACTIVITY	55	-0.53113	-1.895	0	0.002	0.276	5729	tags=56%, list=28%, signal=78%
REACTOME_REGULATION_OF_SIGNALING_BY_CBL	22	-0.56581	-1.7144	0.00488	0.010	0.938	5399	tags=64%, list=27%, signal=87%
REACTOME_REGULATION_OF_TLR_BY_ENDOGENOUS_LIGAND	19	-0.51851	-1.5117	0.03762	0.048	1	2007	tags=32%, list=10%, signal=35%
REACTOME_REGULATION_OF_TNFR1_SIGNALING	33	-0.54028	-1.7639	0.00141	0.006	0.805	5246	tags=61%, list=26%, signal=82%
REACTOME_REGULATION_OF_TP53_ACTIVITY	160	-0.4599	-1.9457	0	0.001	0.142	4626	tags=40%, list=23%, signal=51%
REACTOME_REGULATION_OF_TP53_ACTIVITY_THROUGH_ACETYLATION	30	-0.43002	-1.384	0.07843	0.102	1	5316	tags=47%, list=26%, signal=63%
REACTOME_REGULATION_OF_TP53_ACTIVITY_THROUGH_METHYLATION	19	-0.63659	-1.8291	0.00152	0.004	0.535	4400	tags=58%, list=22%, signal=74%
REACTOME_REGULATION_OF_TP53_ACTIVITY_THROUGH_PHOSPHORYLATION	92	-0.50069	-1.9771	0	0.001	0.08	4525	tags=40%, list=22%, signal=52%

REACTOME_REGULATION_OF_TP53_EXPRESSION_AND_DEGRADATION	37	-0.51457	-1.7427	0.00429	0.008	0.882	4264	tags=49%, list=21%, signal=61%
REACTOME_REPRODUCTION	84	-0.21192	-0.8231	0.77177	0.807	1	5085	tags=27%, list=25%, signal=36%
REACTOME_RESOLUTION_OF_ABASIC_SITES_AP_SITES_	37	-0.42533	-1.4006	0.05951	0.094	1	4558	tags=32%, list=22%, signal=42%
REACTOME_RESOLUTION_OF_AP_SITES_VIA_THE_MULTIPLE_NUCLEOTIDE_PATCH_REPLACEMENT_PATHWAY	24	-0.55698	-1.7221	0.00884	0.009	0.923	4558	tags=50%, list=22%, signal=64%
REACTOME_RESOLUTION_OF_D_LOOP_STRUCTURES	34	-0.37872	-1.2359	0.18519	0.219	1	6154	tags=38%, list=30%, signal=55%
REACTOME_RESOLUTION_OF_D_LOOP_STRUCTURES_THROUGH_SYNTHESIS_DEPENDENT_STRAND_ANNEALING_SDSA_	26	-0.44022	-1.3572	0.10445	0.119	1	5424	tags=38%, list=27%, signal=52%
REACTOME_RESOLUTION_OF_SISTER_CHROMATID_COHESION	125	-0.39256	-1.5897	0	0.029	1	4997	tags=39%, list=25%, signal=52%
REACTOME_RESPIRATORY_ELECTRON_TRANSPORT	90	-0.57476	-2.2704	0	0.000	0.002	4646	tags=56%, list=23%, signal=72%
REACTOME_RESPIRATORY_ELECTRON_TRANSPORT_ATP_SYNTHESIS_BY_CHEMIOSMOTIC_COUPLING_AND_HEAT_PRODUCTION_BY_UNCOUPLING_PROTEINS_	112	-0.58354	-2.3654	0	0.000	0	4646	tags=54%, list=23%, signal=70%
REACTOME_RESPONSE_OF_EIF2AK1_HRI_TO_HEME_DEFICIENCY	15	-0.50954	-1.3848	0.10159	0.102	1	1817	tags=33%, list=9%, signal=37%
REACTOME_RESPONSE_OF_EIF2AK4_GCN2_TO_AMINO_ACID_DEFICIENCY	102	-0.64403	-2.5783	0	0.000	0	4780	tags=72%, list=24%, signal=93%
REACTOME_RESPONSE_OF_MTB_TO_PHAGOCYTOSIS	23	-0.65225	-1.94	0	0.001	0.153	3113	tags=39%, list=15%, signal=46%
REACTOME_RESPONSE_TO_ELEVATED_PLATELET_CYTOSOLIC_CA2_	131	-0.41974	-1.7267	0	0.009	0.918	4052	tags=37%, list=20%, signal=46%
REACTOME_RET_SIGNALING	40	-0.3438	-1.1721	0.23022	0.289	1	4722	tags=40%, list=23%, signal=52%
REACTOME_RETROGRADE_TRANSPORT_AT_THE_TRANS_GOLGI_NETWORK	49	-0.38191	-1.362	0.06784	0.116	1	6831	tags=53%, list=34%, signal=80%
REACTOME_RHO_GTPASE_CYCLE	140	-0.26418	-1.0878	0.30359	0.402	1	2901	tags=19%, list=14%, signal=22%
REACTOME_RHO_GTPASE_EFFECTORS	262	-0.413	-1.8218	0	0.004	0.559	4495	tags=38%, list=22%, signal=48%
REACTOME_RHO_GTPASES_ACTIVATE_CIT	19	-0.3706	-1.0631	0.39171	0.441	1	4420	tags=42%, list=22%, signal=54%
REACTOME_RHO_GTPASES_ACTIVATE_FORMINS	139	-0.37978	-1.5764	0.00353	0.032	1	5021	tags=40%, list=25%, signal=52%
REACTOME_RHO_GTPASES_ACTIVATE_IQGAPS	31	-0.32212	-1.0458	0.40552	0.467	1	4415	tags=35%, list=22%, signal=45%
REACTOME_RHO_GTPASES_ACTIVATE_NADPH_OXIDASES	24	-0.36316	-1.1068	0.33956	0.377	1	3981	tags=29%, list=20%, signal=36%
REACTOME_RHO_GTPASES_ACTIVATE_PAKS	21	-0.36729	-1.0896	0.34743	0.401	1	6914	tags=62%, list=34%, signal=94%
REACTOME_RHO_GTPASES_ACTIVATE_PKNS	34	-0.48269	-1.5894	0.01946	0.029	1	4784	tags=47%, list=24%, signal=61%
REACTOME_RHO_GTPASES_ACTIVATE_ROCKS	19	-0.53507	-1.5272	0.04188	0.044	1	6145	tags=74%, list=30%, signal=106%

REACTOME_RHO_GTPASES_ACTIVATE_WASPS_AND_WAVES	35	-0.61389	-2.0009	0	0.000	0.056	4495	tags=63%, list=22%, signal=81%
REACTOME_RIPK1_MEDIATED_REGULATED_NECROSIS	20	-0.49117	-1.4444	0.06033	0.073	1	4241	tags=60%, list=21%, signal=76%
REACTOME_RMTS_METHYLATE_HISTONE_ARGININES	30	-0.50394	-1.6344	0.01649	0.020	0.999	3377	tags=40%, list=17%, signal=48%
REACTOME_RNA_POLYMERASE_I_PROMOTER_ESCAPE	31	-0.4913	-1.5931	0.01775	0.028	1	5755	tags=61%, list=28%, signal=85%
REACTOME_RNA_POLYMERASE_I_TRANSCRIPTION	51	-0.4742	-1.6711	0.00432	0.015	0.987	6150	tags=59%, list=30%, signal=84%
REACTOME_RNA_POLYMERASE_I_TRANSCRIPTION_INITIATION	47	-0.43845	-1.5667	0.01107	0.034	1	6777	tags=66%, list=33%, signal=99%
REACTOME_RNA_POLYMERASE_I_TRANSCRIPTION_TERMINATION	31	-0.45683	-1.4518	0.05	0.070	1	6933	tags=74%, list=34%, signal=113%
REACTOME_RNA_POLYMERASE_II_TRANSCRIBES_SNRNA_GENES	74	-0.6252	-2.3895	0	0.000	0	4567	tags=59%, list=23%, signal=76%
REACTOME_RNA_POLYMERASE_II_TRANSCRIPTION_TERMINATION	66	-0.57089	-2.1229	0	0.000	0.005	5551	tags=55%, list=27%, signal=75%
REACTOME_RNA_POLYMERASE_III_CHAIN_ELONGATION	18	-0.51134	-1.4388	0.07717	0.075	1	4580	tags=44%, list=23%, signal=57%
REACTOME_RNA_POLYMERASE_III_TRANSCRIPTION	41	-0.58196	-2.0009	0	0.000	0.056	3867	tags=44%, list=19%, signal=54%
REACTOME_RNA_POLYMERASE_III_TRANSCRIPTION_INITIATION_FROM_TYPE_1_PROMOTER	28	-0.53791	-1.6724	0.00452	0.015	0.987	3867	tags=39%, list=19%, signal=48%
REACTOME_RNA_POLYMERASE_III_TRANSCRIPTION_INITIATION_FROM_TYPE_3_PROMOTER	28	-0.55994	-1.7644	0.00295	0.006	0.802	3867	tags=43%, list=19%, signal=53%
REACTOME_RNA_POLYMERASE_III_TRANSCRIPTION_TERMINATION	23	-0.53773	-1.6074	0.02128	0.025	1	3867	tags=43%, list=19%, signal=54%
REACTOME_ROLE_OF_LAT2_NTAL_LAB_ON_CALCIUM_MOBILIZATION	16	-0.55054	-1.4914	0.04058	0.055	1	4222	tags=56%, list=21%, signal=71%
REACTOME_ROLE_OF_PHOSPHOLIPIDS_IN_PHAGOCYTOSIS	25	-0.35161	-1.0606	0.3875	0.444	1	5907	tags=44%, list=29%, signal=62%
REACTOME_RORA_ACTIVATES_GENE_EXPRESSION	18	-0.45864	-1.2876	0.14815	0.172	1	4784	tags=39%, list=24%, signal=51%
REACTOME_ROS_AND_RNS_PRODUCTION_IN_PHAGOCYTES	36	-0.47291	-1.5519	0.02062	0.037	1	3218	tags=33%, list=16%, signal=40%
REACTOME_RRNA_MODIFICATION_IN_THE_NUCLEUS_AND_CYTOSOL	60	-0.43144	-1.5684	0.01083	0.033	1	5321	tags=45%, list=26%, signal=61%
REACTOME_RRNA_PROCESSING	202	-0.52463	-2.2654	0	0.000	0.002	5414	tags=58%, list=27%, signal=78%
REACTOME_RUNX1_INTERACTS_WITH_CO_FACTORS_WHOSE_PRECISE_EFFECT_ON_RUNX1_TARGETS_IS_NOT_KNOWN	37	-0.54923	-1.8355	0.00143	0.003	0.501	3411	tags=41%, list=17%, signal=49%

REACTOME_RUNX1_REGULATES_GENES_INVOLVED_IN_MEGAKARYOCYTE_DIFFERENTIATION_AND_PLATELET_FUNCTION	37	-0.48375	-1.6264	0.00713	0.022	1	5469	tags=49%, list=27%, signal=67%
REACTOME_RUNX1_REGULATES_TRANSCRIPTION_OF_GENES_INVOLVED_IN_DIFFERENTIATION_OF_HSCS	70	-0.51947	-1.9355	0	0.001	0.159	4124	tags=44%, list=20%, signal=55%
REACTOME_RUNX2_REGULATES_BONE_DEVELOPMENT	31	-0.23659	-0.7548	0.81633	0.883	1	5199	tags=29%, list=26%, signal=39%
REACTOME_RUNX2_REGULATES_OSTEOBLAST_DIFFERENTIATION	24	-0.35356	-1.072	0.37288	0.426	1	4977	tags=33%, list=25%, signal=44%
REACTOME_S_PHASE	162	-0.48394	-2.0504	0	0.000	0.035	4626	tags=42%, list=23%, signal=54%
REACTOME_SARS_COV_1_INFECTION	50	-0.52214	-1.8724	0.00139	0.002	0.348	4620	tags=52%, list=23%, signal=67%
REACTOME_SARS_COV_INFECTIONS	86	-0.52417	-2.0373	0	0.000	0.04	4749	tags=51%, list=23%, signal=67%
REACTOME_SCAVENGING_BY_CLASS_A_RECEPTORS	19	-0.41508	-1.1855	0.2654	0.274	1	6241	tags=47%, list=31%, signal=68%
REACTOME_SCF_SKP2_MEDIATED_DEGRADATION_OF_P27_P21	60	-0.52714	-1.9737	0	0.001	0.086	5729	tags=55%, list=28%, signal=76%
REACTOME_SELECTIVE_AUTOPHAGY	81	-0.53139	-2.0457	0	0.000	0.036	4217	tags=49%, list=21%, signal=62%
REACTOME_SELENOAMINO_ACID_METABOLISM	109	-0.59803	-2.4069	0	0.000	0	4780	tags=65%, list=24%, signal=85%
REACTOME_SEMA3A_PAK_DEPENDENT_AXON_REPULSION	16	-0.40632	-1.1325	0.31542	0.343	1	6258	tags=63%, list=31%, signal=90%
REACTOME_SEMA4D_IN_SEMAPHORIN_SIGNALING	24	-0.45994	-1.4218	0.07004	0.083	1	4420	tags=50%, list=22%, signal=64%
REACTOME_SEMA4D_INDUCED_CELL_MIGRATION_AND_GROWTH_CONE_COLLAPSE	20	-0.42425	-1.2393	0.19909	0.216	1	6059	tags=60%, list=30%, signal=85%
REACTOME_SEMAPHORIN_INTERACTIONS	64	-0.37476	-1.4023	0.05836	0.094	1	6258	tags=53%, list=31%, signal=77%
REACTOME_SENESCENCE_ASSOCIATED_SECRETORY_PHENOTYPE_SASP_	52	-0.43527	-1.5592	0.01348	0.035	1	3653	tags=33%, list=18%, signal=40%
REACTOME_SEPARATION_OF_SISTER_CHROMATIDS	190	-0.45231	-1.9586	0	0.001	0.116	4997	tags=42%, list=25%, signal=55%
REACTOME_SHC1_EVENTS_IN_ERBB2_SIGNALING	22	-0.22344	-0.6799	0.89425	0.947	1	6360	tags=41%, list=31%, signal=60%
REACTOME_SIALIC_ACID_METABOLISM	33	-0.26323	-0.8675	0.67338	0.740	1	4479	tags=30%, list=22%, signal=39%
REACTOME_SIGNAL_AMPLIFICATION	33	-0.42763	-1.3975	0.06096	0.096	1	3496	tags=33%, list=17%, signal=40%
REACTOME_SIGNAL_REGULATORY_PROTEIN_FAMILY_INTERACTIONS	16	-0.5326	-1.4793	0.05547	0.059	1	4946	tags=56%, list=24%, signal=74%
REACTOME_SIGNAL_TRANSDUCTION_BY_L1	21	-0.40844	-1.189	0.24094	0.270	1	3549	tags=33%, list=18%, signal=40%
REACTOME_SIGNALING_BY_BMP	28	-0.24171	-0.7627	0.80392	0.875	1	3494	tags=18%, list=17%, signal=22%
REACTOME_SIGNALING_BY_BRAF_AND_RAF_FUSIONS	65	-0.47429	-1.7544	0	0.007	0.845	3444	tags=34%, list=17%, signal=41%
REACTOME_SIGNALING_BY_CYTOSOLIC_FGFR1_FUSION_MUTANTS	17	-0.66868	-1.8828	0.00159	0.002	0.31	4796	tags=71%, list=24%, signal=92%
REACTOME_SIGNALING_BY_EGFR	50	-0.49984	-1.7934	0.00281	0.005	0.683	4722	tags=44%, list=23%, signal=57%

REACTOME_SIGNALING_BY_EGFR_IN_CANCER	25	-0.5755	-1.7805	0.00305	0.005	0.726	4483	tags=56%, list=22%, signal=72%
REACTOME_SIGNALING_BY_ERBB2	50	-0.43106	-1.5465	0.01372	0.039	1	4626	tags=40%, list=23%, signal=52%
REACTOME_SIGNALING_BY_ERBB2_ECD_MUTANTS	16	-0.58481	-1.602	0.02135	0.026	1	4222	tags=50%, list=21%, signal=63%
REACTOME_SIGNALING_BY_ERBB2_IN_CANCER	26	-0.43462	-1.348	0.10423	0.125	1	4222	tags=35%, list=21%, signal=44%
REACTOME_SIGNALING_BY_ERBB4	58	-0.37853	-1.3896	0.04318	0.099	1	4470	tags=34%, list=22%, signal=44%
REACTOME_SIGNALING_BY_ERYTHROPOIETIN	25	-0.47101	-1.4675	0.06056	0.064	1	5834	tags=52%, list=29%, signal=73%
REACTOME_SIGNALING_BY_FGFR	87	-0.428	-1.6808	0.00127	0.013	0.982	4831	tags=43%, list=24%, signal=56%
REACTOME_SIGNALING_BY_FGFR_IN_DISEASE	62	-0.4613	-1.7194	0.00264	0.010	0.928	4430	tags=39%, list=22%, signal=49%
REACTOME_SIGNALING_BY_FGFR1	50	-0.45047	-1.6017	0.01124	0.026	1	4222	tags=38%, list=21%, signal=48%
REACTOME_SIGNALING_BY_FGFR1_IN_DISEASE	37	-0.55669	-1.8435	0.00283	0.003	0.465	3032	tags=35%, list=15%, signal=41%
REACTOME_SIGNALING_BY_FGFR2	73	-0.47107	-1.7777	0.00136	0.006	0.739	4831	tags=47%, list=24%, signal=61%
REACTOME_SIGNALING_BY_FGFR2_IIIA_TM	19	-0.5375	-1.562	0.02188	0.035	1	4412	tags=47%, list=22%, signal=60%
REACTOME_SIGNALING_BY_FGFR2_IN_DISEASE	43	-0.38444	-1.323	0.09155	0.142	1	4412	tags=35%, list=22%, signal=44%
REACTOME_SIGNALING_BY_FGFR3	40	-0.477	-1.6152	0.01289	0.024	1	4722	tags=48%, list=23%, signal=62%
REACTOME_SIGNALING_BY_FGFR4	41	-0.4834	-1.6284	0.01036	0.021	0.999	3249	tags=37%, list=16%, signal=43%
REACTOME_SIGNALING_BY_HEDGEHOG	150	-0.41924	-1.7556	0	0.007	0.843	4255	tags=35%, list=21%, signal=44%
REACTOME_SIGNALING_BY_HIPPO	20	-0.45094	-1.3123	0.13876	0.151	1	3644	tags=35%, list=18%, signal=43%
REACTOME_SIGNALING_BY_INSULIN_RECEPTOR	78	-0.30935	-1.1918	0.18936	0.267	1	3218	tags=24%, list=16%, signal=29%
REACTOME_SIGNALING_BY_INTERLEUKINS	446	-0.35827	-1.6396	0	0.019	0.998	4800	tags=33%, list=24%, signal=43%
REACTOME_SIGNALING_BY_KIT_IN_DISEASE	20	-0.53839	-1.5708	0.03257	0.033	1	5088	tags=55%, list=25%, signal=73%
REACTOME_SIGNALING_BY_MET	79	-0.49752	-1.907	0	0.002	0.24	4722	tags=47%, list=23%, signal=61%
REACTOME_SIGNALING_BY_MODERATE_KINASE_ACTIVITY_BRAF_MUTANTS	45	-0.40534	-1.4268	0.06828	0.081	1	5174	tags=42%, list=26%, signal=57%
REACTOME_SIGNALING_BY_NOTCH	176	-0.41827	-1.7822	0	0.005	0.722	3178	tags=27%, list=16%, signal=31%
REACTOME_SIGNALING_BY_NOTCH1	74	-0.35827	-1.3444	0.07631	0.127	1	5351	tags=36%, list=26%, signal=49%
REACTOME_SIGNALING_BY_NOTCH1_HD_DOMAIN_MUTANTS_IN_CANCER	15	-0.37079	-1.0042	0.44426	0.533	1	3113	tags=27%, list=15%, signal=31%
REACTOME_SIGNALING_BY_NOTCH1_PEST_DOMAIN_MUTANTS_IN_CANCER	58	-0.35669	-1.289	0.1114	0.171	1	5351	tags=36%, list=26%, signal=49%
REACTOME_SIGNALING_BY_NOTCH2	33	-0.42397	-1.3792	0.09224	0.105	1	3760	tags=27%, list=19%, signal=33%
REACTOME_SIGNALING_BY_NOTCH3	49	-0.38457	-1.3449	0.0856	0.127	1	3113	tags=22%, list=15%, signal=26%
REACTOME_SIGNALING_BY_NOTCH4	82	-0.51586	-1.9939	0	0.001	0.062	5555	tags=49%, list=27%, signal=67%
REACTOME_SIGNALING_BY_NTRK2_TRKB_	25	-0.38251	-1.1837	0.23231	0.276	1	5088	tags=44%, list=25%, signal=59%

REACTOME_SIGNALING_BY_NTRK3_TRKC_	17	-0.56007	-1.5679	0.02385	0.033	1	5088	tags=47%, list=25%, signal=63%
REACTOME_SIGNALING_BY_NTRKS	134	-0.35279	-1.4608	0.01185	0.067	1	4773	tags=35%, list=24%, signal=46%
REACTOME_SIGNALING_BY_NUCLEAR_RECEPTORS	237	-0.42388	-1.8521	0	0.003	0.431	5137	tags=42%, list=25%, signal=55%
REACTOME_SIGNALING_BY_PDGF	58	-0.32156	-1.187	0.20822	0.272	1	5088	tags=34%, list=25%, signal=46%
REACTOME_SIGNALING_BY_PDGFR_IN_DISEASE	20	-0.66605	-1.8972	0	0.002	0.272	4185	tags=65%, list=21%, signal=82%
REACTOME_SIGNALING_BY_PTK6	54	-0.39753	-1.4443	0.05049	0.073	1	4626	tags=39%, list=23%, signal=50%
REACTOME_SIGNALING_BY_RETINOIC_ACID	43	-0.29241	-1.0212	0.43634	0.506	1	4476	tags=21%, list=22%, signal=27%
REACTOME_SIGNALING_BY_RHO_GTPASES	392	-0.35472	-1.6192	0	0.023	1	4495	tags=33%, list=22%, signal=41%
REACTOME_SIGNALING_BY_ROBO_RECEPTORS	218	-0.54864	-2.3802	0	0.000	0	5748	tags=63%, list=28%, signal=87%
REACTOME_SIGNALING_BY_SCF_KIT	43	-0.39297	-1.3488	0.08905	0.125	1	4796	tags=47%, list=24%, signal=61%
REACTOME_SIGNALING_BY_TGF_BETA_RECEPTOR_COMPLEX	73	-0.55755	-2.1362	0	0.000	0.005	3335	tags=45%, list=16%, signal=54%
REACTOME_SIGNALING_BY_TGFB_FAMILY_MEMBERS	102	-0.47556	-1.8808	0	0.002	0.313	3601	tags=36%, list=18%, signal=44%
REACTOME_SIGNALING_BY_THE_B_CELL_RECEPTOR_BCR_	110	-0.48356	-1.9551	0	0.001	0.122	5586	tags=49%, list=28%, signal=67%
REACTOME_SIGNALING_BY_VEGF	106	-0.33431	-1.3253	0.05335	0.141	1	4626	tags=36%, list=23%, signal=46%
REACTOME_SIGNALING_BY_WNT	269	-0.38285	-1.705	0	0.011	0.952	4740	tags=37%, list=23%, signal=47%
REACTOME_SIGNALING_BY_WNT_IN_CANCER	34	-0.48085	-1.5714	0.0184	0.033	1	4021	tags=47%, list=20%, signal=59%
REACTOME_SIGNALLING_TO_ERKS	34	-0.39827	-1.2952	0.12428	0.166	1	6019	tags=47%, list=30%, signal=67%
REACTOME_SIGNALLING_TO_RAS	20	-0.20264	-0.5867	0.95513	0.984	1	5088	tags=30%, list=25%, signal=40%
REACTOME_SLC_MEDIATED_TRANSMEMBRANE_TRANSPORT	250	-0.18491	-0.8071	0.89514	0.827	1	4813	tags=24%, list=24%, signal=31%
REACTOME_SLC_TRANSPORTER_DISORDERS	98	-0.40699	-1.6071	0.00375	0.025	1	4813	tags=39%, list=24%, signal=51%
REACTOME_SMAD2_SMAD3_SMAD4_HETEROTRIMER_REGULATES_TRANSCRIPTION	32	-0.59266	-1.8975	0	0.002	0.272	3601	tags=50%, list=18%, signal=61%
REACTOME_SMOOTH_MUSCLE_CONTRACTION	38	-0.32821	-1.1193	0.28973	0.359	1	2387	tags=18%, list=12%, signal=21%
REACTOME_SNRNP_ASSEMBLY	53	-0.61245	-2.1878	0	0.000	0.002	4102	tags=53%, list=20%, signal=66%
REACTOME_SPHINGOLIPID_DE_NOVO_BIOSYNTHESIS	43	-0.36355	-1.256	0.14641	0.199	1	3156	tags=28%, list=16%, signal=33%
REACTOME_SPHINGOLIPID_METABOLISM	87	-0.38809	-1.512	0.00911	0.048	1	3191	tags=28%, list=16%, signal=33%
REACTOME_SPRY_REGULATION_OF_FGF_SIGNALING	16	-0.72848	-2.0184	0	0.000	0.05	4722	tags=75%, list=23%, signal=98%
REACTOME_SRP_DEPENDENT_COTRANSLATIONAL_PROTEIN_TARGETING_TO_MEMBRANE	113	-0.67349	-2.7056	0	0.000	0	4674	tags=73%, list=23%, signal=94%
REACTOME_STABILIZATION_OF_P53	57	-0.58163	-2.108	0	0.000	0.008	3178	tags=40%, list=16%, signal=48%

REACTOME_STING_MEDIATED_INDUCTION_OF_HOST_IMMUNE_RESPONSES	15	-0.36485	-0.9607	0.50256	0.600	1	1228	tags=13%, list=6%, signal=14%
REACTOME_SULFUR_AMINO_ACID_METABOLISM	28	-0.19584	-0.6241	0.93853	0.974	1	3718	tags=21%, list=18%, signal=26%
REACTOME_SUMOYLATION	172	-0.48129	-2.0242	0	0.000	0.047	3755	tags=34%, list=19%, signal=42%
REACTOME_SUMOYLATION_OF_CHROMATIN_ORGANIZATION_PROTEINS	56	-0.6031	-2.1789	0	0.000	0.002	4957	tags=54%, list=24%, signal=71%
REACTOME_SUMOYLATION_OF_DNA_DAMAGE_RESPONSE_AND_REPAIR_PROTEINS	76	-0.57696	-2.1931	0	0.000	0.002	4997	tags=50%, list=25%, signal=66%
REACTOME_SUMOYLATION_OF_DNA_METHYLATION_PROTEINS	16	-0.34687	-0.9593	0.52904	0.602	1	7200	tags=44%, list=36%, signal=68%
REACTOME_SUMOYLATION_OF_DNA_REPLICATION_PROTEINS	45	-0.64742	-2.2462	0	0.000	0.002	4102	tags=53%, list=20%, signal=67%
REACTOME_SUMOYLATION_OF_INTRACELLULAR_RECEPTORS	30	-0.58335	-1.8465	0	0.003	0.456	1454	tags=30%, list=7%, signal=32%
REACTOME_SUMOYLATION_OF_RNA_BINDING_PROTEINS	46	-0.64935	-2.2911	0	0.000	0.001	4957	tags=59%, list=24%, signal=78%
REACTOME_SUMOYLATION_OF_SUMOYLATION_PROTEINS	34	-0.67233	-2.1809	0	0.000	0.002	4729	tags=62%, list=23%, signal=80%
REACTOME_SUMOYLATION_OF_TRANSCRIPTION_COFACTORS	43	-0.55244	-1.8915	0	0.002	0.285	5309	tags=49%, list=26%, signal=66%
REACTOME_SUMOYLATION_OF_TRANSCRIPTION_FACTORS	20	-0.47362	-1.3668	0.13889	0.113	1	3337	tags=35%, list=16%, signal=42%
REACTOME_SUMOYLATION_OF_UBIQUITINYLATION_PROTEINS	38	-0.65762	-2.2327	0	0.000	0.002	4729	tags=58%, list=23%, signal=75%
REACTOME_SWITCHING_OF_ORIGINS_TO_A_POST_REPLICATIVE_STATE	91	-0.51249	-1.9925	0	0.001	0.064	4124	tags=40%, list=20%, signal=49%
REACTOME_SYNDECAN_INTERACTIONS	27	-0.4019	-1.2389	0.18741	0.216	1	5019	tags=44%, list=25%, signal=59%
REACTOME_SYNTHESIS_OF_ACTIVE_UBIQUITIN_ROLES_OF_E1_AND_E2_ENZYMES	30	-0.59506	-1.9169	0	0.001	0.208	5295	tags=63%, list=26%, signal=86%
REACTOME_SYNTHESIS_OF_BILE_ACIDS_AND_BILE_SALTS	34	-0.37583	-1.2447	0.16479	0.211	1	2520	tags=26%, list=12%, signal=30%
REACTOME_SYNTHESIS_OF_BILE_ACIDS_AND_BILE_SALTS_VIA_27_HYDROXYCHOLESTEROL	15	-0.40625	-1.1161	0.32689	0.362	1	5858	tags=47%, list=29%, signal=66%
REACTOME_SYNTHESIS_OF_BILE_ACIDS_AND_BILE_SALTS_VIA_7ALPHA_HYDROXYCHOLESTEROL	24	-0.4185	-1.2734	0.16265	0.184	1	2520	tags=29%, list=12%, signal=33%
REACTOME_SYNTHESIS_OF_PA	39	-0.24368	-0.8331	0.74854	0.793	1	2416	tags=13%, list=12%, signal=15%
REACTOME_SYNTHESIS_OF_PC	28	-0.46551	-1.4876	0.05007	0.056	1	5631	tags=57%, list=28%, signal=79%
REACTOME_SYNTHESIS_OF_PIPS_AT_THE_EARLY_ENDOSOME_MEMBRANE	16	-0.45557	-1.2338	0.1877	0.221	1	5074	tags=38%, list=25%, signal=50%

REACTOME_SYNTHESIS_OF_PIPS_AT_THE_GOLGI_MEMBRANE	18	-0.5582	-1.6092	0.0216	0.025	1	4293	tags=50%, list=21%, signal=63%
REACTOME_SYNTHESIS_OF_PIPS_AT_THE_PLASMA_MEMBRANE	53	-0.45821	-1.6582	0.00274	0.017	0.99	4535	tags=42%, list=22%, signal=53%
REACTOME_SYNTHESIS_OF_PROSTAGLANDINS_PG_AND_THROMBOXANES_TX_	15	-0.32412	-0.8887	0.62679	0.710	1	5377	tags=33%, list=27%, signal=45%
REACTOME_SYNTHESIS_OF_SUBSTRATES_IN_N_GLYCAN_BIOSYTHESIS	62	-0.2932	-1.0882	0.31907	0.402	1	3778	tags=21%, list=19%, signal=26%
REACTOME_SYNTHESIS_OF_VERY_LONG_CHAIN_FATTY_ACYL_COAS	24	-0.26282	-0.8032	0.75155	0.829	1	4554	tags=38%, list=22%, signal=48%
REACTOME_SYNTHESIS_SECRETION_AND_DEACYLATION_OF_GHRELIN	19	-0.38874	-1.1424	0.28885	0.328	1	3353	tags=32%, list=17%, signal=38%
REACTOME_SYNTHESIS_SECRETION_AND_INACTIVATION_OF_GLUCAGON_LIKE_PEPTIDE_1_GLP_1_	20	-0.33752	-0.976	0.51033	0.575	1	3353	tags=30%, list=17%, signal=36%
REACTOME_TAK1_ACTIVATES_NFKB_BY_PHOSPHORYLATION_AND_ACTIVATION_OF_IKKS_COMPLEX	32	-0.48228	-1.5591	0.02193	0.035	1	3926	tags=38%, list=19%, signal=46%
REACTOME_TBC_RABGAPS	44	-0.57017	-1.9986	0	0.000	0.058	3005	tags=41%, list=15%, signal=48%
REACTOME_TCF_DEPENDENT_SIGNALING_IN_RESPONSE_TO_WNT	173	-0.37098	-1.5872	0.00228	0.029	1	4740	tags=36%, list=23%, signal=47%
REACTOME_TCR_SIGNALING	117	-0.59667	-2.4069	0	0.000	0	3572	tags=41%, list=18%, signal=50%
REACTOME_TELOMERE_C_STRAND_LAGGING_STRAND_SYNTHESIS	34	-0.33094	-1.0829	0.35755	0.408	1	5170	tags=35%, list=26%, signal=47%
REACTOME_TELOMERE_EXTENSION_BY_TELOMERASE	23	-0.38701	-1.1615	0.25469	0.303	1	5171	tags=39%, list=26%, signal=52%
REACTOME_TELOMERE_MAINTENANCE	65	-0.38892	-1.4546	0.03426	0.069	1	5171	tags=38%, list=26%, signal=51%
REACTOME_TERMINATION_OF_TRANSLESION_DNA_SYNTHESIS	32	-0.60581	-1.978	0.00142	0.001	0.079	3646	tags=53%, list=18%, signal=65%
REACTOME_TGF_BETA_RECEPTOR_SIGNALING_ACTIVATES_SMADS	32	-0.55083	-1.7957	0.00287	0.005	0.677	3335	tags=44%, list=16%, signal=52%
REACTOME_TGF_BETA_RECEPTOR_SIGNALING_IN_EMT_EPITHELIAL_TO_MESENCHYMAL_TRANSITION_	16	-0.56963	-1.5772	0.02318	0.032	1	4616	tags=69%, list=23%, signal=89%
REACTOME_THE_CITRIC_ACID_TCA_CYCLE_AND_RESPIRATORY_ELECTRON_TRANSPORT	163	-0.53429	-2.2369	0	0.000	0.002	4646	tags=48%, list=23%, signal=62%
REACTOME_THE_NLRP3_INFLAMMASOME	15	-0.47669	-1.2796	0.18434	0.179	1	3892	tags=40%, list=19%, signal=49%
REACTOME_THE_PHOTOTRANSDUCTION_CASCADE	34	-0.18868	-0.6129	0.95954	0.977	1	4608	tags=24%, list=23%, signal=30%
REACTOME_THE_ROLE_OF_GTSE1_IN_G2_M_PROGRESSION_AFTER_G2_CHECKPOINT	78	-0.46557	-1.7923	0	0.005	0.689	4264	tags=38%, list=21%, signal=49%
REACTOME_THE_ROLE_OF_NEF_IN_HIV_1_REPLICATION_AND_DISEASE_PATHOGENESIS	28	-0.44671	-1.4005	0.08663	0.094	1	3565	tags=32%, list=18%, signal=39%

REACTOME_THROMBIN_SIGNALLING_THROUGH_PROTEINASE_ACTIVATED_RECEPTORS_PARS_	32	-0.42767	-1.3954	0.07133	0.096	1	3496	tags=34%, list=17%, signal=41%
REACTOME_THROMBOXANE_SIGNALLING_THROUGH_TP_RECEPTOR	24	-0.39861	-1.2179	0.2003	0.236	1	2462	tags=29%, list=12%, signal=33%
REACTOME_TICAM1_RIP1_MEDIATED_IKK_COMPLEX_RECRUITMENT	19	-0.67735	-1.9335	0.00152	0.001	0.167	3356	tags=68%, list=17%, signal=82%
REACTOME_TIE2_SIGNALING	18	-0.51177	-1.4427	0.07256	0.074	1	5088	tags=61%, list=25%, signal=82%
REACTOME_TIGHT_JUNCTION_INTERACTIONS	30	-0.26164	-0.8316	0.73945	0.795	1	1586	tags=17%, list=8%, signal=18%
REACTOME_TNF_RECEPTOR_SUPERFAMILY_TNFSF_MEMBERS_MEDIATING_NON_CANONICAL_NF_KB_PATHWAY	17	-0.31099	-0.8834	0.62063	0.718	1	3657	tags=29%, list=18%, signal=36%
REACTOME_TNF_SIGNALING	43	-0.54736	-1.8817	0.00273	0.002	0.312	5246	tags=58%, list=26%, signal=78%
REACTOME_TNFR1_INDUCED_NFKAPPAB_SIGNALING_PATHWAY	30	-0.55649	-1.8187	0.00297	0.004	0.568	5246	tags=67%, list=26%, signal=90%
REACTOME_TNFR2_NON_CANONICAL_NF_KB_PATHWAY	101	-0.40414	-1.6133	0.00377	0.024	1	5555	tags=42%, list=27%, signal=57%
REACTOME_TOLL_LIKE_RECEPTOR_10_TLR10_CASCADE	84	-0.49044	-1.9034	0	0.002	0.251	4362	tags=42%, list=22%, signal=53%
REACTOME_TOLL_LIKE_RECEPTOR_4_TLR4_CASCADE	127	-0.48047	-1.97	0	0.001	0.091	4362	tags=40%, list=22%, signal=51%
REACTOME_TOLL_LIKE_RECEPTOR_9_TLR9_CASCADE	95	-0.4671	-1.856	0	0.003	0.416	4021	tags=38%, list=20%, signal=47%
REACTOME_TOLL_LIKE_RECEPTOR_CASCADES	153	-0.47523	-1.9818	0	0.001	0.078	4021	tags=39%, list=20%, signal=48%
REACTOME_TOLL_LIKE_RECEPTOR_TLR1_TLR2_CASCADE	97	-0.45745	-1.8248	0	0.004	0.549	4021	tags=35%, list=20%, signal=44%
REACTOME_TP53_REGULATES_METABOLIC_GENES	83	-0.55394	-2.1318	0	0.000	0.005	4307	tags=52%, list=21%, signal=66%
REACTOME_TP53_REGULATES_TRANSCRIPTION_OF_ADDITIONAL_CELL_CYCLE_GENES_WHOSE_EXACT_ROLE_IN_THE_P53_PATHWAY_REMAIN_UNCERTAIN	21	-0.57438	-1.693	0.00927	0.012	0.97	5300	tags=52%, list=26%, signal=71%
REACTOME_TP53_REGULATES_TRANSCRIPTION_OF_CELL_CYCLE_GENES	49	-0.53002	-1.8723	0.00138	0.002	0.348	5300	tags=51%, list=26%, signal=69%
REACTOME_TP53_REGULATES_TRANSCRIPTION_OF_CELL_DEATH_GENES	44	-0.35097	-1.2076	0.19712	0.248	1	2079	tags=20%, list=10%, signal=23%
REACTOME_TP53_REGULATES_TRANSCRIPTION_OF_DNA_REPAIR_GENES	62	-0.64146	-2.3563	0	0.000	0	4584	tags=55%, list=23%, signal=71%
REACTOME_TP53_REGULATES_TRANSCRIPTION_OF_GENES_INVOLVED_IN_CYTOCHROME_C_RELEASE	20	-0.39756	-1.1429	0.28594	0.328	1	1519	tags=20%, list=7%, signal=22%
REACTOME_TP53_REGULATES_TRANSCRIPTION_OF_GENES_INVOLVED_IN_G2_CELL_CYCLE_ARREST	18	-0.5072	-1.4254	0.07419	0.082	1	5137	tags=44%, list=25%, signal=59%
REACTOME_TRAF6_MEDIATED_INDUCTION_OF_TAK1_COMPLEX_WITHIN_TLR4_COMPLEX	16	-0.70949	-1.9548	0	0.001	0.123	3113	tags=63%, list=15%, signal=74%

REACTOME_TRAF6_MEDIATED_IRF7_ACTIVATION	29	-0.28198	-0.9069	0.58997	0.685	1	4278	tags=28%, list=21%, signal=35%
REACTOME_TRAF6_MEDIATED_NF_KB_ACTIVATION	24	-0.29239	-0.8751	0.64583	0.730	1	5901	tags=38%, list=29%, signal=53%
REACTOME_TRANS_GOLGI_NETWORK_VESICLE_BUDDING	72	-0.49825	-1.8765	0	0.002	0.332	4064	tags=49%, list=20%, signal=61%
REACTOME_TRANSCRIPTION_COUPLED_NUCLEOTIDE_EXCISION_REPAIR_TC_NER_	78	-0.55124	-2.1032	0	0.000	0.009	5097	tags=53%, list=25%, signal=70%
REACTOME_TRANSCRIPTION_OF_E2F_TARGETS_UNDER_NEGATIVE_CONTROL_BY_DREAM_COMPLEX	19	-0.51789	-1.4846	0.05965	0.057	1	6272	tags=63%, list=31%, signal=91%
REACTOME_TRANSCRIPTION_OF_E2F_TARGETS_UNDER_NEGATIVE_CONTROL_BY_P107_RBL1_AND_P130_RBL2_IN_COMPLEX_WITH_HDAC1	16	-0.40276	-1.0974	0.33981	0.390	1	6711	tags=63%, list=33%, signal=93%
REACTOME_TRANSCRIPTION_OF_THE_HIV_GENOME	70	-0.56958	-2.1474	0	0.000	0.004	4571	tags=49%, list=23%, signal=62%
REACTOME_TRANSCRIPTIONAL_ACTIVATION_OF_MITOCHONDRIAL_BIOGENESIS	55	-0.47039	-1.6957	0.00549	0.012	0.965	5845	tags=49%, list=29%, signal=69%
REACTOME_TRANSCRIPTIONAL_ACTIVITY_OF_SMAD2_SMAD3_SMAD4_HETEROTRIMER	44	-0.59681	-2.0907	0	0.000	0.013	3601	tags=52%, list=18%, signal=63%
REACTOME_TRANSCRIPTIONAL_REGULATION_BY_E2F6	34	-0.59429	-1.9902	0.00147	0.001	0.068	4898	tags=53%, list=24%, signal=70%
REACTOME_TRANSCRIPTIONAL_REGULATION_BY_MECP2	61	-0.3065	-1.1283	0.27734	0.349	1	3072	tags=25%, list=15%, signal=29%
REACTOME_TRANSCRIPTIONAL_REGULATION_BY_RUNX1	178	-0.4366	-1.8565	0	0.003	0.414	5555	tags=47%, list=27%, signal=64%
REACTOME_TRANSCRIPTIONAL_REGULATION_BY_RUNX2	120	-0.42002	-1.7072	0	0.011	0.95	5555	tags=43%, list=27%, signal=59%
REACTOME_TRANSCRIPTIONAL_REGULATION_BY_RUNX3	95	-0.45016	-1.7753	0	0.006	0.75	5555	tags=45%, list=27%, signal=62%
REACTOME_TRANSCRIPTIONAL_REGULATION_BY_SMALL_RNAS	46	-0.66595	-2.3517	0	0.000	0	4102	tags=57%, list=20%, signal=71%
REACTOME_TRANSCRIPTIONAL_REGULATION_BY_THE_AP_2_TFAP2_FAMILY_OF_TRANSCRIPTION_FACTORS	38	-0.31158	-1.0427	0.40841	0.471	1	3458	tags=29%, list=17%, signal=35%
REACTOME_TRANSCRIPTIONAL_REGULATION_BY_TP53	359	-0.49833	-2.2245	0	0.000	0.002	4661	tags=44%, list=23%, signal=56%
REACTOME_TRANSCRIPTIONAL_REGULATION_BY_VENTX	40	-0.45927	-1.5528	0.02244	0.037	1	1780	tags=23%, list=9%, signal=25%
REACTOME_TRANSCRIPTIONAL_REGULATION_OF_GRANULOPOIESIS	30	-0.33051	-1.049	0.38791	0.463	1	3458	tags=27%, list=17%, signal=32%
REACTOME_TRANSCRIPTIONAL_REGULATION_OF_WHITE_ADIPOCYTE_DIFFERENTIATION	84	-0.29115	-1.1187	0.27728	0.359	1	4977	tags=33%, list=25%, signal=44%
REACTOME_TRANSFERRIN_ENDOCYTOSIS_AND_RECYCLING	31	-0.52324	-1.6792	0.0071	0.014	0.984	3218	tags=42%, list=16%, signal=50%
REACTOME_TRANSLATION	275	-0.53557	-2.3879	0	0.000	0	4795	tags=53%, list=24%, signal=68%
REACTOME_TRANSLATION_OF_STRUCTURAL_PROTEINS	28	-0.55889	-1.7888	0.00154	0.005	0.695	4436	tags=61%, list=22%, signal=78%
REACTOME_TRANSLESION_SYNTHESIS_BY_POLH	19	-0.59916	-1.7335	0.00784	0.009	0.899	4525	tags=63%, list=22%, signal=81%

REACTOME_TRANSLESION_SYNTHESIS_BY_POLK	17	-0.58612	-1.6268	0.02826	0.022	0.999	5120	tags=71%, list=25%, signal=94%
REACTOME_TRANSLESION_SYNTHESIS_BY_Y_FAMILY_DNA_POLYMERASES_BYPASSES_LESIONS_ON_DNA_TEMPLATE	39	-0.56055	-1.8943	0	0.002	0.277	4525	tags=54%, list=22%, signal=69%
REACTOME_TRANSLOCATION_OF_SLC2A4_GLUT4_TO_THE_PLASMA_MEMBRANE	71	-0.45607	-1.7233	0.00128	0.009	0.922	5107	tags=46%, list=25%, signal=62%
REACTOME_TRANSPORT_OF_BILE_SALTS_AND_ORGANIC_ACIDS_METAL_IONS_AND_AMINE_COMPOUNDS	86	-0.24586	-0.9629	0.52868	0.598	1	4919	tags=31%, list=24%, signal=41%
REACTOME_TRANSPORT_OF_MATURE_MRNAS_DERIVED_FROM_INTRONLESS_TRANSCRIPTS	42	-0.65111	-2.226	0	0.000	0.002	4729	tags=62%, list=23%, signal=81%
REACTOME_TRANSPORT_OF_MATURE_TRANSCRIPT_TO_CYTOPLASM	83	-0.59198	-2.2976	0	0.000	0.001	5551	tags=59%, list=27%, signal=81%
REACTOME_TRANSPORT_OF_THE_SLBP_DEPENDANT_MATURE_MRNA	35	-0.64865	-2.1507	0	0.000	0.004	4729	tags=60%, list=23%, signal=78%
REACTOME_TRANSPORT_OF_VITAMINS_NUCLEOSIDES_AND_RELATED_MOLECULES	44	-0.17176	-0.6004	0.97309	0.981	1	3609	tags=16%, list=18%, signal=19%
REACTOME_TRANSPORT_TO_THE_GOLGI_AND_SUBSEQUENT_MODIFICATION	185	-0.47072	-2.0271	0	0.000	0.046	3413	tags=34%, list=17%, signal=41%
REACTOME_TRIGLYCERIDE_CATABOLISM	24	-0.36418	-1.1195	0.31201	0.359	1	6183	tags=46%, list=31%, signal=66%
REACTOME_TRIGLYCERIDE_METABOLISM	37	-0.34519	-1.1514	0.26829	0.317	1	3876	tags=30%, list=19%, signal=37%
REACTOME_TRISTETRAPROLIN_TTP_ZFP36_BINDS_AND_DESTABILIZES_MRNA	17	-0.49037	-1.3826	0.09486	0.102	1	4811	tags=59%, list=24%, signal=77%
REACTOME_TRNA_AMINOACYLATION	24	-0.24641	-0.7433	0.84759	0.895	1	3922	tags=29%, list=19%, signal=36%
REACTOME_TRNA_MODIFICATION_IN_THE_NUCLEUS_AND_CYTOSOL	42	-0.22255	-0.7787	0.79798	0.857	1	4134	tags=19%, list=20%, signal=24%
REACTOME_TRNA_PROCESSING	105	-0.40597	-1.642	0.00123	0.019	0.997	4134	tags=30%, list=20%, signal=37%
REACTOME_TRNA_PROCESSING_IN_THE_NUCLEUS	57	-0.50984	-1.8762	0	0.002	0.332	4729	tags=42%, list=23%, signal=55%
REACTOME_UB_SPECIFIC_PROCESSING_PROTEASES	186	-0.38555	-1.6546	0	0.017	0.992	4658	tags=37%, list=23%, signal=48%
REACTOME_UCH_PROTEINASES	85	-0.51974	-2.0388	0	0.000	0.038	3610	tags=38%, list=18%, signal=46%
REACTOME_UNFOLDED_PROTEIN_RESPONSE_UPR_	92	-0.46749	-1.8244	0	0.004	0.549	4911	tags=46%, list=24%, signal=60%
REACTOME_UPTAKE_AND_ACTIONS_OF_BACTERIAL_TOXINS	29	-0.35226	-1.1252	0.31184	0.351	1	3722	tags=28%, list=18%, signal=34%
REACTOME_VASOPRESSIN_REGULATES_RENAL_WATER_HOMEOSTASIS_VIA_AQUAPORINS	43	-0.36487	-1.268	0.15092	0.189	1	2496	tags=26%, list=12%, signal=29%
REACTOME_VEGFR2_MEDIATED_CELL_PROLIFERATION	19	-0.3329	-0.9543	0.50077	0.610	1	5907	tags=47%, list=29%, signal=67%

REACTOME_VEGFR2_MEDIATED_VASCULAR_PERMEABILITY	27	-0.24524	-0.7685	0.81426	0.870	1	4626	tags=30%, list=23%, signal=38%
REACTOME_VIRAL_MESSENGER_RNA_SYNTHESIS	43	-0.6782	-2.3395	0	0.000	0	4729	tags=65%, list=23%, signal=85%
REACTOME_VITAMIN_B5_PANTOTHENATE_METABOLISM	17	-0.62275	-1.7165	0.01316	0.010	0.932	4868	tags=65%, list=24%, signal=85%
REACTOME_VXPX_CARGO_TARGETING_TO_CILIUM	21	-0.43289	-1.2621	0.18615	0.194	1	3285	tags=24%, list=16%, signal=28%
REACTOME_WNT_LIGAND_BIOGENESIS_AND_TRAFFICKING	26	-0.29007	-0.9011	0.6009	0.691	1	1367	tags=15%, list=7%, signal=16%
REACTOME_WNT5A_DEPENDENT_INTERNALIZATION_OF_FZD4	15	-0.4817	-1.314	0.15266	0.150	1	3977	tags=33%, list=20%, signal=41%
REACTOME_ZINC_TRANSPORTERS	17	-0.45499	-1.2606	0.18325	0.195	1	3219	tags=35%, list=16%, signal=42%

Table S6: Previousy reported signatures of response / resistance to anti-PD1 therapy and signatures capturing immune cell subsets

aDC	CCL1	EBI3	INDO	LAMP3	OAS3					
B cells	MS4A1	TCL1A	HLA-DOB	PNOC	KIAA0125	CD19	CR2	IGHG1	FCRL2	BLK
	SPIB	BCL11A	GNG7	IGKC	CD72	MICAL3	BACH2	IGL@	CCR9	QRSL1
	COCH	OSBPL10	IGHA1	TNFRSF17	ABCB4	BLNK	GLDC	MEF2C	IGHM	FAM30A
	DTNB	HLA-DQA1	SCN3A	SLC15A2						
CD8 T cells	CD8B	CD8A	PF4	PRR5	SF1	LIME1	DNAJB1	ARHGAP8	GZMM	SLC16A7
	THUMPD1	VAMP2	ZNF91	ZNF22	TMC6	FLT3LG	CDKN2AIP	TSC22D3	TBCC	RBM3
	SFRS7	APBA2	C4orf15	LEPROTL1	ZFP36L2	GADD45A	MYST3	ZEB1	ZNF609	C12orf47
	ABT1	C19orf6	CAMLG	PPP1R2	AES	KLF9	PRF1			
Cytotox	KLRD1	KLRF1	GNLY	CTSW	KLRB1	KLRK1	NKG7	GZMH	SIGIRR	ZBTB16
	RUNX3	APOL3	RORA	APBA2	WHDC1L1	DUSP2	GZMA			
DC	CD209	CCL17	HSD11B1	CCL13	CCL22	PPFIBP2	NPR1			
Eosinophils	IL5RA	KCNH2	TKTL1	EMR1	CCR3	ACACB	THBS1	GALC	RNU2	CLC
	HES1	ABHD2	TIPARP	SMPD3	MYO15B	TGIF1	RRP12	IGSF2	RCOR3	EPN2
	HIST1H1C	CYSLTR2	HRH4	RNASE2	CAT	LRP5L	SYNJ1	THBS4	GPR44	KBTBD11
	C9orf156	SIAH1								
iDC	CD1B	VASH1	F13A1	CD1E	MMP12	FABP4	CLEC10A	SYT17	MS4A6A	CTNS
	CSF1R	HS3ST2	CH25H	LMAN2L	SLC26A6	BLVRB	NUDT9	PREP	TM7SF4	TACSTD2
	GUCA1A	CARD9	ABCG2	CD1A	PPARG	RAP1GAP	SLC7A8	GSTT1	NM_021941	FZD2
	CD1C									
Macrophages	MARCO	CXCL5	SCG5	SULT1C2	MSR1	CTSK	PTGDS	COLEC12	GPC4	PCOLCE2
	BCAT1	RAI14	COL8A2	APOE	CHI3L1	ATG7	CD84	FDX1	MS4A4A	SGMS1
	CHIT1	KAL1	CLEC5A	ME1	DNASE2B	CCL7	FN1	CD163	GM2A	SCARB2
	EMP1	CYBB	CD68							
Mast cells	PRG2	CTSG	TPSAB1	SLC18A2	MS4A2	CPA3	TPSB2	TPS1	GATA2	HDC
	TAL1	ABCC4	PPM1H	MAOB	HPGD	SCG2	PTGS1	CEACAM8	MPO	NR0B1
	LOH11CR2A	SIGLEC6	ELA2	CMA1	PGDS	MLPH	ADCYAP1	SLC24A3	CALB2	KIT
	LOC339524									
Th17 cells	IL17A	IL17RA	RORC							
Th2 cells	PMCH	AHI1	PTGIS	CXCR6	EVI5	IL26	MB	NEIL3	GSTA4	PHEX
	BIRC5	SLC39A14	HELLS	LIMA1	CDC25C	CDC7	GATA3			
	SMAD2	CENPF	ANK1	ADCY1	AI582773	LAIR2	SNRPD1	MICAL2	DHFR	WDHD1
Th1 cells	IFNG	LTA	APBB2	DOK5	IL12RB2	APOD	ZBTB32	CD38	CSF2	CTLA4
	LRRN3	SYNGR3	ATP9A	BTG3	CMAH	HBEGF	SGCB			
	CD70	DPP4	EGFL6	BST2	DUSP5	LRP8	IL22	DGKI	CCL4	GGT1
Tgd cells	TRD@	TARP	C1orf61	TRGV9	CD160	FEZ1				
TFH cells	CHI3L2	CXCL13	MYO7A	CHGB	ICA1	HEY1	CDK5R1	ST8SIA1	PDCD1	BLR1
	PTPN13	KCNK5	ZNF764	MAF	MYO6	SIRPG	THADA	MAGEH1	B3GAT1	SH3TC1
	KIAA1324	PVALB	TSHR	C18orf1	TOX	SLC7A10	SMAD1	POMT1	PASK	MKL2
	HIST1H4K	STK39								
Tem cells	TRA@	PRKY	VIL2	GDPD5	CCR2	MEFV	C7orf54	FLI1	TBC1D5	DDX17
	AKT3	EWSR1	TBCD	NFATC4	LTK					
Tcm cells	CDC14A	ATM	USP9Y	PCNX	FOXP1	KLF12	ST3GAL1	INPP4B	CASP8	MLL
	HNRPH1	STX16	CYLD	SNRPN	TRAF3IP3	NEFL	POLR2J2	AQP3	CG030	PDXDC2
	PCM1	RP11-74E24.2	PHC3	NFATC3	LOC202134	TIMM8A	ATF7IP	REPS1	PSPC1	RPP38
	CLUAP1	DOCK9	CYorf15B	CREBZF	CEP68	TXK	SLC7A6	FYB	MAP3K1	
T helper cells	ICOS	LRBA	ITM2A	FAM111A	PHF10	NUP107	SEC24C	NAP1L4	BATF	ASF1A
	ATF2	CD28	GOLGA8A							
	FRYL	FUSIP1	TRA@	RPA1	UBE2L3	ANP32B	DDX50	C13orf34	PPP2R5C	SLC25A12
T cells	PRKCQ	CD3D	CD3G	CD28	LCK	TRAT1	BCL11B	CD2	TRBC1	TRA@
	ITM2A	SH2D1A	CD6	CD96	NCALD	GIMAP5	CD3E	SKAP1		
NK cells	LOC643313	GAGE2	ZNF747	XCL1	XCL2	AF107846	SLC30A5	NM_014114	MCM3AP	TBXA2R
	ZNF205	AL080130	ZNF528	MAPRE3	BCL2	NM_017616	ARL6IP2	PDLIM4	NM_014274	LDB3
	CDC5L	LOC730096	FUT5	FGF18	MRC2	RP5-886K2.1	SPN	PSMD4	PRX	FZR1
	ADARB1	SMEK1	TCTN2	TINAGL1	IGFBP5	ALDH1B1	NCR1			
NK CD56dim cells	KIR3DL2	SPON2	KIR2DL3	GZMB	KIR3DS1	KIR3DL1	FLJ20699	TMEPAI	IL21R	KIR3DL3
	KIR2DS5	KIR2DS2	GTF3C1	KIR2DS1	EDG8					

NK CD56bright cells	DUSP4	RRAD	XCL1	PLA2G6	NIBP	FOXJ1	44261	MADD	BG255923	MPPED1
	MUC3B									
Neutrophils	CSF3R	CYP4F3	VNN3	FPRL1	KCNJ15	MME	IL8RA	IL8RB	FCGR3B	DYSF
	SLC25A37	BST1	CRISPLD2	G0S2	SIGLEC5	CD93	MGAM	ALPL	FPR1	PDE4B
	FCAR	CEACAM3	HIST1H2BC	HPSE	FLJ11151	CREB5	S100A12	TNFRSF10C	SLC22A4	KIAA0329
	LILRB2									
T cellsmELANOMA	CD8A	CCL2	CCL3	CCL4	CXCL9	CXCL10	ICOS	GZMK	IRF1	HLA-DMA
	HLA-DMB	HLA-DOA	HLA-DOB							
MDSC	CCR2	CXCR4	CXCR2	ITGAM	ITGAX	ANPEP	CD14	FUT4	CD33	CD34
	CCL2	TNF	CXCL12	CSF1R	S100A8	S100A9	STAT1	STAT3	STAT5A	ARG1
	CD38	ENTPD1	PTPRC	CEACAM8	CD80	CSF1R	IL4R	CSF3	CSF2	CXCL8
	NOS2	CD274	TLR3	TLR4	TGFB1	IL10	FOXP3	IDO1	PDCD1	
TLS_nat immunol_Finkin	CCL21	CCL19	CXCL13	CXCL11	CCL8	CXCL10	CXCL9	CCL21	CCL3	CCL18
	CCL5									
Auslander IMPRES	PDCD1	CD28	CIITA	CD3E	CD86	CD28	CD80	CD274	CD86	CD40
	CD28	TNFRSF14	STAT1	GZMB						
POPLAR	CD8A	GZMA	CTLA4	CD40	EOMES	CXCL9	CXCL10	TBX21		
Inflammatory signature (Sangro et al)	CD8A	LAG3	STAT1	CD274						
Cytolytic activity (Rooney et al)	PRF1	GZMA								
Sia Immune Class	NTN3	IGKC	IGKV3D-11	IGLV1-44	IGJ	CCL19	IGHG3	IGHA1	IGHM	IGHG2
	TRBC1	GPR171	GEM	CCL21	TARP	CXCL9	CCL2	TRBC1	IGLJ3	CHIT1
	CD53	PTX3	DCN	CD48	PTPRC	TRAC	FYB	AIM2	DUSP2	CYTIP
	CCL4	STMN2	C11orf96	ID4	CR2	CXCL6	FNDC1	THBS2	LTB	CLIC6
	MGP	TAGLN	CD3D	RAC2	CD27	C16orf54	S100A4	CYR61	PTGIS	COL6A3
	PMEPA1	C7	CORO1A	MS4A1	FAM26F	LAPTM5				
	IGHG1	IGHA2	IGHM	PTGDS	POU2AF1	MMP7	MGC29506	CCL18	GBP5	CD52
	MMP9	IGL@	HLA-DRB5	CXCR4	CD8A	GZMB	LUM	TRBC2	CFTR	GZMK
	CCL5	EFEMP1	LXN	MMP12	AEBP1	IL7R	CD38	POSTN	CXCL14	FAM150B
	ITGB2	GZMH	CCR7	LCP2	RGS1	CD2	SMOC2	LTBP2	GZMA	COL1A2
	SLA	COL1A1	MTHFD2	SAMSN1	PMP22	SRGN	TIMP1	IGLV1-40	GABRP	CTGF
Ayers1 / IFN	IDO1	CXCL10	CXCL9	HLA-DRA	STAT1	IFNG				
WNTscore	APC	APC2	CTNNB1	MYC	SOX11	SOX2	TCF12	TCF7	VEGFA	
WNTTGF_up	DAB2	PLAU	TAX1BP3	RUNX2	RAC2	FZD2	PRKCD	MMP7	PRKX	FZD7
	TCF4	ARRB2	CCND3	PLCB4	DKK3	ROR2	AKT3			
	FRAT2	CDC2	HDAC1	CACYBP	FZD6	DKK2	MVP	PRKCI	MAP1B	SFRP4
WNTTGF_down	TCF1	LRP6	LRP1	PRKCE	WNT16	FZD4	SALL1	WNT1	CAMK2A	NR5A1
	PRKACG									
	WNT8B	CREBBP	DVL1	SOX1	PRKCA	TSHB	WNT10B	NFATC3	NFATC2	CDX1
JerbyArnon_up	BZW2	CCT3	CDK4	GPATCH4	ISYNA1	MDH2	PPIA	RPL31	RPL37A	RPL41
	CHCHD2	CTPS1	EEF1G	EIF2S3	EIF3K	EIF4A1	FARSA	FBL	FKBP4	GAS5
	NONO	PABPC1	PAICS	PFN1	POLD2	PPA1	PTMA	PUF60	RPL10A	RPL11
	RPL28	RPL29	RPL3	RPL36	RPL36A	RPL37	RPL4	RPL5	RPL6	RPL8
	RPS17L	RPS18	RPS19	RPS23	RPS24	RPS27	RPS28	RPS3	RPS4X	RPS5
	SLC25A13	SNHG6	SNRPE	SOX4	SSR2	TIMM50	TOP1MT	TUBB	UQCRFS1	UQCRH
	BOLA2	BOLA2B	BOP1	BTF3	C20orf112	C6orf48	CA14	CACYBP	CBX5	CCT2
	DCAF13	DCT	DCTPP1	DDX21	DDX39A	DDX39B	DLL3	DNAJC9	EEF1B2	EEF1D
	FAM92A1	FBLN1	FOXRED2	FTL	FUS	GABARAP	GGH	GNL3	GRWD1	H3F3A
	IFRD2	ILF3	IMPDH2	ITM2C	KIAA0101	LDHB	LSM4	LSM7	LYPLA1	MAGEA4
	MRPL4	MRPL47	MRPS12	MRPS21	NDUFA11	NDUFA13	NDUFS2	NME2	NOP16	NPM1
	POLR2E	PPP2R1A	PRMT1	PSMA7	PSMD4	RAN	RBM34	RNASEH2A	RNF2	ROMO1
	RPL35A	RPL39	RPL7	RPL7A	RPL9	RPLP2	RPS12	RPS2	RPS20	RPS25
	SLC25A6	SLIRP	SLMO2	SMARCA4	SMIM15	SMS	SNAI2	SNHG15	SNRPB	SNRPC
	TP53	TPI1	TPRKB	TRAP1	TRIM28	TRPM1	TSR1	TUBA1B	TULP4	TXNDC17
	ZFAS1	ZNF286A								
JerbyArnon_down	AHNAK	APOD	ATP1A1	B2M	CD44	CD63	CTSB	CTSD	FOS	GRN

	SERPINE2	TAPBP	TIMP2	A2M	ACSL3	AEBP1	AGA	APOC2	APOE	ATP1B1
	CYP27A1	DAG1	DDR1	EEA1	EMP1	EVA1A	FBXO32	FGFR1	GAA	GPNMB
	MIA	MT2A	NEAT1	NPC1	NSG1	PROS1	S100A6	S100B	SAT1	SCARB2
	TIMP3	TM4SF1	TMED10	TPP1	TSC22D3	TYR	UBC	VAT1	WBP2	XAGE1D
	ATF3	ATP1B3	ATP6V0C	BACE2	BBX	BCL6	C4A	C6orf226	CALU	CARD16
	CLIC4	CORO1A	CRELD1	CRYAB	CSGALNACT1	CXCR4	CYP4V2	DCBLD2	DDX17	DDX5
	FCRLA	FLJ39051	FLJ43663	FLNA	FMN1	FRZB	FSTL3	FTH1	GADD45B	GATSL3
	IFI27	IFI27L2	IFI35	IFI6	IGF1R	IGFBP7	IGSF8	IL1RAP	IL6ST	ITGA6
	LGALS1	LGMN	LINC00518	LOC100126784	LOC100506190	LOC100506714	LOC100507463	LPL	LY6E	LY96
	PDE4DIP	PDK4	PERP	PIK3IP1	PLP2	PRKCDBP	PRNP	PRSS23	PSMB9	PTRF
	MT1X	MTRNR2L1	MTRNR2L10	MTRNR2L2	MTRNR2L3	MTRNR2L4	MTRNR2L5	MTRNR2L6	MTRNR2L7	MTRNR2L8
	S100A13	SCCPDH	SDCBP	SEL1L	SEMA3B	SERINC1	SERPINA1	SGCE	SHC4	SLC20A1
	SPON2	SPP1	SPRY2	SQSTM1	SRPX	ST3GAL6-AS1	ST6GALNAC2	STRIP2	SYNE2	SYNGR2
	TNC	TNFSF4	TRIM22	TRIML2	TSPYL2	TTLL1	TXNIP	UCN2	UPP1	WDFY1
	RPS21	RPS27A	RUVBL2	SAE1	UBA52	AHCY	C17orf76-AS1	C19orf48	C1QBP	CCT6A
	GNB2L1	GPI	HNRNPA1	HNRNPC	IDH2	ILF2	NACA	NCL	NME1	NOLC1
	RPL12	RPL13	RPL13A	RPL13AP5	RPL17	RPL18	RPL18A	RPL21	RPL26	RPL27
	RPLP0	RPLP1	RPS10	RPS11	RPS13	RPS14	RPS15	RPS15A	RPS16	RPS17
	RPS6	RPS7	RPS8	RPS9	RPSA	RRS1	SERPINF1	SET	SHMT2	SLC19A1
	VDAC2	ACTB	AEN	ANP32E	APP	ARMC6	ATP5A1	ATP5D	ATP5G2	ATP5G3
	CCT4	CCT7	CDC123	CDCA7	CFL1	CKS1B	CMSS1	CNRIP1	CS	DARS
	EEF2	EIF3E	EIF3F	EIF3G	EIF3M	EIF4EBP2	ENO1	EXOSC5	FAM174B	FAM60A
	H3F3AP4	HMGA1	HMGB1	HN1	HNRNPA1P10	HNRNPH1	HNRNPM	HSP90AB1	HSPA8	HSPD1
	MAGEC1	MCM7	METAP2	MID1	MIR4461	MKI67IP	MLLT11	MPZL1	MRPL15	MRPL37
	NREP	PA2G4	PAFAH1B3	PET100	PFDN2	PFDN4	PGAM1	PIH1D1	PLEKHJ1	POLR1D
	RPAIN	RPL10	RPL14	RPL15	RPL19	RPL22	RPL27A	RPL30	RPL32	RPL35
	RPS3A	RQCD1	RSL1D1	RTKN	SCD	SCNM1	SERBP1	SF3B4	SKP2	SLC25A3
	SNRPD1	SNRPD2	SNRPF	SNRPG	SRM	SRP14	SSB	TIMM13	TIMM44	TMC6
	TYMS	UBL5	UCK2	UHRF1	USMG5	USP22	VCY1B	VPS72	XIST	YWHAE
	HLA-A	HLA-B	HLA-C	HLA-E	HLA-H	LAMP2	LGALS3	LGALS3BP	NPC2	PSAP
	CD151	CD47	CD58	CD59	CDH19	CSPG4	CST3	CTSA	CTSL1	CTSO
	GSN	HLA-F	HSPA1A	IRF4	ITGA3	KCNN4	KLF4	LEF1-AS1	LRPAP1	MFGE8
	SDC3	SEC11C	SERPINA3	SGK1	SLC26A2	SLC5A3	STOM	STX7	TAPBPL	TIMP1
	ACSL4	ACTA2	ADM	ANGPTL4	ANXA1	ANXA2	APLP2	APOL1	ARL6IP5	ARSA
	CASP1	CAST	CAV1	CAV2	CCND3	CCR10	CD9	CDH1	CHI3L1	CITED1
	DPYSL2	DUSP4	DUSP6	ECM1	EGR1	EPHX2	ERBB3	EZH1	FAM3C	FCGR2C
	GEM	GJB1	GOLGB1	GPR155	GPR56	HLA-DRB5	HLA-G	HPCAL1	HTATIP2	IDI2-AS1
	ITGA7	ITGB1	ITGB3	ITM2B	JMJD7	JUN	KLF6	LAMB2	LCP1	LEPROT
	LYRM9	MAGEC2	MALAT1	MATN2	MCAM	MFI2	MMP14	MPZ	MT1E	MT1M
	PYGB	QPCT	RAB27A	RBP7	RDH5	RNF145	RNF213	RPS4Y1	RTP4	S100A1
	MYO1D	NAV2	NFE2L1	NFKBIA	NFKBIZ	NMRK1	NNMT	NR4A1	P2RX4	PAGE5
	SLC22A18	SLC39A14	SLC7A5P1	SLC7A8	SNX9	SOD1	SORT1	SP100	SPESP1	SPINT1
	SYPL1	TF	TFAP2A	TGOLN2	THBD	TMBIM6	TMED9	TMEM255A	TMEM66	TMX4
	ZBTB20	ZBTB38								
MAPKi resistant melanoma up	ACVR1B	APC2	ARHGAP35	ARID1A	AURKA	BCAP29	BCORL1	BGLAP	BRAF	CCND3
	EGLN2	FANCA	FANCC	FANCE	FGF18	FIGF	FZD5	GATA2	GOT1	GSTP1
	LAMC3	LIFR	MAP1S	MAP2K1	MAPK3	MED12	MEOX2	MLXIPL	MYOD1	NFKBIA
	PIK3R2	PLCG1	POLQ	PPARD	PPM1D	RAB40A	RALBP1	RARB	RCOR2	RPTOR
	VCX3A	WNT6	XIRP2	ZBTB16						
	CCNE1	CD163L1	CDKN2C	CHD8	CIC	CPNE1	CSRNP1	CYCS	DAXX	DOT1L
	HIST1H3C	HSPE1	HTR2C	IGF2	IL6	INPPL1	IPO13	IQSEC1	ITGA2B	JAKMIP2
	NKX3-1	NLRP5	NOTCH2	NPAP1	NRAS	NTRK1	OGDH	PBRM1	PGF	PIAS4
	RXRA	SAMD4B	SMAD3	SRC	STX2	SUFU	SUPT6H	TFEB	THNSL2	TPM3
MAPKi resistant melanoma down	ACADVL	AKT3	AMER1	ANAPC5	ARID2	ASXL1	ATG16L1	ATG4B	ATP1A1	AXIN1
	CTLA4	CTNNA2	DCC	DUSP4	DVL2	EGFR	ERBB3	ESR1	FANCF	FAT1
	GID4	GLI1	GNPTAB	GPR101	H3F3C	HOXD8	IGF1R	ING1	IRF4	ISX
	MLH1	MLL	MLL4	MYC	MYOCD	NCOA4	NFE2L3	NSMAF	OR4A16	PCBP1
	RAC1	RAD51	RARA	RBX1	RHOA	RPS11	RUNX1T1	RXRG	SAMD4A	SLC26A3

	VHL	WNT8B	XBP1	XIAP	YAP1	ZFAND6	ZNF217			
	AXL	B2M	BID	CASP9	CCT8	CDC42	CRIPAK	CRLF2	CTBP1	CTBP2
	FBXW7	FGF1	FGF12	FGF13	FGF2	FGF5	FOXA2	FZD10	FZD3	FZD6
	JAK1	KEAP1	LAMA4	LAMC1	LEF1	LRRK2	MAP2K4	MED23	MEIS2	MGA
	PIAS3	PIK3CB	PLEKHG3	POFUT1	PRKAR1A	PSMA1	PTCH1	PTEN	PTK2	PTPRK
	SMC3	STK36	STK4	TAF1	TIMM44	TNFRSF13B	TP53BP1	TRAF3	TRAF4	TRAF6
Nivolumab (molecular) resistant melanoma up										
	100133445	ABCA5	ABHD12B	ACAD9	ACSBG1	ADAMTS1	ADGRB1	AHNAK2	AHSA2	ANKRD10
	BBS5	BEGAIN	BEST1	C11orf24	C1orf101	C3orf70	CA12	CALCOCO1	CCDC188	CD44
	CREBZF	CRMP1	CSGALNACT1	CSRP1	CTDSPL	CTTN	CYP27C1	CYP4V2	DCBLD2	DDX39B
	EFHC1	EPG5	EVC	FAM131A	FAM188A	FAM210B	FAM86HP	FARP2	FBXL2	FBXO7
	GPM6B	GPR180	GRB10	GSK3B	H1FX-AS1	HERC2P2	HERC2P3	HIBCH	HIST1H3H	HM13-AS1
	ITIH6	KATNAL1	KAZN	KCTD15	KIF13A	KIFC3	KLC1	KLHL41	KPTN	LAMA1
	LOC285593	LOC389834	LOC541473	LOC93429	LPIN3	LRP2BP	LUC7L	LYST	LZTS1	MAP4
	MPZ	MREG	MTRNR2L1	MYBPHL	MYO5A	MYOM3	N6AMT1	NAPB	NAV1	NEAT1
	OSTM1	PABPC1L	PCGF3	PCNX4	PHLDB1	PHLPP1	PIGG	PITRM1	PKD1P1	PKD2
	PTPRS	PTPRZ1	RAB4B	RAB6B	RBM25	RCBTB1	REV3L	RGS12	RHOB	RHOJ
	SLITRK2	SNORD97	SNRNP70	SNX25	SPATA6	SRSF6	ST3GAL4	ST3GAL6-AS1	ST6GALNAC2	ST8SIA6
	TRIB2	TRIM9	TRPM1	TSPAN9	TTC14	TTLL3	TTLL4	TTYH1	UBE2Q2P1	USP31
	ANKRD30B	ANKS1A	AP3M2	ARHGAP5	ARHGAP5-AS1	ARHGEF4	ATG2B	ATP1B3	ATP8B3	B4GALT6
	CDC16	CDC42EP3	CDH4	CELSR2	CHST3	CLCN3	CMYA5	COL16A1	COL7A1	CORO2B
	DIP2C	DLEU1	DLGAP4	DNAJA4	DNAJC13	DNM1P35	DOCK6	DST	DVL3	DYNC1H1
	FHDC1	FLCN	FOXD2	GABBR1	GALNT14	GANC	GAS7	GMFB	GNG12	GPAT4
	HN1L	HSPA12A	HSPG2	IDI2-AS1	IGFL4	IGFN1	INPP5F	ITGA3	ITGA7	ITGB3
	LAMA4	LAMB2	LDB3	LENG8	LINC00681	LINC00920	LOC100499484	LOC100507351	LOC100507577	LOC284080
	MCOLN3	MELTF	MFAP3L	MFGE8	MIA	MIR211	MIR3685	MIR5047	MIR647	MOCOS
	NECTIN1	NEK3	NLGN1	NLGN3	NPHP3	NPHP3-ACAD11	NPIPA1	NPIPA3	NPIPA5	NXF1
	PKNOX2	PLA2G4C	PLAT	PLEKHG3	PLXNB3	PNMA1	POMT2	PRICKLE2	PRMT2	PTPRM
	SAMD4A	SERPINE2	SETD4	SGCD	SLC10A6	SLC22A15	SLC25A27	SLC26A8	SLC4A3	SLC5A3
	STK32A	STK36	TCEAL4	TEAD1	TMED10	TMEM229B	TMOD1	TP53INP2	TPT1-AS1	TRAF3IP2
	USP32P1	UVSSA	VARS2	VN1R1	VPS36	ZC3H7A	ZMAT3	ZNF491	ZNF514	ZNF704
Nivolumab (molecular) resistant melanoma down										
	MARCH1	44440	ABI3	ACAP1	ACRBP	ADA	ADAM28	ADAMDEC1	ADGRG5	ADH1C
	ANKRD29	ANKRD33B	ANKRD55	ANTXR2	ANXA2R	APEX2	APOA1	APOC1	APOC1P1	ARHGAP15
	ATP8A1	BCAS4	BCL11A	BCL2L14	BHMT	BLNK	BTG2	BTK	C15orf57	C16orf54
	CCL19	CCL21	CCL24	CCR4	CCRL2	CD180	CD2	CD247	CD27	CD28
	CD6	CD68	CD69	CD7	CD72	CD74	CD79A	CD83	CD84	CD86
	CETP	CFD	CHDH	CHIT1	CHRNA1	CHST13	CISH	CLECL1	CLU	CNTNAP2
	CYBA	CYP2C8	CYP2C9	CYTH1	CYTIP	DAPP1	DEF6	DENND1C	DENND2D	DGKD
	EFCAB1	EMG1	ERP27	EVI2A	EVI2B	EXOSC1	FAM107B	FAM151A	FAM159A	FAM172BP
	FRAT1	FRAT2	FTL	FUCA1	GABRR1	GALNT13	GAPT	GCHFR	GCNT1	GCSAM
	GPRIN3	GRAP	GRAPL	GRIN3A	GSTA1	GSTK1	GTSF1	GZMH	GZMK	HAVCR2
	HLA-DQA1	HLA-DQA2	HLA-DQB1	HLA-DQB2	HLA-DRA	HLA-DRB1	HLA-DRB5	HLX	HS3ST2	HSH2D
	IL32	INPP5D	IQGAP2	IRF8	ITGAD	JCHAIN	KBTBD8	KCNJ5	KCNQ1	KCTD12
	LINC00693	LIPA	LOC100505622	LOC389641	LOC606724	LOC653786	LOC728989	LPAR1	LPAR5	LPCAT3
	MGAT4C	MGC70870	MPEG1	MSL3P1	MYO1A	MYO7B	NAPSB	NCF1	NCF1B	NCF1C
	P2RX5	P2RY10	P2RY13	P2RY14	P2RY8	PACSIN1	PAOX	PCED1B	PCED1B-AS1	PDE1A
	PKD2L1	PKHD1L1	PKIB	PLA2G2D	PLA2G7	PLAC8	PLCG2	PLCL2	PLCXD2	PLD4
	PROC	PRSS12	PRUNE2	PSD4	PTGER4	PTPN6	PTPRC	PTPRCAP	PTPRN2	RAB3C
	RGN	RGS7	RGS9	RHOH	RHOU	RILPL2	RNASE6	RNASET2	RND1	RNLS
	SDS	SEL1L3	SELENOP	SERPINB9	SERPINF2	SH2D1A	SH2D1B	SH2D2A	SIGLEC10	SIGLEC12
	SLC25A53	SLC26A7	SLC27A2	SLC29A3	SLC38A1	SLC40A1	SLC45A3	SLC46A3	SLC47A1	SMAP2

	STK17B	SURF1	SUSD3	SYK	SYTL3	TAGAP	TBC1D10C	TBC1D22A	TBC1D30	TDRD6
	TMEM37	TMIGD2	TMSB4X	TNF	TNFAIP8	TNFAIP8L2	TNFRSF17	TNFSF8	TOX	TRAF3IP3
	VAV1	VAV3	VCAM1	VOPP1	WDFY4	XCL1	ZBTB18	ZBTB8OS	ZC3H12D	ZC4H2
	ADORA2A-AS1	ADORA3	AKNA	AKR1B1	AKR1C1	AKR1C2	AKR1C3	ALDH2	ALDOB	ANKRD19P
	ARHGAP25	ARHGDIB	ARID3A	ARL11	ARRB2	ASAH2	ASAH2B	ASGR2	ATP2A3	ATP6V0D2
	C1orf54	C4BPA	C4BPB	C5	CARD11	CBLN2	CCDC28A	CCDC69	CCDC88C	CCL18
	CD300LF	CD37	CD3D	CD3E	CD3G	CD40LG	CD48	CD5	CD52	CD53
	CD8B	CD96	CDC42SE2	CEACAM21	CEBPA	CEBPA-AS1	CECR1	CENPH	CEP120	CERKL
	CORO1A	CP	CREG1	CRTAM	CSF2RB	CTSH	CTSS	CXCL13	CXCL16	CYB5R4
	DHDH	DLL3	DNAJC5B	DOCK11	DOCK2	DOK3	DPEP2	EAF2	EDARADD	EDN3
	FAM58A	FBN2	FBP1	FCER1G	FCRL3	FCRL5	FGD3	FKBP5	FLI1	FNDC5
	GM2A	GNGT2	GP1BA	GPC3	GPR160	GPR174	GPR18	GPR183	GPR35	GPR88
	HCLS1	HCN1	HEIH	HLA-DMA	HLA-DMB	HLA-DOA	HLA-DOB	HLA-DPA1	HLA-DPB1	HLA-DPB2
	HTRA4	HVCN1	ICAM3	ICOSLG	IGFLR1	IGSF6	IKZF1	IKZF3	IL21R	IL2RG
	KLHL6	KLRB1	LAIR1	LAPTM5	LCK	LGALS2	LGALS9	LILRA4	LILRB1	LILRB4
	LSP1	LTA	LTB	LY86	LY9	LYZ	MAP4K1	MEF2C	MFNG	MFSD6L
	NCR3	NELL2	NINJ2	NLRP2	NR2F1	NTS	NUAK2	NUB1	NUGGC	ORM2
	PDE6G	PDE7A	PHYHIPL	PIK3AP1	PIK3CG	PIK3IP1	PILRA	PIM2	PIP5K1B	PIPOX
	PLEK	PNOC	POC1B	POU2AF1	POU2F2	PPARG	PPP1R16B	PRDM8	PRIM1	PRLR
	RAB42	RAB8A	RASGEF1B	RASSF5	RBM47	RBP5	RCSD1	RELB	RFC2	RFTN1
	RPA2	RPA3	RPL10	RPS14P3	RPS6KA1	RSPO3	SASH3	SCIMP	SCN3A	SCTR
	SIGLEC7	SIGLEC8	SIRPG	SIT1	SLAMF1	SLAMF6	SLAMF8	SLC12A3	SLC1A2	SLC25A38
	SNAI3	SOCS1	SOWAHD	SP140	SPOCK2	SSBP1	SSR4	ST6GALNAC1	ST8SIA4	STAP1
	TESPA1	TFEB	TFR2	TIFA	TIFAB	TLCD1	TLR7	TMEM156	TMEM176A	TMEM176B
	TRAT1	TREM2	TRG-AS1	TSPAN13	TSPAN33	TST	TTF1	TYROBP	UBASH3A	UPB1
	ZNF101	ZNF48	ZNF890P	ZNRF2	ZSCAN2					
Nivolumab resistant melanoma up	ARSI	C1orf116	CAMK2A	CEACAM19	ELFN1	FAM189A2	FGFR3	FLCN	H1FX-AS1	LINC00571
	LINC01024	PMP22	SHROOM1	SLC9A3	TACR2	ZNF577				
Nivolumab resistant melanoma down	ATP2A3	ATP5EP2	BACH2	BANK1	BMP6	C4BPA	CARD11	CCL24	CCR6	CD19
	ERCC6L	FAM129C	FAM159A	FCRL3	GPC3	GPR174	GPR88	GRAP	HAR1A	KLHDC8A
	P2RY8	PCDH11X	POLA2	POU2F2	PPP1R16B	PRDM8	PSMA7	RBM38	RHOH	SAMD5
	CD22	CD79B	CFI	CLEC17A	CXCL13	CXCR5	CYFIP2	DGKD	DGKE	DNASE1L3
	LINC00643	LRMP	LRRC55	LSM14B	MAP4K1	MLC1	NELL2	NLRC3	NUGGC	P2RX5
	SLC26A4	SUSD3	TAF4	TNR	UBAP1L	ZNF101				
On Nivolumab up	SEPT1	ABCB1	ACOD1	ADGRE2	AKAP5	ALPK1	ANKRD22	APOL1	APOL3	ASCL2
	CD2	CD247	CD274	CD300LF	CD3D	CD3E	CD3G	CD5	CD6	CD7
	CTLA4	CTNND2	CXCL10	CXCL9	CXCR6	CYFIP2	DBH	DTHD1	DTX3L	EBI3
	FCRL3	FCRL6	GADD45B	GADD45G	GBP1	GBP1P1	GBP2	GBP4	GBP5	GCH1
	HLA-C	HLA-DQA2	HLA-DRB6	HLA-E	HLA-F	HLA-H	HLA-L	HS3ST3B1	HSD11B1	ICOS
	IL32	IRAK2	IRF1	ITGAL	ITK	JAKMIP1	KLHDC7B	LAG3	LCK	LILRA3
	PLEK	PRF1	PSD4	PSMB9	PSTPIP2	PTPN22	PTPRC	RAB37	RAC2	RARRES3
	SIRPG	SIT1	SKAP1	SLA2	SLAMF6	SLAMF7	SLAMF8	SLC27A2	SLC2A6	SLC6A12
	THEMIS	TIGIT	TLR8	TMEM155	TMEM176A	TMEM176B	TMPRSS3	TNFAIP3	TNFRSF1B	TNFRSF9
	BATF	BCL11B	BCL6	BIRC3	CA11	CCL4	CCL4L1	CCL5	CCL8	CCR5
	CD72	CD80	CD8A	CD8B	CD96	CIITA	CLEC4E	CP	CRTAM	CST7
	EOMES	ETV7	EZR	FADS2	FAM179A	FAM26F	FASLG	FCGR1A	FCGR1B	FCGR1CP
	GJD3	GPR132	GPR171	GPR68	GRIN3A	GZMA	GZMB	GZMH	GZMK	HLA-B
	IDO1	IFNG	IGFLR1	IKZF3	IL12RB1	IL18BP	IL21R	IL2RA	IL2RB	IL2RG
	LILRB1	LY75	MFSD6	MIAT	NKG7	NLRC5	PDCD1	PDCD1LG2	PIK3AP1	PLA2G2D
	RASGEF1B	RASGRP1	RILPL2	RIPK3	RNF144B	SECTM1	SERPINA1	SH2D1A	SIGLEC10	SIGLEC11
	SLC9A3R1	SMCO4	SOD2	SPATA13	SPOCK2	SQRDL	STAT3	TAP1	TAPBP	TGM2
	TNIP3	TOX	TOX2	UBASH3A	ZAP70	ZC3H12A				
On Nivolumab down	CBX1	GAP43	GYPE	HOXA2	HOXD4	KIAA1024	MPP4	NCAM1	NIFK	NYAP1

	PIR	POPDC3	RPL7	TRAM1L1	WASF1					
Responders on Nivolumab up	SEPT1	LOC728875	ABCB1	ABCC9	ABCD2	ABI3	ABRACL	ACAA1	ACAP1	ACOD1
	AES	AFTPH	AGAP2	AGFG2	AIM1	AIM2	AKAP5	AKNA	AKR1C4	AKTIP
	APOL2	APOL3	APOL6	ARHGAP15	ARHGAP27	ARHGAP30	ARHGAP9	ARHGEF3	ARID5A	ARNTL
	BATF	BCL2L11	BCL3	BCL6	BID	BIN2	BIRC3	BLOC1S2	BTN3A1	BTN3A2
	C2orf81	C4B_2	C5AR2	CA11	CA2	CABP4	CALCOCO2	CARD11	CARHSP1	CASP7
	CCR5	CCRL2	CD14	CD163	CD1D	CD2	CD226	CD244	CD247	CD27
	CD40	CD47	CD48	CD5	CD53	CD6	CD7	CD72	CD74	CD80
	CFLAR	CHI3L1	CHST7	CIITA	CLMN	CORO1A	CP	CPPED1	CREG1	CRLF3
	CXCL16	CXCL2	CXCL9	CXCR3	CXCR6	CYB5R4	CYBA	CYFIP2	CYLD	CYTH1
	DOCK8	DOK2	DPYD	DRAM1	DSE	DTHD1	DTX3L	DYSF	ELF3	ELL
	FAM192A	FAM20A	FAM20C	FAM26F	FASLG	FBP1	FBXO6	FCGR1A	FCGR1B	FCGR1CP
	FUOM	FXYD1	FYB	GADD45B	GADD45G	GALM	GBP1	GBP1P1	GBP2	GBP3
	GIMAP6	GJD3	GLDC	GLRX	GMFG	GMIP	GNB5	GNLY	GPR132	GPR171
	HAVCR2	HCG26	HCLS1	HCP5	HCST	HGD	HK3	HLA-A	HLA-B	HLA-C
	HLA-E	HLA-F	HLA-H	HLA-L	HMHA1	HS3ST3A1	HS3ST3B1	HSD11B1	HSD3B7	ICAM3
	IKZF1	IKZF3	IL10	IL10RB	IL12RB1	IL15	IL18BP	IL21R	IL24	IL2RA
	IRF2	IRF8	ISG20	ITGAL	ITGB2	ITGB7	ITK	JAK3	JAKMIP1	JAKMIP2
	KLHDC7B	KLHL2	KLRC2	KLRD1	KMO	KYNU	LACTB	LAG3	LAIR1	LAMP3
	LINC00324	LINC00623	LINC00649	LLGL2	LOC100499489	LOC100506585	LOC100507412	LOC153684	LOC606724	LOC728752
	MAFB	MAN1C1	MAN2A1	MAN2B2	MAP3K14	MAP3K7CL	MAP3K8	MAP4K1	MAPK13	MBD4
	MPO	MPPE1	MR1	MT1E	MT1L	MVP	MYD88	MYL12A	MYLK	MYO1F
	NFKBIB	NKAPP1	NKG7	NLRC3	NLRC5	NMI	NR1H3	NSMCE4A	NTN4	NTSR1
	P4HTM	PARP11	PARP12	PARP14	PARP15	PARP9	PATL2	PCED1B-AS1	PCGF5	PDCD1
	PLPP6	PNRC1	PPM1M	PPP3CC	PRF1	PROX1	PRR5L	PSD4	PSMB10	PSMB8
	PTPRC	PTPRCAP	PZP	RAB11B-AS1	RAB20	RAB37	RAB8A	RAC2	RAP2C	RARRES2
	RGS14	RGS9	RHOH	RILPL2	RIN3	RIPK3	RLTPR	RNASET2	RNF166	RNF213
	SCP2	SCPEP1	SECTM1	SEMA4D	SERPINA1	SERPINB1	SERPINB8	SERPING1	SGPP1	SH2D1A
	SLA	SLA2	SLAMF1	SLAMF6	SLAMF7	SLAMF8	SLC14A1	SLC15A3	SLC16A13	SLC27A2
	SLC9A3R1	SLC9A3R2	SLC9A7	SLCO2B1	SLFN12L	SMAP2	SMCO4	SNORD89	SNX20	SOD2
	STAT1	STAT3	STAT4	STAT5B	STX11	STX4	STXBP2	SULT1A1	SUN2	SUSD3
	TC2N	TCIRG1	TFEC	TGFB1	TGFB1I1	TGM2	THBS1	THEMIS	THSD4	TIFA
	TMEM176A	TMEM176B	TMPRSS3	TNF	TNFAIP3	TNFAIP8L1	TNFAIP8L2	TNFRSF10A	TNFRSF1B	TNFRSF4
	TRG-AS1	TRIM21	TRIM22	TRIM8	TTC39B	TUBA4A	TXK	TXNDC11	TYMP	UBA7
	VASP	VAV1	VNN1	VNN2	VPS13C	WAS	WIPF1	WISP1	WTAP	XPO6
	ACOT2	ACP2	ACSF3	ACSL5	ACTR3	ADAM28	ADAMTS9-AS2	ADAP1	ADAP2	ADCY3
	ALPK1	AMFR	AMPD3	ANKRD22	ANKRD29	ANPEP	APBB1IP	APOBEC3F	APOBEC3G	APOL1
	ARNTL2	ARPC4	ARRB2	ARRDC1	ASCL2	ASGR1	ATF5	ATF7IP2	ATP6V0D1	B2M
	BTN3A3	C10orf76	C12orf75	C16orf54	C17orf62	C18orf8	C19orf38	C1RL	C1S	C2
	CASP8	CCBE1	CCDC64	CCDC88B	CCL16	CCL3	CCL4	CCL4L1	CCL5	CCL8
	CD274	CD28	CD300A	CD300C	CD300LF	CD38	CD3D	CD3E	CD3G	CD4
	CD82	CD84	CD86	CD8A	CD8B	CD96	CDC40	CDC42SE2	CEBPD	CFB
	CRTAM	CSF1	CST7	CTAGE1	CTAGE5	CTLA4	CTSH	CTSS	CTSW	CXCL10
	CYTH4	DAZAP2	DBH	DDHD1	DENND1B	DENND1C	DHRS1	DHRS3	DNAJC5B	DNASE2
	EOMES	EPHA1	EPSTI1	ERAP1	ERMARD	EVL	F11R	FAM107B	FAM111A	FAM179A
	FCN1	FCRL6	FERMT3	FGD2	FLT3LG	FLVCR2	FMNL1	FPGS	FRMD4B	FTL
	GBP4	GBP5	GCH1	GCHFR	GCLC	GCNT1	GFI1	GGT5	GIMAP2	GIMAP4
	GPR65	GPR68	GSAP	GSDMD	GZMA	GZMB	GZMH	GZMK	HAAO	HAMP
	HLA-DMA	HLA-DMB	HLA-DOA	HLA-DPA1	HLA-DPB1	HLA-DQB1	HLA-DRA	HLA-DRB1	HLA-DRB5	HLA-DRB6
	ICOS	ID2	IDNK	IDO1	IFITM1	IFITM10	IFITM2	IFNAR2	IFNG	IGFLR1
	IL2RB	IL2RG	IL32	IL4R	INHBB	INPP5D	IPCEF1	IRAK2	IRAK4	IRF1
	JUN	KBTBD8	KCNA1	KCNK6	KCNMA1	KCNMB1	KDM8	KIAA1324	KIAA1551	KIF19
	LAP3	LAPTM5	LAT2	LCK	LCP1	LCP2	LEPR	LILRA3	LILRB1	LILRB4
	LPAR5	LPIN2	LRG1	LRRC25	LSR	LY75	LY9	LYN	LYRM9	MAF
	MED29	MFNG	MFSD2A	MFSD8	MIAT	MICB	MIR155HG	MKNK1	MOB1A	MOB3C
	MYO1G	MYO7A	N4BP2L1	NAAA	NAT1	NCF1	NCF1B	NCF1C	NCKAP1L	NFKBIA
	NUBP1	NUDT16P1	NUMB	OASL	OCIAD2	ODF3B	OSCAR	OTOF	OXER1	P2RY14
	PDCD1LG2	PHF11	PI4K2B	PIGR	PIK3AP1	PILRA	PITPNM1	PLEK	PLEKHF1	PLIN2
	PSMB8-AS1	PSMB9	PSME1	PSME2	PSTPIP1	PSTPIP2	PTK2B	PTPN22	PTPN6	PTPN7
	RARRES3	RASAL3	RASGEF1B	RASGRP1	RASSF4	RASSF5	RASSF7	RCSD1	REC8	RELB

	RNF34	RNF4	RPS6KA1	RRAD	S1PR4	SAMD3	SAMSN1	SASH3	SCARF1	SCIMP
	SH3BP2	SHKBP1	SIGIRR	SIGLEC11	SIGLEC14	SIGLEC16	SIPA1	SIRPG	SIT1	SKAP1
	SLC29A3	SLC2A6	SLC30A1	SLC31A2	SLC41A2	SLC47A1	SLC6A1	SLC6A12	SLC8A1	SLC8B1
	SOWAHD	SP100	SP140L	SPATA13	SPI1	SPN	SPOCK2	SQRDL	SSTR2	STARD4
	SUSD6	SYTL3	TAB2	TANK	TAP1	TAPBP	TAPBPL	TARP	TBC1D10C	TBC1D2
	TIGIT	TLR2	TLR6	TLR8	TMC8	TMEM102	TMEM123	TMEM155	TMEM170A	TMEM175
	TNFRSF9	TNFSF13	TNFSF14	TNIP1	TNIP3	TOX	TOX2	TPRG1	TRADD	TRAF3IP3
	UBASH3A	UBASH3B	UBE2F	UBE2L6	UBE2QL1	UNC13D	UNC5A	VAMP5	VAMP8	VASN
	ZAP70	ZBED1	ZBTB32	ZC3H12A	ZC3H12D	ZDHHC18	ZNF101	ZNF438	ZNF831	ZNRF2
Responders on Nivolumab down	SEP3	AACS	ABCB6	ABCF1	ABCF2	ADGRL1	AHCYL2	AKT3	ALX1	AMMECR1L
	ATP1A1	ATP6V0A4	ATP6V1B1	ATP9A	BACE2	BAMBI	BBS9	BCAN	BEST1	BEX3
	C16orf59	C19orf57	C2orf88	C5orf22	C5orf30	C8orf33	CABLES1	CAPN3	CASKIN1	CBX1
	CDK16	CDK2	CDK5R1	CDKN2B	CDKN3	CDYL	CELSR2	CENPA	CENPF	CERS1
	COLGALT2	COPG2	CORO2B	CRNDE	CRTAP	CS	CSE1L	CSNK1E	CSNK2A1	CSPG4
	DLL3	DNAJC2	DNER	DONSON	DPF1	DROSHA	DSCC1	DSTYK	DTL	E2F1
	EN2	EPHA5	EPRS	ESF1	ESRP1	ETV4	EWSAT1	EXO1	EXTL1	FABP7
	FARSB	FASN	FAXC	FGD1	FIGNL1	FKBP10	FKBP14	FMN1	FMN2	FOXM1
	GEMIN5	GGCT	GINS4	GJC3	GLI3	GLMP	GOLGA2P10	GOLGA2P7	GPATCH4	GPM6B
	H2AFZ	HAGLR	HAS2	HCN1	HEY1	HHATL	HILS1	HMGXB4	HNRNPA1	HNRNPA1L2
	IGF1R	IGFBPL1	IGSF11	IMPDH2	INPP5F	IPO11	IPO4	IPO7	IPO9	IQGAP3
	KIAA1024	KIF20A	KIF4A	KIFAP3	KIFC1	LAPTM4B	LDHB	LEF1	LGI3	LHFPL3-AS1
	LINC01278	LINC01531	LOC100126784	LOC100130370	LOC100505912	LOC285000	LOC642423	LOC646762	LONRF1	LRP12
	MCOLN3	MCUR1	MDGA2	MECR	MED20	MEIS2	METAP1D	MGC16275	MID1	MITF
	MSTO1	MSTO2P	MSX2	MTAP	MTBP	MYC	MYEF2	MYH14	MYO10	MYT1
	NKAIN1	NLE1	NME1	NOL11	NONO	NOP16	NOP56	NPM1	NRG3	NRM
	PABPC1	PABPC3	PAICS	PAPSS1	PARVB	PAX3	PBK	PCGF2	PDCD7	PDE11A
	PLCB4	PLEKHA5	PLEKHA8P1	PLEKHH1	PLOD3	PLXNB3	PMS2	PNCK	PNMAL1	POGK
	PPT2	PRAME	PRC1	PRELID2	PRR11	PRRT3-AS1	PRSS33	PRTG	PTK2	PTP4A3
	RASSF8	RASSF8-AS1	RBBP7	RCOR2	RECQL4	RGS20	RIMS2	RLBP1	RNF144A	RNF2
	RTCB	RTTN	S100A1	SAMM50	SCIN	SEMA6A	SERPINB7	SERPINE2	SFTPC	SGCD
	SLC6A10P	SLC6A15	SLC6A17	SLC6A8	SLC7A1	SLC7A5	SLCO4A1-AS1	SMIM13	SMYD5	SNCA
	SPIRE2	SPRY1	SPRY4	SRP68	SRPK1	SRPK2	SRRD	ST13	ST13P4	STEAP1
	TCEAL4	TCTN3	TEAD1	TEX10	TEX15	TEX41	TFAP2A	TFAP4	TICRR	TIMM8A
	TONSL	TOP1MT	TPTE	TRAM1L1	TRIM63	TRIM9	TRIP13	TRMT12	TROAP	TSPAN10
	TYRP1	TYW3	UBAP2L	UBE2H	UBE2T	UBFD1	UCK2	URB1	URB2	USP51
	XRCC2	ZBTB9	ZC2HC1A	ZIC2	ZNF106	ZNF16	ZNF212	ZNF280B	ZNF330	ZNF343
	AMOT	ANKRD7	ANLN	AP1S2	ARC	ARHGAP39	ARHGAP5-AS1	ARPC1A	ASB11	ATP10B
	BICD1	BMS1	BMS1P17	BMS1P18	BNC2	BTBD3	BUB1B	BYSL	BZW2	C10orf90
	CC2D2A	CCDC140	CCDC34	CCNB1	CCT2	CCT3	CCT6A	CCT8	CDC45	CDC6
	CHAF1B	CHGA	CHML	CHST10	CIT	CITED1	CKAP2L	CNNM1	CNPY4	COL25A1
	CTSV	CXorf56	CYTH3	DARS2	DCAF13	DCT	DENR	DGAT1	DHX33	DKC1
	E2F3	ECD	EFNA5	EFR3B	EIF2S3	EIF3B	EIF3D	EIF3E	EIF3H	EIF3L
	FAM127C	FAM161A	FAM169A	FAM174B	FAM20B	FAM57A	FAM64A	FAM69C	FAM83D	FAM86C2P
	FSTL4	FSTL5	FXR1	GABRA3	GABRB3	GAPDHS	GAR1	GAS5	GDAP1	GDF11
	GPR143	GPRIN1	GPSM2	GREB1	GSTA4	GTF2IP4	GTF3C4	GTSE1	GYG2	GYS1
	HNRNPA1P33	HOXB9	HPS4	HS6ST2	HSP90AB1	HSPA12A	HSPA2	HSPA4	HTATSF1	IARS2
	IRX5	IRX6	ISPD	ISYNA1	JARID2	KAZN	KBTBD2	KCNH1	KCNQ5	KDM1A
	LINC00461	LINC00473	LINC00511	LINC00622	LINC00673	LINC00681	LINC00997	LINC01021	LINC01102	LINC01158
	LRRC39	LRRN4CL	LUZP1	MAGEC1	MAGED2	MAP7D2	MAPK12	MAPK4	MAPT	MCM8
	MLANA	MLPH	MMP16	MMP17	MOB3B	MOK	MORF4L2	MPP4	MPPED2	MRPS25
	NARS	NARS2	NAT9	NAV2	NBEA	NCAPG2	NCBP2	NCL	NFYA	NIFK
	NSG1	NT5DC3	NUBPL	NVL	NYAP1	OCRL	OSBPL1A	OTUD7B	P2RX6	P3H4
	PDHA1	PEG10	PES1	PEX5	PFKM	PHLPP1	PIAS3	PIR	PJA1	PKNOX2
	POLA1	POLD2	POLR1C	POLR3G	POMT2	POPDC3	PPEF1	PPIL1	PPP1R14C	PPP1R9A
	PTPN13	PTPN14	PTTG1	PUM3	PUS7	PWP2	PYCR1	QPCT	QTRT2	RAB6B
	RNF216P1	ROPN1	ROPN1B	RP9	RP9P	RPL7	RPS10	RPS6KC1	RRP15	RRS1
	SH3TC2	SLC19A2	SLC24A5	SLC25A23	SLC25A32	SLC35B4	SLC39A10	SLC39A6	SLC41A1	SLC45A2
	SNHG16	SNHG4	SNHG6	SNX12	SORT1	SOX10	SOX12	SOX6	SOX9	SPIRE1
	STEAP1B	STK32A	STRADB	STX7	STXBP6	TAF4B	TAF9B	TBC1D16	TBC1D7	TBRG4

TMCC2	TMEM120B	TMEM164	TMEM201	TMEM215	TMEM237	TMEM241	TMEM55A	TMEM98	TOMM20
TSPAN3	TSR1	TTC21B	TTC26	TUBB	TUBB4A	TULP3	TYMS	TYR	TYRO3
USP54	UTP14A	UTP15	VLDLR-AS1	WASF1	WDR3	WDR46	WDR63	WDR91	XPO5
ZNF367	ZNF462	ZNF696	ZNF697	ZNF704	ZNF74				

Table S7: Performance of previously reported signatures and IFNAP in frontline cohort

	IFN	Inflammatory signature	POPLAR	Cytolytic Activity	IFNAP
Accuracy	82%	82%	68%	68%	82%
Sensitivity	67%	67%	50%	50%	67%
Specificity	94%	94%	81%	81%	94%
PPV	89%	89%	67%	67%	89%
NPV	79%	79%	68%	68%	79%
AUC	0.85	0.82	0.76	0.67	0.87

Table S8: Genes incorporated in the IFNAP signature

Genename
STAT1
GBP1
HLA-DRA
HLA-DRB5
HLA-DQA1
TRIM25
FCER1G
SEC24A
CTSS
CXCL9
B2M

Table S9: Clinicopathological characteristics of patients treated with anti-PD1 in 2nd/3rd line

	All (n = 55)	Objective response (n=13)	No response (n=42)	p
Age (years), median (range)	63.0 (28-86)	63.0 (51-86)	63.5 (28-83)	0.48
>65 years, n(%)	25 (45.5)	6 (46.2)	19 (45.2)	1.0
Sex, n (%)				0.16
Male	42 (76.4)	12 (92.3)	30 (71.4)	
Female	13 (23.6)	1 (7.7)	12 (28.6)	
Region, n (%)				0.67
US	9 (16.4)	1 (7.7)	8 (19.0)	
Europe	46 (83.6)	12 (92.3)	34 (81.0)	
Aetiology, n (%)				
HBV	11 (20.0)	5 (38.5)	6 (14.3)	0.11
HCV	13 (23.6)	1 (7.7)	12 (28.6)	0.16
Uninfected	31 (56.4)	7 (53.8)	24 (57.1)	
BCLC stage, n (%)				0.71
Intermediate (B)	12 (21.8)	2 (15.4)	10 (23.8)	
Advanced (C)	43 (78.2)	11 (84.6)	32 (76.2)	
Sample origin, n (%)				0.62
Primary tumor	49 (89.1)	11 (84.6)	38 (90.5)	
Metastasis	6 (10.9)	2 (15.4)	4 (9.5)	
Specimen type, n (%)				0.75
Resection	35 (63.6)	9 (69.2)	26 (61.9)	
Biopsy	20 (36.4)	4 (30.8)	16 (38.1)	
Child Pugh Score, n (%)				0.34
A	48 (87.3)	10 (76.9)	38 (90.5)	
B	7 (12.7)	3 (23.1)	4 (9.5)	
Advanced Fibrosis F3-4, n (%)*	15 (44.1)	4 (44.4)	11 (44.0)	1.0
Platelets >100,000 / mm3, n (%)	41 (74.5)	10 (76.9)	31 (73.8)	1.0
AFP (ng/mL), median (range)	58 (1-675,400)	4.4 (1-93,238)	97.9 (1-675,400)	0.03
AFP (ng/ml) > 200, n (%)	23 (41.8)	3 (23.1)	20 (47.6)	0.20
Macrovascular invasion, n (%)	12 (22.2)	4 (30.8)	8 (19.5)	0.45
Extrahepatic disease, n (%)	39 (70.9)	10 (76.9)	29 (69.0)	0.73
Anti-PD1 drug, n (%)				0.59
Nivolumab	42 (76.4)	9 (69.2)	33 (78.6)	
Pembrolizumab	12 (21.8)	4 (30.8)	8 (19.0)	
Tislelizumab	1 (1.8)	0 (0.0)	1 (2.4)	
Median time on therapy (months)	3.9	21.0	2.78	<0.001

* data missing from 21 cases

Molecular markers of response to anti-PD1 therapy in advanced hepatocellular carcinoma

INDEX OF SUPPLEMENTARY INFORMATION

Supplementary materials and methods

Study population and endpoints

Gene expression profiles from 347 patients undergoing anti-PD1 therapy were analysed for the purpose of our study, including our HCC cohort of 83 cases established under the umbrella of an international consortium comprising 13 referral centers. Cases from our cohort were recruited from the following institutions: Icahn School of Medicine at Mount Sinai, the Inselspital University of Bern, KU Leuven, University of Mainz, Hannover Medical School, University College London Cancer Institute, Lausanne University Hospital, Mayo Clinic, Hospital Universitari Vall d'Hebron, IRCCS Istituto Nazionale Tumori (Milan, Italy), University of Frankfurt, Charité University Medicine Berlin and the Geffen School of Medicine at UCLA. The transcriptomic data from the remaining 240 cases were previously published and obtained from public repositories[1-4]. Clinico-pathological data and follow-up for patients included in the internal cohort of 83 patients are summarized in **Tables 1, S2-3**.

RNA extraction and gene expression profiling

We collected 111 archived formalin-fixed paraffin-embedded tissue blocks (**Table S1**), including both resection specimen and biopsies, of patients undergoing anti-PD1 therapy for advanced HCC. The study protocol was approved at each contributing center and informed consent obtained from subjects. An expert liver pathologist (ST) validated HCC as the disease entity and discerned tumor tissue from adjacent non-tumoral hepatic parenchyma based on haematoxylin/eosin (H&E) staining. Briefly, tumor tissue was

macrodissected in FFPE sections and RNA as well as gDNA isolated using the miRNAeasy FFPE and QIAmp DNA FFPE tissue kit (QIAgen), respectively.

Transcriptomic studies were performed using the Clariom S human Array (Affymetrix) with 400ng of total RNA as input. We performed the microarrays in two different batches of 58 samples and 29 cases, respectively. The latter batch included 4 technical replicates from the first batch, in order to allow for subsequent batch correction, if necessary. Nonetheless, after applying an empirical Bayes framework with ComBat –integrated in sva bioconductor package[5] - no differences were observed between batches, and therefore technical replicates were removed from the first set. Commands mod=NULL, and par.prior=TRUE were used in ComBat. Background correction and quantile normalization of the raw expression data was carried out using the R *oligo* package with *rma* modules. Differential gene expression based on the distinct response subtypes was conducted using the *limma* package. We performed Wilcoxon rank sum test on an individual gene level and used a nominal p value threshold <0.01 and a fold change (FC) of 1.5 as cut-offs to define differentially expressed genes (DEG). Functional characterization of DEGs was performed using Gene Ontology enrichment analysis with FDR corrected p values. We further tested previously reported gene-expression signatures that define states of inflammation and immune cell subsets using the Molecular Signature Database gene sets (MSigDB, www.broadinstitute.org/msigdb) and individually curated gene sets[6-13] (signatures are shown in **Table S6**). This included signatures that have been previously linked to response to immunotherapy in HCC and other cancer types. Gene sets with an upregulation of all included genes were tested via single sample Gene set enrichment analysis (ssGSEA) after normalization. Assessment of pathway

activation was performed using Gene Set Enrichment Analysis (GSEA) and ssGSEA. Other signatures that incorporate up-and downregulation of genes as well as previously reported molecular HCC classes[11, 14, 15] were tested using the GenePattern Nearest Template Prediction module[16]. Samples were assigned to a given class when the FDR<0.05 unless otherwise stated in the original publication. Microenvironmental deconvolution was performed with CIBERSORTx[17] in batch corrected mode.

Generation of the IFNAP signature

To generate a gene-expression signature associated with objective response to anti-PD1 single-agent therapy, differential expression analysis was performed between responders and non-responders and genes with a Fold Change > 1.5 and a p-value by Wilcoxon-rank sum test p<0.01 selected for further analysis. The resulting 140 genes were able to distinguish responding from non-responding cases based on principal component analysis (**Figure S2A**). We next cross-referenced the 140 genes with the two top Gene Ontology terms associated with these genes pertaining to IFN signalling (GO:0060333) and antigen presentation (GO:0019886). We added *CXCL9* (FC=3.4, p<0.01) and *B2M* (FC=1.7, p=0.01) that were enriched in responders in our dataset as well. *CXCL9* is a key chemokine, facilitating tumoral T-cell infiltration that has been shown in a recent metaanalysis to be significantly enriched among responding patients across cancer types[18]. *B2M* is a part of the antigen-presentation machinery, where loss of heterozygosity (LOH) and deletions have been linked to primary resistance in melanoma[19]. The resulting 11 genes were incorporated into a gene set titled IFNAP that was then tested to predict response and survival in our HCC cohort and four validation datasets. We defined high

expression of IFNAP as patients within the 3rd tertile, whereas the remaining patients were characterized as the Rest. A summary of the generation of the signature is depicted in **Figure S13**.

Validation of IFNAP in external datasets

After ensuring acceptable predictive ability in our dataset, we then sought to test the predictive potential of IFNAP in five independent external datasets that were previously published:

1. Prat et al, Cancer research 2017 : 65 patients (Melanoma, NSCLC, HNSCC)[3]
2. Jung et al, Nat. Comm. 2019: 27 patients (NSCLC)[1]
3. Liu et al, Nature Med. 2019 : 151 patients (Melanoma)[2]
4. Hugo et al, Cell 2016 : 28 patients (Melanoma)[4]
5. Hsu et al, Liver Cancer 2021 : 24 patients (HCC)[20]

As in our internal cohort, IFNAP expression was defined as high for the top tertile whereas the remaining patients were grouped as the Rest in each of the datasets. In the cohort by Jung et al, response was defined as patients having a durable clinical benefit (DCB), meaning the patient had either OR or SD for at least 6 months.

In all datasets, tissue was obtained before the initiation of anti-PD1 therapy. In the Liu et al cohort, however, one patient had an on-treatment biopsy. This patient was therefore excluded from the analysis.

In both pure melanoma datasets, response rates exceeded 33% and therefore the applied cut-off for the third tertile limited the predictive ability of IFNAP. In these datasets, chi² p values are 1-sided.

The effect of TKIs on tumoral and microenvironmental signaling was studies by repurposing a previously published report where a syngeneic HCC model was generated by injecting 5x106 Hepa1-6 cells in 5-6-week old female C57BL/6J mice[21]. Tumor samples from the model were collected 13 days after treatment with either lenvatinib or vehicle and subjected to gene expression microarray studies using the Clariom S Mouse Array (Affymetrix, Santa Clara, CA; GSE153203). Normalization, background correction and log-transformation were were carried out using the limma package and single sample gene set enrichment analysis performed using GenePattern.

Immunohistochemistry and assessment of immune infiltration

The presence and severity of an immune infiltrate was assessed by an expert pathologist (ST) using HE stained slides. A previously published scoring system was applied grading the overall amount of the immune infiltrate applying a semi-quantitative score from 0-4, where 0= absence of immune cell infiltration, 1= minimal, 2=mild infiltration, 3= moderate infiltration and 4= severe infiltration[11]. We applied the previously established threshold of 2, up to which samples are defined to have low infiltration where grades 3-4 are considered to have high infiltration. Scoring was performed both within the tumoral compartment as well as at the invasive margin when available.

Assessment of the tumor infiltration lymphocytes (TILs) and scoring was performed following the International Immuno-Oncology Biomarkers Working Group recommendations[22].

Immunohistochemistry (IHC) for PD-1 and PD-L1 was performed on 3-µm-thick FFPE tissue sections after heat-induced antigen retrieval in microwave with 10 mM TRIS-EDTA (pH=9). Primary antibodies used for anti-PD-L1 and anti-PD1 were Abcam clone 28-8 and clone NAT105, respectively. Positive staining for PD1 was measured as previously characterized using a semi-quantitative (high vs. low) score[11]. PD-L1 expression was assessed in HCC cells where the percentage of neoplastic cells with membranous staining was defined and tumors with 1% or more of positively stained cells were classified as positive.

CTNNB1 mutation status

As mutations in *CTNNB1* have been implicated in driving primary resistance to anti-PD1 therapy, we performed Sanger sequencing using primers to amplify *CTNNB1* exon 3. Mutations were confirmed by sequencing a second amplification product on both strands. Primers used were 5' to 3' GATTTGATGGAGTTGGACATGG (forward) and TGTTCTTGAGTGAAGGACTGAG (reverse).

Statistical analysis

Supplementary analysis were performed using the R statistical package. Correlations between expression of gene signatures and objective response were performed by Chi^2 test and Wilcoxon rank-sum test for categorical and continuous data, respectively. Kaplan-Meier estimates and log-rank test were performed to investigate the association

of IFNAP expression with progression-free- and overall survival using the *survminer* package.

Molecular Data availability

Publically available datasets used in this study are detailed in the supplementary materials and methods. The normalized gene expression data and clinical data from the HCC cohort has been deposited at European Genome archive (EGAS00001005477). All reasonable requests for raw data will be promptly reviewed by the corresponding author to determine whether the request is subject to any intellectual property or confidentiality obligations.

References

1. Jung H, Kim HS, Kim JY, et al. DNA methylation loss promotes immune evasion of tumours with high mutation and copy number load. Nature Communications 2019;10:4278.
2. Liu D, Schilling B, Liu D, et al. Integrative molecular and clinical modeling of clinical outcomes to PD1 blockade in patients with metastatic melanoma. Nature Medicine 2019;25:1916-1927.
3. Prat A, Navarro A, Paré L, et al. Immune-Related Gene Expression Profiling After PD-1 Blockade in Non–Small Cell Lung Carcinoma, Head and Neck Squamous Cell Carcinoma, and Melanoma. Cancer Research 2017;77:3540-3550.
4. Hugo W, Zaretsky JM, Sun L, et al. Genomic and Transcriptomic Features of Response to Anti-PD-1 Therapy in Metastatic Melanoma. Cell 2016;165:35-44.
5. Leek JT, Johnson WE, Parker HS, et al. The sva package for removing batch effects and other unwanted variation in high-throughput experiments. Bioinformatics 2012;28:882-3.
6. Ayers M, Lunceford J, Nebozhyn M, et al. IFN-γ-related mRNA profile predicts clinical response to PD-1 blockade. J Clin Invest 2017;127:2930-2940.
7. Rooney MS, Shukla SA, Wu CJ, et al. Molecular and genetic properties of tumors associated with local immune cytolytic activity. Cell 2015;160:48-61.
8. Sangro B, Melero I, Wadhawan S, et al. Association of inflammatory biomarkers with clinical outcomes in nivolumab-treated patients with advanced hepatocellular carcinoma. J Hepatol 2020;73:1460-1469.
9. Auslander N, Zhang G, Lee JS, et al. Robust prediction of response to immune checkpoint blockade therapy in metastatic melanoma. Nat Med 2018;24:1545-1549.
10. Fehrenbacher L, Spira A, Ballinger M, et al. Atezolizumab versus docetaxel for patients with previously treated non-small-cell lung cancer (POPLAR): a multicentre, open-label, phase 2 randomised controlled trial. The Lancet 2016;387:1837-1846.
11. Sia D, Jiao Y, Martinez-Quetglas I, et al. Identification of an Immune-specific Class of Hepatocellular Carcinoma, Based on Molecular Features. Gastroenterology 2017;153:812-826.

12. Pinyol R, Montal R, Bassaganyas L, et al. Molecular predictors of prevention of recurrence in HCC with sorafenib as adjuvant treatment and prognostic factors in the phase 3 STORM trial. Gut 2019;68:1065-1075.
13. Bindea G, Mlecnik B, Tosolini M, et al. Spatiotemporal dynamics of intratumoral immune cells reveal the immune landscape in human cancer. Immunity 2013;39:782-95.
14. Hoshida Y, Nijman SM, Kobayashi M, et al. Integrative transcriptome analysis reveals common molecular subclasses of human hepatocellular carcinoma. Cancer Res 2009;69:7385-92.
15. Chiang DY, Villanueva A, Hoshida Y, et al. Focal gains of VEGFA and molecular classification of hepatocellular carcinoma. Cancer Res 2008;68:6779-88.
16. Brunet J-P, Tamayo P, Golub TR, et al. Metagenes and molecular pattern discovery using matrix factorization. Proceedings of the National Academy of Sciences 2004;101:4164.
17. Newman AM, Steen CB, Liu CL, et al. Determining cell type abundance and expression from bulk tissues with digital cytometry. Nature Biotechnology 2019;37:773-782.
18. Litchfield K, Reading JL, Puttick C, et al. Meta-analysis of tumor- and T cell-intrinsic mechanisms of sensitization to checkpoint inhibition. Cell 2021;184:596-614.e14.
19. Sade-Feldman M, Jiao YJ, Chen JH, et al. Resistance to checkpoint blockade therapy through inactivation of antigen presentation. Nature Communications 2017;8:1136.
20. Hsu CL, Ou DL, Bai LY, et al. Exploring Markers of Exhausted CD8 T Cells to Predict Response to Immune Checkpoint Inhibitor Therapy for Hepatocellular Carcinoma. Liver Cancer 2021;10:346-359.
21. Torrens L, Montironi C, Puigvehí M, et al. Immunomodulatory Effects of Lenvatinib Plus Anti-Programmed Cell Death Protein 1 in Mice and Rationale for Patient Enrichment in Hepatocellular Carcinoma. Hepatology 2021.
22. Hendry S, Salgado R, Gevaert T, et al. Assessing Tumor-Infiltrating Lymphocytes in Solid Tumors: A Practical Review for Pathologists and Proposal for a Standardized Method from the International Immuno-Oncology Biomarkers Working Group: Part 2: TILs in Melanoma, Gastrointestinal Tract Carcinomas, Non-Small Cell Lung Carcinoma and Mesothelioma, Endometrial and Ovarian Carcinomas, Squamous Cell Carcinoma of the Head and Neck, Genitourinary Carcinomas, and Primary Brain Tumors. Adv Anat Pathol 2017;24:311-335.

Supplementary Figures

S1: Depiction showing the time between sample acquisition and treatment initiation.

S2: Pathway activation in responding patients and clinical outcomes according to the HCC molecular classes.

S3: Performance of histological markers and inferred TMB in patients treated with anti-PD1 frontline and $2^{nd}/3^{rd}$ line

S4: Principal component analysis and composition of IFNAP and other signatures.

S5: Association of outcomes and individual genes in response signatures

S6: Validation of IFNAP in two independent melanoma cohorts.

S7: Performance of previously reported response signatures in two validation datasets.

S8: Validation of IFNAP in independent HCC cohort.

S9: Microenvironmental deconvolution with CIBERSORTx.

S10: Outcomes according to CTNNB1 mutational status.

S11: Performance of response signatures in patients treated with anti-PD1 after previous TKI therapy.

S12:Prior TKI therapy interferes with the readout of inflammatory signatures as biomarkers of response

S13: Generation of IFNAP signature.

Fig. S1: Depiction showing the time between sample acquisition and treatment initiation. The time difference between the acquisition of the biological specimen and the initiation of systemic therapies was 4 months in patients treated with anti-PD1 in frontline and 12.8 months for patients treated in 2nd or 3rd line.

Fig. S2: Pathway activation in responding patients and clinical outcomes according to the HCC molecular classes. (A) GO-term analysis for cellular components among the 140 DE genes revealed a strong association enrichment in genes associated with MHC class II expression and formation (FDR<0.001). (B) Gene set enrichment analysis (GSEA) between responding patients treated with anti-PD1 in frontline (n=12) compared to non-responders (n=16) confirmed an upregulation of genesets associated with an active immune response and antigen presentation (FDR<0.001). (C) Outcome analysis in patients treated with anti-PD1 in frontline revealed a trend towards longer mPFS in the *Inflamed HCC* subclass was observed. (D) Patients with an aggressive phenotype, as accounted for by the molecular classes *S1* and *S2* had a markedly longer mPFS than the remaining patients.

Fig. S3: Performance of histological markers and inferred TMB in patients treated with anti-PD1 frontline and 2nd/3rd line. (A) No difference was observed between responders and non-respondes treated in frontline based on histological assessment of tumor infiltrating lymphocytes within the tumor (top panel) or at the invasive margin (bottom panel). (B) In patients treated in 2nd and 3rd line, a similar observation was made, where the severity of TIL infiltration was not linked to response. (C) Expression of

previously reported signatures inferring high mutational burden (TMB) and the presence of tertiary lymphoid structures (TLS) was not linked to response status in frontline or in 2nd/3rd line.

Fig. S4: Principal component analysis and composition of IFNAP and other signatures. (A) Principal component analysis (PCA) using the 140 DE genes reveals a clear separation between responding and non-responding patients, with IFNAP positive patients clustering together. (B) Individual compositions of gene expression signatures previously reported and IFNAP are shown highlighting the unique composition of IFNAP. Red squares indicate the inclusion of an individual gene in the respective signature. (C) Re-analysis of a previously published cohort of 30 samples from 15 large HCC tumors revealed expression of IFNAP to be highly correlated between two samples of a given tumor indicating that intratumoral heterogeneity does not mitigate the robustness of the signature.

Fig. S6: Association of outcomes and individual genes in response signatures. Analysis of the genes included in the IFNAP and IFN signature revealed a significant enrichment of all individual IFNAP genes in responders (A). Superior clinical outcomes were observed with regard to Objective response when performing binary logistic regression and to PFS with Cox regression analysis (B). Of the 6 genes included in the IFN signature only the ones overlapping with IFNAP were positively linked with OR and longer PFS whereas the remaining 3 genes (IFNG, CXCL10 and IDO1) were not (C).

Fig. S6: Validation of IFNAP in two independent melanoma cohorts. Correlations between response signature expression, according to the top tertile vs remaining cases, and objective response rates as well as Kaplan-Meier estimates for progression-free survival and overall survival are shown. (A-L) In a third dataset, including only melanoma cases treated with anti-PD1, only IFNAP was able to consistently show significant differences in terms of objective response (A), progression-free- (B) and overall survival (C). Conversely, none of the previously reported response signatures (D-L) were able to elicit significant differences in terms of OR (D,G,J), PFS (E,H,K) and OS (C,F,I,L). (M-P) Validation was performed in a further RNA-seq based dataset of melanoma patients treated with anti-PD1 (Hugo et al). Of the tested signatures, only high Expression of IFNAP was associated with an increase in ORR (M), whereas neither the 6-gene *IFN* signature, nor *POPLAR* and the *Inflammatory* signature predicted response (N-P). No data on PFS was available in this dataset. P values in Chi^2 tests represent a 1-sided significance level.

Fig. S7: Performance of previously reported response signatures in 2 validation datasets. Correlations between response signature expression, according to the top tertile vs remaining cases, and objective response rates as well as Kaplan-Meier estimates for progression-free survival are shown. (A-F) In the nanostring-based datasets with non-small cell lung cancer, melanoma or head and neck squamous cell cancer patients, none of the previously reported signatures were associated with response (A,C,E), while high expression of the IFN signature was able associated with longer PFS (B). (G-L) In the RNA-seq based dataset by Jung et al, comprising NSCLC patients, only IFNAP and the IFN signature was associated with response (G) and longer PFS (H) while

the remaining signatures had no predictive values (I-L). A cut-off at between 2nd and 3rd expression tertile was applied to separate the groups. P values in Chi^2 tests represent a 2-sided significance level.

Fig. S8: Validation of IFNAP in independent HCC cohort. Validation was performed **i**n an independent cohort of 24 HCC patients treated with either nivolumab (n=13) or combination (n=11). Among the patients treated with nivolumab, high expression of IFNAP was associated with significantly longer OS (A), whereas a trend was observed towards higher ORR in patients with high IFNAP expression. In those patients treated with combination, however, high IFNAP expression was neither associated with neither OS (C) nor OR (D). P values represent log-rank test in KM curves as well as asymptotic Chi² tests with a 2-sided significance level.

Fig. S9: Microenvironmental deconvolution with CIBERSORTx. Complete results of CIBERSORTx are shown based on expression of IFNAP. High expression was defined as the top tertile, whereas remaining patients were summarized as the Rest. Analysis was performed with 100 permutations in batch-correction mode. P values represent Wilcoxon-rank sum tests.

Fig. S10: Outcomes according to CTNNB1 mutational status. Kaplan-Meier estimates for PFS and OS are shown for patients treated with anti-PD1 in frontline. While responders had markedly longer mPFS and mOS than non-responders, no differences were observed when comparing responders based on CTNNB1 mutational status. Likewise, outcomes of non-responders were similar as well between CTNNB1 mutated cases and CTNNB1 wildtype (WT) patients. P values represent a log rank test.

Fig. S11: Performance of response signatures in patients treated with anti-PD1 after previous TKI therapy. Correlations between response signature expression, according to the top tertile vs remaining cases, and objective response rates as well as Kaplan-Meier estimates for progression-free- and overall survival are shown for patients treated with anti-PD1 therapy in either 2nd or 3rd line in our dataset. Neither IFNAP nor previously reported signatures of response were able to predict any differences in ORR (A,D,G,J), progression-free- (B,E,H,K) and overall survival (C,F,I,L). The lack of discrimatory ability by these signatures suggests that previous TKI therapy can reshape the tumoral microenvironment to render initially inflamed tumors no longer amenable to anti-PD1 therapy. P values in Chi^2 tests represent a 2-sided significance level.

Fig. S12: Prior TKI therapy interferes with the readout of inflammatory signatures as biomarkers of response. (A) Heatmap of patients treated with anti-PD1 in 2nd and 3rd line and previously characterized response signatures. (B) Depiction of normalized expression scores from GO-based gene set enrichment analysis in patients with low IFNAP expression based on whether they responded (IFNAP low OR, pink) or not (IFNAP low NR, navy blue). (C) Boxplot representation of CIBERSORTx in patients with low IFNAP expression identifies severe Treg infiltration as an obstacle to achieve OR to anti-PD1 in patients treated in 2nd and 3rd line. (D) A previously reported murine model was re-analyzed to investigate the impact of TKI treatment via lenvatinib on the tumoral microenvironment. (E) In the murine model, lenvatinib elicited a shift in the cellular

composition within the tumoral microenvironment and was able to augment inflammatory signalling. P values for KM analysis derive from log-rank test whereas those in the boxplot representation represent Wilcoxon-rank sum test.

Fig. S13: Generation of IFNAP signature. IFNAP signature was created based on differential expression analysis using highly differentially expressed genes that overlapped with known Gene Ontology terms with the addition of CXCL9 and B2M.

Supplementary Tables

Table S1: Participating centers.

Table S2: Cohort characteristics based on treatment line.

Table S3: Clinicopathological characteristics of patients treated with anti-PD1 in frontline.

Table S4: Differentially expressed genes between responders and non-responders in frontline treated patients.

Table S5: GSEA between responding and non-responding patients treated in frontline.

Table S6: Previously reported signatures of response / resistance to anti-PD1 therapy and signatures capturing immune cell subsets.

Table S7: Performance of previously reported signatures and IFNAP in frontline cohort.

Table S8: Genes incorporated in the IFNAP signature.

Table S9: Clinicopathological characteristics of patients treated with anti-PD1 in 2nd/3rd line.